Development of a self-silencing adenovirus for the efficient manufacture of adeno-associated virus vectors



Weiheng Su
Exeter College
The University of Oxford

A thesis submitted for the degree of Doctor of Philosophy to the Department of Oncology, University of Oxford
Hilary Term 2021

To ah Ma – nothing would have been possible without your support and sacrifice

Abstract

Adeno-associated virus (AAV) shows great promise for gene therapy, however scalability, yield and quality remain significant issues. The most common 'helper-free' method used to produce recombinant AAV (rAAV) for pre-clinical/clinical application is based on plasmid transfection of HEK293 cells to provide all the components required for rAAV replication. While versatile and easy to adopt, the helper-free method is limited by a lack of scalability and vector yield.

Here we describe novel rAAV manufacturing strategies using 'helper' adenoviruses that self-inhibits its major late promoter (MLP) to truncate its own replication. Modification of the adenovirus MLP *in situ* to provide inducible repression has not previously been demonstrated, primarily because the virus DNA polymerase coding sequence is in the opposing DNA strand. We show that strategic insertion of tetracycline repressor binding sites into the MLP and encoding the tetracycline repressor under its transcriptional control allows for normal adenovirus replication in the presence of doxycycline, but only enhanced genome amplification and early gene expression (important for the 'helper' functions) in its absence.

Using this negative feedback system, we developed a complete transfection-free 'self-repressing' helper-vector approach to produces AAV particles. We demonstrate delivery of adenoviral helper functions, the rAAV transfer genome, and the AAV genes including rep, known to be toxic to adenovirus, to yield up to a 1000-fold increase in infectious rAAV2 compared to the helper-free plasmid system. We further extended this approach to produce rAAV5, -6, -8, -9 vector serotypes, and in all cases, yielding significant increases in intact particles over the standard manufacturing approach with over 8 log reduction in contaminating adenoviruses. To reduce manufacturing complexity and encapsidation of illegitimate DNA within rAAV particles, we also explored a unique strategy to manufacture rAAV vectors by

propagating rAAV particles using self-silencing adenoviral vectors expressing the AAV components. This included a *trans*-pseudotyping or 'capsid-exchange' method to generate rAAV-5, -6, -8, and -9 from rAAV2 particles. We propose these as high-yielding contaminant-free production systems suitable for scalable rAAV manufacture.

Lastly, in exploring the use of the self-silencing adenovirus to promote rAAV production from mammalian cells stably encoding the AAV genes, we provide direct evidence that factor(s) expressed from the MLP during adenovirus replication was required to support CARE-dependent amplification, a unique mechanism that results in 100-1000 fold DNA amplification of the integrated AAV genes, and a prerequisite for high-titre rAAV production from the stable AAV packaging cells.

Declaration of Authentication

The work presented in this thesis was performed under the supervision of Professor Leonard Seymour, Department of Oncology, Division of Medical Sciences, University of Oxford, and Dr Ryan Cawood CEO, Oxford Genetics Ltd. This work is wholly my own, and any contribution to the thesis made by others has been acknowledged. The work submitted here does not form part of another thesis in this or any other university.

Weiheng Su

March 2021

Acknowledgements

This thesis is dedicated to Max, for all the time we missed together.

I am eternally grateful to Dr. Ryan Cawood and Professor Len Seymore for offering me the opportunity to undertake this DPhil. Their friendship, mentorship, scientific and intellectual guidance have proved invaluable and inspirational over these past four years. I consider myself one of the luckiest of students to have benefitted from their supervision.

I would like to thank the Seymour Group, an extremely bright and talented bunch, for letting me be a part of the team and always providing the best of support through challenging times. In particular – Arthur and Sally for providing never-ending support and advice. I would like to thank Margaret – for the opportunity and privilege to have been one of your students. Despite brief, your supervision and advice have been invaluable. I would like to thank the OXGENE friends and colleagues, both past and present - Anna, Lucia, Stefania, Emma, Maria, Corinne, and Shalome. Working together have made the day shorter every day.

I'm grateful for my parents and siblings for their support. Mostly, to Gosia – for keeping everything in order and for your support.

Table of Content

Abstract 3
Declaration of Authentication 5
Acknowledgements 6
List of Abbreviations 12
Chapter 1 14
Introduction 14
1.1 Gene therapy 14
1.2 Adeno-associated virus (AAV) 17
1.2.1 History of AAV 17
1.2.2 General biology of AAV 18
1.2.3 AAV genome organisation 19
1.2.4 Life cycle of AAV 21
1.2.5 AAV cellular entry and transduction 23
1.2.6 AAV genome replication cycle 25
1.2.7 Vectorization of AAV 28
1.2.8 Development of the helper-free method 29
1.2.9 Manufacture of rAAV vectors 32
1.3 Adenovirus 36
1.3.1 Adenovirus classification 36
1.3.2 Adenovirus structure 37
1.3.3 Adenovirus attachment and entry 39
1.3.4 Adenovirus genome organisation 41
1.3.5 Adenovirus genome replication 43
1.3.6 Adenovirus major late promoter 45
1.3.7 Adenovirus tripartite leader 47
1.3.8 Adenovirus packaging 48
1.3.9 Adenovirus Vectorization 49
1.4 Inducible gene regulation systems 51
1.4.1 Tetracycline inducible systems 51
1.4.2 Cumate gene-switch systems 54
1.5 Thesis overview and aims 56
1.5.1 Thesis overview 56
1.5.2 Thesis aims 58

Chapter 2 59
Materials and Methods 59
2.1 Molecular biology 59
2.1.1 Bacterial transformation 59
2.1.2 Plasmid DNA purification 60
2.1.3 Plasmid restriction digest 60
2.1.4 DNA ligation 60
2.1.5 Gibson assembly 61
2.1.6 Polymerase chain reaction (PCR) 61
2.1.7 Agarose gel electrophoresis 62
2.1.8 DNA quantification 63
2.1.9 Sanger Sequencing 63
2.2 Cell culture 63
2.2.1 Maintenance of cell lines 63
2.2.2 DNA transfection 64
2.2.3 siRNA transfection 64
2.2.4 Adenovirus infection in HEK293 cells and Flp-In-T-Rex-293 cells 65
2.2.5 Flow cytometry 65
2.3 Viral vectors 67
2.3.1 Adenovirus recovery and small-scale amplification 67
2.3.2 Large-scale amplification and purification by caesium chloride gradients 68
2.3.3 rAAV production using adenovirus and the helper-free system 70
2.3.4 TCID50 assay for determining infectious adenovirus and rAAV 71
2.3.5 AAV cell internalisation assay 72
2.3.6 Determining intact adenovirus particles by PicoGreen assay 72
2.3.7 DNA quantification using qPCR 72
2.3.8 RNA extraction and reverse transcription 74
2.3.9 Western blotting 75
2.3.10 Transmission electron microscopy 76
2.3.11 Statistical analysis 76
Chapter 3 77
Engineering and characterisation of a Tetracycline Enabled Self-Silencing Adeno virus 'TESSA' for rAAV manufacture 77
3.1 Introduction 77
3.2 Chapter aims 81
3.3 Results 82

3.3.1 Engineering Tet-responsive elements into the MLP EGFP reporter plasmids 82
3.3.2 Insertion of TetO sites do not affect Ad5 MLP basal activity 84
3.3.3 Engineering adenovirus vectors with TetO MLPs 88
3.3.4 Repression of TetO modified Adenovirus vectors in Flp-In T-REx 293 cells 89
3.3.5 Adenovirus genome replication is maintained during MLP repression 90
3.3.6 MLP repression blocks adenovirus spread in Flp-In T-REx 293 92
3.3.7 Engineering of TESSA – expression of TetR under control of the virus MLP 95
3.3.8 Assessing the potency of the TESSA MLP self-repression loop 98
3.3.9 TESSA maintains expression of early genes and helper functions for AAV production 101
3.3.10 Engineering TESSA to encode the rAAV transfer genome 103
3.3.11 Transcription of TetR from the MLP is higher in the presence of doxycycline but the TetR protein is unable to mediate promoter self-repression 107
3.3.12 Repression of MLP inhibits expression of adenovirus structural proteins 108
3.3.13 Repression of MLP from TESSA enhances DNA replication 111
3.3.14 Expression of transgenes from TESSA 112
3.3.15 Production of rAAV2 from TESSA-AAV-EGFP 114
3.3.16 Contamination of infectious adenovirus is repressed from TESSA during AAV production 115
3.4 Chapter discussions 118
3.5 Chapter conclusions 122
Chapter 4 123
Encoding AAV rep and cap in TESSA to support efficient rAAV manufacture 123
4.1 Introduction 123
4.2 Chapter aims 126
4.3 Results 127
4.3.1 AAV Rep proteins repress MLP activity 127
4.3.2 Development of single-switch virus for repression of AAV Rep 128
4.3.3 Cloning and evaluation of the rTetR-E37A-P39K TetO-4C5G system 129
4.3.4 Evaluation of TESSA-DS expressing EGFP from the 4C5G-inducible promoter 132
4.3.5 Evaluation of TESSA-DS expressing BAX from the 4C5G-inducible promoter 133
4.3.6 Design and construction TESSA-DS expressing Rep and Cap from the 4C5G-inducible promoter 135
4.3.7 Exploring the Cumate-inducible gene expression system 138
4.3.8 Engineering TESSA vectors expressing AAV Rep and Cap from the cumate-inducible system 139
4.3.9 Construction of TESSA encoding promoterless AAV rep 144

4.3.10 Assessment of rAAV production using TESSA encoding the AAV transfer genome and Rep *in cis* 146
4.3.11 rAAV2 production via TESSA^{v1} approach (co-infection of TESSA-Rep with TESSA-AAV-EGFP-Cap2) 149
4.3.12 rAAV2 derived from TESSA^{V1} vectors exhibit enhanced cell transduction 153
4.3.13 Reverse DNA packaging in AAV2 vectors 154
4.3.14 Production of AAV-hFIX vectors using TESSA-Rep 156
4.3.15 Assessment of AAV9 vector production using 159
TESSA-AAV-EGFP-Cap9 159
4.3.16 Construction of TESSA-AAV-EGFP-Cap5 160
4.3.17 Cap5 coding sequence is lost from TESSA-AAV-EGFP-Cap5 at sequential passages 161
4.3.18 Assessment of AAV5 production via co-infection of TESSA-AAV-EGFP-Cap5 with TESSA-Rep 162
4.3.19 Construction and assessment of TESSA-AAV-EGFP expressing Cap5 from Cumate-inducible promoter 164
4.3.20 Construction of TESSA-RepCap2 167
4.3.21 Production and characterisation of rAAV2 particles from TESSA2.0 168
4.3.22 rAAV2 derived from TESSA2.0 exhibit enhance cell entry and transduction 170
4.3.23 All Rep proteins are expressed from TESSA 172
4.3.24 Replication and stability assessment of TESSA-RepCap2 175
4.3.25 siRNA knockdown of cap2 mRNA increase production of TESSA-RepCap2 177
4.3.26 Construction of TESSA-RepCap5, -6, -8 and -9 vectors 181
4.3.27 Production of rAAV5, rAAV6, rAAV8 and rAAV9 using the TESSA2.0 system 182
4.3.28 Assessment of rAAV5, rAAV6, rAAV8 and rAAV9 transduction *in vitro* 185
4.3.29 Stability assessment of TESSA-RepCap5, -6, -8 and -9 vectors 190
4.4 Chapter discussion 193
4.5 Chapter conclusions 198
Chapter 5 199
Production of rAAV via propagation and capsid-exchange using TESSA 199
5.1 Introduction 199
5.2 Chapter aims 201
5.3 Results 202
5.3.1 Propagation of AAV2 using TESSA-RepCap2 202
5.3.2 Assessment of transduction 203
5.3.3 Assessment of contaminating adenoviruses 203
5.3.4 Assessment of capsid composition 204

5.3.5 Assessment of contaminant DNA 204
5.3.6 Assessment of AAV2 particles by TEM 205
5.3.7 Capsid-exchange for the propagation of rAAV5, -6 and -9 209
5.3.8 Analysis of rAAV5, -6 and -9 derived from the capsid-exchange method 211
5.3.9 Production of AAV8 via capsid-exchange using TESSA-RepCap8 216
5.4 Chapter discussion 221
5.5 Chapter conclusions 224
Chapter 6 225
Production of rAAV from stable AAV packaging cell line using TESSA 225
6.1 Introduction 225
6.2 Chapter aims 227
6.3 Results 228
6.3.1 Expression from the adenovirus MLP is required for rAAV production from HeLaRC32 stable AAV packaging cell line 228
6.3.2 Expression from the adenovirus MLP is required to maintain AAV rep and cap DNA amplification from HeLaRC32 AAV packaging cells 230
6.3.3 siRNA knockdown of Ad5 E2B recovered rep and cap amplification in TESSA-E1-infected HeLaRC32 cells during MLP repression 234
6.3.4 Expression of the intermediate & late L4 22/33K unit is required for rAAV production from HelaRC32 cells 238
6.4 Chapter discussion 241
6.5 Chapter conclusions 243
Chapter 7 244
Final Discussion 244
7.1 Overview of the thesis 244
7.2 Repression of the MLP 246
7.3 Packaging of illegitimate DNA into rAAV 247
7.4 The potency of rAAV from TESSA 249
7.5 Potential applications to TESSA encoding AAV rep and cap 250
Concluding remarks 253
References 254

List of Abbreviations

AAV	adeno-associated virus
Ad	adenovirus
Ad Pol	adenovirus polymerase
ANOVA	analysis of variance
bp	base pair
Cap	AAV capsid gene
CAR	coxsackie and adenovirus receptor
CMV	cytomegalovirus
CO_2	carbon dioxide
CPE	cytopathic effect
cTA	cumate transactivator
DMEM	Dulbecco's modified Eagle's medium
DNA	deoxyribonucleic acid
Dox	doxycycline
dsDNA	double-stranded DNA
E	adenovirus early gene
EDTA	ethylenediaminetetraacetic acid
FBS	foetal bovine serum
FDA	Food and Drugs Administration
FLuc	firefly luciferase
g	gravity
GC	genome copies
h	hour
HEK	human embryonic kidney
ITR	inverted terminal repeat
kb	kilobase
kDa	kilodalton
L	adenovirus late gene
L	litre

mins	minutes
mL	millilitre
MLP	adenovirus major late promoter
mM	millimole
MOI	multiplicity of infection
ng	nanogram
ORF	open reading frame
p	plasmid
PCR	polymerase chain reaction
pH	potential of hydrogen
pTP	pre-terminal protein
qPCR	quantitative polymerase chain reaction
Ref	reference
Rep	AAV replication gene
RNA	ribonucleic acid
rTA	reverse tetracycline transactivator
SA	splice acceptor
SD	standard deviation
SDS	sodium dodecyl sulphate
TCID50	tissue culture infectious dose 50
Tet	tetracycline
TetR	tetracycline repressor
TESSA	tetracycline enabled self-silencing adenovirus
tTA	tetracycline transactivator
TPL	tripartite leader
UPE	upstream promoter element
UTR	untranslated region
VA	viral associated
VP	viral particle
WT	wildtype

Chapter 1

Introduction

1.1 Gene therapy

Initial concepts for gene therapy first emerged in the early 1960s with the development of immortalised cell lines and demonstrations that exogenous DNA can be stably introduced into a cell to provide new genetic functions (Friedmann 1992; Szybalska and Szybalski 1962). Gene therapy is defined as the therapeutic approach to deliver nucleic acids into patients' cells for correction of a genetic disorder. This is usually accomplished by correction, addition, or silencing of a targeted gene and is aimed at treating a variety of human diseases that include both dominant and recessive genetic disorders, cardiovascular and neurodegenerative diseases, and cancer (Lapteva et al. 2020; Mali 2013).

Gene delivery into patients' cells may occur by two routes, *ex vivo* or *in vivo*. In the *ex vivo* route, cells of interest are temporarily isolated from the patient for introduction of the therapeutic construct, before the modified cells are re-introduced back into the patient (Gowing, Svendsen, and Svendsen 2017; Anguela and High 2019). While this approach can ensure a stringent quality control process to confirm successful genetic modification and minimise the likelihood of unintentional mutations, *ex vivo* gene therapy is an expensive and laborious process, and only applicable to cells that are accessible for isolation and genetic manipulation (Naldini 2011; Mejia-Toiber, Castillo, and Giordano 2011). In the *in vivo* gene delivery approach, which may be local or systemic, vectors carrying the nucleic acids of interest are directly introduced into the patient for targeting cells and tissues at their native anatomical

locations (Kumar et al. 2016). *In vivo* gene delivery remains the gold standard approach to gene therapy as it is the least invasive method, with the theoretical potential to target any cell in the body. Several criteria are critical to achieve success in *in vivo* gene therapy, including the use of vectors that are safe and efficient, and which can be economically produced in sufficient quantities to meet clinical demands (Macpherson and Rasko 2014; Herzog, Cao, and Srivastava 2010; Goncalves and Paiva 2017; van der Loo and Wright 2016).

Vectors for delivery of gene therapy can usually be classified as viral or non-viral (Boulaiz et al. 2005). In the non-viral approach, therapeutic DNA is usually complexed with carrier molecules such as cationic lipids to facilitate cell entry and transduction. These carrier-DNA complexes can mediate cellular entry either by endocytosis or simply by disruption of the lipid bilayer in the plasma membrane. Alternatively, physical methods of nucleic acid delivery into cells have also been explored, such as microinjections, ultrasound-mediated approaches, and ballistic approaches such as the gene gun (Yin et al. 2014; Li and Huang 2000). While non-viral delivery methods are sometimes seen as safer alternatives to viral vectors and usually exhibit low immunogenicity, widespread utility is hindered by the low efficiency of transfection and limited target specificity (Al-Dosari and Gao 2009; Nguyen et al. 2007).

Viral gene delivery is, in most cases, more efficient than the non-viral approach as they utilise viruses highly evolved for cell entry and transduction (Finer and Glorioso 2017). Viruses generally exhibit a broad tropism to allow receptor-mediated gene delivery into a wide range of cells and tissues. Most vectors are derived from viruses (pathogenic and non-pathogenic) that are genetically modified by deletion of essential genes required for virus replication (Waehler, Russell, and Curiel 2007). However, most viruses elicit significant immune responses and integrating viruses may pose risks of insertional mutagenesis, limiting their use for therapeutic gene delivery (Knight, Collins, and Takeuchi 2013; Shirley et al. 2020; Kohn,

Sadelain, and Glorioso 2003). Most commonly use viral vectors for gene therapy include adenovirus, adeno-associated virus (AAV), retrovirus/lentivirus, and herpes simplex virus type 1-derived vectors (Lundstrom 2018; Kotterman, Chalberg, and Schaffer 2015). In general retrovirus/lentivirus and AAV are used to achieve long-term gene expression, with AAV the vector of choice for post-mitotic cells and retrovirus/lentivirus preferred for proliferating cells, whereas adenovirus and herpes are used for more short term expression such as cytotoxic cancer treatment or vaccination (Milone and O'Doherty 2018; Yi, Noh, and Lee 2011; Riviere, Danos, and Douar 2006; Wold and Toth 2013; Herold et al. 2002).

The first gene transfer trial was approved by the National Institutes of Health (NIH) in 1989. In that study, autologous tumour-infiltrating lymphocytes were transduced with a neomycin-tagged retroviral vector before reinfusing into patients to investigate the biodistribution and long-term survival of the transduced cells. Importantly, this showed for the first time that human cells can be genetically modified *ex vivo* and returned to patients safely (Cournoyer and Caskey 1990). Additionally, a landmark gene therapy trial was initiated in 1990 for delivery of the adenosine deaminase (ADA) gene into T cells of severe combined immunodeficiency patients using a retroviral vector. This trial successfully showed long-term persistence of ADA activity in one of the two patients following 11-12 infusions of the transduced T cells over 2 years (Blaese et al. 1995; Culver, Anderson, and Blaese 1991). However, progress in the gene therapy field was badly hit in 1999 following the controversial death of Jesse Gelsinger who received a high intra-arterial dose (3.8×10^{13} virus particles) of an E1- and E4-deleted adenovirus vector for the treatment for Ornithine Transcarbamylase (OTC) deficiency (Gao, Yang, and Wilson 1996; Raper et al. 2003). This led to a temporary cessation of all gene therapy trials in the USA and EU. In 2002 a clinical study of an adenovirus vector encoding p53, developed in the US by Schering Plough, showed impressive efficacy in phase I trials and was sold to a Chinese company SiBiono Gene Technologies. The virus, known as Gendicine, was

awarded a product licence in China in 2004 (Buller et al. 2002; Zhang et al. 2018). A resurgence in the gene therapy field led to the approval of Glybera in 2012 by the European Commission for the treatment of lipoprotein lipase deficiency using AAV1 vectors (Bryant et al. 2013).

Building on this proof of principle, the past five years have seen a rapid growth in the gene and cell therapy field with the FDA approval of cell therapies such as Kymriah (lentiviral-based vector for treatment of acute lymphoblastic leukaemia), Yescarta, (retroviral-based vector for treatment of large B cell lymphoma), and Tescartus (retroviral-based vector for treatment mantle cell lymphoma) and two AAV-based gene therapies Luxturna and Zolgensma for the treatment RPE65-associated Leber congenital amaurosis and spinal muscular atrophy, respectively (Ali et al. 2020; AlDallal 2020; Bulaklak and Gersbach 2020). To date, over 4000 gene therapy clinical trials have been completed or ongoing, targeting numerous disorders (Maldonado, Jalil, and Wartiovaara 2020).

1.2 Adeno-associated virus (AAV)

1.2.1 History of AAV

The discovery of the AAV is generally regarded as an accident, although the virus has now emerged as one of the most versatile and promising vectors for laboratory applications and gene therapy purposes. AAV was initially identified as contaminating defective particles from an adenovirus preparation in 1965 by R.W Atchinson and colleagues using electron microscopy imaging. These small particles were described as nonautonomous and required co-infection with adenovirus for replication, for which its name was derived. AAV was isolated away from adenoviruses and used for assessing pathogenicity by infecting newborn mice and hamsters. It

was concluded that AAV is not pathogenic as the animals displayed no signs of illness after inoculation (Atchison, Casto, and Hammon 1965). Within the human population, it has been estimated that up to 80% of individuals have been exposed to AAV and display reactive antibodies, but no diseases have yet been correlated with the virus (Erles, Sebokova, and Schlehofer 1999; Boutin et al. 2010). To date, thirteen natural serotypes of human AAV have been identified and hundreds of variants have been isolated from species ranging from mammals, reptiles, and birds (Tobiasch et al. 1998; Flotte and Berns 2005; Pillay et al. 2017). Over the last three decades AAV serotype 2 (AAV2) has been the most widely researched, reflecting its amenability to cell culture, and since it was the first serotype identified it is generally regarded as the prototypic AAV (Wu, Asokan, and Samulski 2006).

1.2.2 General biology of AAV

AAV is a small non-enveloped DNA virus that belongs to the family of Parvoviridae in the genus of Dependoparvovirus. It is approximately 22 nm in diameter and composed of an icosahedral capsid structure consisting of 60 viral protein (VP) subunits, VP1, VP2, and VP3 at an estimated 1:1:10 ratio (Johnson, Ozer, and Hoggan 1971; Xie et al. 2002). The capsid encompasses a ~4.7Kb single-strand DNA genome that is framed by GC-rich 145 bp inverted terminal repeat sequences (ITRs). Each viral ITR contains a 125 bp palindromic sequence to form a T-shaped hairpin structure at each end of the linear genome. They are important *cis*-active elements influencing multiple stages of the virus replicative cycle. For example, the ITRs serve as the initiation element for self-primed second strand synthesis required for gene expression and viral genome replication, but also act as a packaging signal for genome encapsidation (Srivastava, Lusby, and Berns 1983; Pegoraro et al. 2006; Xiao et al. 1997; Daya and Berns 2008). The single-stranded DNA genome can exist in both plus and minus forms, and during

productive replication both forms are packaged into virions at equal efficiency (Kapranov et al. 2012; Ling et al. 2015).

1.2.3 AAV genome organisation

The AAV genome encodes two main open reading frames (ORFs) situated in a sense orientation between the ITR hairpin structures (**Figure 1.1**). The first ORF encodes the rep gene that transcribes four non-structural Rep protein isoforms (Rep78, Rep68, Rep52, and Rep40) that regulate all stages of the AAV replication cycle. The largest Rep protein (Rep78) is transcribed from the p5 promoter and the smaller Rep68 is also produced from this transcript by alternative splicing. Rep78 and Rep68 perform a diverse range of functions that include acting as transcription activators to increase expression of AAV genes for replication, repressing AAV gene expression in its latent phase, and also providing DNA binding, helicase and site-specific endonuclease activities. The remaining Rep52 and Rep40 are transcribed from the p19 promoter embedded within the rep78/68 coding sequence. While Rep52 is expressed from the full-length mRNA, Rep40 is a smaller splice variant produced from this transcript. Rep52 and Rep40 proteins are important for the accumulation of single-stranded AAV genome from double-stranded DNA intermediates and packaging into viral capsids (King et al. 2001; Chejanovsky and Carter 1989).

The second ORF encodes AAV cap and is transcribed by the p40 promoter situated within the rep coding sequence. The viral capsid subunits VP1 VP2 and VP3 are expressed by alternative splicing and use of alternative start codons. The p40 mRNA transcript can be spliced from a single 5’ donor site to two 3’ acceptor sequences to generate different mRNAs transcripts (Weger et al. 1997; McCarty, Christensen, and Muzyczka 1991). The largest capsid unit VP1 is

expressed from a less abundant mRNA transcript with the weaker 3´splice acceptor sites, whereas VP2 and VP3 are expressed from the second major spliced mRNA transcript using the stronger 3´splice acceptor sequence. From this transcript, VP2 is translated inefficiently as it uses the upstream near-cognate start codon ACG, and VP3 is translated in abundance from the AUG start sequence (Trempe and Carter 1988; Stutika et al. 2016). The assembly-activating protein (AAP) is expressed from an alternative ORF embedded within the cap gene and translated using a near-cognate start codon (CUG) from the major spliced mRNA transcript. AAP was shown to be 23 kDa in size and essential for directing capsid subunits to the nucleolus and for capsid assembly in the majority of AAV serotypes (Sonntag, Schmidt, and Kleinschmidt 2010; Maurer et al. 2018). More recently, an additional protein, Membrane-associated accessory protein (MAAP), was also identified to be expressed from the major spliced cap transcript and via a CUG start codon. The function of the MAAP remains to be determined precisely, but it is thought to play a role in the productive replication cycle of the virus (Ogden et al. 2019).

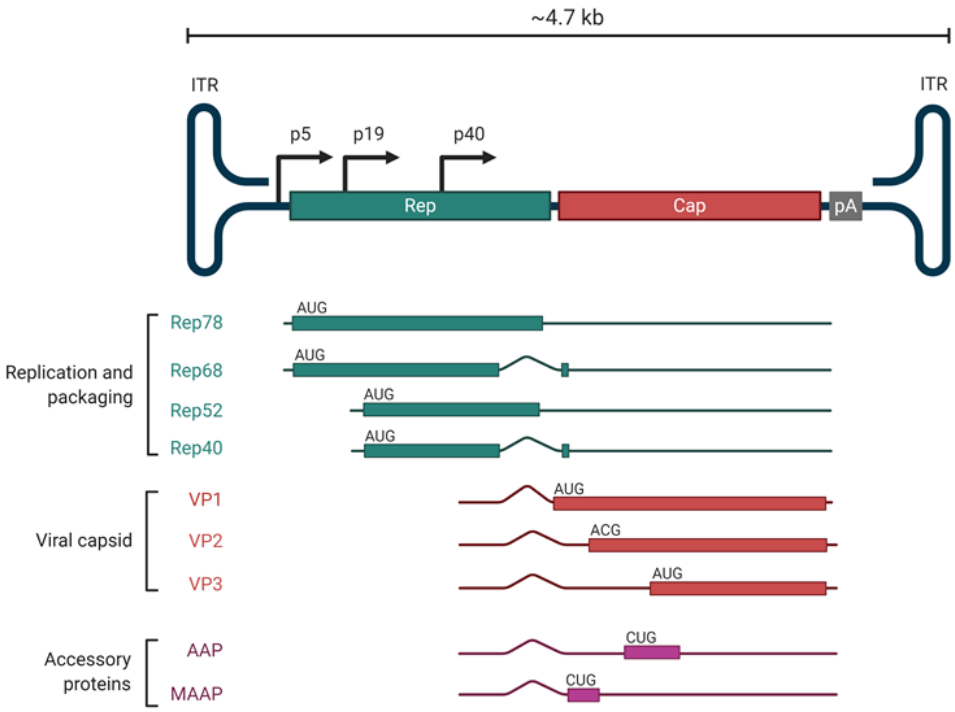


Figure 1.1 - Organisation of the AAV2 genome. AAV-2 genome organization. T-shaped black structures indicate the ITRs. Introns are indicated by broken lines. The first ORF encodes the four Rep regulator proteins expressed from the p5 and p19 promoter. Capsid proteins VP1 VP2 VP3 are encoded within the second ORF expressed from the p40 promoter. Alternative splicing results in the production of two transcripts. VP1 is translated from the first transcript. The second transcript encodes VP2, VP3, and the accessory proteins AAP and MAAP, which arise from initiation at different translation start sites. Diagram created using Biorender, not drawn to scale.

1.2.4 Life cycle of AAV

AAV may enter either a latent or lytic phase of its replication cycle after infection. In the absence of a helper virus co-infection, such as an adenovirus, AAV establishes a latent phase wherein viral gene expression is largely repressed. Under these conditions, the AAV genome can persist episomally as a double-stranded circular DNA or it can integrate into the AAVS1 locus within the PPP1R12C gene, located on chromosome 19 (q13.4) (Kotin et al. 1990; Daya,

Cortez, and Berns 2009). The occurrence of non-specific integration into the cell's chromosome is extremely rare, and site-specific integration of the AAV genome requires both cellular and viral components. AAV Rep78 or Rep68 proteins can bind to the Rep-binding site (RBS) in the 'integration efficiency' element within the AAV genome, a 138 bp sequence located within the p5 promoter, and also to an RBS-like element present within the AAVS1 for targeted integration (Philpott, Gomos, et al. 2002; Philpott, Giraud-Wali, et al. 2002). In the presence of a helper virus co-infection, AAV undergoes a lytic infection wherein its viral genes are expressed to induce genome replication and production of progeny viruses. Although adenovirus was identified as the first AAV helper virus, other viruses such as Cytomegalovirus (CMV), Herpes simplex virus (HSV), and Vaccinia virus are now known to act as helpers for AAV replication (McPherson, Rosenthal, and Rose 1985; Moore, Dong, et al. 2015). In general, the helper viruses contribute proteins involved in the induction of AAV gene expression and regulating host cell proteins to enable a promiscuous environment for AAV replication. The helper genes provided by adenovirus have been extensively characterised and involve E1a, E1b-55K, E2a, and E4Orf6 genes, and the VA RNAs, while the contributions provide by helper viruses HSV and CMV are less well understood (Timpe, Verrill, and Trempe 2006; Alazard-Dany et al. 2009; Nayak and Pintel 2007; Meier, Fraefel, and Seyffert 2020). Interestingly, during co-infection with adenoviruses, cellular DNA polymerase was shown to responsible for AAV genome replication, while the HSV-1 DNA polymerase performed this function in models using HSV as helper viruses for AAV replication, indicating distinct requirements in different helper systems (Ward et al. 2001; Alazard-Dany et al. 2009).

1.2.5 AAV cellular entry and transduction

Most of our current understanding of AAV biology, from cellular entry to transduction, comes from *in vitro* and *in vivo* studies of recombinant AAV (rAAV) vectors. The mechanisms of cellular entry by AAV remains poorly understood, however, it was shown to involve various negatively charged glycans as primary receptors for initial cell-surface attachment, and subsequently engaging with a wide range of cell receptor molecules for internalisation into the cytoplasm (Mietzsch, Broecker, et al. 2014; Shen et al. 2012). AAV2 displays a broad range of tropism and was identified to use heparan sulfate proteoglycans (HSPG) for cell attachment. Co-receptors shown to facilitate AAV2 entry include human fibroblast growth factor receptor 1 (FGFR1), hepatocyte growth factor receptor (c-MET), laminin receptor (LamR), and αVβ5/α5β1 integrin (Summerford and Samulski 1998; O'Donnell, Taylor, and Chapman 2009). In contrast, the most divergent natural serotype, AAV5, was shown to use α2–3 N-linked sialic acid and platelet-derived growth factor receptor (PDGFR) for cell entry (Di Pasquale et al. 2003; Wu et al. 2006). Receptor usage by other AAV serotypes is less well characterised, including serotypes AAV7, AAVrh10, AAV11, and AAV12 where the receptor/co-receptor(s) have not been identified, and it is thought that the unique tropisms observed from different serotypes arise from the combination of different glycans and co-receptor affinity to the virus capsid (Pillay and Carette 2017; Madigan and Asokan 2016). More recently, a universal receptor was identified by genetic screening, entitled AAV receptor (AAVR), which facilitated AAV infection from all serotypes assessed, except for AAV4 and related variants, and was confirmed to be significant in *in vivo* mice models (Pillay et al. 2016; Dudek et al. 2018).

After initial cell attachment, AAV is internalised by endocytosis and this may involve multiple pathways. Early studies showed that internalisation of rAAV vectors occurs through clathrin-mediated endocytosis (CME). In these studies, expression of a dominant-negative mutant of

dynamin, a membrane fission protein essential for CME, was sufficient to inhibit rAAV transduction (Duan et al. 1999; Bartlett, Wilcher, and Samulski 2000). However, clathrin-independent endocytosis, micropinocytosis, and transcytosis have all been shown to contribute towards AAV internalisation (Nonnenmacher and Weber 2011; Di Pasquale and Chiorini 2006; Weinberg et al. 2014). Post-entry virions are directed towards 'infectious competent' pathways (eventual trafficking to the cell's nucleus) or 'non-infectious' pathways that can result in sequestration and degradation of virions (Nonnenmacher and Weber 2012). This post-entry fate of AAV particles is likely dependent on serotype and cell target, as cell lines NIH3T3, HeLa, and HEK293s are comparably efficient at internalisation of rAAV2 vectors, but intracellular trafficking and transduction in NIH3T3 cells were shown to be impaired (Hansen et al. 2000).

Once internalised, AAV undergoes endosomal trafficking along microtubules towards the trans-Golgi network. Mechanisms of cytoplasmic escape of AAV from the Golgi apparatus or endoplasmic reticulum remain unclear, but maybe pH-dependent as acidification within the endocytic compartments was shown to be important for transduction using different AAV serotypes (Nonnenmacher and Weber 2012; Douar et al. 2001). Evidence suggests that endosomal processing induces a conformational change within the virus capsid to expose the N-terminal domain of VP1 and/or VP2 required for cytoplasmic release. In support, the VP1 subunit of AAV2 was shown to harbour a hidden phospholipase A2 domain important for transduction, and mutations within this domain result in virion accumulation in the Golgi compartment (Johnson et al. 2010). However, exposure of AAV2 to low pH *in vitro* was unable to induce conformational changes and externalisation of the VP1/2 N-termini from the capsid, indicating the presence of further processing requirements within the endocytic compartments (Kronenberg et al. 2005). Importantly, viral processing within different endosomal compartments appears to be a prerequisite for nuclear entry and transduction as

AAV2 particles directly introduced into the cytoplasm by microinjection, thereby bypassing the normal entry route, failed to accumulate in the cell's nucleus. In this same study, direct injection of intact viruses to the nucleus also resulted in relatively low transduction levels (Sonntag et al. 2006).

Nuclear entry of AAV remains poorly understood, however, immunofluorescence imaging have shown accumulation of intact virions in the nucleus, and isolation of infectious virions from the nuclei of infected cells suggests that intact AAV particles are directly translocated across the nuclear membrane (Johnson and Samulski 2009). Within the nucleus, the efficiency of AAV uncoating and genome release appears to be serotype- and cell-dependent as internalisation and nuclear trafficking of rAAV2, 6 and 8 vectors were comparable in hepatocytes, but AAV2 displayed significant time delay for genome release and transduction (Thomas et al. 2004). Once released from the capsid, the AAV genome is converted to double-stranded DNA, which occurs either by annealing of the plus and minus single-stranded virus genomes (if a cell was infected by multiple AAV) or *de novo* second-strand DNA synthesis initiated at the 3' end of the ITR hairpin structure, which serves as a primer for DNA replication. From recombination of ITR sequences, the double-stranded AAV genome may persist as circular and linear concatamers if cell division is not ongoing (Xiao, Li, and Samulski 1996; Schnepp et al. 2003).

1.2.6 AAV genome replication cycle

The accepted model for AAV genome replication involves a self-primer and strand-displacement mechanism, and is shown in **Figure 1.2** (Goncalves 2005; Nash et al. 2007). Several cellular proteins were identified previously to be important for AAV genome replication, including DNA polymerase δ, minichromosome maintenance complex, replication

factors A & C, and proliferating cell nuclear antigen (Ni et al. 1998; Nash, Chen, and Muzyczka 2008). AAV replication is initiated at the 3’ end of the ITR hairpin by a DNA polymerase, and DNA synthesis extends to convert the single-stranded genome into a double-stranded molecule (a duplex monomer consisting of one genome sequence). Here, one end of the hairpin is covalently closed and resolved by Rep endonuclease activity to induce DNA nicking at the terminal resolution site, within the ITR of the parental strand. As a result, DNA synthesis processes from the newly generated 3' hydroxyl groups of the parental strand, with unwinding and copying of the opposing ITR template. Hairpin structures are formed at the terminal end of each strand of the linear duplex molecule. Subsequently, DNA synthesis processes from the free 3' hydroxyl groups for the displacement of the two strands, resulting in the formation of a single-stranded genome and a duplex monomer. Alternative intermediates are formed if Rep fails at nicking of the TRS. In this scenario, DNA synthesis can proceed through a closed hairpin to generate a duplex dimer molecule consisting of two double-stranded genomes, in a head-to-head or head-to-tail configuration. These duplex dimer molecules can be resolved to monomers through the ITR sequences by Rep (Cervelli, Backovic, and Galli 2011; Ward, Elias, and Linden 2003; Goncalves 2005).

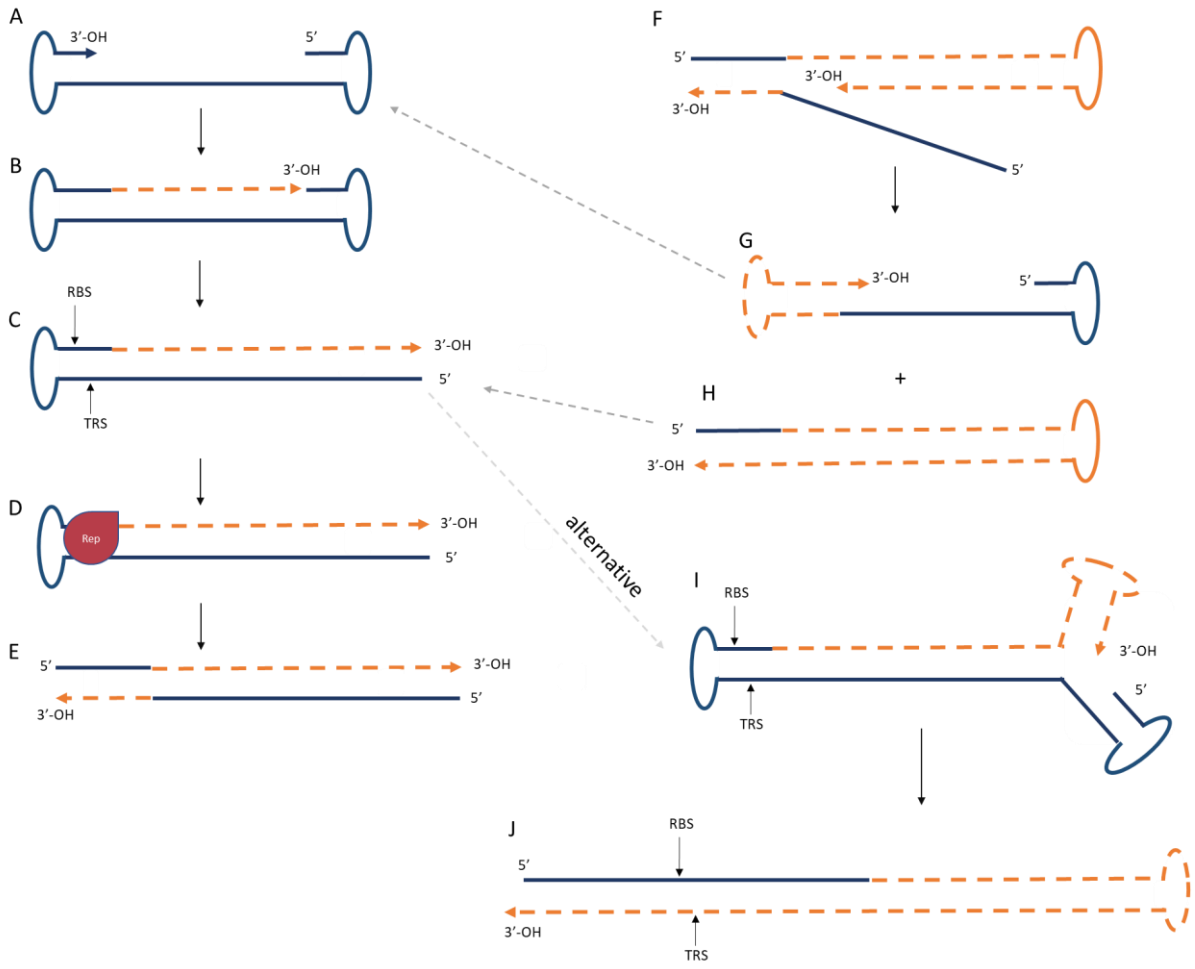


Figure 1.2 – Diagram schematic of the AAV genome replication model. **A**) Single-stranded AAV genome containing a 3' hydroxyl groups (-OH). **B**) Replication is initiated at the 3’ end of the ITR. **C**) Synthesis extends to convert the single-stranded genome into a double-stranded molecule. **D**) Rep endonuclease activity induce nicking at the TRS of the parental strand. **E**) DNA synthesis processes from the newly generated 3’-OH with unwinding and copying of the opposing ITR template. **F**) Hairpin structures are formed at the terminal end of each strand of the linear duplex molecule. DNA synthesis proceeds for the displacement of the two strands to generate a (**G**) single-stranded genome and a (**H**) duplex monomer. **I**) Alternative, if Rep fails at nicking of the TRS at (**C**) DNA synthesis can proceed through a closed hairpin to generate a (**J**) duplex dimer molecule consisting of two double-stranded genomes. These duplex dimer molecules can be resolved to monomers through the ITR sequences by Rep.

1.2.7 Vectorization of AAV

AAV is in many ways an ideal vector for transgene delivery for research and gene therapy purposes. These characteristics include its non-autonomous replicative capacity, low toxicity, and its ability to transduce a wide range of cell targets for sustained transgene expression.

Genetic manipulation of the AAV genome first occurred in the early 1980s. In pioneering work from Samulski et al. and Laughlin et al., the entirety of the AAV2 genome was inserted into a DNA plasmid and shown to be capable of producing AAV when transfected into mammalian cells that were infected with a helper adenovirus (Samulski et al. 1982; Laughlin et al. 1983). In early attempts to vectorize AAV for gene transfer purposes, the cap gene was replaced with the desired transgene sequence, with the rep gene intact, and rAAV vectors were generated by *trans*-complementation to provide the missing cap genes. As the Cap proteins were generally provided from a wildtype (wt) AAV, or one that had been genetically modified to reduce encapsidation, significant levels of wt AAV contaminations were detected due to unwanted packaging of the wt AAV genome (Hermonat and Muzyczka 1984; Tratschin et al. 1984; Tratschin et al. 1985).

Eventually, it was shown that only the 145-nucleotide viral ITR sequences were required *in cis* for replication of AAV, and the viral genes can be exchanged in place of a transgene sequence. The packaging capacity of AAV is limited to ~4.7kb due to the size limit of the virus capsid. In these early experiments, rAAV vectors were generated by supplying the rep and cap genes *in trans* by plasmid transfection and infection with wt adenovirus as a helper. By inactivation of the helper adenovirus contaminant with heat-treatment, rAAV vectors were shown to be capable of gene transfer and the rAAV genome persisted episomally in cells (Lebkowski et al. 1988; Samulski, Chang, and Shenk 1989). In subsequent iterations of this approach, the use of wt adenoviruses was replaced with an E1/E3-deleted adenovirus (E1/E3Δ-Ad) vector to

alleviate safety concerns with using replicating wt adenoviruses. To accommodate this change, rAAV production was also transitioned to HEK293-based cell lines to provide adenovirus E1 proteins required for inducing AAV replication *in trans* (Zhang et al. 2009). Alongside, HeLa-based stable packaging and producer cell lines were also being developed and pursued for efficient AAV production. These cells are stably integrated with the AAV rep and cap genes, with or without additional integration of the recombinant vector genome. AAV production is induced by infection with wt adenovirus for delivery of helper functions and p5 transcription of the integrated rep. However, a significant disadvantage shared amongst these approaches is the concomitant production of adenovirus contaminants alongside AAV vectors (Clark et al. 1995; Tamayose, Hirai, and Shimada 1996).

1.2.8 Development of the helper-free method

Early work had defined the minimal set of adenovirus genes required for helper functions for AAV replication. In the late 1990s, the widely utilise helper-free method was developed with subcloning of the helper genes VA RNA, E4orf6, and E2A, into a DNA plasmid to allow complete contaminant-free production of AAV vectors (Xiao, Li, and Samulski 1998; Matsushita et al. 1998). AAV production requires transfection of three plasmids, containing the following components – (i) AAV transfer genome encoding the gene of interest (pAAV), (ii) the rep and cap genes (pRepCap), and (iii) the adenovirus helper genes (pHelper), into HEK293-base cell lines to provide the E1 proteins. As variations of the helper-free system, construction of a single plasmid encoding the AAV rep and cap, and the adenovirus helper genes was explored and shown to improve vector yields (Grimm, Kay, and Kleinschmidt 2003). Interestingly, while the minimum set of helper genes (E1, VA RNA, E4orf6, and E2A) were required for optimal AAV

replication from the standard rep cap plasmid with its native promoters, expression of the rep and cap from heterologous promoters using a mouse metallothionine 1 promoter and CMV, respectively, was shown to only require E4Orf6 in HEK293 cells for producing AAV vectors (Allen, Halbert, and Miller 2000). Early studies indicated that downregulation of Rep78 protein and expression of Cap from a strong CMV promoter increased AAV production. Vincent et al showed that overexpression of Rep78/68 using an RSV promoter resulted in reduced expression of Cap protein. It was suggested by the authors, and indirectly shown, that high Rep78 levels induced translational repression of cap mRNAs (Vincent, Piraino, and Wadsworth 1997). Similar observations were reported by Li et al and further demonstrated by downregulating Rep78/68 expression using an ACG alternative start codon to achieve a 10-fold increase in AAV titre (Li, Samulski, and Xiao 1997). Furthermore, increases in AAV vector production by a factor of 10 was also reported from reducing Rep78/68 expression using an LTR promoter from the mouse mammary tumour virus (MMTV). While Rep 78/68 is required for efficient transcription of cap mRNA from the p40 promoter, these studies suggest tight regulation of its levels is important to achieve optimal AAV yields (Grimm et al. 1998). More recently, segregation of the rep and cap into two plasmids were shown to improve the titre of intact AAV vectors by 12-fold with a 5-fold increase in transduction. In this configuration, expression of Rep78 was ablated, and Rep coding was split into two expression cassettes, one expressing Rep68 and the other expressing Rep52/40. Additionally, the Cap coding sequences were expressed from a separate plasmid using its native p40 promoter. Increased productivity from this segregated plasmid system was shown to be correlated with increased expression of Cap and Rep68 (Emmerling et al. 2016).

With the discovery and isolation of new AAV serotypes from many animal species including non-human primates, humans and canines, vectorization of these serotypes quickly emerged. Initially, serotype-specific vectors, including AAV3, AAV4, AAV5, and AAV6, were engineered

by subcloning of the AAV genome into plasmid DNA and, subsequently, exchange of the rep and cap genes with the transgene of interest. The rep and cap genes from these serotypes were also subcloned into plasmids for complementing vector production *in trans* (Rutledge, Halbert, and Russell 1998; Chiorini et al. 1997; Chiorini et al. 1999). However, it was soon realised that only the cap ORFs of different AAV serotypes were required and different vector serotypes can be generated by complementing with ITRs and rep from AAV2. This pseudotyping strategy, wherein recombinant genome ITRs and rep are AAV2-based, was rapidly adopted for simplicity reasons as it follows the same production approach as the well characterised AAV2 vectors. This approach is now used almost exclusively for production of all AAV serotypes (Gao, Alvira, et al. 2002; Rabinowitz et al. 2002).

Dependent upon the AAV vector serotype and efficiency of transduction, production of progeny virions was shown to range from tens to several thousand of intact particles per transduction event (Rodriguez-Estevez, Asokan, and Borras 2020). In probing this variability it was estimated that only approximately 30% of AAV particles typically reach the nucleus after cellular uptake (Xiao et al. 2012). AAV transduction requires successful nuclear trafficking, uncoating and conversion of the single-stranded genomes to double-stranded sequences, which are essential for gene transcription. Conversion to a double-stranded genome may occur from stand annealing of the plus and minus ssAAV genome or ITR primed second-strand synthesis, and is thought to be a relatively slow and inefficient process. To eliminate this potentially rate-limiting step, self-complementing AAV (scAAV) genomes were constructed by deletion of the terminal resolution site (TRS) from one ITR sequence. Production of monomeric AAV genomes during replication requires efficient resolution of the two ITRs, following each round of DNA synthesis, by AAV Rep endonuclease activity. Dimeric or self-complementing AAV genomes are enriched by deletion of the TRS from one ITR sequence to prevent nicking by Rep. Following infection and uncoating, the scAAV genomes fold by intramolecular base pairing to

form double-stranded genomes. This approach was shown to increase transduction by over 140% and enabled more rapid transgene expression (McCarty 2008; McCarty, Monahan, and Samulski 2001).

1.2.9 Manufacture of rAAV vectors

As previously mentioned, AAV vectors were initially produced by transfection of plasmids encoding the ITR transfer vector, rep and cap sequences into mammalian cells, followed by infection with helper adenoviruses. This process yielded both AAV vector stocks and contaminating adenoviruses. The development of plasmids encoding the adenovirus helper functions overcame this problem and enabled production of adenovirus-free AAV stocks when co-transfected with plasmids encoding the AAV genome, and rep and cap. While this helper-free system remains the most widely used approach for AAV production for research, a major limitation is the difficulty to up-scale production at an industrial level required for widespread clinical applications due to its dependency on DNA transfection (Merten, Geny-Fiamma, and Douar 2005). More recently, attempts to up-scale production of AAV vector for pre-clinical use have expanded to evaluation of suspension-adapted HEK293 cells, but production per cell is generally lower compared to their adherent counterparts (Grieger, Soltys, and Samulski 2016; Blessing, Deglon, and Schneider 2018). For manufacture of clinical-grade AAV vectors, GMP (good manufacturing practice) certification is required from each component including the DNA plasmids, transfection reagents and the producer cell line, significantly increasing manufacturing costs (Clement and Grieger 2016). To overcome these limitations, various rAAV production systems have been explored, including baculovirus expression systems, herpesviruses complementation systems, and the generation of stable AAV packaging/producer cell lines (Penaud-Budloo et al. 2018).

1.2.9.1 Insect cells - baculoviral expression systems

Production of AAV vectors using baculovirus was first demonstrated by Sollerbrant and colleagues (Sollerbrant et al. 2001). Here, a three-virus vector system was adopted that employed two recombinant baculoviruses, encoding rep and the AAV transfer vector, respectively, and a third E1/E3-deleted adenovirus vector to introduce the cap genes for AAV production in HEK293 cells. Soon after, insect Sf9 cells were shown to be capable of producing rAAV vectors using a three baculoviral vector system, encoding the AAV rep, cap and the ITR transfer genome components (Urabe, Ding, and Kotin 2002). In subsequent iterations to simplify the process, a two baculovirus vector approach was adopted to allow expression of the rep and cap genes from one baculovirus vector, and the ITR transfer genome is encoded within the second baculovirus. However, significant genetic instability was observed in baculoviruses encoding the AAV rep and cap genes after a few serial passages. More recently, stable Sf9 insect cell lines expressing Rep and Cap proteins have also been developed requiring infection with one baculovirus encoding the ITR transfer genome to enable produce AAV vectors (Mietzsch, Grasse, et al. 2014). While initially cumbersome, the baculovirus-Sf9 platform represents a common alternative, and high-yielding, approach for manufacturing AAV vectors in non-mammalian cells, and with GMP-compliant platforms already established (Kotin and Snyder 2017). Major challenges that limit wide-spread utility of the baculovirus-Sf9 include reduced potency of baculovirus-derived AAV vectors compared to HEK293-derived counterparts, and detailed characterisation of contaminants in baculoviral-derived AAV particles (such as nucleic acid impurities, proteins and baculovirus contaminants) (Mietzsch et al. 2017; Bulcha et al. 2021).

1.2.9.2 Herpesvirus complementation systems

Although less common than the baculovirus-Sf9 platform, use of recombinant HSV-1 vectors has also been explored for production of AAV vectors. Early studies confirmed the potential use of HSV as helper viruses for facilitating AAV replication, and the HSV-derived helper genes were designated UL5, UL8, UL52, which codes for the HSV helicase-primase complex and the UL29 DNA-binding protein (Weindler and Heilbronn 1991).

Conway et al initially developed a none-replicating ICP27-deleted HSV-1 vector encoding the AAV rep and cap genes, and assessed production of AAV vectors in HEK293 cells via transfection of the ITR transfer plasmid or cell lines with stable integration of the ITR genome (Conway et al. 1999). As the ICP27-deleted strains were propagated in ICP27-expressing Vero cells, they were unable to replicate in HEK293 cells and reducing vector contaminations during the AAV production process. Subsequently, two recombinant rHSV-1 vector systems (non-replicating, ICP27-deleted) were developed wherein the AAV rep and cap genes, and the ITR transfer genome are encoded between the two rHSV-1 vectors (Booth et al. 2004). While the yield of AAV vector serotypes 1, 2 and 9 generated from this approach was reported to be comparable to the helper-free system, these results were not recapitulated for production of AAV5 (Kang et al. 2009; Wustner et al. 2002). Use of replication competent HSV-1 has also been explored, but was shown to be less efficient at producing AAV vectors than ICP27-deleted HSV-1 vectors. While the HSV-1 platform offers scalability by bypassing requirements for plasmid transfection, further characterisation and removal of HSV-1 derived contaminants are required for clinical application (de Oliveira and Fraefel 2010; Penaud-Budloo et al. 2018).

1.2.9.3 Stable mammalian packaging/producer cells

In the stable AAV packaging/producer cell line approach, rep and cap genes (devoid of viral ITRs) are integrated into the cell's chromosome, usually A549- or Hela-based cell lines (Farson et al. 2004; Liu, Clark, and Johnson 1999). The ITR transfer genome may be introduced into the system by additional integration into the cell's chromosome or via infectious with an adenovirus vector encoding the recombinant AAV genome. Production of AAV vectors is achieved by infection with a wt adenovirus to provide helper functions, such as the E1A protein to induce AAV gene expression from the cells. Interestingly, upon infection with the wt adenovirus, the integrated rep and cap genes undergo exponential DNA amplification, with levels reported ranging from 100-1000 copies per cell (Tessier et al. 2001; Chadeuf et al. 2000). While the mechanisms and factors responsible for this amplification process remain unclear, it is essential for production of high titre AAV vectors. As previously discussed, this approach offers several advantages that include scalability to bioreactor sizes and GMP certification of a single master cell bank. However, the major disadvantages include requirement to establish a new producer/packaging cell line for each desired capsid serotype and ITR-genome transgene sequence, the concurrent production of both helper adenovirus and AAV vectors, and intricate purification procedures to remove the contaminant adenovirus.

1.3 Adenovirus

1.3.1 Adenovirus classification

Adenoviruses are members of the large adenoviridae family, found abundantly in vertebrates that include fish, reptiles, amphibia, birds and mammals. The genus Mastadenovirus comprises adenoviruses that only infect mammalian species. Adenoviruses were initially classified by hemagglutination and neutralisation reactions in serum but more recent classification is based on genomic and bioinformatic analysis (Ghebremedhin 2014; Sarantis et al. 2004). To date, about 110 human adenoviruses have been identified and are grouped into seven species (denoted by a letter of A - G) accordingly to types and genotypes, and recognised in the database of the International Committee on Taxonomy of Viruses (http://ictv.global/virusTaxonomy.asp)(Greber 2020).

Since their first isolation for human adenoids in the early 1950s, adenoviruses have been studied extensively as a model system in fundamental eukaryotic cellular process, such as apoptosis and gene expression (Rowe et al. 1953; Lion 2014; Logan and Shenk 1982; Nemerow and Flint 2019). Adenovirus research has also yielded landmark discoveries that include mRNA splicing and DNA replication with reconstituted components (Stillman 1983; Berk 2016). As a result, our in-depth understanding of adenovirus biology has enabled its widespread utilisation from an efficient vector tool for gene delivery in basic research, to the field of gene therapy, oncolytic viral therapy, and virally vectored vaccination (Wold and Toth 2013).

In general, adenovirus infections can result in self-limiting respiratory (group B, -C, -E), ocular (group C, -D), urinary tract (group B) and gastrointestinal infections (group A, -F, -G). However, diseases can be particularly severe in individuals who are immune compromised. As infections can be highly contagious, local epidemic outbreaks have been documented to occur with

profound consequences (Lynch and Kajon 2016; Lion 2014). While there are no specific therapies for adenovirus infections, live vaccines against adenovirus type 4 and 7, most often associated with acute respiratory disease, are available to personnel in the US military. Although this vaccine uses live virus and can be transmissible to other individuals, phase 1 and 3 clinical studies with military recruits showed that it was safe with adverse effects comparable to the placebo control group (Choudhry et al. 2016; Gaydos and Gaydos 1995). Immunity to some adenovirus serotypes are widespread within the population. Specifically, dependent on the geographical location, around 80 - 100% of the population was shown have seroreactive antibodies against adenovirus type 5 (Pilankatta et al. 2010; Sun et al. 2011).

1.3.2 Adenovirus structure

Adenoviruses are non-enveloped icosahedral virus of approximately 90nm in diameter. Hexon is the most abundant adenovirus structural protein and contributes ~80% of the capsid mass (Rux and Burnett 2004). The capsid polyhedron structure is composed of 252 capsomeres. This includes twelve copies of assembled hexon trimers that form each of the twenty faces of the polyhedron. At each of the twelve vertices the penton base forms pentamers and each can be anchored by non-covalent interactions with one or more copy of the trimeric fiber spike of 9-77.5 nm in length (Hess et al. 1995; Penzes et al. 2014; San Martin 2012). As shown in **Figure 1.3**, adenovirus hexon, penton and fibre form the major capsid proteins, and the minor capsid proteins (IIIa, VI, VIII, and IX) functions to maintains particle stability, and are important for intracellular trafficking and post-entry capsid disassembly. While their arrangements are still unclear, the adenovirus particle also contain core proteins V, VII, X, IVa2, viral protease, and the ITR-associated terminal proteins (Reddy and Nemerow 2014; Mangel and San Martin

2014). These core proteins primarily function to condense viral genomic DNA in clusters to facilitate encapsidation within the size-constrained particle and to modulate viral genome release (Martin-Gonzalez et al. 2019). Dependent on the encapsidated DNA genome and processing events by viral protease, virions can be produced in four different forms. Empty capsids are the lightest particles as they do not contain a copy of the virus genome. Alternatively, encapsidation of the left portion (containing the virus packaging signal element) produces light intermediate virions while heavy intermediate are immature virions containing the full virus genome with capsid proteins unprocessed by the viral protease. Mature virions are infectious particles that are proteolytically processed and contain the full adenovirus genome (Perez-Berna et al. 2009; Ostapchuk and Hearing 2005; Condezo et al. 2015).

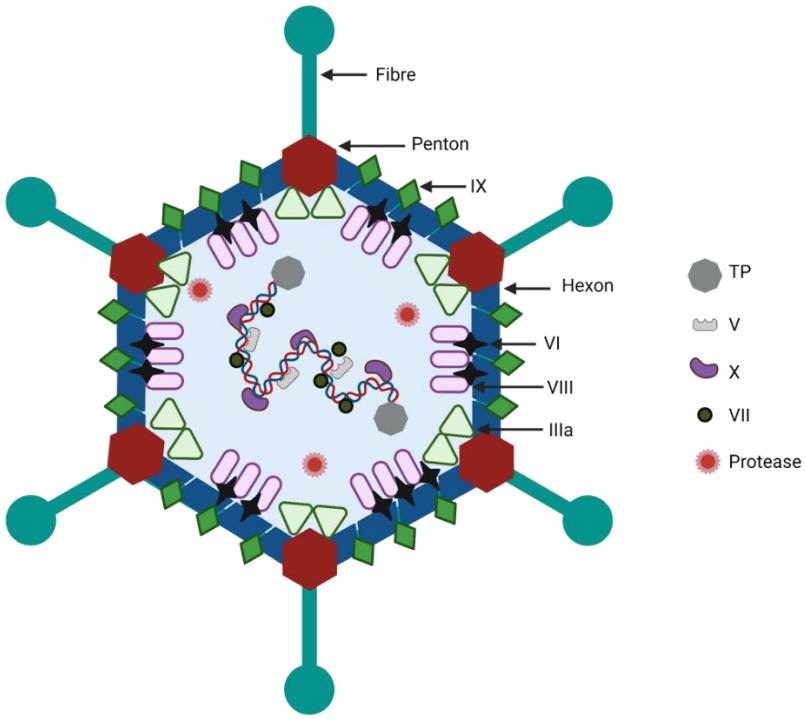


Figure 1.3 – Schematic representation of a cross-section of an adenovirus particle. The structural capsid proteins (Fibre, Penton, Hexon, IIIa, VI, VIII, and IX) and core proteins (TP, V, X, VII, and protease) are shown. Diagram created using Biorender, not drawn to scale.

1.3.3 Adenovirus attachment and entry

Cell receptors and attachment factors used by adenovirus for cell entry varies depending on the serotype. Adenoviruses with respiratory, ocular, and gastrointestinal tropisms, including the group C adenovirus serotype 5, uses the cell surface coxsackie and adenovirus receptor (CAR) for primary attachment (**Figure 1.4**) (Zhang and Bergelson 2005). As CAR is commonly expressed at tight junctions and adherens junctions of epithelia cells, strong attachments are formed by binding of CAR with the fibre knob domain to enable docking of virion to the cell surface (Cohen et al. 2001; Houri, Huang, and Nalbantoglu 2013). In contrast, CD46 was identified as the primary attachment receptor for group B adenoviruses, alongside desmoglein-2. Following this high-affinity binding, cell surface integrins (αVβ3 & αVβ5) interact with the penton base located at the vertices of the capsid to facilitate uptake by clathrin and dynamin-mediated endocytosis (Lyle and McCormick 2010; Gaggar, Shayakhmetov, and Lieber 2003; Meier and Greber 2004). Within the endosomes, shedding of fibre protein and limited released of protein VI, a membrane lytic protein facilitates virion escape to the cytosol (Nakano et al. 2000; Wiethoff et al. 2005). After endosomal escape, virions are trafficked along microtubules via a dynein/dynactin-dependent mechanism and then dock at the nuclear pore complex. Uncoating of the capsid and disruption of the nuclear pore complex is mediated by kinesin-1 motor protein to allow nuclear entry of viral genomes (Strunze et al. 2011).

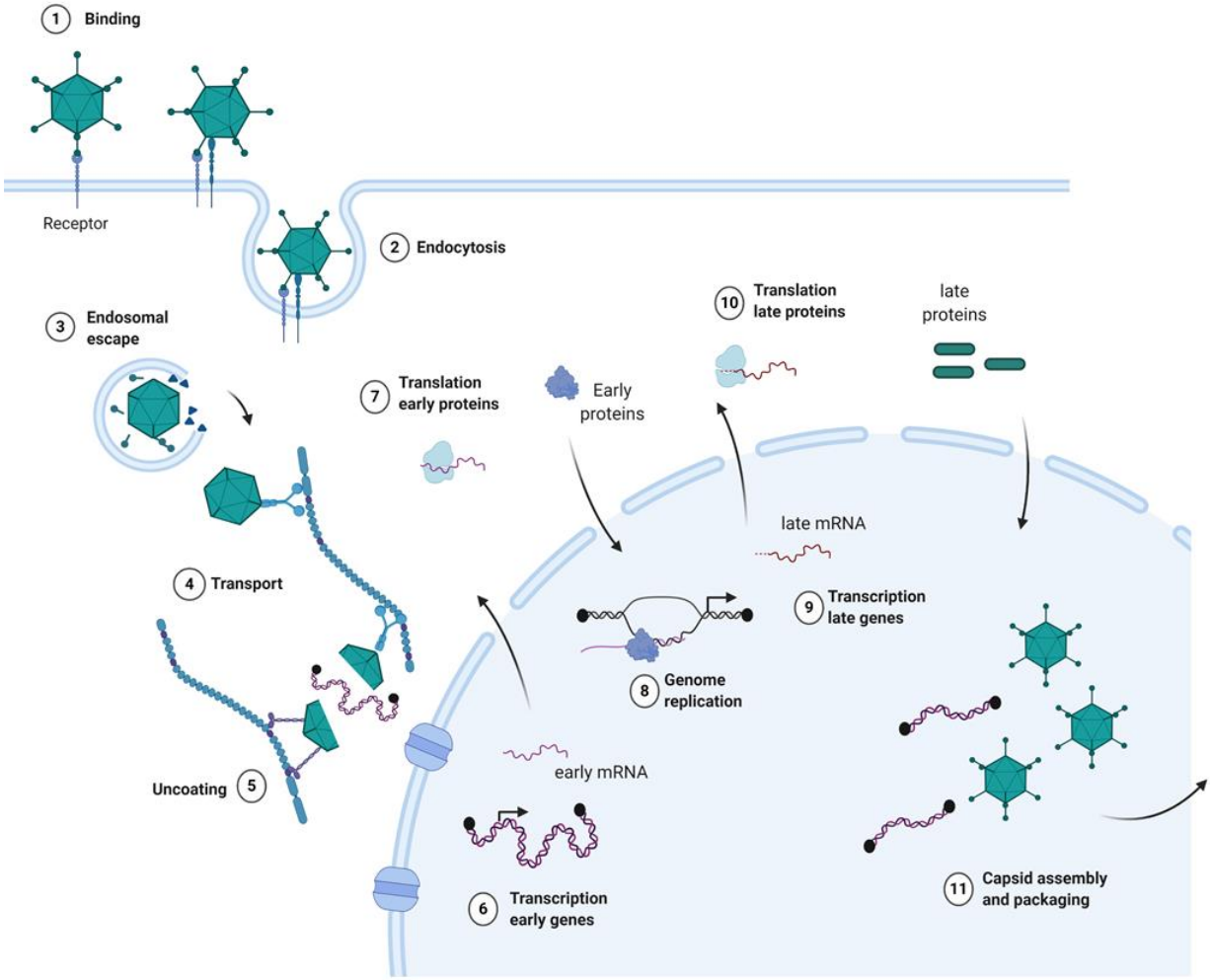


Figure 1.4 – Life cycle of the adenovirus. (1) Initial attachment is facilitated by interactions between the fibre protein and cell surface receptors. (2) Virus uptake by clathrin and dynamin-mediated endocytosis is mediated by interactions of penton base with cell surface integrins (αVβ3 & αVβ5). (3) Within the endosomes, shedding of fibre protein and limited released of protein VI promotes virion escape to the cytosol virions are trafficked (4) towards the nucleus and docking at nuclear pore complex via microtubules network and Dynein dependent mechanism. (5) Uncoating of capsid and disruption of nuclear pore complex is mediated by kinesin-1 motor protein to allow nuclear entry of viral genomes. (6) Transcription and translation (7) early viral genes, which functions to inhibit apoptosis, transition of the cell cycle to S phase, and promote (8) viral genome replication. (9) Transcription of late vial genes by the MLP to produce viral structural and non-structural proteins (10), which are trafficked back into the nucleus for capsid assembly and genome encapsidation (11). Diagram created using Biorender, not drawn to scale.

1.3.4 Adenovirus genome organisation

Of the human adenovirus species, serotype five is most extensively studied and contributes significantly to our understanding of virus biology and virus-cell interactions. The adenovirus genome is a linear double-stranded DNA genome of about 36 kb and flanked by ~100 bp inverted terminal repeats sequences (ITR) that contain the origins of viral DNA replication (**Figure 1.5**). Terminal proteins (pTP) are covalent attached at the 5' end of each ITR sequences and are essential for initiating virus DNA replication (Mei et al. 2003; Pronk and van der Vliet 1993). The adenovirus genome is efficiently organised to maximise coding potential by utilising a strategy of overlapping ORFs and encoding of transcriptional units on both strands of the DNA. The genome encodes over 40 proteins that are sequentially and temporally expressed to meet requirements at different phases of the virus replication cycle (Reddy et al. 1998; Saha, Wong, and Parks 2014). Specifically, adenovirus genes are divided into early or late genes depending on the timing of initiation of transcription, that is prior or post DNA replication of the virus genome, respectively. The genome encodes five early transcription units (designated E1A, E1B, E2, E3 and E4) and one late transcription unit that is subdivided into L1 to L5 (Fessler and Young 1998). The intermediate-expressed proteins (IX and IVa2), are expressed after initiation of viral DNA replication (Vales and Darnell 1989; Pardo-Mateos and Young 2004). E1A is the first gene to be expressed after infection, and its mRNA transcripts are alternatively spliced to produce five different proteins (289R, 243R, 217R, 171R, 55R). The E1A proteins function to enable transcription of other early viral genes and to facilitate efficient viral DNA replication by inducing transition to the S phase of the cell cycle (Gallimore and Turnell 2001; Radko et al. 2015). The E1B transcription unit is detected shortly after E1A and it produces two principal proteins, E1B-19K and E1B-55K, that blocks E1A induced-apoptosis. The E2 region encodes proteins to direct DNA replication of the virus genome, such as the virus DNA

polymerase (E2B) (Hidalgo et al. 2019; Swaminathan and Thimmapaya 1995). While proteins from the E3 units modulate immune responses and are dispensable in adenoviral vectors, E4 encodes proteins that are multifunctional and important for regulating transcription, the cell-cycle, cell signalling and DNA repair (Lichtenstein et al. 2004; Evans and Hearing 2003; Reichel et al. 1989). At late stage of infection, the virus structural proteins encoded within L1-L5 are transcribed from the major late promoter (Farley, Brown, and Leppard 2004; Young 2003). Adenovirus derived VA RNA and VA RNAII are important non-coding RNA products that are expressed in the late phase of the virus replication cycle and modulate a range of functions that include regulating translation of late viral genes, antagonising host interferon responses, and interfering with cellular micro (mi)RNA processes (Ma and Mathews 1996; Vachon and Conn 2016).

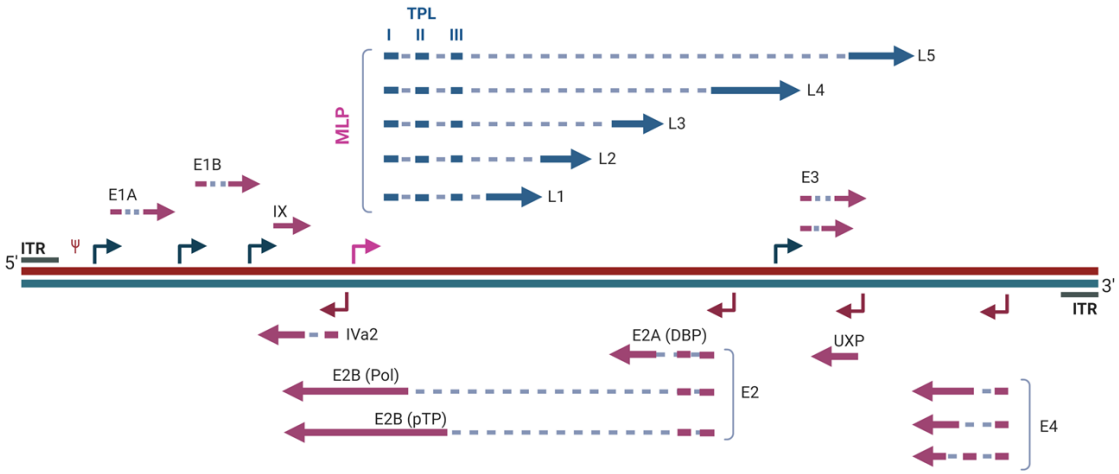


Figure 1.5 - Organisation of the adenovirus genome. The left and right ITRs are indicated at either ends of the virus genome. Transcripts are indicated by solid lines. Introns are indicated by broken lines. Early/intermediate viral genes (E1, E2, E3 and E4) expressed from their respective promoters are indicated by purple lines. Late viral mRNAs (L1-L5) expressed from the MLP are indicated by blue lines. Diagram created using Biorender, not drawn to scale.

1.3.5 Adenovirus genome replication

Adenovirus replication occurs in the nucleus and virions are released by cell lysis (Jiang et al. 2011). *In vitro* reconstitution of the adenovirus DNA replication system showed a requirement for three viral-derived proteins encoded within the E2 transcription unit, namely precursor terminal protein (pTP), DNA polymerase (Ad pol), and the DNA binding protein (DBP). The Ad pol harbours both DNA polymerase and 3'-5' exonuclease proofreading activity and forms heterodimers with the pTP in early viral infection (van der Vliet, van Dam, and Kwant 1984; Enomoto et al. 1981). The abundantly expressed DBP (~ $1x10^7$ copies per cell) binds to ssDNA and dsDNA, and is essential for elongation of the replicating genome (Chang and Shenk 1990; Caravokyri and Leppard 1996). Two cellular transcription factors, nuclear factor I (NFI) and nuclear factor III (Oct-1) were also shown to be required for viral DNA replication (Mul, Verrijzer, and van der Vliet 1990).

Adenovirus DNA replication occurs via a mechanism of strand displacement and efficiently produces a large quantity of viral genomes, approximately $1x10^6$ genome copies per infected cell at 40 hours. Replication fidelity is governed by the DNA polymerase via its selectivity to incorporate correct bases and 3'-5' exonuclease proofreading activity to excise mistakenly incorporated nucleotides (Hoeben and Uil 2013). The adenovirus DNA polymerase was identified as a α-like, B-family of polymerases and contains a series of conserved motifs that are important for functions that include dNTP binding, DNA template binding, and polymerase activity. The DNA polymerase proofreading domain is located in the N-terminal peptide sequence and consists of three highly conserved Exo motifs (Exo I, II, and III) which are responsible for the 3'-5' exonuclease function. The C-terminal peptide sequence contains the conserved polymerase (Pol) motifs, consisting of seven domains (Pol I – Pol VII), that are components of the Pol catalytic site (Brenkman, Breure, and van der Vliet 2002). The intrinsic

proofreading ability of the Ad pol enables faithful replication with estimated spontaneous mutation rate of 1.3 x 10^{-7} per base per cell infection cycle (Liu, Naismith, and Hay 2000; Risso-Ballester, Cuevas, and Sanjuan 2016).

The virus origin of replication, consisting of a core region (1-18 bp) and auxiliary region (25-48 bp), is positioned at the terminal ends of each ITR sequence (Rawlins et al. 1984). The pre-initiation complex is formed by binding of NFI and Oct-1 to the auxiliary sequence, and facilitated by the DBP, to alter origin confirmation and recruit the pTP-Pol complex to the core region. Genome replication initiates by a protein primer mechanism with the covalent attachment of the pTP to the first nucleotide of the nascent strand by the virus polymerase (Hoeben and Uil 2013). In the case of group C adenoviruses, a dCMP nucleotide is attached to Serine 580 of the pTP by the Ad pol, followed by formation of a pTP-CAT trinucleotide intermediate. Initially, pTP-CAT intermediates pairs with the 3'-GTA-5' nucleotides at position 4 to 6 of the origin template, but slides back to a 3'-GTA-5' residue at nucleotides position 1 to 3 following a "jumping back" mechanism. Subsequently, Ad pol dissociates from the pTP for synthesis of the nascent strand, generating a new DNA duplex genome and displacing the existing strand. DPB facilitates to unwind of the dsDNA genome and oligomerises the displaced ssDNA as replication continues. Annealing of the two ITR sequences from the displaced strand results in the formation of new origins of replication that can enter in subsequent rounds of DNA replication along with the new DNA duplex genome (Mysiak et al. 2004; de Jong, van der Vliet, and Brenkman 2003).

1.3.6 Adenovirus major late promoter

In the late 1970s, genetics and biochemical analysis of the adenovirus MLP provided fundamental insights into the mechanisms of gene expression, from RNA transcription to splicing and nuclear export. These studies were pivotal in mapping canonical transcriptional activators and enhancer elements regulating gene control, and also isolation of transcription factors that bind to these DNA elements. As a result, the MLP is studied in-depth as a model for mammalian promoters (Young 2003; Lu et al. 1997).

The major late transcription unit (MLTU), encoding all but one of the adenovirus structural proteins and three non-structural polypeptides, is transcribed from the MLP (Donovan-Banfield et al. 2020). During early infection, the MLP is active at low levels, and transcription terminate at the L1 region to yield the L1 52/55K protein. The MLP is fully activated after DNA replication and transcription can proceed through the entire length (approximately 2.8kb) of the MLTU (Morris, Scott, and Leppard 2010). Processing of this large transcript by alternative splicing and usage of different polyadenylation sites results in the production of over 20 mature mRNAs that are grouped into five families L1 to L5, where each family shares a common polyadenylation sequence. In addition, each mature late viral mRNAs share a common 5' non-coding sequence of approximately 200 bp known as the tripartite leader sequence (TPL), consisting of leaders -1, 2 and 3. The TPL facilitates efficient production of late viral proteins by modulating nuclear export, mRNA stability and cap-independent translation (Young 2003; Ramke et al. 2017).

Proper functioning of the MLP is essential for completion of the adenovirus replication cycle. The transition of early-to-late phase of the virus life cycle coincides with decrease expression of early genes and full activation of the virus MLP to produce large quantities of late structural proteins. While the mechanism of MLP activation remains unclear, transcription is stimulated

by E1A 289R proteins and initiation, but not ongoing, of DNA replication of the adenovirus genome appears to be a prerequisite for full activation (Nevins 1981; Carter and Ginsberg 1976; Thomas and Mathews 1980).

Initiation of genome replication generally occurs 7 hours post-infection. Using genotype-distinguishable adenoviruses in co-infection experiments, Thomas and Matthew showed that superinfection of cells already in the late stage of adenovirus infection and therefore expressing MLP trans-activating factors, do not display late MLTU patterns from the super-infecting genomes unless they themselves had undergone DNA replication (Thomas and Mathews 1980). These observations suggest that a cis-acting change in the DNA template is required to facilitate late transcription from the MLP. It was suggested that the temporal control of late gene expression from the MLP allows accumulation of new genomes before large quantities of capsid proteins are made to ensure efficient assembly of virions.

Genetic analysis of the MLP showed a relatively simple core structure consisting of a consensus TATA box and an initiator element (Inr), and two *cis*-acting upstream elements, an inverted CAAT box and an upstream promoter element (UPE). As shown in **Figure 1.6**, directly flanking the MLP TATA box are unique GC-rich sequences at position -36 and -18 relative to the initiator site, that binds MAZ and SP1 transcription factors, respectively (Young 2003). In transient expression studies, MLP activity was increase up to 200-fold by interactions between E1A and the MAZ or Sp1 transcription factor (Parks and Shenk 1997). Furthermore, downstream of the Inr are enhancer elements (entitled DE1 and DE2b/a) which are recognised by viral-derived IVa2 and L4 22K proteins for stimulating late transcription from the MLP (Lan et al. 2017). As the L4-22K is expressed from the MLP at late stage of viral infection, it may provide a forward-feed mechanism to stimulate further MLP activity. Moreover, it was shown that the L4 22K protein also mediates a suppressive effect on both E1 and the MLP expression, with the latter

due to binding, at both DNA and single standard RNA level, to the R1 region within the first intron of the MLTU. Overall, these studies suggest that the L4-22K, essential in the packaging process, is also important for the transition from early-to-late phase of infection and may enable fine-tuning of transcription from the MLP (Wu, Orozco, and Hearing 2012; Lan et al. 2017).

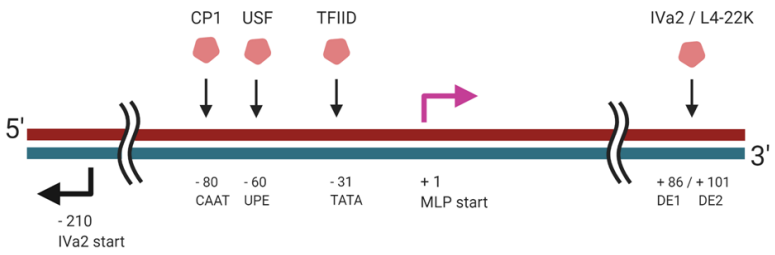


Figure 1.6 - Genetic structure of the MLP of group C adenoviruses. The MLP transcription start site (+1) is indicated by pink arrow. DNA sequence elements (CAAT, UPE, TATA, DE/DE2) and factors to which they bind are indicated. IVa2 transcriptional start site in the opposing DNA strand is indicated by a black arrow. Diagram created using Biorender, not drawn to scale.

1.3.7 Adenovirus tripartite leader

At the late phase, large quantities of adenovirus capsid proteins are efficiently produced from infected cells, comprising up to 40% of total cell protein. This prodigious productivity results from the significant increase in genome templates, late phase activity of the MLP and function of the 5' untranslated TPL in late viral transcripts (Schneider 1995).

The TPL sequence is present in all mature mRNAs derived from the MLP. It consists of three exon leaders 1, 2 and 3, that are processed by alternative splicing from a primary transcript of approximately 3.7 kb. The TPL is important to mediate late viral mRNA transport and accumulation in the cytoplasm and preferential mRNA translation by cap-independent mechanisms. At the late phase, nuclear export of cellular derived mRNAs is significantly

inhibited and late viral mRNAs are selectively exported, in a process involving the E1b-55K/E4 Orf6 complex. Additionally, efficient translation of late viral mRNA requires the MLP-derived L4 100K protein, which plays an important role in downregulating translation of cellular-derived mRNA (Logan and Shenk 1984; Berkner and Sharp 1985). Normally, translation of cellular mRNAs requires binding of the 5'm7GpppN (cap) structure to the cap-initiation complex eIF-4F (composed of cap-binding protein eIF4E, an ATP-dependent RNA helicase, eIF4A; and the scaffold protein eIF4G). Function of the cap-initiation complex eIF-4F is blocked by binding of the adenoviral 100K protein to the scaffold protein eIF4G, which results in displacement of protein kinase Mnk1 required for phosphorylation of eIF4E. In addition, binding of the TPL at the RNA-binding domain of the 100K protein, and subsequent interactions with the scaffold protein eIF4G enables ribosome shunting for efficient translation of late viral mRNAs (Adam and Dreyfuss 1987; Riley and Flint 1993; Xi, Cuesta, and Schneider 2005). It has been estimated that up to 90-95% of total mRNAs translated at this stage of the virus life cycle are late viral transcripts containing the tripartite leader sequence (Schneider 1995).

1.3.8 Adenovirus packaging

The adenovirus packaging sequence involved a series of seven functionally redundant A-repeats, referred as A1-A7, (TTTGN8CG) of approximately 200 bp and situated between the virus left ITR sequence and the E1 transcription unit. Packaging of the adenovirus genome occurs in a polar fashion and capsids containing only the left arm portion of the viral genome can be obtained. The packaging signal was shown to maintain efficient function only when positioned within 600bp of either the left or right ITR sequence. Although unclear, this observation may suggest involvement of the ITR sequence and terminal protein in the

packaging process (Hearing et al. 1987). While the mechanism of adenovirus packaging remains to be fully established, production of empty capsids from virally infected cells suggest a model of 'sequential assembly' to form infectious virions. In this model, particles are first assembled from hexon trimers and penton with incorporation of the minor and non-structural proteins. Subsequently, genome packaging occurs by a process of recognition of the virus packaging element by a packaging complex, that results in insertion of the DNA genome through a portal at an unidentified unique vertex of the capsid. Adenovirus proteins associated with the packaging signal include IVa2, L4 33K, L4 22K, L1 52/55K and IIIa (Ostapchuk and Hearing 2003; Ahi and Mittal 2016). The intermediate-expressed IVa2 protein is multifunctional and important in stimulating transcription of late viral genes and the genome encapsidation process. The current model of adenovirus packaging suggests IVa2 binds, in a co-dependent complex, with the L4 22K protein to the CG motif within the A repeats of the packaging sequence (Wu, Orozco, and Hearing 2012). This complex further recruits packaging associated proteins L1-52/55K and IIIa, which were shown to contribute to packaging of serotype-specific adenovirus genomes. IVa2 exhibits ATPase function and may serve as a motor protein, in the presence of adenovirus genome and L4 33K, for threading of the genome through the capsid portal (Ahi et al. 2015).

1.3.9 Adenovirus Vectorization

Adenovirus vectors, particularly based on serotype 5 (Ad5), has received tremendous attention over the past three decades as a vector for gene therapy, vaccines, oncolytic virotherapy and protein expression. They exhibit a range of desirable characteristic, including an in-depth characterisation of Ad5 biology, they can be economically produced and purified to a high titre (approximately 1×10^{12}- 1×10^{13} virus particles per mL). Additionally, they can infect a wide

variety of dividing or nondividing cells, and once inside the cell the adenovirus is one of the most effective method for gene delivery with approximately 80% of viral genome reaching the nucleus within 1-hour post infection (Leopold and Crystal 2007; Wold and Toth 2013).

In general, there are two groups of adenoviral vectors, replication-defective and replication-competent (including conditionally replicating) (Nemerow and Flint 2019). While replication-competent adenoviral vectors are mainly used for oncolytic cancer therapy, replication-defective vectors were initially generated for gene therapy and are usually deficient of the essential viral E1 genes (E1A and E1B) (Wold and Toth 2013). In addition, they are usually also deleted of the E3 genes, normally involved in immune modulation and dispensable for viral replication (Lee et al. 2017). These vectors constitute the first-generation E1/E3-deleted adenovirus vectors and can accommodate up to 8.2kb of exogenous DNA, generally inserted into the E1-deleted region of the vector. E1/E3-deleted vectors can be engineered from plasmid DNA that encodes the recombinant virus genome. They are initially recovered by transfection of the recombinant genome into 293-based cell line to provide the E1 genes *in trans*, and subsequently amplified further in these producer cells to high titre (Danthinne and Imperiale 2000).

As the first-generation E1/E3-deleted vectors elicit significant immune responses *in vivo* due to leaky expression of both early and late viral genes that resulted in immune-mediated clearance, second-generation and helper-dependent adenoviral vectors were developed (Lee et al. 2017). In the second-generation vectors, additional viral genes are deleted including the E2 and E4 transcription units, and they are produced in complementing cell lines that are engineered to produce the missing viral proteins *in trans*. While these vectors can accommodate a large payload of ~14kb and exhibit reduced immunogenicity *in vivo*, widespread utility is hindered by difficulty in production to high titre (Wang and Finer 1996).

Similarly, helper-dependent adenoviruses are vectors devoid of all viral genes with the exception of the cis-acting ITR sequences and virus packaging signal. These helper-dependent vectors are propagated in the presence of a 'helper' adenovirus to provide the early and late genes *in trans* to facilitate adenovirus replication. DNA recombinase systems, such as Cre-lox and FlP-FRT recombination, are typically used for removal of the packaging signal of the 'helper' virus genomes in attempts to eliminate encapsidation of the helper adenovirus. These vectors can accommodate up to 37 kb of exogenous DNA, but their production is laborious with significant contamination by the infectious 'helper' adenovirus, which has been reported to range from 0.1-10% of virus genomes (Alba, Bosch, and Chillon 2005; Sakhuja et al. 2003).

1.4 Inducible gene regulation systems

1.4.1 Tetracycline inducible systems

Temporal control of gene expression is fundamental and applicable to almost all aspects of research, including examination of gene and cellular functions, biologics discovery and production, and gene therapy. Numerous approaches have been developed to enable temporal control of gene expression and these can be divided into two classes – endogenous or exogenous control systems. Whereas the former requires environmental or physiological stimuli, such as hypoxia, interferons or metal ions, to regulate gene expression, exogenous control requires external factors, such as a drug molecule, to induce or switch-off gene expression (Naidoo and Young 2012; Ryals et al. 1985; Mayo, Warren, and Palmiter 1982).

The most widely explore exogenous gene control approach is the tetracycline regulated gene expression system developed from the Tn10-encoded tetracycline resistance operon in

Escherichia coli (E. coli) (Gossen and Bujard 1992). In bacteria, antibiotic resistance to tetracycline is mediated by the TetA protein, which functions as a tetracycline efflux pump located in the cytoplasmic membrane. The tetracycline regulated mechanism is highly evolved, both in sensitivity for detecting intracellular tetracycline and the control response in antibiotic clearance. As overexpression of TetA is lethal to the bacteria, its expression is tightly regulated at the transcription level by a repressor protein TetR. Binding of TetR to the tetracycline operator sites (tetO1 and tetO2) within the tet operon repress transcription of both both TetR and the TetA resistance gene. Influx of tetracycline results in high affinity binding to the TetR and its disassociation from the tetO sites, resulting in rapid expression of TetA and TetR to remove the intracellular tetracycline, and subsequent gene repression to avoid TetA-induced lethality (Ramos et al. 2005; Das, Tenenbaum, and Berkhout 2016).

There are three different variations to this TetR inducible system (**Figure 1.7**) - Tet-Off, Tet-On and the unmodified TetR system. The unmodified TetR represents the most basic configuration and consists of insertion of tetO sites in the target promoter. Transcriptional repression is mediated by the TetR which interferes with binding of transcription factors and RNA polymerase to the target promoter (Alba, Bosch, and Chillon 2005; Yao et al. 1998). Early studies by Gatz and Quail showed for the first-time repression of a eukaryotic plant promoter in tobacco protoplast using the TetR. Here, the target CaMV 35S promoter was modified with TetO sites flanking the TATA element (Gatz and Quail 1988). Repression of promoters utilising RNA polymerase I, II and III were subsequently demonstrated using the TetR, but highlighted significant variations in the positioning of TetO sites in these different models that was important for efficient gene regulation (Yan, Myler, and Stuart 2001; Frohberg, Heins, and Gatz 1991; Dingermann et al. 1992). In a common configuration to regulate gene expression in mammalian cells, two tetO sites are positioned at approximately 10 bp downstream of the CMV TATA box element to enable TetR-mediated transcriptional repression. Repression can be

alleviated by addition of tetracycline, to disrupt binding of the TetR to its operator elements (Wu et al. 2010; Yao et al. 1998).

In both Tet-Off and Tet-On approaches, tetO sequences (usually x7 copies, termed tetracycline responsive elements (TRE)) are positioned upstream of the minimal constitutive promoter of a gene target. In the Tet-Off configuration, a transactivator proteins (tTA), consisting of TetR fused to the VP16 transactivator domain from herpes simplex virus type 1 is introduced to enable automatic expression of the target gene. Addition of tetracycline to cell cultures binds and inhibits activity of the tTA to silence gene expression (Kim et al. 1995; Toniatti et al. 2004). Conversely, the Tet-on configuration utilises a mutant tTA, entitled reverse tTA (rtTA), that binds in the presence of tetracycline to the TetO elements within the target promoter to facilitate gene expression. In this configuration, the absence of tetracycline results in target gene repression (Ramos et al. 2005).

TetR inducible expression system offers many advantages as a gene control platform and are often explored in conjunction with viral vectors, such as adenoviruses, AAV and lentiviruses, for both fundamental research and gene therapy application (Goverdhana et al. 2005; Chen et al. 2015). Tetracycline and its analogue doxycycline are antibiotics that are well characterised with a high safety margin in both clinical and preclinical application (Moore, Ling, et al. 2015). However, a major concern of the TetR inducible system is a tendency for leaky gene expression. To improve upon this, attempts have included fusion of the TetR to the Krüppel-associated box (KRAB) repressor domain of human KOX1, use of a minimal promoter from the modified mouse mammary tumor virus (MMTV) for inducible transcription, codon optimisation of the rtTA and identification of novel rtTA by PCR mutagenesis or error-prone reverse transcription using RNA viruses (Deuschle, Meyer, and Thiesen 1995; Hofmann, Nolan, and Blau 1996; Wells et al. 1999; Zhou et al. 2006; Urlinger et al. 2000).

1.4.2 Cumate gene-switch systems

A number of other exogenous inducible systems have been explored in mammalian cells and include the cumate gene-switch system, rapamycin-regulated systems, and the TRiP translational repression system (Mullick et al. 2006; Maunder et al. 2017; Naidoo and Young 2012). Of these approaches, the cumate gene-switch is most analogous to the tet-inducible system, in which it was developed from a bacterial repressor, the *p-cmt* and *p-cym* operon in *Pseudomonas putida* (Eaton 1997). Further similarities to the TetR approach include the cumate gene-switch has three configurations where (I) the repressor protein CmyR can be used to block transcription of the target promoter by binding to operator sequences (CuO), or (II) a chimeric transactivator (cTA) composed of CymR fused to the VP16 activator domain can be used to induce transcription of a minimal promoter encoding six-copies of CuO upstream, or (III) a reverse transactivator (rcTA) can be used to facilitate transcription from the targeted CuOx6 minimal promoter. While activity of the cTA is inhibited with addition of the cumate drug, function of rcTA is activated by cumate. While the cumate gene-switch system shares some problems with the TetR-inducible approach, such as its propensity to repress highly active promoters, such as CMV, or leaky expression from minimal promotors, it provides a useful alternative in biological systems requiring simultaneous temporal control of multiple transcription units (Mullick et al. 2006).

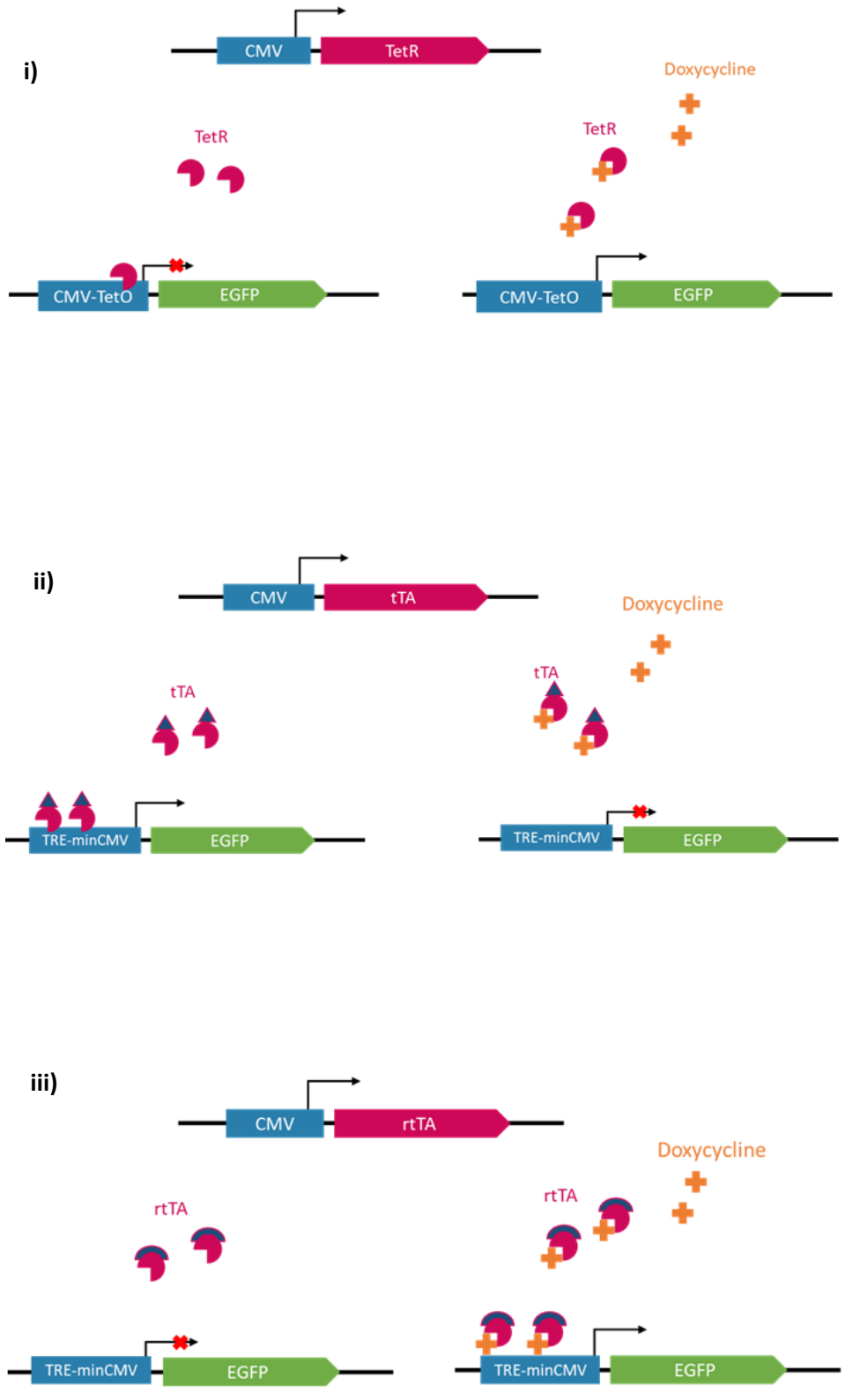


Figure 1.7 – Tetracycline inducible gene expression systems. Schematic diagram illustrating the three variations of the TetR inducible system repressing transcription of the EGFP reporter - **i**) TetR, **ii**) Tet-Off, and Tet-On. Diagram not drawn to scale.

1.5 Thesis overview and aims

1.5.1 Thesis overview

Efficient manufacture of high titre and high quality rAAV vectors remains a significant challenge in the gene therapy field. The issue of vector quality has been highlighted particularly by recent observations of severe toxicity associated with high dose rAAV to treat myotubular myopathy and muscular degenerations ('High-dose AAV gene therapy deaths' 2020). Work in this thesis explores the engineering and use of improved 'helper' adenoviral vectors to allow more efficient manufacture of higher quality AAV vectors. By inserting a TetR binding site into the MLP and encoding the repressor TetR under its transcriptional control, it was hypothesised that this would allow normal adenovirus replication in the presence of doxycycline but only genome amplification and early gene expression (the 'helper' functions) in its absence. The improved helper adenovirus developed here uses this strategy to self-inhibit transcription from its endogenous MLP, and thereby truncates its own virus replication allowing scalable and efficient AAV manufacture.

rAAV production requires the adenovirus early genes for its helper functionalities, whilst late adenoviral mRNAs expressed from the MLP encodes virus structural proteins. Transcriptional regulation of the MLP should maintain essential AAV helper function but inhibit expression of adenoviral capsids, and thereby removing adenovirus contamination of an AAV preparation. Late adenovirus infection is accompanied by exponential viral genome replication and shut-down of cellular protein synthesis. Likely, high expression of the TetR and its translation by virus-dependent mechanisms are required for tight repression of the MLP, and can be achieved by encoding it under transcriptional control of the MLP. This should create an efficient negative feedback loop regulating adenovirus structural gene expression, but allowed adenovirus

production with the addition of doxycycline. It was unclear, however, whether significant modification to the virus endogenous MLP allowed production of viable vectors as its transcriptional activity is intricately regulated throughout the virus replication cycle, and the essential E2 and IVa2 transcriptional units are encoded in the opposing DNA strand.

This thesis further explored novel approaches for rAAV manufacture using the MLP-regulated adenovirus helper. Firstly, we explored the utility of the adenoviral vector in delivering the rAAV transfer genome and helper functions for rAAV manufacture in cells, transiently or stably, harbouring the AAV rep and cap genes. Secondly, the AAV rep and cap genes, known to be toxic to adenovirus replication, and the rAAV transfer genome were encoded within two adenovirus helpers. These viral vectors were explored in-depth for their capacity to delivery helper functions and the AAV genes required for efficient replication of AAV vectors. Lastly, production of rAAV via serial propagation using rAAV vectors in combination with adenovirus vectors encoding AAV rep and cap was explored.

1.5.2 Thesis aims

I. Determine whether the adenovirus MLP can be modified to enable transcription control of its late proteins whilst avoiding compromising vector viability

II. Demonstrate whether the MLP-regulated adenovirus vector can be used for efficient manufacture of rAAV and to reduce adenovirus contaminations

III. Determine whether the AAV rep and cap can be modified to enable stable propagation within the MLP-regulated adenovirus and use for facilitating AAV replication

Chapter 2

Materials and Methods

2.1 Molecular biology

2.1.1 Bacterial transformation

For plasmid amplification and cloning, XL1-Blue competent *Escherichia coli* (*E. coli*) was used (Agilent, USA). For bacterial transformation with plasmid DNA, an aliquot (100 µL) of competent cells was thawed on ice and added to plasmid DNA (10 – 500 ng). For transformation with DNA ligation or Gibson assembly mixture, 4 µL of the reaction was used for bacterial transformation. Mixtures were incubated on ice for 20 minutes before heat-shock in a water bath at 42 °C for 90 seconds and then rested on ice for a further 2 minutes. 900 µL of S.O.C. medium (ThermoFisher, USA) were added to the transformed bacteria and incubated at 37°C for 60 minutes with shaking at 210 RPM. Samples were either poured or streaked into Luria Bertani (LB) agar plates (Sigma-Aldrich, USA) containing 50 µg/mL of Kanamycin Sulfate (Sigma-Aldrich, USA) or 50 µg/mL of Ampicillin sodium salt (Sigma-Aldrich, USA). Individual bacterial colonies were picked into LB broth (Sigma-Aldrich, USA) containing Kanamycin or Ampicillin and cultured overnight at 37 °C with shaking at 210 RPM.

2.1.2 Plasmid DNA purification

Plasmids were either purified from 4 mL of bacteria culture by mini-prep using the FastGene Plasmid Mini Kit (Nippon Genetics Europe GmbH, Germany) or 50 mL of bacteria culture by midi-prep using QIAGEN Plasmid Midi Kit (Qiagen, UK). Plasmids were confirmed by test/diagnostic restriction digest and Sanger sequencing.

2.1.3 Plasmid restriction digest

Restriction endonucleases were used for diagnostic digests of plasmids to generate unique DNA patterns for confirmation of clones, and generate DNA ends (blunt and sticky ends) for ligation with DNA fragments. Restriction endonucleases were either purchased from New England Biolabs (UK) or Promega (UK) and used according to the manufacturer's specifications. For diagnostic digest, plasmid DNA (50-300 ng) was incubated (~2 hours) with the appropriate enzyme(s) and buffer in a 10 µL reaction before visualisation by gel electrophoresis. For digestion of plasmid DNA in molecular cloning, 5 µg of DNA were incubated with the appropriate enzyme(s) and buffer in a 70 µL reaction for 2-3 hours. DNA fragments were visualisation by gel electrophoresis and purified from the agarose gel using FastGene Gel/PCR Extraction Kit (Nippon Genetics Europe GmbH, Germany).

2.1.4 DNA ligation

Restriction enzyme(s) were used to linearised the recipient plasmid (vector), extraction of DNA fragment from donor plasmids, or generation sticky ends from PCR amplicons as discussed above. The vector is additionally treated with calf intestinal alkaline phosphatase for 1-2 hours at 37°C to

de-phosphorylate each end of the DNA. DNA inserts and vectors are then gel-purified and used in a 10 µL ligation reaction with T4 DNA Ligase (New England Biolabs, UK) carried out according to the manufacturer's protocol.

2.1.5 Gibson assembly

For plasmid cloning via Gibson assembly, overlapping sequences with homology shared between the DNA insert and linear vector are generated (as specified in the particular construct) by PCR amplification or unique restriction enzyme digestion of the donor/recipient plasmid. A 10 µL reaction containing compatible linear vectors and DNA inserts was carried out using Gibson Assembly Mastermix (New England Biolabs, UK) or SnapFast Mastermix (OXGENE, UK) according to the manufacturer's protocol.

2.1.6 Polymerase chain reaction (PCR)

PCR primers were either custom synthesised by Sigma-Aldrich (USA) or Integrated DNA Technologies (USA). PCR amplification was carried out using Q5 High-Fidelity Master Mix (New England Biolabs, UK) according to the manufacturer's protocol. In a PCR, 1-10 ng of the template DNA was used for amplification with the relevant forward and reverse primer at a final concentration of 0.5 µM each in a 50 µL reaction. PCR cycles are as follows - 30 seconds at 98°C for initial denaturation, then 25 iterative cycles of denaturation (98°C for 10 seconds), annealing (55-65 °C dependent on primer annealing temperature for 15 seconds), and extension (72°C for 30 seconds per kb). The final extension step was carried out at 72°C for 5 minutes and hold at 4°C.

2.1.7 Agarose gel electrophoresis

DNA fragments were visualised using agarose gel electrophoresis to validate PCR reactions, the efficiency of restriction enzyme digestion, and plasmid fragment patterns after diagnostic restriction digest. The size of DNA fragments was determined by comparing against a molecular weight marker (**Figure 2.1**) (1 kb DNA Ladder, New England Biolabs, UK). Briefly, samples were resolved by size using a 1% agarose gel (Sigma-Aldrich, USA) containing 1X Midori Green nucleic acid stain (Nippon Genetics Europe GmbH, Germany) in Tris-acetate-EDTA (TAE) Buffer (ThermoFisher, USA). Gel electrophoresis was carried out at 10 volts per cm gel length for 40-60 minutes in DNA electrophoresis gel tanks (Bio-Rad Laboratories Ltd, UK). DNA was visualised in the gel either using a Dark Reader transilluminator (GRI, UK) or Gel Doc XR+ System (Bio-Rad Laboratories, UK).

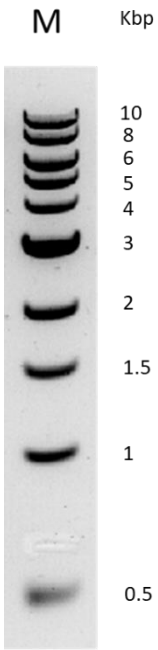


Figure 2.1 – NEB 1Kb D DNA ladder. A reference ladder to estimate size of DNA fragments by agarose gel electrophoresis.

2.1.8 DNA quantification

DNA concentration was quantified using a Nanodrop 2000 spectrophotometer (ThermoFisher Scientific, UK). Nanodrop was initially blanked with elution buffer or nuclease-free water before sample measurement.

2.1.9 Sanger Sequencing

Sanger sequencing of plasmids were carried out by Genewiz (UK) or GATC (Germany) using custom primers. Sequence reads were confirmed by alignment a predicted plasmid sequence map using SnapGene software (USA).

2.2 Cell culture

2.2.1 Maintenance of cell lines

HEK293-AD cells (referred to as HEK293; ATCC, USA), Flp-In T-REX 293 cells (ThermoFisher, USA), and U-87 MG (ATCC, USA) were cultured in Dulbecco's Modified Eagle Medium (DMEM; Sigma-Aldrich, USA) supplemented with 10% (v/v) heat-inactivated foetal bovine serum (FBS; Gibco, MA, USA) and maintained at 5% CO2, 37°C, and 95% humidity. Cells were subculture in T175 tissue culture treated flasks and split every 2-4 days. For subculture, the growth medium was removed, and cells were washed with phosphate-buffered saline (PBS, Thermo Fisher, UK). Cells were detached using trypsin/ethylenediaminetetraacetic acid (EDTA; 0.25% trypsin and 0.02% EDTA; Sigma-Aldrich, USA). Subsequently, 10% of cells were added to a T175 tissue culture treated flask

with 25 mL of growth medium for subculturing. Cells were routinely tested for mycoplasma (carried out by Genewiz, USA).

2.2.2 DNA transfection

HEK293 cells were seeded for 24-hours in 48-well tissue culture plates at 6.5 x10^4 cells per well. Each well was transfected with 0.75 µg of plasmid DNA complexed using Lipofectamine 2000 according to the manufacturer's protocol. For co-transfections, plasmids pCMV-TetR and pMLP-TetO were used at a 1:1 ratio of DNA mass. Transfection mixture diluted in Opti-MEM (Gibco, MA, USA) were exchanged with DMEM containing 10% FBS, and supplemented with dox 0.5 µg/mL (unless specified) or DMSO, at 4 hpi.

2.2.3 siRNA transfection

Dicer-Substrate Short Interfering RNAs (DsiRNAs) were designed (using IDT online designer tool, unless specified) and synthesised by IDT (USA). List of siRNAs used in this thesis is presented in **Table 2.1**. siRNA transfections were performed using Lipofectamine RNAiMAX (ThermoFisher, USA) according to the manufacturer's protocol. Reverse transfection of HEK293 cells with siRNA was carried out in 48-well plate format. For each well, 3 pmol of siRNA diluted in 30 µL of OptiMEM (Life Technologies, UK) was complexed with 1 µL of RNAiMAX suspended OptiMEM. Reaction was incubated at ambient temperature for 10 minutes before adding to the well. Subsequently, 300 µL of cells suspended in DMEM containing 10% FBS was added to each well and the plate was transferred to a 37°C incubator. After 24 hours, cells were infected with adenovirus vectors as indicated in the experiments.

Table 2.1 List of siRNA sequences used in this thesis

Name	Sense	Antisense	Origin
Ad5 Pol	CAACGUCUUCCAGCGUCCAACCAUA	UAUGGUUGGACGCUGGAAGACGUUG	(Kneidinger et al. 2012)
100K A	CAGUACCAACAGAGGAUAAAAAGCA	UGCUUUUUAUCCUCUGUUGGUACUGAG	Custom
100K B	GUACCAACAGAGGAUAAAAAGCAAG	CUUGCUUUUUAUCCUCUGUUGGUACUG	Custom
22/33K	GAACAAGAGCUGAAAAUAAAAAACA	UGUUUUUUAUUUUCAGCUCUUGUUCUU	Custom
L4 A	ACCUUGGAUUACAUCAAGAUCAUCT	AGAUGAUCUUGAUGUAAUCCAAGGUUA	Custom
L4 B	AACUGUCCUAACCUUGGAUUACATC	CGUUGACAGGAUUGGAACCUAAUGUAG	Custom
Cap2 3'UTR A	GCGUUUGUCUAUAUGUUAUUUUCCA	UGGAAAAUAACAUAUAGACAAACGCAC	Custom
Cap2 3'UTR B	UGCGUUUGUCUAUAUGUUAUUUUCC	GGAAAAUAACAUAUAGACAAACGCACA	Custom
Cap2 C	GUGGACAUUGAAAAGGUCAUGAUTA	UAAUCAUGACCUUUUCAAUGUCCACAU	Custom
Cap2 D	GUACCUGUAUUACUUGAGCAGAACA	UGUUCUGCUCAAGUAAUACAGGUACUG	Custom

2.2.4 Adenovirus infection in HEK293 cells and Flp-In-T-Rex-293 cells

HEK293 cells were seeded in 48-well tissue culture plates, at a density of 7.5 x10^4 cells per well, for 24-hours before infection with adenoviruses diluted in DMEM containing 2% FBS. Infectious medium was exchanged with fresh DMEM containing 2% FBS, supplemented with doxycycline 0.5 µg/mL (unless specified) or DMSO, at 4-6 hpi.

2.2.5 Flow cytometry

Cells were harvested for flow cytometry at the indicated timepoint treatment by trypsinisation. Flow cytometry was performed on an Attune NxT Flow Cytometer (ThermoFisher, USA) or accuri

C6 flow cytometer (BD Biosciences, USA). A flow cytometry gating strategy is shown in **Figure 2.2**. The side scatter area (SSC-A) is plotted against the forward scatter (FSC-A) area for exclusion of cell debris and gating of the live population. A second gate, FSC-H (height) and FSC-A (area) of the forward scatter was plotted for exclusion of doublets. In the remaining population is plotted as a histogram to display the proportion of cells positive in the BL1-A channel.

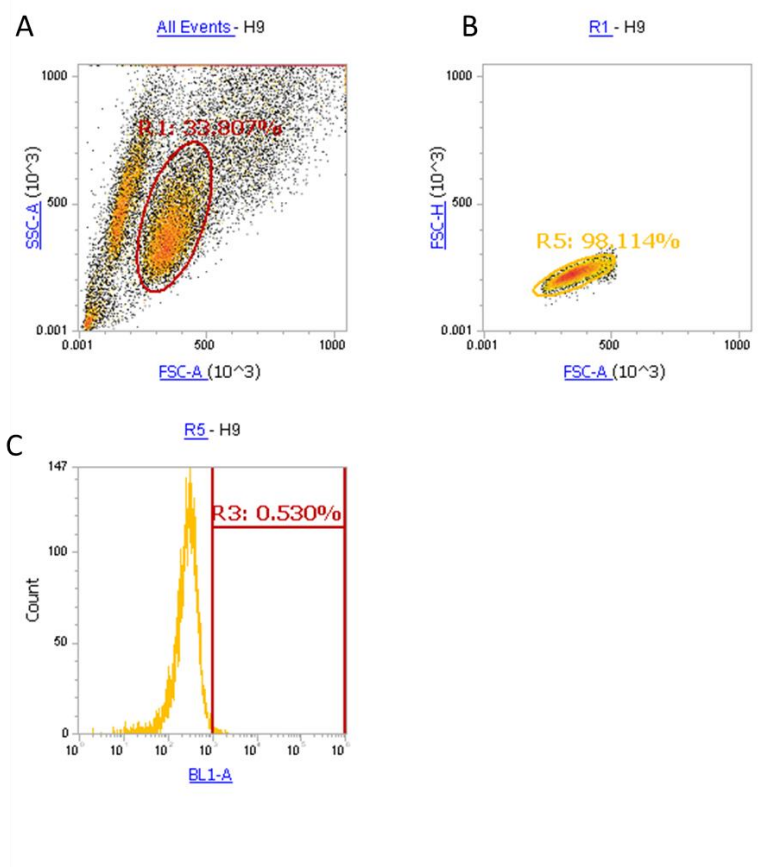


Figure 2.2 Flow cytometry (Attune NxT software) gating strategy for defining EGFP negative population of HEK293 cells are shown. A) SSC-FSC plot selecting live cell population. B) FSC-H and FSC-A gate for the exclusion of doublets. C) BL1-A channel gating to measure EGFP expression.

2.3 Viral vectors

2.3.1 Adenovirus recovery and small-scale amplification

All recombinant adenoviruses and adenoviral vectors were initially recovered in HEK293 cells from plasmid DNA encoding each viral genome. For the recovery process, plasmids (20 µg) were linearised with SwaI restriction enzyme to release virus ITRs from the bacterial plasmid backbone and purified using genomic Purelink DNA extraction kit (Invitrogen, USA) or DNeasy Blood & Tissue Kit (Qiagen, UK). For the recovery of the TESSA-E1 and Ad5-E1 virus, the plasmid DNA was linearised using PacI restriction enzyme to release the virus ITRs. HEK293 cells were seeded in T25 tissue culture flasks, at a density of 2 x10^6 cells per flask, for 24-hours before transfection. Each flask was transfected with 2.5 µg of linearised DNA suspended in 300 µL of OptiMEM (Life Technologies, UK) and complexed using Lipofectamine 2000 (Invitrogen) according to the manufacturer's protocol. After 4-6 hours, transfection media were exchanged with fresh DMEM containing 2% FBS and supplemented with doxycycline 0.5 µg/mL or DMSO as indicated. Recombinant viruses were harvested from growth media ~12-15 days post-transfection upon observation of advanced CPE. Cells and growth medium were collected and subjected to three rounds of freeze-thaw cycle by transferring between a 37°C incubator and a -80°C freezer. Cellular debris was pelleted by centrifugation at 2500 x g for 20 minutes and supernatant passed through a 0.2 µm filter and stored at -80°C. Adenoviral vectors were amplified by a further two rounds in HEK293 cells. In the first round, HEK293 cells were seeded in T75 tissue culture flasks for 24 hours so that cells are ~90% confluent. Cells were replenished with fresh DMEM containing 2% FBS (supplemented with doxycycline 0.5 µg/mL or DMSO) and infected with 100-1000 µL of the primary virus stock. After three days, cells were harvested and suspended in ~4 mL of growth medium. Viruses were released by three rounds of freeze-thaw using a 37°C incubator and a -

80°C freezer. Cellular debris was pelleted by centrifugation at 2500 x g for 20 minutes and supernatant passed through a 0.2 µm filter and stored at -80°C. This process was repeated at a T175 tissue culture flask scale for the second round of amplification.

2.3.2 Large-scale amplification and purification by caesium chloride gradients

For large-scale virus amplification, HEK293 cells were seeded in Corning HYPERFlask (Sigma-Aldrich, MO, USA) for 48-hours so that they are ~95% confluent before infection. Growth medium was replenished with fresh DMEM containing 2% FBS (supplemented with doxycycline 0.5 µg/mL for TESSA-based adenoviruses) with viral stocks (purified or crude lysates). Cells were harvested upon display of advanced CPE, usually observed at 48-72 hpi, and resuspended in ~16 mL of growth medium. Viruses were released by three rounds of freeze-thaw using a 37°C incubator and a -80°C freezer. Lysates were incubated with water-saturated n-butanol (diluted 1:100) for 60 minutes at 4°C and cell debris pelleted by centrifugation at 2500 g for 20 minutes. The supernatant was collected for purification by a caesium chloride (CsCl) gradient.

In brief, the CsCl gradient was prepared in ultra-clear centrifuge tubes (Beckman Coulter UK Ltd) and consists of 3 mL of 1:32 ρ CsCl (32.0g CsCl, 6.8 mL of 0.5 M Tris-HCl at pH 7.9, 61.2 mL dH2O), underlaid with 2 mL of 1:45 ρ CsCl (20.5g CsCl, 2.9 mL 0.5 M Tris-HCl at pH 7.2, 28.5 mL dH2O), and 2 mL of PBS 40% Glycerol added on top of the gradient. Approximately 4.5 mL of viral supernatant was added on top of each ultra-clear centrifuge tube. The gradients were centrifuged (30,000 g, 120 minutes, 10°C) using a Thermo Sorvall WX90 plus ultracentrifuge with a TH-641 rotor (ThermoFisher, USA). After centrifugation, two discrete bands were obtained (**Figure 2.3**) – intact virus particles are presented in the lower band, while the upper band consists of

incomplete/empty capsids. Viruses were extracted from the lower band by puncturing the centrifuge tube with a 21 g needle attached to a 6 mL syringe. Virus mixture was injected into a 10K molecular weight cut off Slide-A-Lyzer dialysis cassette (ThermoFisher, UK) and CsCl was removed by four-rounds of dialysis using ~500 mL of PBS in each round. Viruses were extracted from the dialysis cassette using a 21 g needle and a syringe and subsequently treated with benzonase 250 U/mL (Sigma-Aldrich, MO, USA), supplemented with magnesium chloride (2 mM), for 1 hour at room temperature. After treatment, the virus mixture was re-injected into a Slide-A-Lyzer cassette for three further rounds of dialysis using PBS. The final dialysis step was carried out using PBS containing 10% glycerol and 10mM HEPES buffer (Sigma-Aldrich, USA). Viruses were extracted and stored at -80°C.

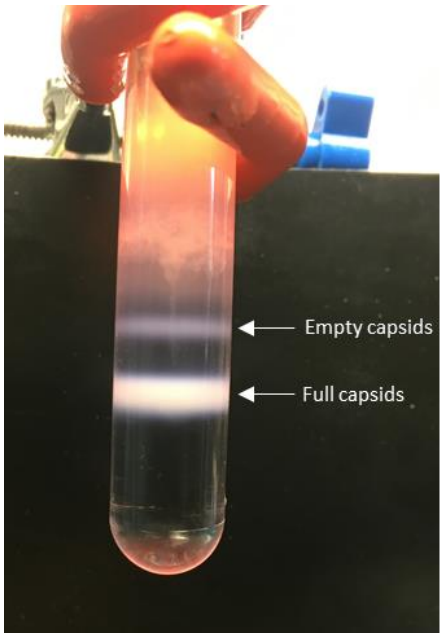


Figure 2.3 Purification of adenovirus by CsCl gradient banding. Representative image of adenovirus preparation after one round of ultracentrifugation. The lower larger band corresponds to intact viral particles containing the virus genome. The upper smaller band is formed by empty particles.

2.3.3 rAAV production using adenovirus and the helper-free system

HEK293 cells were seeded in 48-well tissue culture plates, at a density of 9 x10^4 cells per well, for 24-hours before production. Helper-free rAAV production was carried out according to Takara AAVpro Helper-Free System (Clontech, USA). Plasmids provided by OXGENE. Each well was transfected with 0.75 µg of plasmid DNA, containing pHelper (Q1364), pRepCap (Cap2 ref: Q1311; -5 ref: Q4658; -6 ref: R444; or -8 ref: Q5207; -9 ref: Q6293), and the rAAV transfer vector (pAAV-CMV-EGFP ref: Q4346; pAA-hFIX ref:pSU908; or pscAAV-hFIX ref:pSU878) diluted with Opti-MEM (Gibco, USA) at a DNA mass ratio of 1:1:1, and complexed using linear PEI 25kDA (Polysciences, USA) at a 1:3 DNA to PEI mass ratio. For AAV production using the TESSA2.0 system (including TESSA2.0-AAV5, -AAV6, -AAV8, and -AAV9), HEK293 cells were co-infected (at the indicated vector dose) with TESSA-RepCap and TESSA-AAV-EGP diluted in DMEM containing 2% FBS. For propagation of rAAV using rAAV vectors (including the capsid-exchange method), HEK293 cells were co-infected with rAAV2 vectors (at the indicated doses) with TESSA-RepCap (Cap2, -5, -6, or -9) at the indicated vector dose and diluted in DMEM containing 2% FBS. Transfection and infection media were exchanged with fresh DMEM containing 2% FBS (supplemented with dox 0.5 µg/mL or DMSO as indicated) 4-6 hours post-treatment. To determine the efficiency of the DNase reaction in degrading free-DNA, a helper-free production control was included with each experiment, wherein the stuffer plasmid pUC19 (provided by OXGENE) was used in place of pRepCap. Similarly, for production control using the TESSA2.0 system, HEK293 cells were only infected with TESSA-AAV-EGFP. At 96 hpt, rAAV vectors released from the cells via three rounds of freeze-thaw cycles by transferring plates between a 37°C incubator and a -80°C freezer. Cell debris was pelleted by centrifugation at 3000 g for 20 minutes and supernatant stored at -80 °C.

2.3.4 TCID50 assay for determining infectious adenovirus and rAAV

Infectious adenoviruses were determined using the Tissue Culture Infectious Dose (TCID50) assay. HEK293 cells were seeded in 96-well tissue culture plates at a density of 1 $x10^4$ cells per well for 24-hours. Eight 10-fold serial dilutions of each adenovirus stock were made in DMEM containing 2% FBS at a total volume of 1.2 mL. For quantification of TESSA-based vectors, DMEM was additionally supplemented with doxycycline 0.5 µg/mL. Ten replicates of each diluted sample (1 $x10^{-5}$ to $1x10^{-12}$) were added at a volume of 100 µL per well on each plate. For determining contamination of infectious adenoviruses, a low dilution of $1x10^{-1}$ to $1x10^{-8}$ were generated. 100uL of DMEM containing 2% FBS were added to the final two columns as a negative control. Plates were monitored over 12 days for the presence of viral plaques in each well under a light microscope. For adenoviral vectors encoding the EGFP reporter, expression of EGFP is used as a proxy for infectious events. To measure rAAV transduction, the TCID50 assay was carried out as above. However, samples were diluted at a lower range (approximately $1x10^{-2}$ to $1x10^{-10}$) dependent on the assessed serotype, and plates were observed for the presence of EGFP expressing cells from each well at 6 days post-infection using a EVOS FL imaging system (ThermoFisher Scientific, USA). Infectious adenovirus and rAAV determined as TCID50 per mL using KÄRBER formula (Cawood et al. 2009).

$$\text{Titre (TCID50/mL)} = 10^{\,1 + D\,(S - 0.5)}$$

$$D = \log(\text{dilution factor})$$

$$S = \text{sum of the ratios of wells with infection to infection-free wells}$$

2.3.5 AAV cell internalisation assay

HEK293 cells were seeded in 48-well tissue-culture treated plates at 7.5 x10^4 for 24 hours. Cells were counted before infection and AAV2 derived from TESSA2.0 or helper-free method were used to infect at an MOI of 50 GC per cell. At 6 hpi, cells were trypsinised and extensively washed for three rounds with PBS before extraction of total DNA using a DNeasy Blood & Tissue Kits (Qiagen, UK). Viral genomes were quantified by qPCR.

2.3.6 Determining intact adenovirus particles by PicoGreen assay

Intact adenovirus particles in purified stocks were determined using the PicoGreen dsDNA assay (Invitrogen, UK) which uses a fluorescent nucleic acid stain specific for double-stranded DNA. Purified viral stocks were diluted in TE buffer containing 0.1% SDS, 25mM EDTA and incubated at 37°C for 15 minutes to disassociate the virus capsid. Samples and the standard curve generated using bacteriophage lambda DNA were measured using the PicoGreen dsDNA assay kit according to the manufacturer's instructions. Concentration of intact particles was calculated based upon 1 µg is equivalent to 2.7 ×10^{10} genome intact particles(Murakami and McCaman 1999).

2.3.7 DNA quantification using qPCR

For quantification viral genomes extracted using genomic DNA extraction kits (as discussed above), 5 µL of sample eluent was in a qPCR reaction using TaqMan Fast Advanced Master Mix (Applied Biosystems, CA, USA) in a StepOnePlus Real-Time PCR System (Applied Biosystems, CA, USA). For quantification of genome encapsulated rAAV and intact adenoviral particles, 2 µL of viral crude lysate preparations were treated with 1U of TURBO DNase (ThermoFisher Scientific,

USA) in a 20 µL reaction for 2 hours at 37°C. TURBO DNase was heat-inactivated at 75°C for 10-minutes. Five microlitres of samples diluted at 1:200 using nuclease-free water and 5 µL were used in the qPCR reaction. Standard curves for qPCR analyses were generated using a gBLOCK gene fragment encoding the qPCR amplicon sequences (appendix 1; Integrated DNA Technologies, USA) and CT values of PCR reaction used to calculate DNA copy number by extrapolation to the standard curves. rAAV productivity per cell determined from total rAAV vectors produced by cell count at the time of virus treatment or plasmid transfection. Primers and probe sequences are presented in (**Table 2.2**). qPCR cycle conditions are as follows - 95˚C 10 min; 40 times (95˚C 1s, 60˚C 20s). Shown in **Figure 2.4** is a representative qPCR assay carried out using EGFP-specific qPCR against gBlock DNA standard.

Table 2.2 qPCR primers and probe sequences

Target	Forward 5'-3'	Reverse 5'-3'	Probe 5'-3'
fibre	TGGCTGTTAAAGGCAGTTTGG	GCACTCCATTTTCGTCAAATCTT	TCCAATATCTGGAACAGTTCAAAGTGCTCATCT
hexon	CACTCATATTTCTTACATGCCCACTAT	GGCCTGTTGGGCATAGATTG	AGGAAGGTAACTCACGAGAACTAATGGGCCA
Ad5 Ψ PS	CACATGTAAGCGACGGATGT	CTTACTCGGTTACGCCCAAAT	TTGTCACTTCCTGTGTACACCGGC
TetR	ATGAGGTGGGAATTGAAGGAC	CAGCATTTCGATGGCAAGC	AAGAATAAACGGGCGCTCCTAGACG
EGFP	GAACCGCATCGAGCTGAA	TGCTTGTCGGCCATGATATAG	ATCGACTTCAAGGAGGACGGCAAC
hFIX	GTGTTCCCTGATGTGGACTATG	ACCCTGGTGAAGTCATTGAAG	AGGCTGAAACCATCCTGGACAACA
E4Orf6	CACTACGACCAACACGATCT	GATGATCCTCCAGTATGGTAGC	AGACGATCCCTACTGTACGGAGTGC
E2A DBP	GACAGCGAGGAAGAAAGAGAA	CTCCTTTGCCATGCTTGATTAG	CGCTACAAATGGTGGGTTTCAGCA
Ampicillin	GCTGAATGAAGCCATACCAAAC	CTAGAGTAAGTAGTTCGCCAGTTAAT	TGACACCACGATGCCTGTAGCAAT
AAV2 rep	GGCCTCATACATCTCCTTCAAT	AGTCAGGCTCATAATCTTTCCC	TCCAACTCGCGGTCCCAAATCAA
AAV2 cap	CGACCCAAGAGACTCAACTTC	GAACCGTGCTGGTAAGGTTAT	AAAGAGGTCACGCAGAATGACGGT

AAV5 cap	CGCTTCGTGAGCACAAATAAC	TTGTAGGTGTTGGCGTATCTC	TGGCGGAGTCCAGTTCAACAAGAA
AAV6 cap	GACCGGAGATGTGCATGTTAT	GTCCATCCGTGTGAGGAATTT	AATGGTGTGGCAAGACAGAGACGT
AAV8 cap	GGACTGCTGGGACCAAATAC	AGGATCCCGTTACTGGGAAA	ACACAAAGACGACGAGGAGCGTTT
AAV9 cap	GATGAATCCTGGACCTGCTATG	GTTGTCTCTTCCAGTTCCTTGT	AACGGTCCTCTCCTTCTTTGTGGC

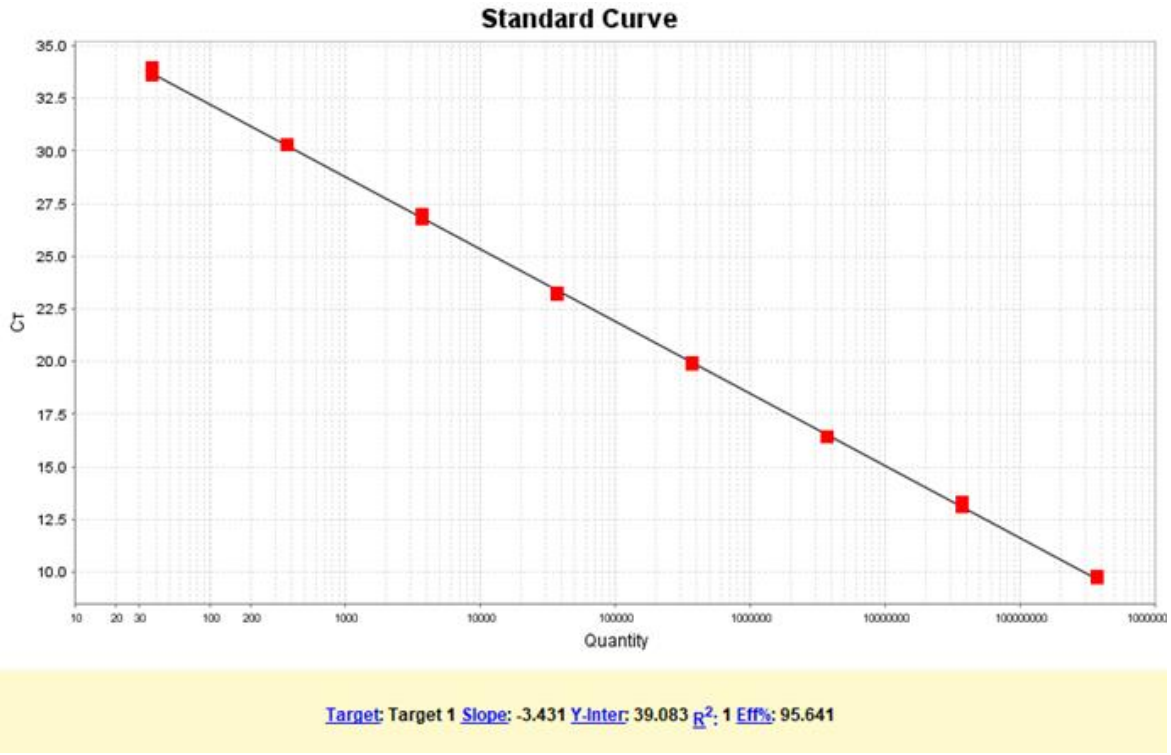


Figure 2.4 - example qPCR standard curve using EGFP primers and probe. Known concentration of gBlock DNA fragment standard encoding the EGFP amplicon were diluted in nuclease-free water and qPCR carried out using TaqMan Fast Advanced Master Mix reagent. Data shows that the efficiency of the reaction was 95.64% and a slope of -3.431.

2.3.8 RNA extraction and reverse transcription

Total RNA was extracted using RNeasy Mini Kit (Qiagen, UK). RNA eluent (5 µL) was used for cDNA synthesis in a reverse transcription reaction (RT) using SuperScript IV First-Strand Synthesis System (Invitrogen, USA). Five microlitres of each RT reaction was used as template for qPCR to quantify viral RNA expression using primers and probe as specified.

2.3.9 Western blotting

Detection of adenovirus capsid proteins by western blotting was carried out using Wes automated system (ProteinSimple, USA) according to the manufacturer's instructions. Adenovirus was harvested from culture medium and HEK293 cell lysate 3 days post-infection by three rounds of freeze-thaw. Cell debris was pelleted by centrifugation and lysates were probed using polyclonal antibodies directed against adenovirus type 5 (ab6982, Abcam, UK) and used at 1:50 dilution. For detection of TetR and BAX using Wes automated system (ProteinSimple, USA), cellular extracts were harvested using RIPA buffer (ThermoFisher, USA) and probed using Anti-TetR antibody (ab25845; Abcam, UK) or anti-FLAG tag antibody (F3165, Sigma-Aldrich, USA) used at 1:50 dilution. For detection of AAV2 Rep and GAPDH, cellular extracts were harvested from HEK293 cells using RIPA buffer. For detection of AAV capsid proteins, crude lysate preparations were used. Equal amounts (25 uL) of total cellular extracts were resolved in SDS-PAGE (10%, Tris-Glycine; ThermoFisher, USA) for detection AAV Rep and capsid proteins. Proteins were transferred to a nitrocellulose membrane using iBlot 2 Dry Blotting System (ThermoFisher, MA, USA) and probed with anti-AAV2 Rep antibody used at a 1:200 dilution (65172, Progen, Germany), anti-GAPDH used at 1:1000 dilution or anti-AAV VP1/VP2/VP3 monoclonal antibody used at 1:200 dilution (65158, Progen, Heidelberg, Germany). Secondary antibody donkey anti-mouse, HRP (ThermoFisher, USA) was used at a 1:5000 dilution and detected with TMB substrate solution (Sigma-Aldrich, USA). Membrane was imaged using a Gel Doc XR+ System.

2.3.10 Transmission electron microscopy

Electron microscopy imaging of AAV particles was carried out by the Dunn School Bioimaging Facility, University of Oxford. For TEM imaging of purified AAV2 produced in bioreactor HEK293 suspension culture cells from the TESSA2.0 or helper-free transfection method, 10 µL of neat HF-derived AAV or TESSA-derived AAV diluted 1:5 in PBS, were further diluted 1:1 with water and applied to freshly glow discharged carbon formvar 300 mesh copper grids for 2 mins, blotted with filter paper and stained with 2% uranyl acetate for 10 seconds. Grids were imaged in a FEI Tecnai 12 TEM at 120 kV using a Gatan OneView CMOS camera.

2.3.11 Statistical analysis

Data presented as mean ± standard error of mean (SEM), unless otherwise stated. All data are shown as biological triplicates unless specified. For grouped datasets, two-way ANOVA test was used. Unless otherwise stated, significance evaluated using unpaired, two-tailed Student's t-test, and denoted on the graphs as *P≤0.05 **P≤0.01, ***P≤0.001, ****P≤0.0001.

Chapter 3

Engineering and characterisation of a Tetracycline Enabled Self-Silencing Adeno virus 'TESSA' for rAAV manufacture

3.1 Introduction

Production of recombinant AAV vectors (rAAV) for clinical use is limited by current manufacturing approaches. The most common 'helper-free' method is based on plasmid transfection of HEK293 cells to provide all the components (rAAV transfer genome, packaging plasmids and the Ad helper plasmid) required for rAAV replication. While versatile and easy to adopt, the helper-free method is limited by lack of scalability and vector yield (Xiao, Li, and Samulski 1998; Clement and Grieger 2016). Alternatively, the use of wildtype (wt) adenoviruses to deliver essential helper functions for rAAV replication from stable producer cells have been explored extensively. Here, stable producer cells, typically HeLa or A549-based, are integrated with the AAV rep and cap genes, and ITR transfer genome encoding the transgene cassette (Clark 2002; Chadeuf et al. 2000; Gao, Lu, et al. 2002). AAV replication is induced by infection with wt helper adenovirus. As a variation to this approach, the ITR transfer genome may be delivered using an E1/E3-deleted adenovirus vector (E1/E3Δ-Ad). While scalable, and production of high-quality particles have been reported, the use of wt replicating adenoviruses raises some safety concerns and the extensive purification

steps required for their removal from the product undermines cost-effectiveness (Zhang et al. 2009; Clement and Grieger 2016; Sun et al. 2003).

Packaging cells based on HEK293 cells, which harbor the adenovirus E1 genes, might enable the use of safer E1/E3Δ-Ad as helper viruses for rAAV production, however previous attempts to engineer them have met with limited success. In some cases this was attributed to E1A induced activation of the AAV p5 and p19 promoters leading to expression of the Rep proteins, which are well recognized to be cytotoxic (Yang, Chen, and Trempe 1994).

In an attempt to generate 293-based AAV packaging cells, Nakamura et al. integrated the AAV rep and cap, and adenovirus helper genes (VA RNA, E2A and E4) into 293T cells using a multi-step lentivirus transduction approach. While the packaging cell line was capable of generating rAAV by transfection of the ITR genome at early passages, productivity diminished by over 100-fold when cells were grown to the 7^{th} passage. Interestingly, cell lines solely integrated with the rep and cap maintained rAAV vector production following transfection with the rAAV genome and Ad helper plasmid (Nakamura et al. 2004). This suggested that the harmful effects of Rep alone may be tolerated, but the adenovirus genes promoted significant cytotoxicity when integrated into the cells. Similarly, attempts to integrate adenovirus helper genes (E2A, E4, VA RNA) into HeLa cell lines stably encoding the rep and cap was also unsuccessful with observed toxicity (Qiao et al. 2002). Gene products from the E2A and E4 regions are toxic to the cells and their controlled expression for producing complementation cell lines to support replication of adenovirus (ΔE2A and ΔE4) have been extensively explored (Kovesdi and Hedley 2010; Li et al. 2005).

Elaborate systems to generate rAAV producer cell lines from HEK293 cells have also been explored in order to eliminate both the requirement for transient transfection and use of wt adenoviruses. For example, Yuan et al. developed a splicing switch system to manipulate stably integrated AAV rep and cap in 293 cells. Here, Rep induced cytotoxicity is alleviated by insertion of an intron and

polyadenylation elements to disrupt the coding sequence of all four Rep proteins. Rep expression is reconstituted by infection using an E1/E3Δ-Ad expressing Cre recombinase, to splice the loxP-flanked rep disruptive element, for rAAV replication. Advantages of this approach allows scalability and a significantly better safety profile by using E1-defective Ad vectors compared to wt helper viruses. Interestingly, rAAV vector yield from this system were reported to be greater than from the helper-free approach with particles (rAAV2) displaying over 6-fold increase in infectivity. However, a significant drawback of this system is the difficulty in generation of the complex DNA construct and producer cell line (Yuan et al. 2011). Timeline ranging from months to years are required for construction of each (transgene and capsid serotype specific) cell line due to multiple rounds of plasmid integration and antibiotic selection (Lai, Yang, and Ng 2013). Furthermore, E1/E3Δ-Ad particles are abundantly generated in parallel to rAAV vectors which, while regarded as safer than using wt adenoviruses, still requires complex purification procedures to remove them from the final preparation.

These studies demonstrate the challenges in generating 293-based rAAV packaging and producer cells but also highlight the benefits for scalable production of high-quality rAAV particles using helper Ad vectors. As a superior alternative approach, we set out to develop a more sophisticated adenovirus helper by exploiting the fact that the adenovirus life cycle involves early and late temporal phases. rAAV production requires only the early phase for its helper functionalities, whilst the late phase is required only by adenovirus for production of its own structural proteins These proteins are mainly transcribed from the adenoviral major late promoter (MLP) (Samulski, Chang, and Shenk 1989; Young 2003; Penaud-Budloo et al. 2018). Therefore, the use of a conditionally-replicating helper adenovirus, where production of its late structural proteins can be selectively turned-off during rAAV manufacture, should produce rAAV vectors free of adenovirus capsid proteins and reduce safety concerns over adenovirus contamination.

Utility of an adenovirus encoding an inducible MLP was initially conceptualized and pursued in the early 2000s for improving vector safety and transgene delivery (Young 2003). However, modification to the virus endogenous MLP to provide inducible repression have not previously been demonstrated, most likely because it would requires disruption of the virus DNA polymerase coding sequence and IVa2 transcriptional unit on the opposing DNA strand, both of which are essential for virus replication (Brunet et al. 1987; Mei et al. 2003; Pardo-Mateos and Young 2004).

In this chapter, we explored the tetracycline-controlled (TetR) system for regulating transcription from the adenovirus MLP as it allows silencing of gene transcription in the absence of tetracycline, or its derivatives such as doxycycline (Ramos et al. 2005). We aimed to develop a self-silencing adenovirus vector that provides all the necessary helper functions for rAAV manufacture in the absence of doxycycline, but is unable to complete its own replication cycle and thereby avoids contamination of the rAAV preparation. We hypothesized that insertion of tetracycline operator (TetO) sites into the MLP, if it could be achieved without disrupting the coding sequence on the opposite strand, should allow tetracycline repressor protein (TetR)-mediated control of the adenovirus life cycle. In addition, we hypothesized that encoding the TetR itself under the control of the MLP, would enable a negative feedback loop that self-inhibits further transcription activity to completely silence structural gene expression. Since doxycycline binds to the TetR and prevents it binding to the TetO and inhibiting the MLP, this approach should create a switchable virus life-cycle, wherein addition of doxycycline will alleviate repression of the MLP and allow production of the 'self-silencing' helper vector when required.

3.2 Chapter aims

1. Design and engineer inducible MLP reporter plasmids to assess transcriptional repression using the TetR system
2. Explore the feasibility of modifying the adenovirus MLP to enable transcriptional control of its capsid proteins whilst avoiding compromising vector viability by extensive changes to the sequence of the opposing DNA strand.
3. Encode the repressor protein TetR under transcriptional control of its repressible MLP to generate an autoregulated loop of self-repression within the Ad vector
4. Characterise this self-silencing Ad vector and assess its utility to deliver helper functions and the ITR transfer genome for rAAV manufacture

3.3 Results

3.3.1 Engineering Tet-responsive elements into the MLP EGFP reporter plasmids

As illustrated in **Figure 3.1A**, the TetR system allows regulated gene transcription depending on the presence or absence of doxycycline (Yao et al. 1998). In the absence of doxycycline, the repressor protein TetR, expressed from the constitutive CMV promoter, recognizes and binds to TetO within the MLP to suppress transcription activity. As doxycycline as added to the system, it binds to the TetR at high affinity and triggers a conformational change to prevent its binding to its cognate TetO elements for promoter repression.

Numerous TetR-repressible promoters have been described; however, they can differ in the positioning and amount of tetO elements embedded within the core promoter sequence (Bertram and Hillen 2008). As a first step, we sought to identify regions within the adenovirus MLP that allow insertion of TetO sites whilst maintaining good transcription functionality. While the adenovirus MLP appears relatively simple, as previously discussed (Introduction 1.3.5), genetic mutation analysis suggests a more complex structure as sequences surrounding the Inr or TATA element were shown to be important by *in vitro* transcription assays, but may also function in a redundant manner as single point-mutations in these elements, including the TATA box and Inr, was not detrimental to virus replication compared to when introduced in parallel (Lu et al. 1997; Reach, Xu, and Young 1991; Song and Young 1997).

To assess possible strategies, we inserted a single TetO sequence upstream (MLP-TetO1a), downstream (MLP-TetO1b) or flanking (MLP-TetO2) the TATA element by direct sequence

exchange to minimally disturbed the structure of the MLP (**Figure 3.1B**). Where possible we used synonymous codons to preserve the coding sequence of the virus polymerase on the opposing DNA strand and avoided introduction of termination codons to this C-terminal peptide sequence (Hoeben and Uil 2013). The modified sequences of the polymerase are shown in **Figure 3.1C** and they are thought unlikely to affect the replication fidelity of the polymerase, as the three highly conserved Exo motifs (I, II and III) within the 3'-5' exonuclease domains, are located away at the N-terminal portion and at a distance of over 240 amino acids (Uil et al. 2011; Brenkman, Breure, and van der Vliet 2002; Capella et al. 2012). These MLP variants were initially cloned, alongside the wildtype (wt) MLP, into plasmid constructs driving EGFP expression.

For the construction of these MLP reporter plasmids, the Ad5 wt-MLP, MLP-TetO1a, MLP-TetO1b and MLP-TetO2 sequences were generated by *de novo* synthesis into a pUC57 plasmid backbone (Genewiz, USA) and used as template for PCR with forward primer 5'-GAACATTTCTCTGTCGACCAACTAGTCGCCCTCTTCGGCATCAAG-3' and reverse 5'-GGCCCTCGCAGA CAGCGATGCGGAAGAGAG-3'. This generate DNA fragments with flanking homology sequences corresponding to the SalI restriction site position of plasmid pSF-pA-PromMCS (OG186; provided by OXGENE) and the first-leader sequence of the adenovirus tripartite leader (TPL) (accession no: AY339865). A second DNA fragment encoding the EGFP reporter, wherein its start codon is fused to the Ad5 tripartite leader I-II-III exon was extracted by PCR from plasmid pSU109 using forward primer 5'-TCTCTTCCGCATCGCTGTCTGCGAGGGCC-3' and reverse 5'-AGCTGAAGGTACGCTGTATC-3'. Each MLP-TetO promoter fragment was inserted alongside the EGFP coding sequence into plasmid pSF-pA-PromMCS linearized with SalI and NheI using SnapFast assembly reagent (provided by OXGENE). This generate the corresponding plasmids pMLPwt-EGFP, pMLP-TetO1a-EGFP, pMLP-TetO1b-EGFP, or pMLP-TetO2-EGFP shown in **Figure 3.1B.** Plasmids were confirmed by restriction digest and Sanger sequencing (not shown).

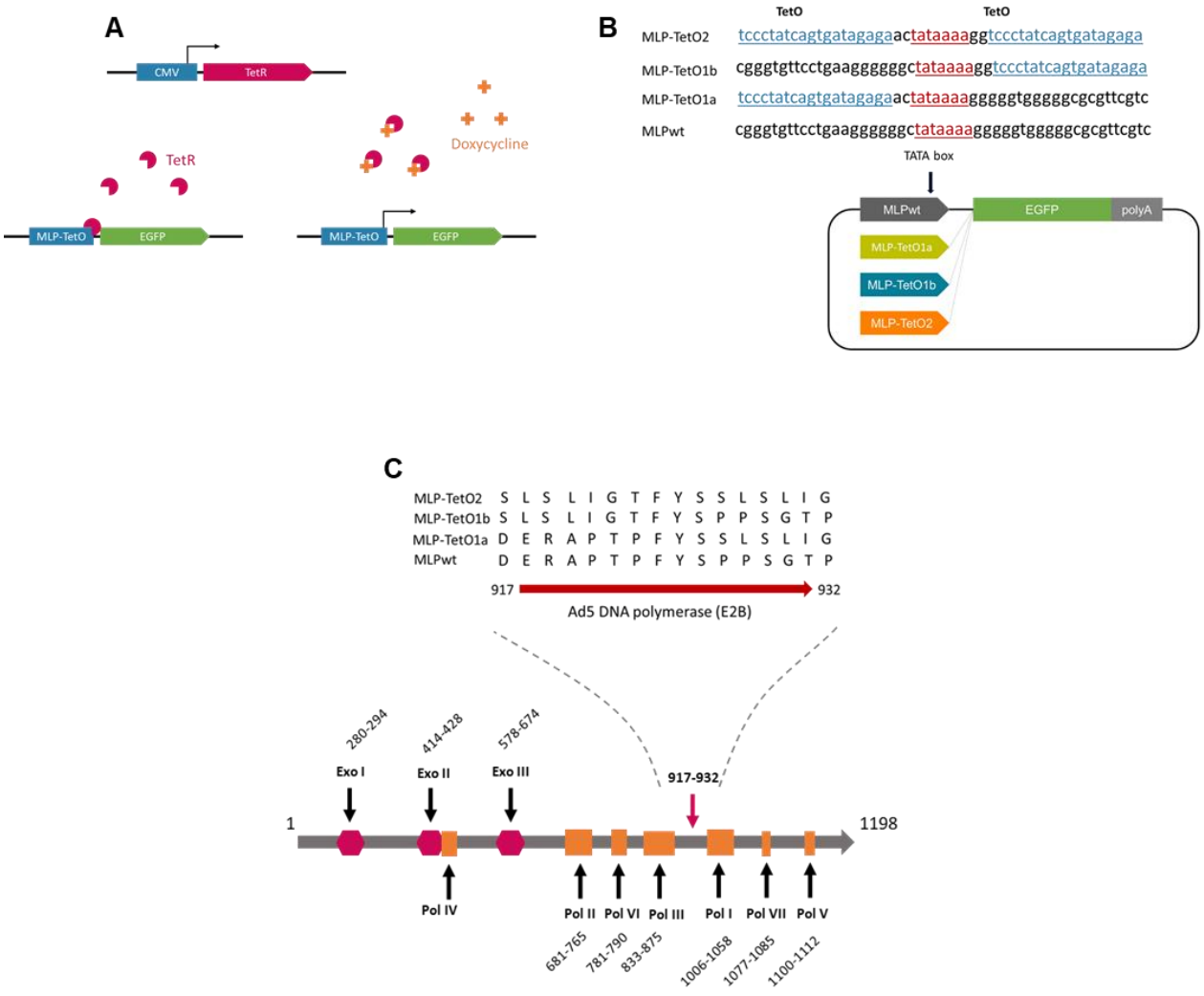


Figure 3.1 A) Schematic diagram of the TetR system. TetR expressed from the CMV promoter induce transcriptional repression from MLP-TetO promoter. Addition of doxycycline alleviate MLP repression by binding to TetR proteins. **B)** Schematic of Ad5 MLP expression plasmids and positioning of TetO sequences relative to the promoter TATA-box. **C)** Amino acid changes in the Ad5 DNA polymerase due to insertion of TetO sequences in the MLP. Conserved residues within the exonuclease and polymerase domains in the Ad E2B DNA polymerase are also illustrated.

3.3.2 Insertion of TetO sites do not affect Ad5 MLP basal activity

Prior to testing of MLP EGFP reporter plasmids, parameters were optimized for transient transfection of HEK293 cells using linear PEI. Cells seeded for 24 hours in 48-well tissue culture treated plates were transfected with increasing amounts of a CMV EGFP reporter plasmid complexed with linear PEI at the indicated DNA to PEI mass ratio. Cells were analyzed by flow

cytometry 48 hours post-transfection (hpt) for the proportion of EGFP expressing cells (**Figure 3.2A**). While transfection with 750ng and 1000ng of plasmid DNA per well achieved >80% efficiency, optimal results (>86% EGFP positive cells) were achieved using 750ng of plasmid DNA with a 1:3 ratio DNA to PEI mass. This transient transfection parameter was selected for subsequent experiments.

To assess transcription activity of the TetO modified MLP, HEK293 cells were transfected with EGFP reporter plasmids driven by the wt-MLP (pMLP-EGFP) or TetO modified MLPs (pMLP-TetO1a-EGFP, pMLP-TetO1b-EGFP, pMLP-TetO2-EGFP) and cells were analyzed by flow cytometry 24, 48 and 72hpt. In parallel, cells were transfected with a promoter-less EGFP expression plasmid (pMCS-EGFP) as a mock-transfection control for background EGFP expression. Expression of EGFP (determined by mean fluorescent intensity (MFI) of EGFP positive cells) from TetO modified MLP were comparable to the wt promoter with levels increasing over the 72 hours assessed period (**Figure 3.2B**). While MLP-TetO1a and MLP-TetO1b showed a slight, but significant, increase in EGFP expression compared the wt MLP sequence, MLP-TetO2 showed a non-significant decrease in promoter activity.

To assess whether expression from the MLP plasmids were influenced by an ongoing adenovirus infection, HEK293 cells were transfected with the TetO-modified MLPs or the wt MLP-EGFP reporter plasmids and infected with wt Ad5 at an MOI of 5. Cells were harvested 48 hours post-treatment (hpt) and MFI of EGFP positive cells were compared to non-adenovirus infected cells. As shown in **Figure 3.2C**, EGFP expression was comparable in Ad-infected cells that were transfected with the wt-MLP or TetO-modified MLP plasmids. As expected, presence of the wt Ad did not increase MLP activity outside of its endogenous viral contexts as it is primarily activated after the onset of adenovirus replication (Thomas and Mathews 1980).

As the TetO-modified MLPs showed comparable activity to the wt promoter sequence, we further determined whether basal transcription activity of the MLP could be repressed by the TetR. HEK293 cells were co-transfected using plasmids pMLP-TetO1a-EGFP, pMLP-TetO1b-EGFP, pMLP-TetO2-EGFP, or pMLP-WT-EGFP with pSF-CMV-TetR, wherein the TetR is expressed from a CMV promoter, and treated with doxycycline or DMSO. Here, doxycycline alleviates transcription repression by binding at high affinity to TetR, thereby preventing TetR from binding to MLP-TetO sites. In addition, cells were also co-transfected in parallel using a pMCS-EGFP with pCMV-TetR, as a mock-transfection to control for background EGFP expression. Cells were harvested for flow cytometry analysis at the indicated timepoint post-transfection. Although EGFP expression from MLP-TetO1a was not repressed by the TetR, both MLP-TetO1b and -TetO2 exhibited >80% promoter repression by TetR (****P≤0.0001) at 72hpt, when compared to the activity of wt-MLP (**Figure 3.2D**). This suggested that only the TetO site downstream of the TAT box was functional, and that binding of TetR downstream of the MLP TATA box is required to inhibit basal transcription activity. Notably, MLP-TetO2 showed relatively limited activity even in the presence of doxycycline, whereas the MLP-TetO1b exhibited full alleviation from TetR repression with doxycycline at 24, 48 and 72 hpt.

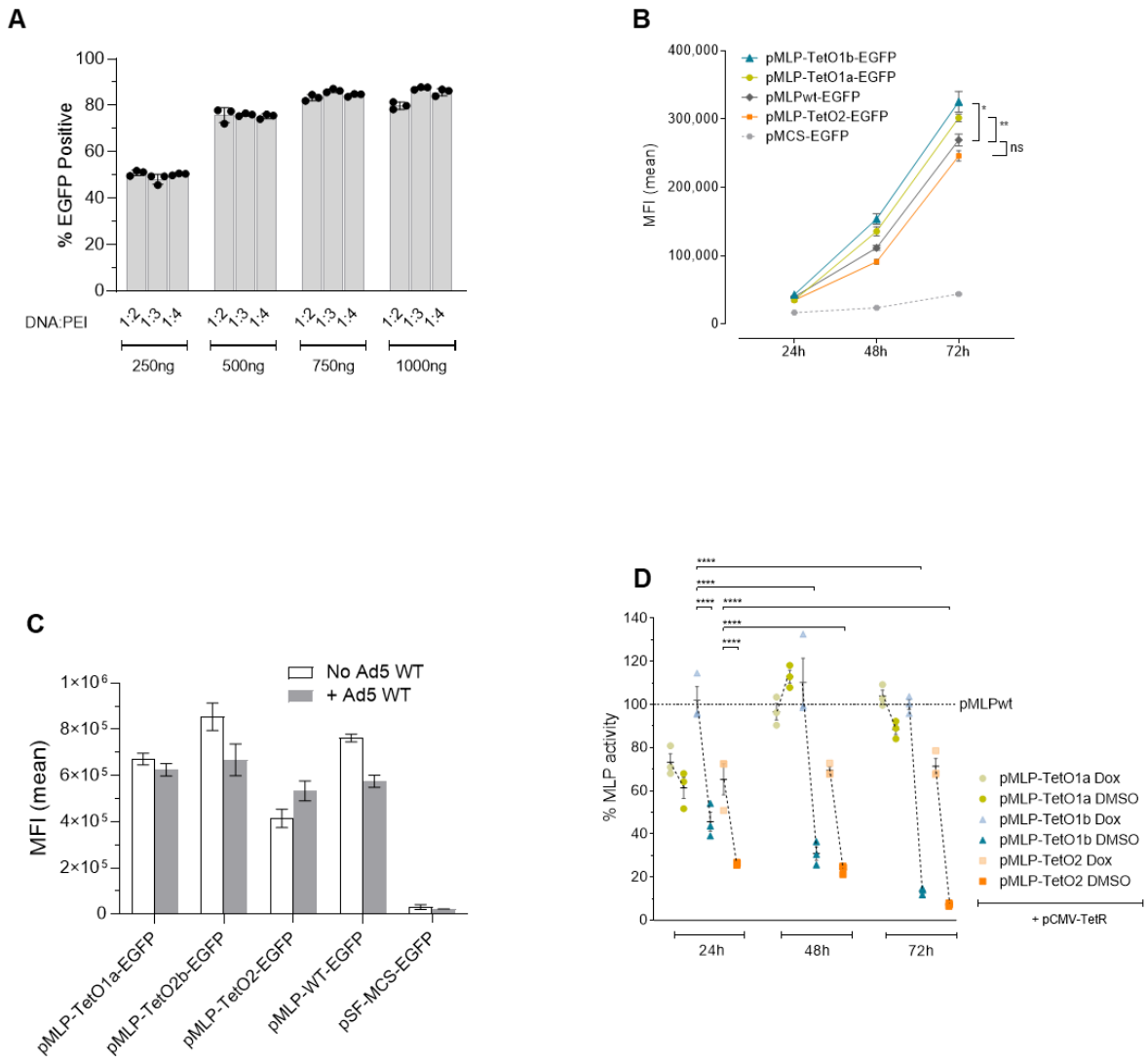


Figure 3.2 Repression of MLP expression plasmids by TetR. A) Optimizing transient transfection of HEK293 cells using linear PEI. Increasing amounts (ng) of a CMV EGFP expression plasmid was complex using linear PEI (25kDA) at the indicated DNA:PEI mass ratio and transfected into HEK293 cells. EGFP expression was measured by flow cytometry at 48hpt. Data presented as percentage of EGFP positive cells. **B**) Mean fluorescent intensity (MFI) of EGFP expressing HEK293 cells transfected with pMLP-TetO, pMLPwt or promoterless (pMCS) EGFP plasmids. **C**) MFI of HEK293 cells transfected with MLP plasmids, either infected with WT Ad5 (MOI5) or left untreated. Cells were analysed by flow cytometry at 48hpt. **D**) Transcriptional repression of MLP-TetO promoters by plasmid encoding TetR in HEK293 cells treated with doxycycline 0.2 µg/mL or DMSO. Data presented as percentage of MLP transcription activity, based on MFI of EGFP-positive cells, compared to wildtype pMLPwt promoter. Data normalised for background EGFP expression using pMCS-EGFP and presented as mean ± SEM of triple biological replicates. Significance determined by two-way ANOVA ** P≤0.05, *** P≤0.01, ****P≤0.0001.

3.3.3 Engineering adenovirus vectors with TetO MLPs

To explore whether viable adenovirus vectors can be recovered despite such significant alterations to its MLP, an E1/E3Δ-Ad5 was engineered to encode MLP-TetO1a, MLP-TetO1b or MLP-TetO2 in place of its wt-MLP promoter sequence.

Initially, a shuttle plasmid was constructed to encode the Ad5 E2/MLP sequence corresponding to nucleotides 4840 to 10816 of wt Ad5 (accession no: AY339865.1) to increase the availability of unique restriction sites available for cloning. Here, a 4.2 Kb fragment encompassing the wt-Ad5 MLP was extracted from a plasmid encoding the genome of a wt Ad5 (T38; provided by OXGENE) by PCR (primers: appendix 2.1) and inserted via Gibson assembly into the ClaI position of a kanamycin resistance (KanR) plasmid (OG10; provided by OXGENE). Subsequently, this intermediate plasmid (P4481) was further modified by insertion of an extended DNA sequence mapping to the E2B region of Ad5. The 2.7 Kb E2B fragment was extracted by PCR (primers: appendix 2.2) from an E1/E3-Ad5 plasmid (OG268; provided by OXGENE) and inserted into P4481 linearised with BsrGI and NheI via Gibson assembly. As a result, this created the Ad5 E2/MLP-shuttle plasmid pSU43 (not shown), which was used for DNA sequence exchange of the wildtype MLP sequence in place of MLP-TetO1a, MLP-TetO1b, or MLP-TetO2. Here, the MLP-TetO promoter fragments were excised from pUC57 backbone plasmids using PcII and DraIII and cloned into Ad5-E2/MLP-shuttle plasmid digested with the same enzymes to generate the corresponding Ad5-E2/MLP-TetO1a (pSU51), -TetMLP-O1b (52) and -MLP-TetO2 (pSU48) shuttle plasmids.

Schematic diagram for the exchange of the wt MLP in place of TetO modified variants using Ad5-E2/MLP-shuttle plasmids is illustrated in **Figure 3.3A**. A 5.7kb DNA fragments encoding the MLP-TetO1a, MLP-TetO1b, or MLP-TetO2 were extracted from the Ad5-E2/MLP-shuttle plasmid using SphI and NheI and cloned E1/E3-Ad5 genome plasmid (OG268; provided by OXGENE) that was linearized using Bstz17I and XbaI. The Ad5-E2/MLP-shuttle plasmid was designed for efficient

insertion into the large E1/E3-Ad5 genome by DNA assembly method using SnapFast assembly reagent (OXGENE), as digest with SphI and NheI generated a 5.7kb MLP-TetO-encoding fragment with a 5' homology arm (625bp) and 3' homology arm (220bp) corresponding to 3' and 5' arms, respectively, of the Bstz17I and XbaI digested E1/E3-Ad5 genome plasmid. The resulting plasmids encoding the E1/E3-Ad5 genome with TetO modified MLPs, Ad5-MLP-TetO1a (pSU208), Ad5-MLP-TetO1b (pSU196), and Ad5-MLP-TetO2 (pSU233), were confirmed by DNA digest using enzymes XbaI and ClaI (**Figure 3.3B**), and Sanger sequencing. Throughout this thesis, the chosen clone is indicated by red tick symbol.

To assess recovery of viable vectors, DNA plasmids encoding the Ad-MLP-TetO genomes alongside the control E1/E3Δ-Ad5 were linearized with SwaI to release the Ad5 genome from the bacterial backbone and transfected into HEK293 cells. Surprisingly, plaques were visible from all Ad vectors at ~8 days post-transfection, indicating viable vectors can be produced despite the modifications to the MLP and opposing E2B region. All four Ad vectors were harvested at 14 days post-transfection and further amplified in HEK293 cells for subsequent characterisation.

3.3.4 Repression of TetO modified Adenovirus vectors in Flp-In T-REx 293 cells

To assess whether repression of the MLP inhibits virus spread, we initially assessed replication of MLP-TetO modified vectors in Flp-In T-REx 293 cells, stably expressing the TetR. Crude vector preparations were used to infect (at a MOI of 1) Flp-In T-REx 293 cells and subsequently treated with doxycycline or DMSO. Cell monolayers were monitored using light microscopy for adenovirus cytopathic-effect (CPE) over a 10 day period (**Figure 3.3C**). As expected, vector replication of the control E1/E3Δ-Ad5 or Ad5-MLP-TetO1a were not hindered in the cells as CPE can be observed at

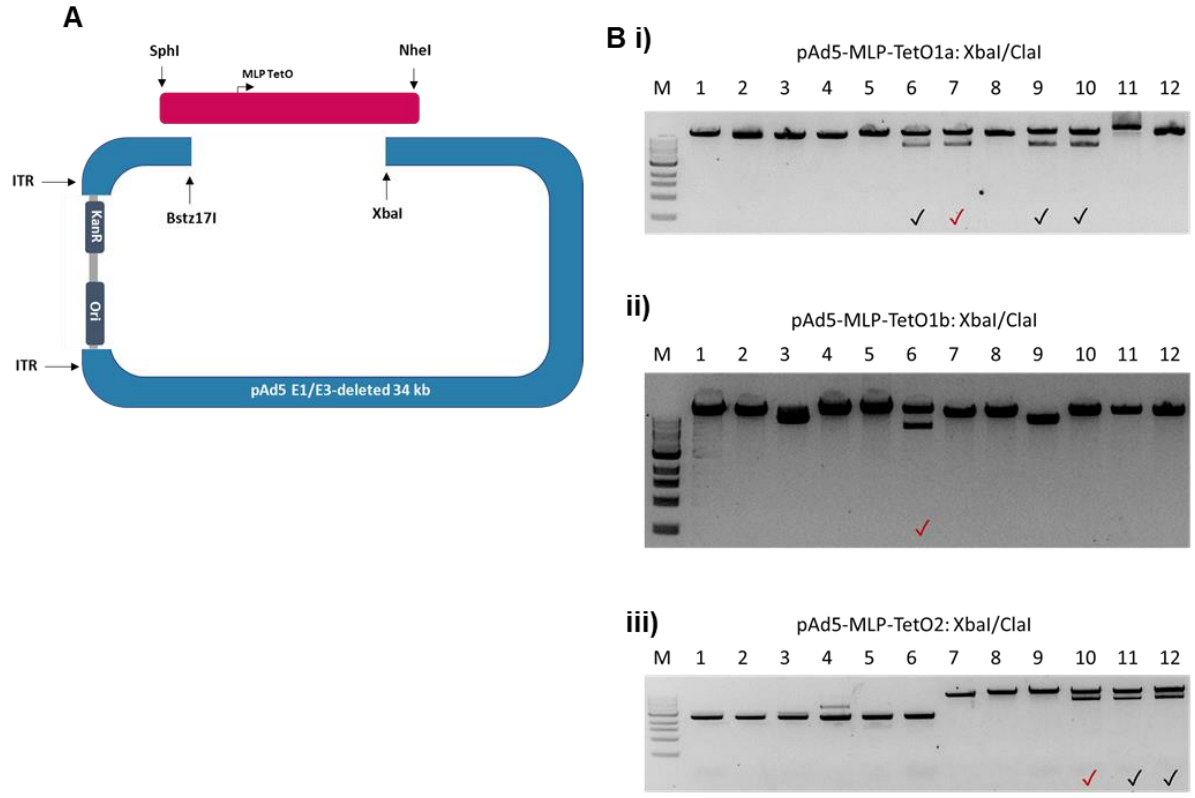
day 4 post-infection (data not shown) in both the DMSO and doxycycline treated samples. This was expected because neither virus is sensitive to the TetR. In Flp-In T-REx 293 cells infected with Ad5-MLP-TetO1b and Ad5-MLP-TetO2, viral plaques were only observed when the cells were cultured with doxycycline, while the DMSO control group exhibited an attached monolayer without viral plaques. This was also as expected, because the TetR should inhibit the latter life cycle stages of both viruses except in the presence of doxycycline.

At day 10, cells infected with E1/E3Δ-Ad5 or Ad5-MLP-TetO1a exhibited advance CPE, with full detachment of the monolayer and cells rounding up, in both the DMSO and doxycycline-treated groups. However, advance CPE were only observed in Flp-In T-REx 293 cells infected with Ad5-MLP-TetO1b or Ad5-MLP-TetO that were treated with doxycycline, while in the DMSO group cells still exhibited a healthy attached monolayer with only a few cells rounding up. This result, consistent with evaluation of the MLP reporter plasmids using TetR (**Results 3.3.2**), indicates that promoters MLP-TetO1b and MLP-TetO2 can be repressed by the TetR from Flp-In T-REx 293 cells to control viral replication and the additional of doxycycline alleviated this control.

3.3.5 Adenovirus genome replication is maintained during MLP repression

The lytic life cycle of Ad5-TetO1b and Ad5-TetO2 was inhibited in Flp-In T-REx 293 cells, which stably express the TetR. Since the TetR is intended to inhibit the MLP but not necessarily adenovirus genome replication, we assessed whether genome replication was inhibited or not. Total DNA was extracted from Flp-In T-REx 293 cells at day 10 post-infection from TetO modified Ad5 or the control Ad5 vectors. Viral genomes were determined by QPCR using primers and probe directed against the virus fibre gene sequence. As shown in **Figure 3.3D**, control E1/E3Δ-Ad5, Ad5-

TetO1a and Ad5-TetO1b showed comparable levels of viral genomes in both the doxycycline and DMSO-treated groups. This indicates that DNA amplification is maintained unaffected in Ad5-TetO1b even in the absence of doxycycline, despite repression of virus spread observed under light microscopy (Figure 3.3B). Ad5-TetO2 exhibited a slight reduction in adenovirus genomes (**P≤0.01) when cells were treated with DMSO (where the MLP was repressed) compared to doxycycline. Therefore, we decided to proceed to prioritize adenoviruses encoding MLP-TetO1b for future work as that configuration allowed similar levels of genome replication when the MLP was repressed (DMSO-treated group) compared to during active virus replication (doxycycline-treated group).



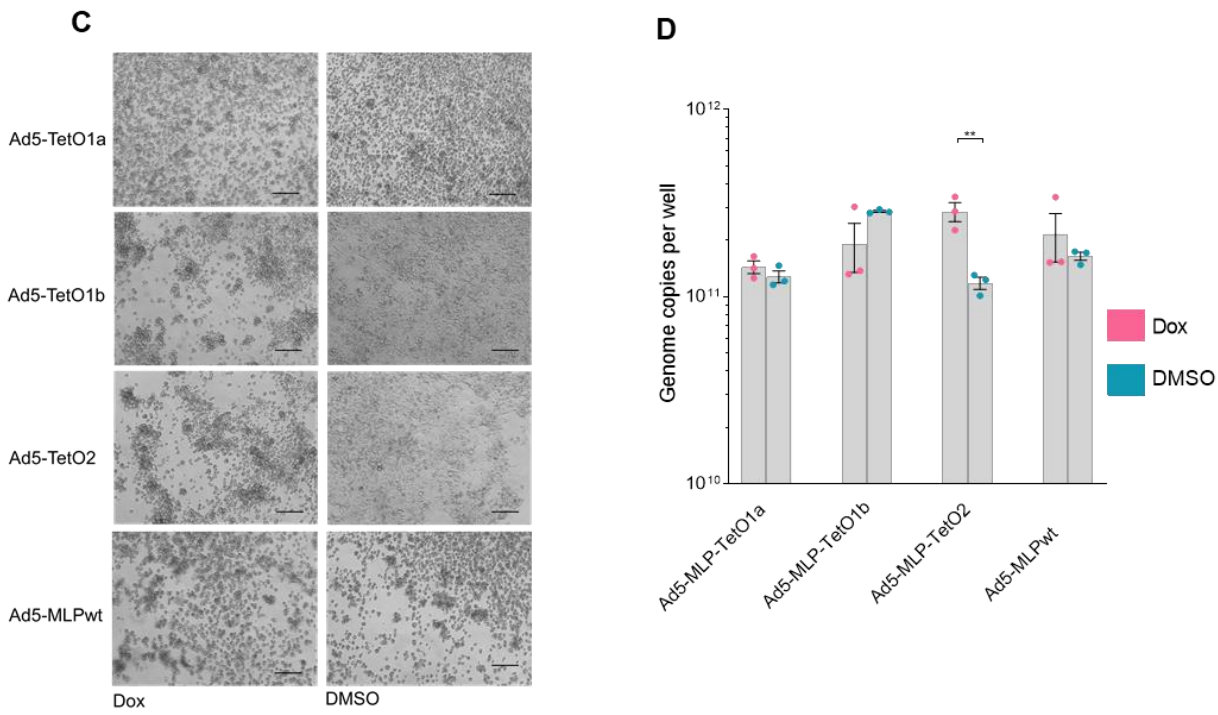


Figure 3.3 Repression of Adenovirus MLP by TetR inhibits virus replication. A) Cloning schematic for exchange of wt MLP for TetO-modified MLP variants via DNA assembly cloning. **B)** XhoI and ClaI restriction digest to confirm correct insertion of (i) MLP-TetO1a, (ii) MLP-TetO1b, and (iii) TetO2-MLP into pAd5-E1/E3-deleted plasmid. **C)** Flp-In-T-Rex-293 cells infected with Ad5-MLPwt, Ad5-TetO1a, Ad5-TetO1b or Ad5-TetO2 (MOI of 1) and treated with doxycycline 0.2 µg/mL or DMSO. Cell monolayer imaged by brightfield microscopy 10 days post-infection. Scale bar, 250 µm. **D)** Adenoviral genome replication in Flp-In-T-Rex-293 cells. Total DNA harvested 10 days post infection and viral genomes quantified by qPCR against Ad5 fibre. Data are presented as mean ± SEM of triple biological replicates. Significance determined by Unpaired t-test **P≤0.01.

3.3.6 MLP repression blocks adenovirus spread in Flp-In T-REx 293

To visually monitor repression of Ad5-MLP-TetO1b replication in Flp-In T-REx 293, a CMV-EGFP reporter expression cassette was inserted into the E1-deleted region of Ad5-MLP-TetO1b or the control E1/E3Δ-Ad5. To this end, the EGFP coding sequence was extracted from plasmid pSF-CMV-EGFP (OG4728; provided by OXGENE) using NcoI and NheI, and inserted into the multiple-cloning-site MCS of an E1-shuttle plasmid pSF-E1A-CMV-Shuttle (P7842; provided by OXGENE) linearized

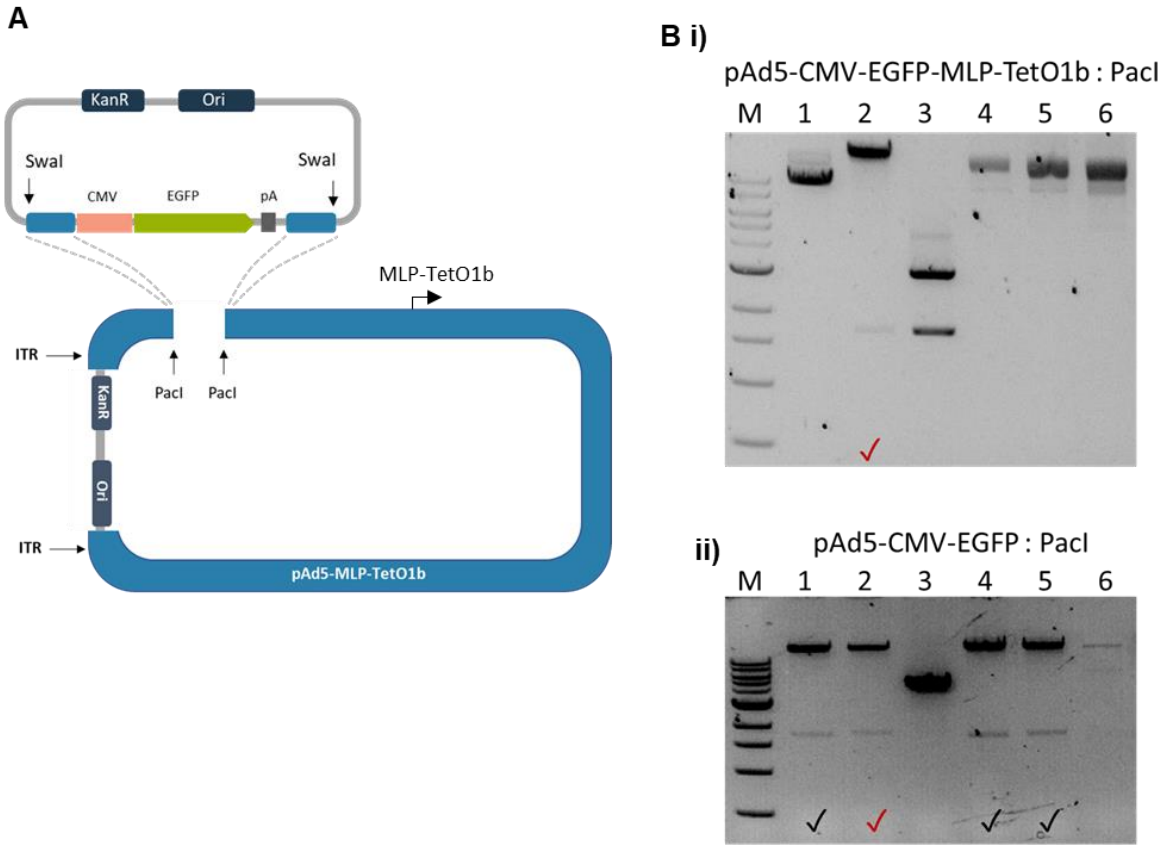
with the same enzymes. Clones were screened by restriction digest and confirmed by Sanger sequencing (appendix).

As shown in **Figure 3.4A**, the E1-shuttle plasmid is designed for efficient insertion of transgenes into the E1-deleted region of the Ad5 vector. Flanking the transgene expression cassette is a 5' homology arm (~190bp) and a 3' homology arm (~110bp) corresponding to 3' and 5' arms, respectively, of the PacI digested E1/E3-Ad5 genome plasmid. The DNA homology arms enable efficient cloning into the large E1/E3-Ad5 genome plasmid via exonuclease-based method such as Gibson assembly (Chao, Yuan, and Zhao 2015). For insertion into the Ad vector genome, the CMV-EGFP expression cassette was excised using SwaI from the E1-shuttle EGFP plasmid (pSU151) and cloned into the PacI position of Ad5-MLP-TetO1b or the control Ad5 vector using Snapfast assembly reagents (provided by OXGENE). As shown in **Figure 3.4B**, positive clones for Ad5-MLP-TetO1b (**i**) or E1/E3Δ-Ad5 (**ii**) encoding the CMV-EGFP cassette were screened by PacI restriction digest.

For Ad vector recovery, plasmid DNA encoding the Ad5-CMV-EGFP-MLP-TetO1b and Ad5-CMV-EGFP were linearized with SwaI to release the Ad5 ITRs from the bacterial backbone and transfected into HEK293 cells. Vectors were harvested 14 days after transfection. Ad5-CMV-EGFP-MLP-TetO1b and Ad5-CMV-EGFP were used for infection of Flp-In T-REx 293, expressing TetR, at an MOI of 0.1 and cultured with DMSO or doxycycline. EGFP expression was monitored for 6 days post-infection using fluorescence microscopy. As shown in **Figure 3.4C**, while viral replication and spread, determined by EGFP expression across the cell monolayer and presence of viral plaques, was not inhibited in the control Ad, spread of Ad5-CMV-EGFP-MLP-TetO1b was repressed as expected in the absence of doxycycline, presumably by the endogenous TetR. Assessment of EGFP expression showed that the vector was largely confined to isolated cells, probably those infected

from the initial inoculation. In contrast, in the presence of doxycycline, replication of Ad5-CMV-EGFP-MLP-TetO1b, was comparable to the control virus.

However, although replication of Ad5-CMV-EGFP-MLP-TetO1b was significantly repressed in Flp-In T-REx 293 (in the absence of doxycycline) as expected, there was also some evidence of escape from repression with the appearance of viral plaques, particularly as the infection timepoint progressed or when the vector was used at a high MOI (>10) (not shown). This suggested the ability of TetR in Flp-In T-Rex 293 cells to inhibit the MLP could be overcome when the level of virus genomes was sufficiently high.



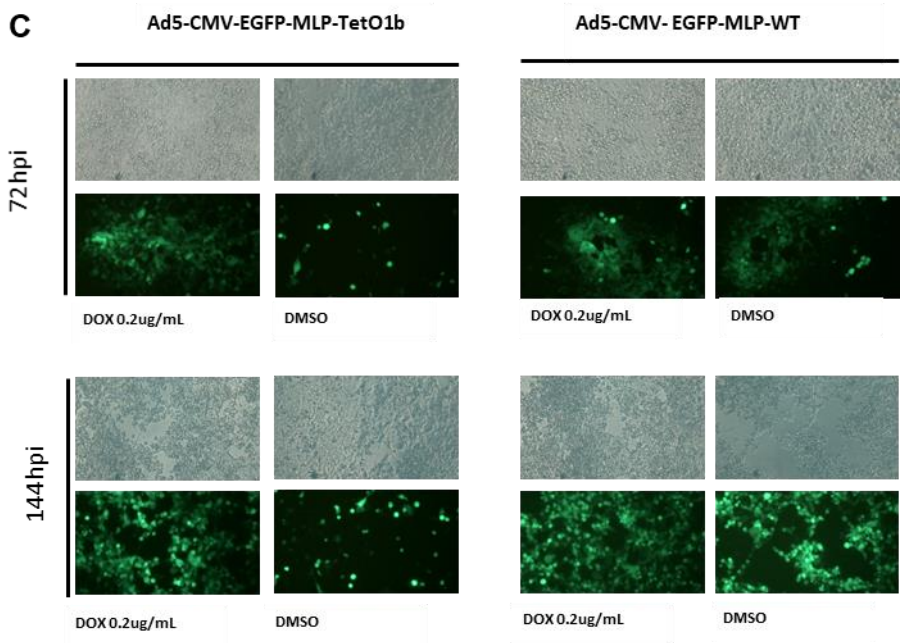


Figure 3.4 Repression Adenovirus MLP inhibits virus spread. A) Cloning schematic for insertion of the CMV-EGFP expression cassette into the MLP-TetO1b modified and MLP-WT Ad5 E1/E3-deleted control plasmid via DNA assembly cloning. **B**) PacI restriction digest for screening correct insertion of the CMV-EGFP into the (i) MLP-TetO1b or (ii) MLP-WT Ad5 E1/E3-deleted plasmid. **C**) HEK293 cells transduced with control Ad5 or Ad5 MLP-TetO1b vector encoding CMV-EGFP at an MOI 0.1 and treated with doxycycline 0.2 µg/mL or DMSO. Cells imaged at day 6 post-infection by fluorescence microscopy.

3.3.7 Engineering of TESSA – expression of TetR under control of the virus MLP

As the Ad5-CMV-EGFP-MLP-TetO1b genomes are exponentially amplified in the Flp-In T-REx 293 cell following infection, the observed escape of vector repression from control by TetR may be due to the limited production of TetR proteins from the Flp-In T-Rex 293 cells or perhaps to inhibition of cellular cap-dependent translation machineries by the Ad5 vector, a strategy adopted by adenovirus to prioritise viral derived mRNA transcripts (Schneider 1995). Furthermore, the requirement to provide the TetR protein *in trans* to inhibit the encoded MLP-TetO1b limits the

broad utility of the adenoviral vector and effectively restricts its use to 293-based TetR expressing cell lines.

To address these issues, Ad5-TetO1b was further engineered to encode a TetR adjacent to a splice-acceptor site under transcriptional control of the virus MLP, meaning the active MLP actually expresses TetR and thereby providing a negative-feedback loop to allow MLP self-repression. This strategy should be more resilient when the adenovirus genome replicates because each copy has the ability to produce TetR if the MLP starts to activate, whilst simultaneously maintaining the ability of doxycycline to reverse the suppression. The resulting adenovirus is entitled TESSA (*Tetracycline Enabled Self-Silencing Adenovirus*). Schematic of TESSA is shown in **Figure 3.5A**.

To engineer TESSA an E3-shuttle plasmid (pSU149) encoding the Ad5 L4-E3-L5 coding segments was initially modified by insertion of a splice acceptor element and the TetR coding sequence. The tetR, including SV40 polyA termination, sequence was extracted by PCR (primers: appendix 2.3) from template pSF-CMV-TetR (OG4156; provided by OXGENE) and inserted into the E3-shuttle plasmid linearized with SalI to generate the plasmid pE3-TetR-shuttle (pSU375). Positive clones were isolated and confirmed by restriction digest (**Figure 3.5B**) and Sanger sequencing.

Subsequently, a 4.1kb DNA fragment containing TetR embedded between the L4 and L5 coding sequence was excised from pE3-TetR-shuttle (pSU375) using NdeI and AscI and ligate into the Ad5-MLP-TetO1b (pSU196) genome plasmid, that was digested with the same enzymes. Cloning strategy is shown illustrated in **Figure 3.5C**. This generated an intermediate genome plasmid (pAd5-MLP-TetO1b-ΔL2-4-tetR (pSU382)) as digest of the Ad5-MLP-TetO1b (pSU196) with AscI also released the L2-L4 coding sequence. Positive clones of pAd5-MLP-TetO1b-ΔL2-4-tetR were isolated and confirmed by restriction digest (**Figure 3.5D**) and Sanger sequencing.

To reinsert the L2-L4 coding sequence for reconstitution of the full Ad5 genome, a large 13.1kb DNA fragment containing L1-L4 was excised from the Ad5-MLP-TetO1b (pSU196) plasmid and inserted into pAd5-MLP-TetO1b-ΔL2-4-tetR (pSU382) linearized with AscI using Snapfast assembly reagent (provided by OXGENE), as shown in **Figure 3.5E**. This reconstituted plasmid DNA encoding the full TESSA genome (pSU390; Ad5-MLP-TetO1b-SA-TetR). Clones were isolated and confirmed by restriction digest (**Figure 3.5F**) and Sanger sequencing.

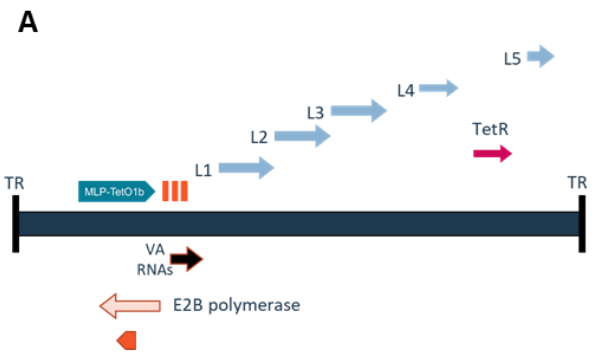
For vector recovery, plasmid DNA encoding TESSA linearized with SwaI was transfected into HEK293 cells. Cells were subsequently cultured with doxycycline (to inhibit activity of the TetR protein produced by the active MLP) or DMSO. In parallel, HEK293 cells were transfected with a E1/E3Δ-Ad5 genome as a control for vector recovery. Viral plaques were observed on the cell monolayer from ~6-7 days post-transfection in cells transfected with the E1/E3 Δ -Ad5 genome or with TESSA only in the presence of doxycycline. This suggested that this configuration of TetR inserted into the E3-deleted region did not affect the production of viable vectors and that activity of the TetR was inhibited by doxycycline. This result was consistent up to day 13 post-transfection, when TESSA vectors were harvested from the doxycycline-treated group displaying advance CPE, while cells transfected with TESSA and cultured in DMSO still showed no noticeable plaques (data not shown). These observations suggest that expression of the TetR from TESSA (in the absence of doxycycline) enabled self-repression of MLP-TetO1b to block production of viral structural proteins and thereby prevent particle formation.

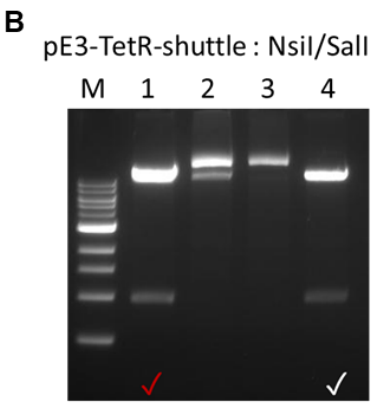
TESSA was sequentially passaged alongside the control Ad5 for two further rounds in HEK293 cells, with doxycycline added to TESSA infected cell cultures, and crude preparation used for inoculation of HEK293 cells seeded in HYPERFlasks. After two sequential rounds of CsCl gradient banding, the control Ad5 and TESSA yielded high titre viral particles of 7.65×10^{12} (viral particles (vp)) per HYPERFlask and 7.05×10^{12} vp per HYPERFlask, respectively. Comparable yields obtained

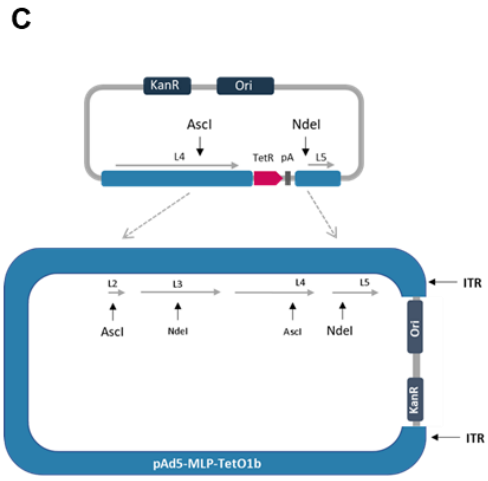
between the control Ad5 and TESSA suggest that the vector is stable as it exhibited similar replication kinetics.

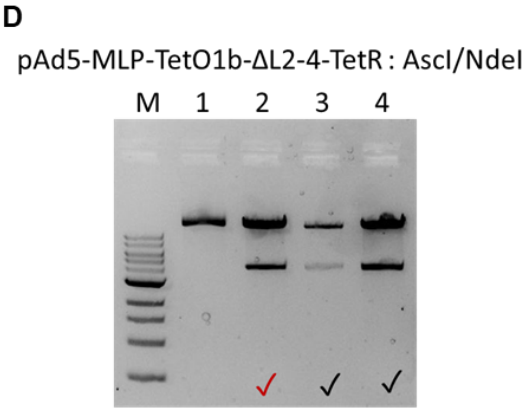
3.3.8 Assessing the potency of the TESSA MLP self-repression loop

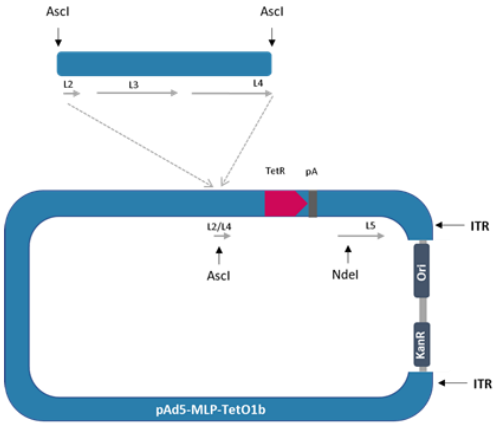
To assess the ability of the encoded TetR to repress TESSA viral replication, HEK293 cells were infected with TESSA or the control Ad5 (at an MOI of 5) and treated with DMSO or doxycycline. At day 3 post-infection vectors were harvested and levels of infectious adenoviruses were quantified using a TCID50 assay in HEK293 cells supplemented with doxycycline (to enable replication of any TESSA vectors). TCID50 assay results confirmed that TESSA produced from HEK293 cells in the presence of doxycycline yielded an equivalent titre compared to the control virus (>1e8 TCID50/mL), while the DMSO group showed over 5 x 10^7-fold reduction in infectious vectors (**Figure 3.5G**). Representative brightfield microscopy images of the TCID50 assay taken at day 9 post-infection is shown in **Figure 3.5H**. Viral plaques were notable in all wells (10/10) infected at 1 in 1x10^6 volume dilution with the control-Ad5 or TESSA produced from HEK293 cells with doxycycline, indicating that TESSA produced in this way shows equivalent plaque-forming potency as the control virus. In contrast, at the much higher virus concentration (1 in 10 volume dilution of the crude preparations), while the control virus showed extensive plaque formation, only ~2-3 out of 10 wells showed plaques from TESSA produced in DMSO. This virtual absence of infectious viruses indicates that the MLP-TetO1b structure, with MLP-controlled TetR, gives almost total repression of adenovirus production in the absence of doxycycline.

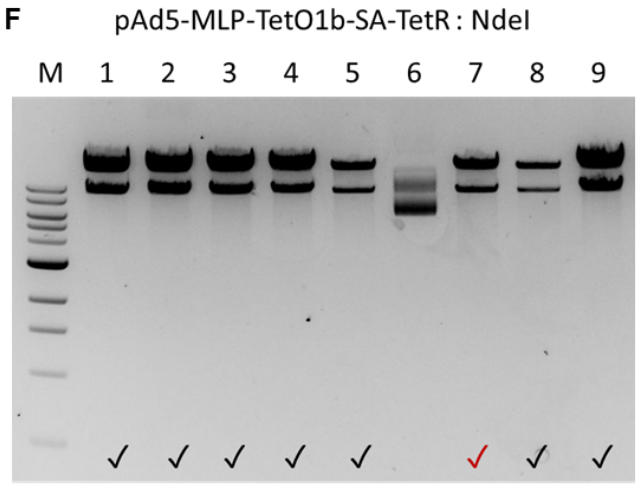

A
L5
L4
L3
L2
L1
TetR
TR
MLP-TetO1b
TR
VA
RNAs
E2B polymerase


B
pE3-TetR-shuttle : NsiI/SalI
M 1 2 3 4


C
KanR
Ori
AscI
NdeI
L4
TetR
pA
L5
L2
L3
L4
L5
AscI
NdeI
AscI
NdeI
ITR
Ori
KanR
ITR
pAd5-MLP-TetO1b


D
pAd5-MLP-TetO1b-ΔL2-4-TetR : AscI/NdeI
M 1 2 3 4


E
AscI
AscI
L2
L3
L4
TetR
pA
L2/L4
L5
AscI
NdeI
ITR
Ori
KanR
ITR
pAd5-MLP-TetO1b


F
pAd5-MLP-TetO1b-SA-TetR : NdeI
M 1 2 3 4 5 6 7 8 9

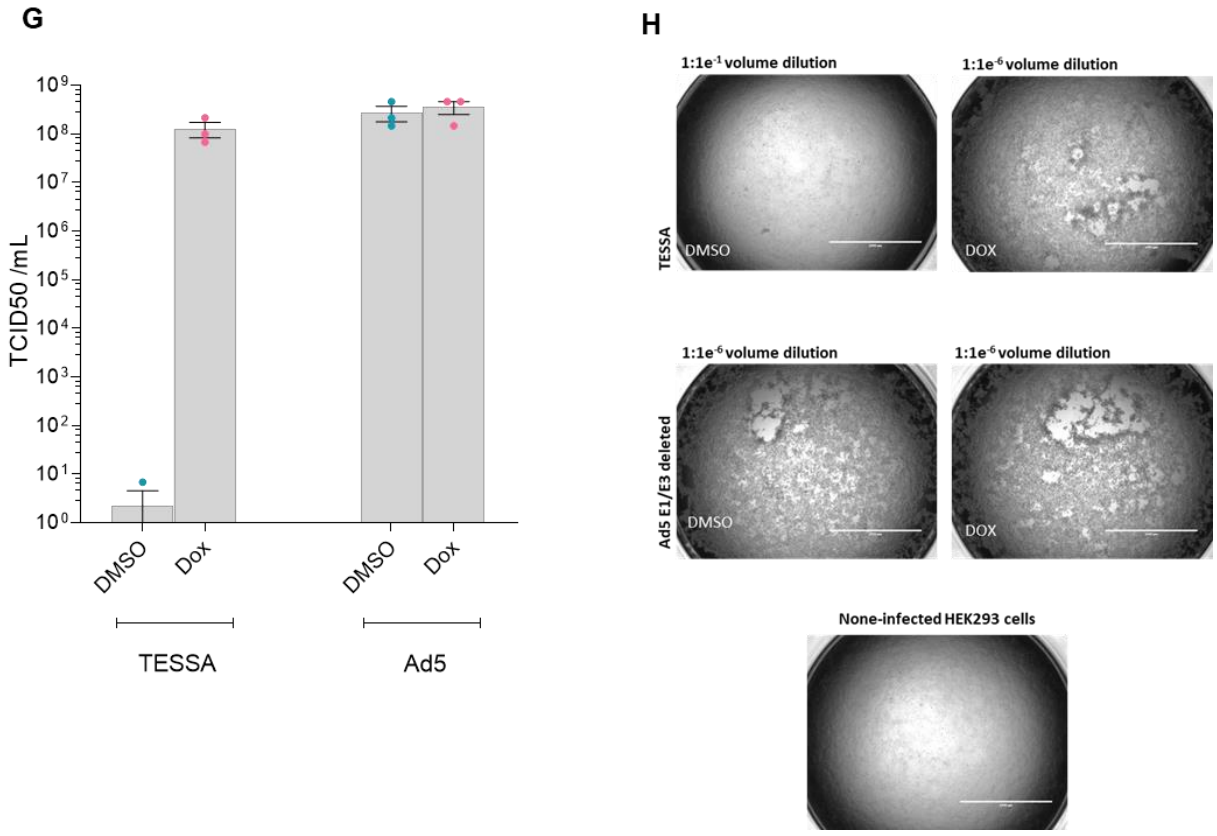


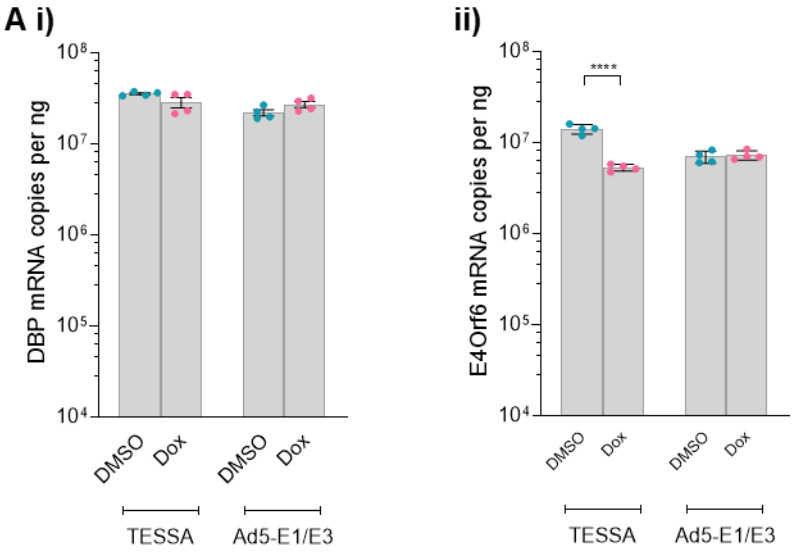
Figure 3.5 TESSA expresses TetR to enable self-repression of MLP and adenovirus replication. A) Genome schematic of TESSA encoding TetR under transcriptional control of MLP-TetO1b. **B**) NsiI and SalI restriction digest for screening correct insertion of tetR in the Ad5 E3-shuttle plasmid. **C**) Cloning schametic for insertion of the TetR coding sequence into plasmid pAd5-MLP-TetO1b. As shown, restriction cloning resulted in removal of Ad5 E2-E4 coding sequence. **D**) AscI and NdeI restriction digest for screening correct insertion of tetR into the intermediate plasmid (pAd5-MLP-TetO1b-ΔE2-E4-TetR). **E**) Cloning schametic for re-insertion of the Ad5 E2-E4 coding sequence into pAd5-MLP-TetO1b-ΔE2-E4-TetR and (**F**) screening correct clones by NdeI restriction digest. **G**) TCID50 assay for quantification of infectious TESSA or control Ad5 vectors produced in HEK293 cells. HEK293 cells were innoculated with TESSA or Ad5 vectors at an MOI of 5 and cultured with DMSO or doxycycline 0.5 µg/ml. Vectors were harvested 72hpi and infectious particles from crude preparations were quantified by the TCID50 assay using HEK293 cells, and cultured with doxycline 0.5 µg/ml. **H**) Representative brightfield images of HEK293 cells infected, at the indicated dilution, with crude preparation of TESSA and Ad5 vectors (both doxycycline and DMSO group). Cells were cultured doxycycline 0.5 µg/mL and imaged at day 9 post-infection.

3.3.9 TESSA maintains expression of early genes and helper functions for AAV production

We next determined the effect of MLP repression on expression of adenovirus early genes E2A DBP and E4Orf6, which are known to be important for AAV replication. HEK293 cells were infected with TESSA or control-Ad5 at an MOI of 10 and cultured with DMSO or doxycycline. Total RNA was extracted 72 hpi and quantified by RT-qPCR using primers and probe against Ad5 E2A and E4Orf6. As shown in **Figure 3.6A**, comparable levels of (**i**) E2B DBP mRNA were detected from the control-Ad5 or TESSA replication in HEK293 cultured with DMSO or doxycycline. Intriguingly we observed a ~3-fold increase in (**ii**) E4Orf6 mRNA levels in TESSA cultured in DMSO compared to doxycycline. The exact reason for this is not yet known, but might suggest that MLP repression somehow increases production of E4Orf6. Similarly, increase in expression of adenovirus early genes from virus mutant deficient in transcription from the MLP was reported (Fessler and Young 1998).

TESSA is designed to express all of the adenovirus early genes and none of the late genes. Since the late genes are not thought to play a role as helper proteins in AAV production, we hypothesise that TESSA will provide all of the essential helper functionalities. To assess whether this is the case, HEK293 cells were infected, at an MOI of 10, with TESSA or the E1/E3-deleted Ad5 control and co-transfected using plasmid pRepCap2 with the AAV transfer vector encoding an EGFP reporter (pSF-AAV-EGFP). rAAV2 production was compared to transfection of the helper-free plasmids (pRepCap2, with pHelper and pAAV-EGFP). Vectors were harvested 96 hpt and treated with Turbo® DNase I to degrade cellular and non-encapsidated DNA. To determine efficiency of the DNAse treatment and control unencapsidated vector genomes, cells were transfected in parallel with pRepCap2, pAAV-EGFP and stuffer DNA pOG10 (in place of pHelper; OXGENE). Intact rAAV vectors were measured by EGFP-specific qPCR. As shown in **Figure 3.6B**, while comparable yields of rAAV2 (~$1.7x10^9$ GC/mL) were observed from the between cells infected with the TESSA-

helper and transfected with the helper-free plasmids, cells infected with the control Ad5 produced 9.8x10^8 GC/mL of intact rAAV2. Levels of contaminating adenovirus particles were also measured by Hexon-specific qPCR. As expected, while intact Ad5 vectors were measured at ~5x10^8 GC/mL from cells infected with the E1/E3Δ-Ad5, adenovirus contaminations were not detected from the TESSA-infected cells, with average Ct values >36 and comparable to the helper-free samples. This result confirmed that TESSA can inhibit production of adenovirus particles and can function effectively as a helper virus for promoting rAAV production from cells transfected with pRepCap and the rAAV genome plasmid.



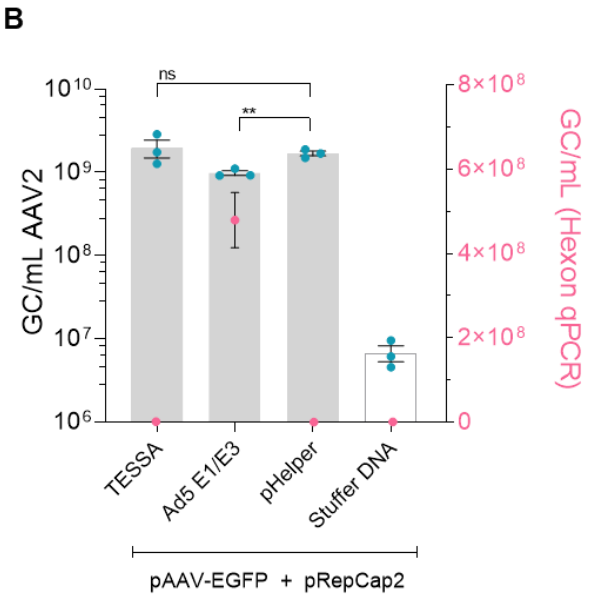


Figure 3.6 Adenovirus early genes are repressed during MLP repression to enable AAV replication. **A**) Expression of adenovirus early genes DBP (i) and E4Orf6 (ii) from TESSA or control-Ad5. HEK293 cells were infected with TESSA or Ad5 (MOI-10) and cultured with doxycycline 0.5 µg/mL or DMSO. Total RNA was extracted at 48 hpi and E4Orf6 and DBP mRNA levels quantified by RT-qPCR. Data is N=4 (mean ± SEM). **B**) Production of rAAV2 encoding EGFP using TESSA as helper virus. HEK293 cells were triple-transfected with the helper-free plasmids, or co-transfected using plasmid pRepCap2 with the AAV transfer genome and infected with TESSA or the control Ad5 E1/E3 deleted at an MOI10. Vectors were harvested 96hpt and encapsidated genomes quantified by EGFP-specific qPCR. Data presented as genome copies (GC) per mL. Data presented mean±SEM of triple biological replicates. Significance determined by Unpaired t-test **P≤0.01.

3.3.10 Engineering TESSA to encode the rAAV transfer genome

As TESSA enables delivery of all of the helper functions required for inducing AAV replication, we also explored its use in encoding the rAAV transfer genome to improve the efficiency of rAAV production. If successful, this approach would remove the need for transfecting the rAAV genome into packaging cells and should thereby increase the efficiency of the overall process. We introduced an rAAV genome encoding a CMV-EGFP expression cassette into the E1-deleted region of TESSA (creating TESSA-AAV-EGFP; genome schematic shown in **Figure 3.7A**). This hybrid virus was designed to exploit the extensive genome replication of adenovirus for amplification of the

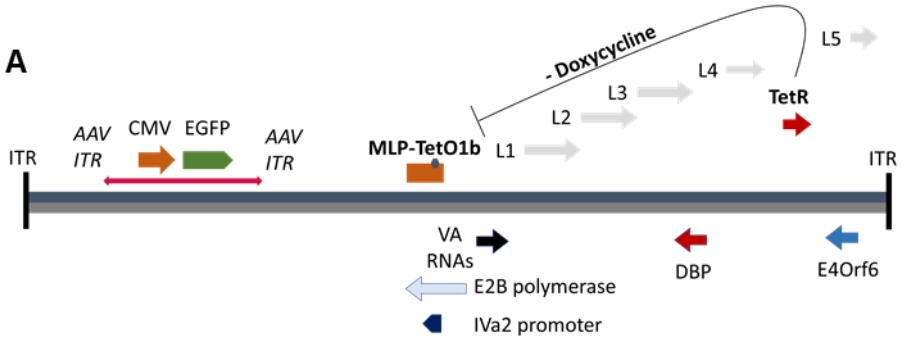
integrated rAAV sequence, allowing improved rAAV rescue and subsequent rAAV genome replication (Fisher et al. 1996). In parallel, as a control vector was constructed wherein the rAAV transfer vector was inserted into the E1-deleted region of a E1/E3Δ-Ad5.

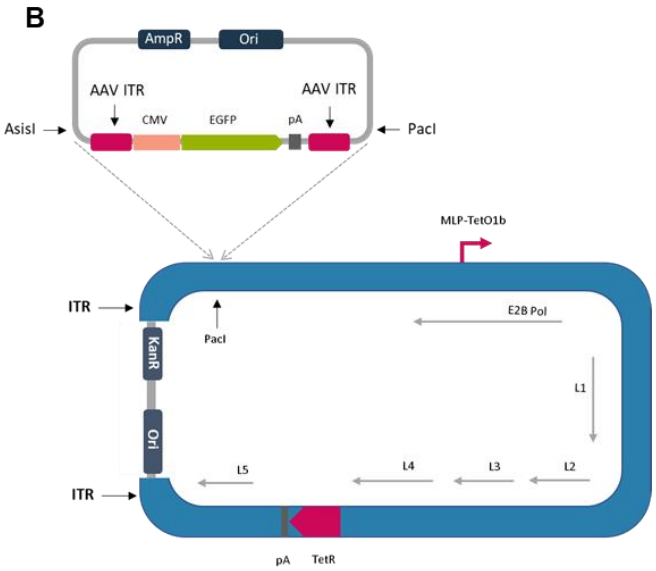
To construct TESSA or E1/E3Δ-Ad5 with the rAAV genome, a DNA fragment encoding the rAAV2 ITR-CMV-EGFP sequence was excised from plasmid pSF-AAV-EGFP (provided by OXGENE) using AsisI and PacI and ligated into PacI linearised plasmids encoding TESSA (pSU390) or E1/E3-deleted Ad5 (OG268) to generate TESSA-AAV-EGFP (pSU468) and Ad5-AAV-EGFP (pSU467), respectively (**Figure 3.7B**). Positive clones isolated and confirmed by restriction digest (**Figure 3.7C**).

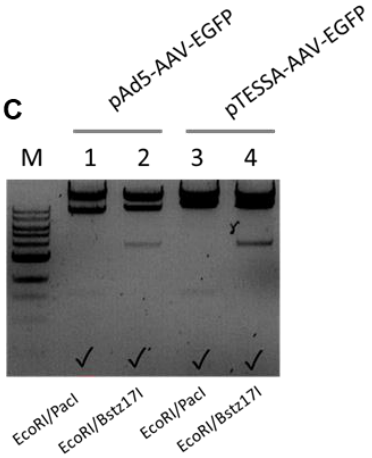
For vector recovery, plasmids encoding TESSA-AAV-EGFP and Ad5-AAV-EGFP were linearised with SwaI to release the Ad5 genome from the bacterial backbone and transfected into HEK293 cells. Both vectors were sequentially passaged for two further rounds in HEK293 cells and then amplified in HYPERFlasks. Following two rounds of CsCl-gradient banding, vectors were titred using the TCID50 assay and particles determined via PicoGreen assay. Infectivity and particle titres are shown in **Figure 3.7D**. The control Ad5-AAV-EGFP yielded was 3.1 x10 ^{12} vp/mL with a particle to infectivity ratio of 4.37, while TESSA-AAV-EGFP yielded a comparable titre of 3.1 x10 ^{12} vp/mL with a particle to infectivity ratio of 6.00. Purified TESSA-AAV-EGFP particles were further validated by negatively stained transmission electron microscope (carried out by Dunn School Bioimaging Facility, University of Oxford). As shown in **Figure 3.7 E&F**, TESSA-AAV-EGFP particles were indistinguishable from the control Ad5-AAV-EGFP.

Representative images of HEK293 cells infected with Ad5-AAV-EGFP or TESSA-AAV-EGFP are shown on **Figure 3.7G**. Cells were infected with purified vectors at 1 x 10^{-7} volume dilution and imaged at day 2 and day 9 post-infection. EGFP expression was positive from cells infected with both TESSA-AAV-EGFP and Ad5-AAV-EGFP at day 2 post-infection. However, while the Ad5-AAV-EGFP infection eventually spread across the well at day 9 and cells display advance CPE with cell

lysis and release of EGFP into the media, the spread of TESSA-AAV-EGFP is inhibited and remains confined to cells from the initial inoculation, confirming that self-repression of MLP-TetO1b from TESSA-AAV-EGFP remained intact.







D

Name	TCID50/mL	VP/mL	P/I ratio
Ad5-AAV-EGFP	7.1×10^{11} (SD ± 8.2×10^{10})	3.1×10^{12} (SD ± 1.6×10^{11})	4.37
TESSA-AAV-EGFP	6.5×10^{11} (SD ± 1.5×10^{11})	3.9×10^{12} (SD ± 1.4×10^{11})	6.00

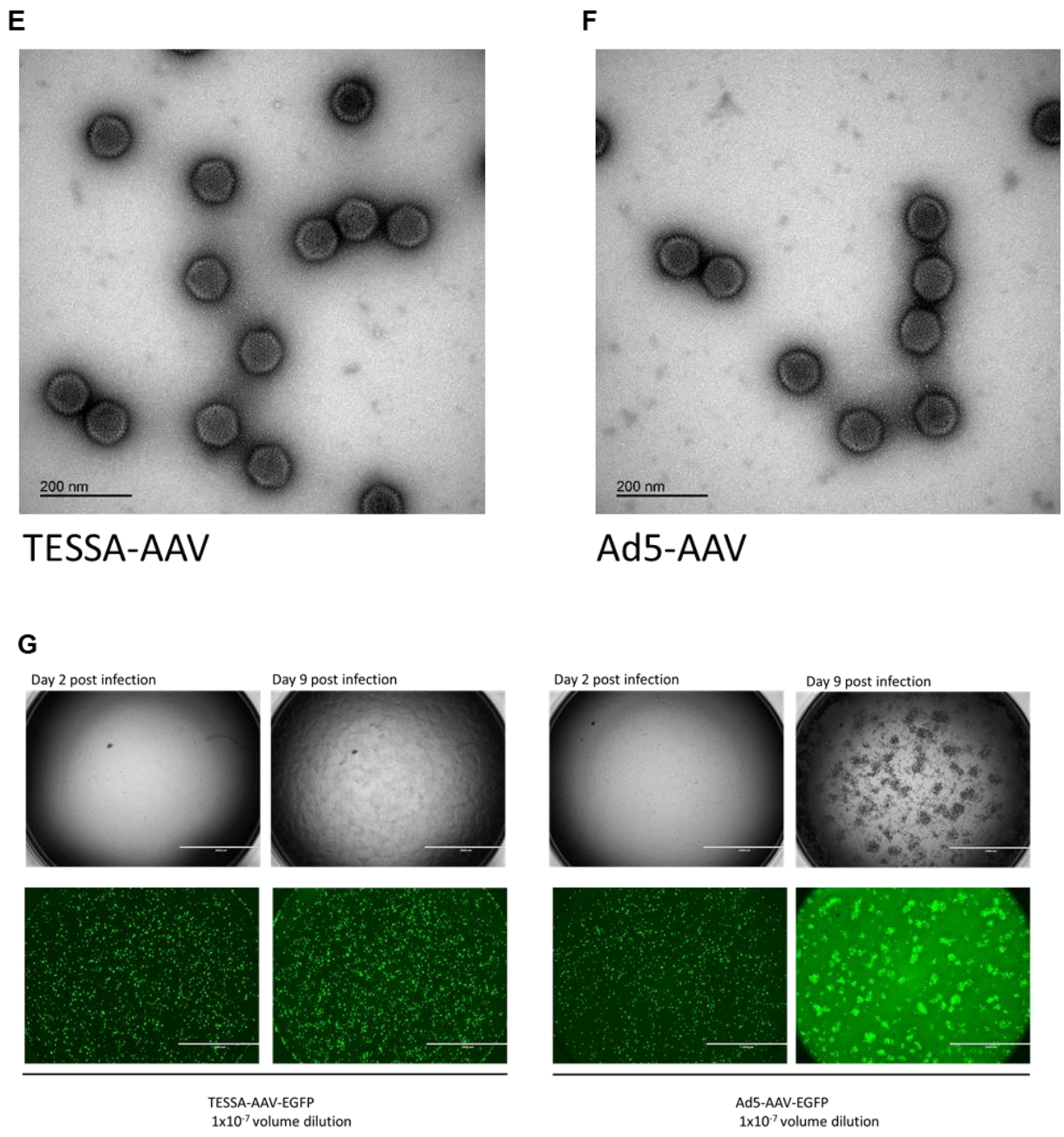


Figure 3.7 TESSA encoding the AAV transfer genome can be produced and purified at high titre. A) Genome schematic of TESSA-AAV-EGFP encoding the AAV transfer genome in the E1-deleted region of the adenovirus. **B**) Schematic for insertion of the AAV transfer genome into TESSA or the Ad5 E1/E3-deleted plasmid by restriction cloning. **C**) Restriction digest (restriction enzymes indicated) for screening correct clones with the insertion of AAV transfer genome. **D**) Comparison of infectious (TCID50/mL) and viral particle (vp/mL) titres determined using a TCID50 and PicoGreen assay, respectively, from TESSA-AAV-EGFP and Ad5-AAV-EGFP. Data N=3 and mean ± SD. Negatively stained electron microscopy images of purified (**E**) TESSA-AAV-EGFP and (**F**) Ad5-AAV-EGFP particles. **G**) Replication and spread of TESSA-AAV-EGFP is inhibited in HEK293 cells. Cells were infected with purified TESSA-AAV-EGFP or Ad5-AAV-EGFP at a 1 x 10^{-7} volume dilution and imaged at day 2 and day 9 post-infection.

3.3.11 Transcription of TetR from the MLP is higher in the presence of doxycycline but the TetR protein is unable to mediate promoter self-repression

In the absence of doxycycline, TESSA-AAV-EGFP is expected to undergo minimal MLP activity that produces sufficient TetR to inhibit the MLP, whereas in the presence of doxycycline the MLP remains active and the levels of TetR produced (which will be inactivated by binding to doxycycline) might be much higher. We therefore compared the levels of TetR mRNA produced by TESSA-AAV-EGFP in the presence and absence of doxycycline. Total RNA was extracted from HEK293 cells infected at an MOI of 10 with TESSA-AAV-EGFP and TetR mRNA measured by RT-qPCR. As shown in **Figure 3.8A**, at 24 hpi with TESSA-AAV-EGFP, a ~7-fold increase in TetR mRNA was already observable from cells treated with doxycycline (1.9×10^9 copies/well) compared to the DMSO group (3.3×10^8 copies/well). Transcription of TetR mRNA from the doxycycline-treated group increased by ~20-fold to maximum levels (4×10^{10} copies/well) measured at 48 hpi, with a slight decrease to 2.2×10^{10} copies/well at 72 hpi. This suggests high-level transcription of TetR from the virus, coupled with functional inhibition of the TetR protein by doxycycline to prevent repression of the MLP-TetO1b. In contrast, expression of TetR mRNA from TESSA-AAV-EGFP in the DMSO-treated group decline further to 2×10^8 copies/well and 1.3×10^8 copies/well at 48hpi and 72hpi, respectively. This represents a 202-fold fewer TetR mRNA transcript at 48hpi compared to doxycycline treatment and confirmed that the TetR can inhibit further transcription from MLP-TetO1b.

Expression of TetR protein was also determined using western blot. HEK293 cells infected at an MOI of 10 with TESSA or the control Ad5, and treated with doxycycline or DMSO, were harvested at 72 hpi for western blot analysis using an anti-TetR antibody. Similar to the mRNA expression

pattern, TetR protein was only detectable following infection with TESSA in the group treated with doxycycline (**Figure 3.8B**).

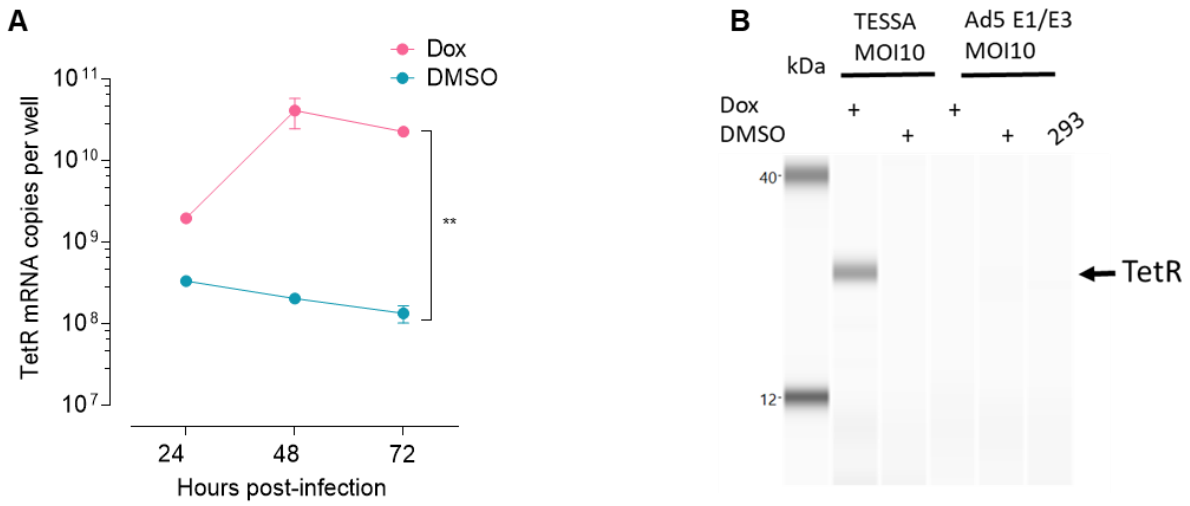


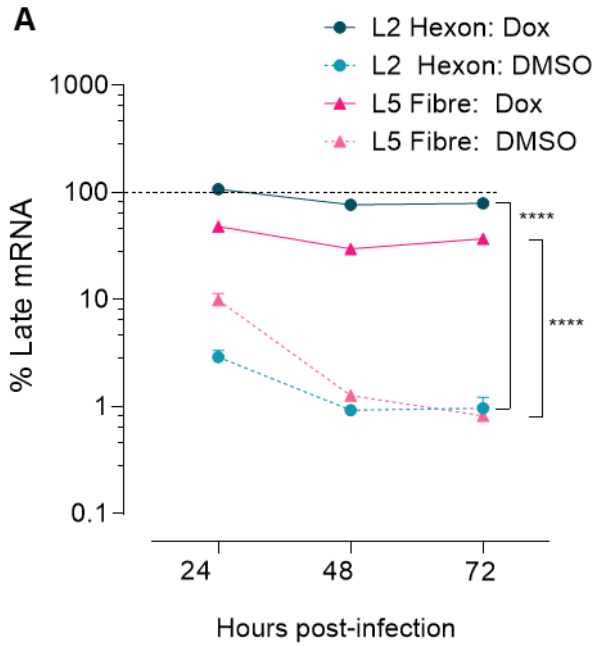
Figure 3.8 TetR is expressed from the endogenous MLP and induces promoter self-repression in the absence of doxycycline. A) TetR mRNA expression from TESSA-AAV (MOI-10) in HEK293 cells treated with 0.5 µg/mL doxycycline or DMSO. Total RNA was harvested at each time point and quantified by reverse transcription (RT) qPCR. Data presented as mean ± SEM of triple biological replicates. Significance determined by two-way ANOVA ** P≤0.05. **B**) Expression of TetR from TESSA. HEK293 cells were infected with TESSA or E1/E3Δ-Ad5 at an MOI of 10 and cultured with either DMSO or doxycycline 0.5 µg/mL. Cellular extracts (5uL of total lysate) were probed with anti-TetR antibody and detected using automated western blot.

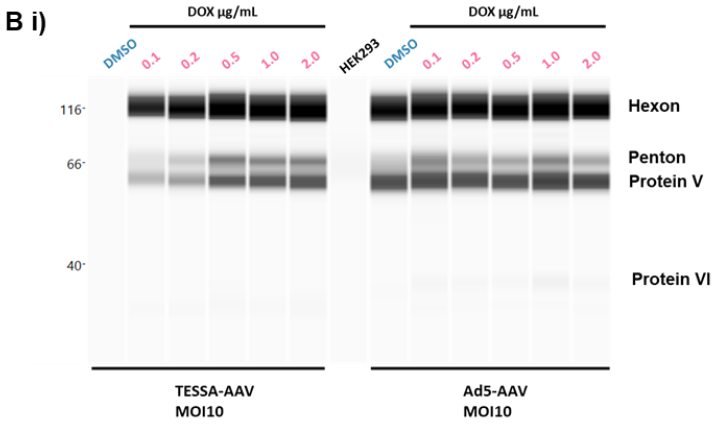
3.3.12 Repression of MLP inhibits expression of adenovirus structural proteins

Late viral mRNAs encoding adenoviral structural proteins were quantified to determine the extent of MLP repression from TESSA-AAV-EGFP. HEK293 cells infected with TESSA-AAV-EGFP or control Ad5-AAV-EGFP at an MOI of 10 and treated with DMSO or doxycycline. Expression of late viral mRNA coding for Hexon and Fibre, encoded within L2 and L5 respectively, were determined by

RT-qPCR. In the DMSO-treated HEK293 cells, TESSA-AAV-EGFP shows 35-fold lower (at 24hpi) and >100-fold lower (at 48hpi and 72hpi) levels of Hexon mRNA compared to the control Ad5-AAV-EGFP (**Figure 3.9A**). Similarly, TESSA-AAV-EGFP expressed >140-fold less fibre mRNA compared to the control virus at 72hpi. Unexpectedly, we also observed a 2-3-fold reduction in fibre mRNA expressed from TESSA-AAV-EGFP compared to the control virus in the presence of doxycycline, which may be a consequence of the additional splice acceptor site placed upstream of fibre to regulate the TetR expression. However, both TESSA-AAV-EGFP and Ad5-AAV-EGFP yielded comparable virus titres after scale-up production suggesting that viral infectivity and replication was unaffected (**Figure 3.7D**). This fits with the observation that capsid proteins (including fibre) are normally expressed in excess during the late phase of viral infection (Rebetz et al. 2009; Yan et al. 2017).

In addition to measuring late viral mRNA from TESSA-AAV-EGFP, we also assessed the expression of adenovirus capsid proteins by western blot. HEK293 cells were infected (at an MOI of 10 and 100) with TESSA-AAV-EGFP or the control Ad5-AAV-EGFP and cultured with DMSO or increasing doses of doxycycline. Samples were harvested at 72hpi and adenovirus capsid proteins from lysate preparations were probed using anti-Ad5 antibody and detected by automated western blot. As shown in **Figure 3.9B**, comparable levels of adenovirus capsid proteins were detected from replication of the control Ad-AAV-EGFP in DMSO or the varying doses of doxycycline at MOI 10 (**i**) and MOI 100 (**ii**). In contrast, while adenovirus capsid proteins were not detected from TESSA-AAV-EGFP (MOI 10 and -100) when cultured with DMSO in HEK293 cells, the addition of doxycycline alleviated MLP repression and expression of structural proteins from TESSA was observed to be dose-dependent up to 0.5 µg/mL.


A
L2 Hexon: Dox
L2 Hexon: DMSO
L5 Fibre: Dox
L5 Fibre: DMSO
% Late mRNA
1000
100
10
1
0.1
****
****
24
48
72
Hours post-infection


B i)
DOX µg/mL
DMSO
0.1
0.2
0.5
1.0
2.0
HEK293
116
66
40
Hexon
Penton
Protein V
Protein VI
TESSA-AAV
MOI10
Ad5-AAV
MOI10

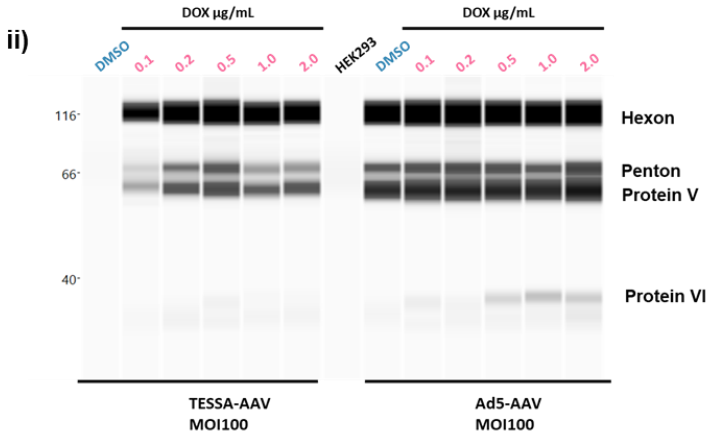

ii)
DOX µg/mL
DMSO
0.1
0.2
0.5
1.0
2.0
HEK293
116
66
40
Hexon
Penton
Protein V
Protein VI
TESSA-AAV
MOI100
Ad5-AAV
MOI100

Figure 3.9 Repression of the MLP in TESSA inhibits transcription of late viral mRNA and expression of virus capsid proteins are doxycycline dose-dependent. A) Hexon and fibre mRNA are repressed by TESSA-AAV. HEK293 cells were infected with TESSA-AAV or Ad5-AAV (MOI-10) and cultured with 0.5 µg/mL doxycycline or DMSO. Total RNA extracted at the indicated timepoints and hexon and fibre mRNA quantified by RT-qPCR. Data are presented as percentage of mRNA levels versus control Ad5-AAV. Significance determined by two-way ANOVA ****P≤0.0001. Adenovirus structural protein expression from TESSA-AAV is doxycycline-dependent. HEK293 cells were infected with TESSA-AAV and Ad5-AAV at an MOI10 (**B i**) and MOI100 (**ii)** and culture with DMSO or increasing doses of doxycycline. Samples were harvested at 72 hpi and detected by western blot using anti-Ad5 antibody.

3.3.13 Repression of MLP from TESSA enhances DNA replication

Efficient replication of adenovirus vectors is important to maintain stable propagation of important transgenes over multiple passages. Replication kinetics of TESSA was assessed in-depth to determine whether modifications to the MLP and encoding TetR under its transcription control hindered virus growth. HEK293 cells were infected with TESSA-AAV-EGFP or control Ad5-AAV-EGFP at an MOI of 10 or -100 and treated with DMSO or doxycycline. Total DNA was extracted from cells and growth media at the indicated timepoint and quantified by fibre-specific qPCR. As adenovirus DNA replication usually occurs at 12 hpi, the 4 hpi group is provided as a control for the quantification of input vectors. As expected, a ~3-log increase in adenovirus genomes was already observed at 24 hpi (MOI 10 and -100) from both TESSA-AAV-EGFP or Ad5-AAV-EGFP, with levels reaching a plateau at 48-72 hpi (**Figure 3.10A i&ii**). Genome replication of Ad5-AAV-EGFP was unaffected by either the presence or absence of doxycycline and TESSA-AAV-EGFP exhibited similar levels of progeny genomes when doxycycline was added to the culture to alleviate MLP repression. In contrast, in the absence of doxycycline, TESSA-AAV-EGFP produced up to 10-fold (P≤0.0001) more virus genomes from both assessed MOI. This raises the possibility that repression of adenovirus structural protein production could allow more metabolic resources to be used for viral genome synthesis.

3.3.14 Expression of transgenes from TESSA

We further tested whether repression of MLP-TetO1b influenced transgene expression embedded in the E1-deleted region of TESSA. HEK293 cells were infected at an MOI of 10 with TESSA or the control-Ad5 encoding the CMV-EGFP and treated with doxycycline or DMSO. EGFP expression was analyzed by flow cytometry. At 24 hpi, comparable levels of EGFP determine by the median fluorescent intensity (MFI) were observed from the control-Ad5 (in both the DMSO and doxycycline-treated group) and TESSA, with the DMSO-treated TESSA group showing a 40% increase in EGFP expression (**Figure 3.10B**). This increase remained consistent after 48 hpi and 72 hpi, with a maximal expression of EGFP observed at 48 hpi at which point the DMSO-treated TESSA group showed a significant 2.2-fold increase compared to the control virus. This increased EGFP expression from self-repression of MLP-TetO1b in TESSA may be reflected by the availability of more metabolic resources and the increase in viral genome copies providing more EGFP template for transcription.

Expression of EGFP and adenovirus proteins at 72 hpi were also analyzed by western blot. Equal amounts of crude lysates were probed using anti-EGFP and anti-Ad5 antibody showed high levels of EGFP and Ad5 capsid proteins from cells infected with Ad5-CMV-EGFP (**Figure 3.10C**). As expected, while Ad5 capsids and EGFP proteins were detected from TESSA in the doxycycline-treated group, Ad5 proteins were undetectably in the DMSO-group.

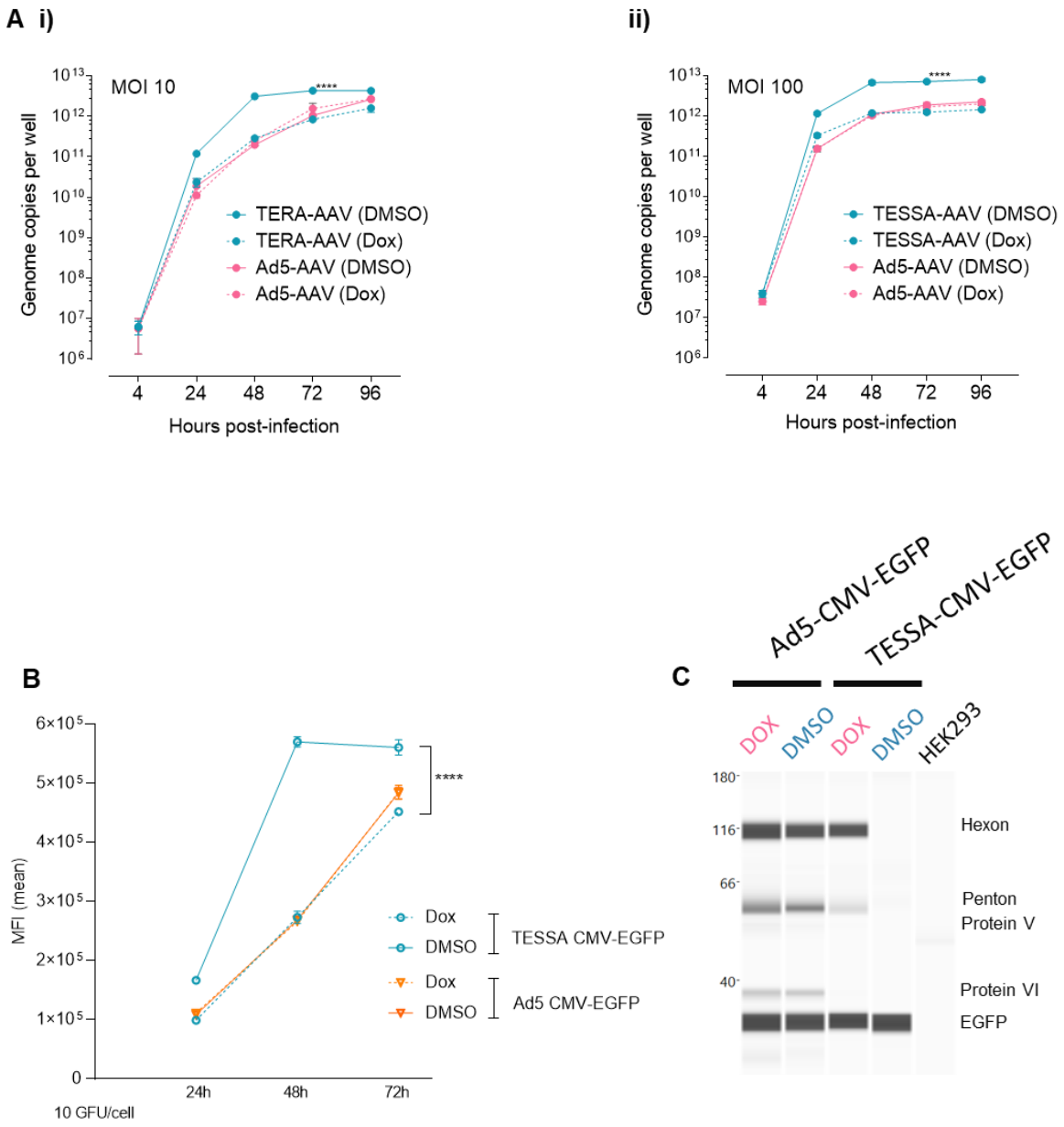


Figure 3.10 Repression of the MLP in TESSA enhances viral genome replication and transgene expression. A) Genome replication of TESSA-AAV and Ad5-AAV. HEK293 cells were infected with TESSA-AAV or Ad5-AAV at a MOI of 10 (**i**) or -100 (**ii**) and treated with 0.5 µg/mL doxycycline or DMSO. Total DNA was extracted at each timepoint and adenovirus genomes quantified by qPCR directed against Ad5 fibre. **B**) Expression of EGFP from TESSA-CMV-EGFP or the control Ad5-CMV-EGFP. HEK293 cells were infected at an MOI of 10 with each vector and cultured with doxycycline 0.5 µg/mL or DMSO. Cells were harvested for flow cytometry analysis at the indicated timepoint post infection. Data is N=3 (mean ± SEM). Significance determined using two-way ANOVA ****P≤0.0001. **C**) Detection of adenovirus proteins and EGFP transgenes by western blot. HEK293 cells were infected with Ad5-CMV-EGFP or TESSA-CMV-EGFP at an MOI of 10 and cultured with doxycycline 0.5 µg/mL or DMSO. Samples were harvested at 72 hpi and equal amounts of cell lysates were analyzed by automated western blot and multiplexed using anti-EGFP and Anti-Ad5 antibodies.

3.3.15 Production of rAAV2 from TESSA-AAV-EGFP

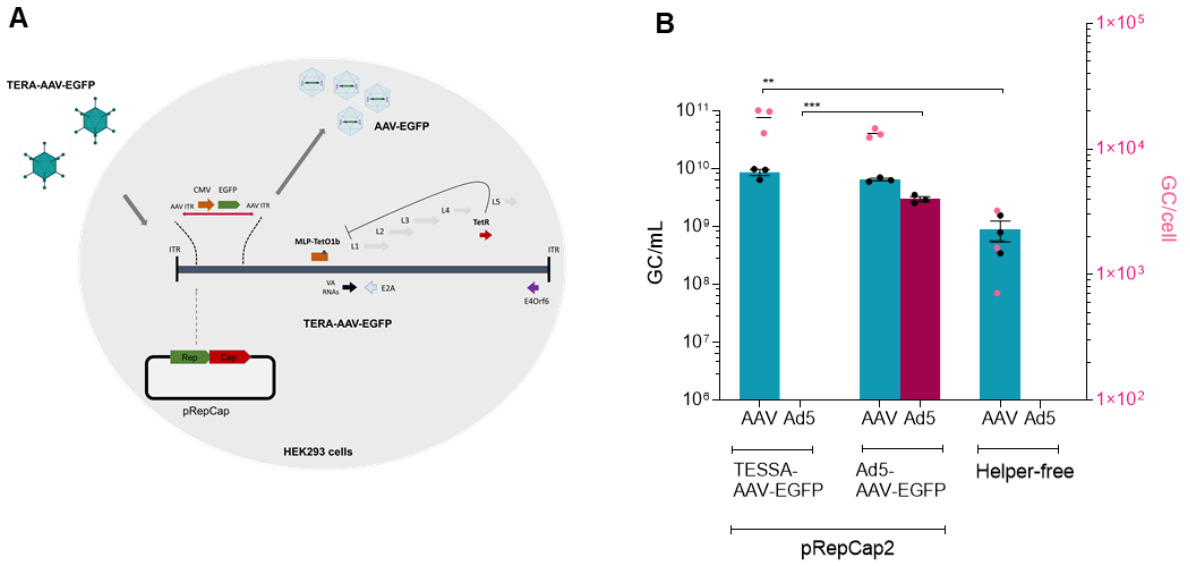
To explore the utility of TESSA-AAV-EGFP for rAAV production, HEK293 cells were transfected with plasmid pRepCap2 (encoding the AAV2 rep and cap genes) and infected with TESSA-AAV-EGFP or helper Ad5-AAV-EGFP at an MOI of 500. rAAV production was compared to the helper-free method wherein cells were transfected with pAAV-CMV-EGFP, pRepCap2 and pHelper. Schematic of rAAV production using TESSA-AAV-EGFP with pRepCap2 is shown in **Figure 3.11A**. To determine efficiency of the DNAse treatment and control for input rAAV vector genome, cells were also transfected in parallel with pHelper, pAAV-EGFP and stuffer DNA (in place of pRepCap). Vectors were harvested at 96 hpt, treated with DNase to degrade free-DNA, and encapsulated rAAV2 genomes quantified by EGFP-specific qPCR. As the EGFP sequence is also encoded within TESSA-AAV-EGFP and control Ad5-AAV-EGFP vectors, levels of rAAV2 produced from these systems were determined by subtraction of intact adenoviral vectors measured from the Hexon-specific qPCR. As shown in **Figure 3.11B**, comparable levels of rAAV2 were observed from the Ad5-AAV-EGFP and via production from the helper-free system which yielded $1.5x10^9$ GC/mL. We observed almost 7-fold ($P \leq 0.01$) more rAAV2 produced from TESSA-AAV-EGFP, which yielded $1x10^{10}$ GC/mL, compared to the helper-free system. Crucially, however, use of helper Ad5-AAV-EGFP was characterized by high levels of contaminating adenovirus accounting for ~50% of total vectors, whereas using the TESSA-AAV-EGFP system contaminating adenovirus was below qPCR detection limits (ct >35).

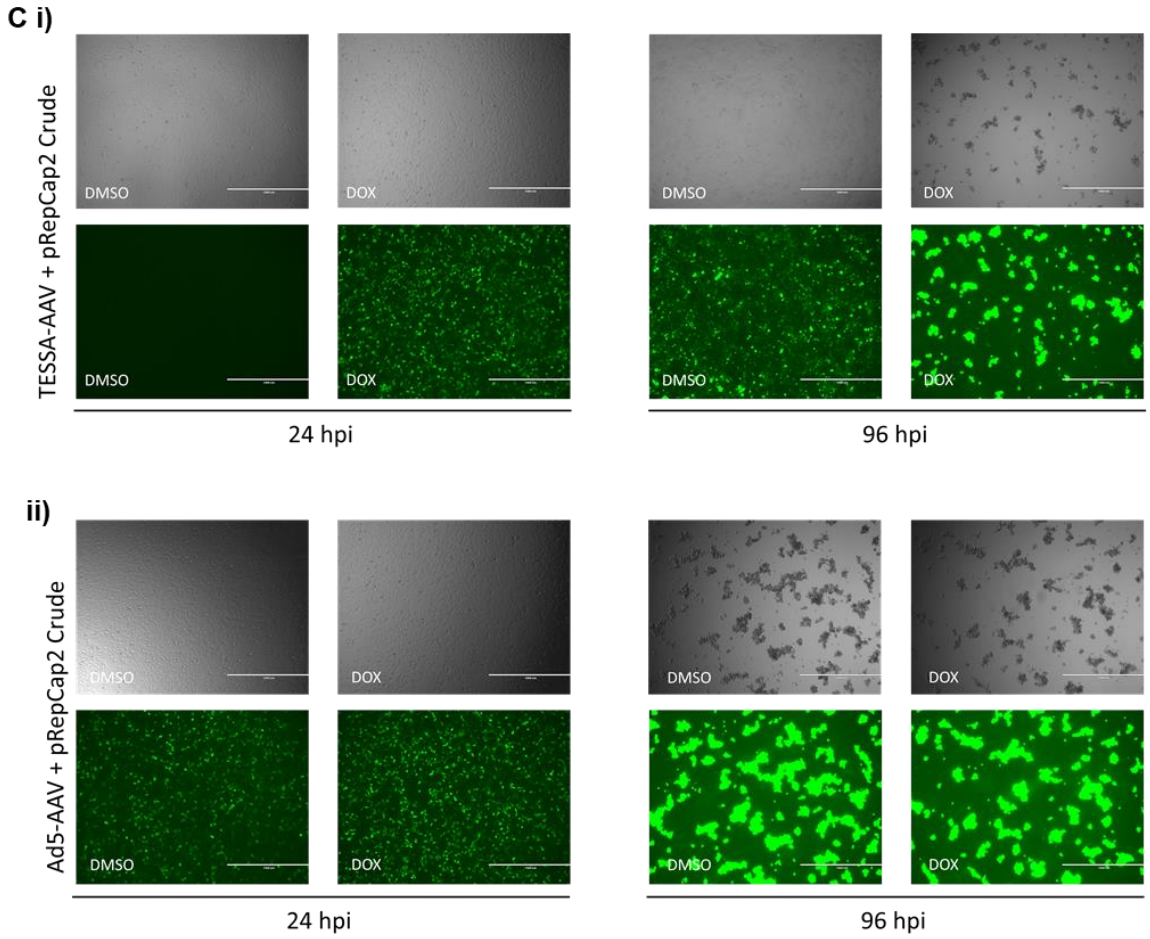
3.3.16 Contamination of infectious adenovirus is repressed from TESSA during AAV production

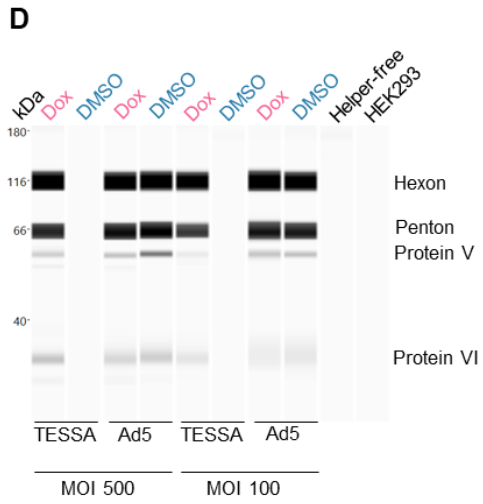
Contaminating adenovirus was initially assessed by adding crude rAAV preparations produced from TESSA-AAV-EGFP or Ad5-AAV-EGFP (in the presence of doxycycline or DMSO), at a 1:100 volume dilution to fresh HEK293 cells that were subsequently cultured with doxycycline. Representative brightfield and fluorescent images at 24 hpi and 96 hpi are shown in **Figure 3.11C**. Transduction of HEK293 cells with crude rAAV produced by Ad5-AAV-EGFP or TESSA-AAV-EGFP in doxycycline cultured HEK293 cells results in early and high levels of EGFP expression that was easily notable at 24 hpi, thought to reflect adenovirus-encoded EGFP. This interpretation was supported by the presence of advanced adenovirus CPE at 96 hpi. In contrast, rAAV-EGFP produced by TESSA-AAV-EGFP without doxycycline showed delayed EGFP expression, typical of the expression kinetics of AAV and presumably due to the requirement for second-strand synthesis of the single-stranded AAV genome (Afione et al. 1999). Importantly, the cell monolayer remained intact, suggesting a lack of adenovirus contamination. In addition there was no sign of focal spreading of EGFP, again characteristic of adenovirus vector contamination.

The absence of adenovirus contamination in the TESSA product was further confirmed by western blot analysis (**Figure 3.11D**). Equal amounts of crude rAAV2 lysates produced using TESSA-AAV-EGFP or Ad5-AAV-EGFP used at MOI of 500 or 100, or via helper-free method were probed using anti-Ad5 antibody and detected using automated western blot. While the helper Ad5-AAV system showed a strong presence of all the main adenovirus capsid proteins, no contaminating capsid proteins were detectable in rAAV crude lysates produced using TESSA-AAV-EGFP (in the absence of doxycycline) or helper-free samples.

Levels of contaminating infectious adenovirus were also quantified using a TCID50 assay in HEK293 cells (**Figure 3.11E**). As expected, no infectious adenoviruses were found using the helper-free method whereas Ad5-helper produced high levels of contaminating adenovirus (>2x10^9 TCID50/mL). TESSA in the presence of doxycycline yielded 60-80% as much contaminating adenovirus as the Ad5-helper, but without doxycycline contamination levels were decreased to negligible quantities of 0.007% and 0.00004% , compared to compared to the helper-Ad5 control, when used at an MOI of 500 and -100.




C i)
TESSA-AAV + pRepCap2 Crude
DMSO
DOX
24 hpi
96 hpi
ii)
Ad5-AAV + pRepCap2 Crude


D
kDa
Dox
DMSO
Helper-free HEK293
180
116
66
40
Hexon
Penton
Protein V
Protein VI
TESSA
Ad5
MOI 500
MOI 100

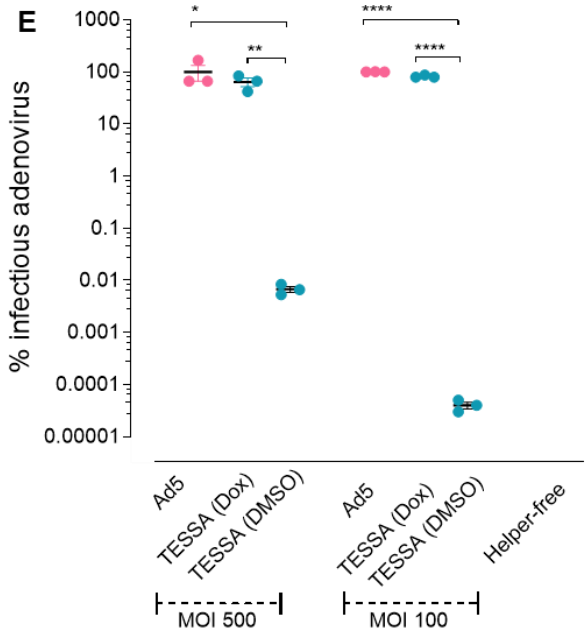

E
% infectious adenovirus
1000
100
10
1
0.1
0.01
0.001
0.0001
0.00001
*
**
****
Ad5
TESSA (Dox)
TESSA (DMSO)
Helper-free
MOI 500
MOI 100

Figure 3.11 TESSA-AAV-EGFP enables delivery and rescue of the AAV genome for enhanced production of AAV vectors while inhibiting the production of contaminating adenovirus in HEK293 cells. **A**) Schematic diagram of AAV production in HEK293 cells using TESSA-AAV-EGFP encoding the AAV transfer genome and cells were transfected with plasmid pRepCap. **B**) AAV2 production using TESSA-AAV-EGFP, helper Ad5-AAV-EGFP (encoding recombinant AAV2 genome) or helper-free method. HEK293 cells were transfected with plasmid expressing AAV2 Rep and Cap genes prior to transduction (MOI500) with helper Ad5-AAV or TESSA-AAV, or via helper-free plasmid transfection. Viruses extracted 96hpt and encapsulated adenovirus and AAV2 quantified by qPCR. AAV2 productivity (GC) per HEK293 cell is shown on the right axis. **C**) Crude rAAV lysates produced from TESSA-AAV-EGFP or Ad5-AAV-EGFP (MOI500), in the presence of DMSO or doxycycline 0.5ug/mL, was used for infection of fresh HEK293 cells at a 1:100 volume dilution and supplemented with doxycycline 0.5ug/mL. Cells imaged by brightfield and fluorescent microscopy at 24hpi and 96hpi. **D**) Contaminating adenovirus proteins from rAAV2 crude lysates produced using TESSA-AAV-EGFP, Ad5-AAV-EGFP (cultured with doxycycline 0.5 µg/mL or DMSO) or helper-free method determined by western blot and infectious adenovirus confirmed using a TCID50 assay (**E**). Data presented as mean ± SD of triple biological replicates. Significance determined by Unpaired t-test *p P≤0.05, **P≤0.01, ***P≤0.001.

3.4 Chapter discussions

Traditionally, infectious adenoviruses are used for transducing producer mammalian cells for high titre rAAV vector production. Although this approach provides the benefit of scalable and higher titre production over commonly used helper-free systems, contamination by infectious adenovirus is highly undesirable due to safety concerns and costs associated with their removal (Thorne, Takeya, and Peluso 2009; Clement and Grieger 2016). We therefore set out to use rational adenovirus engineering to develop a safer and more efficient helper adenovirus that enables manufacture of rAAV vectors without adenovirus contaminants.

In this study, we developed a novel adenoviral vector, TESSA, wherein the endogenous MLP was engineered both to transcribe the TetR and to be inhibited by it. This enabled expression or self-repression of viral structural proteins, in the presence or absence of doxycycline, respectively.

We initially explored the feasibility of repressing the adenovirus MLP by using EGFP reporter plasmids, wherein TetO sites were inserted within the MLP core promoter element to assess for transcriptional repression by the TetR (**Figure 3.2**). Subsequently, E1/E3Δ-Ad5 vectors were constructed with the TetO insertions into the endogenous virus MLP to assessed recovery of viable vectors, and its capacity to inhibit virus replication in HEK293 cells expressing the TetR (**Figure 3.3**). Our data suggest that sequences immediately upstream and downstream of the MLP TATA box, and the divergent DNA polymerase, can tolerate a level of mutations and nonsynonymous substitutions, respectively, without hindering viral replication; but only TetO site positioned between the MLP TATA element and transcriptional start site was able to mediate promoter repression.

While we have not assessed the replication fidelity of TESSA, the synonymous substitutions incorporated into the DNA polymerase by modification of the MLP to incorporate the TetO1b site is located approximately 640, 500 and 340 amino acids away from the conserved Exo -I, -II and III motifs within the 3'-5' exonuclease domains, respectively, and therefore not expected to hinder its proofreading functions (Liu, Naismith, and Hay 2000). In addition, these MLP modifications did not affect any conserved Pol residues located at the C-terminal portion of the polymerase, which was shown to be largely essential for the adenovirus, as single amino acid changes within these putative sequences significantly decreased or abrogated viral genome replication (Capella et al. 2012; Uil et al. 2011).

It is reasonable to speculate that as the adenoviral genomes exponentially replicate within the cell, exponential production of TetR is required to maintain tight repression of each transcriptionally activate MLPs. Consistent with this hypothesis, escape of adenovirus repression was also infrequently observed from 293 Flp-in TREx cells infected with the MLP-TetO1b-modified Ad vector, which contained a TetO site allowing MLP repression when bound by TetR produced

by the host cell. To improve upon the repression system, we coupled expression of the TetR to activity of the MLP so that TetR would be produced in proportion to adenovirus genome replication. This self-silencing adenoviral vector 'TESSA' showed normal replication kinetics in the presence of doxycycline, but repressed generation of infectious adenovirus while yielding increase copies of viral genomes in its absence (**Figure 3.10**). While the mechanisms responsible for this increase in viral genomes during MLP repression remains unclear, it may be that additional cellular resources can be dedicated to DNA replication when the expression of Ad structural proteins are inhibited. More recently, it was shown that a small RNA, termed MLP-TSS-sRNA, was transcribed from the MLP and functions to reduce DNA polymerase and pre-terminal proteins (pTP) mRNA, which are essential for adenovirus DNA replication (Kamel and Akusjarvi 2017). Likely, the expression of this MLP-TSS-sRNA is inhibited during MLP repression in TESSA. Importantly, we demonstrated the utility of the TESSA vector for delivering adenovirus helper functions and the rAAV transfer genome into cells, thereby yielding more than 10-fold increase in rAAV2 vector production, with an almost 8-log reduction in infectious adenovirus vectors (**Figure 3.11**).

There have been a few previous, largely unsuccessful, attempts to develop inducible MLP structures. For example, one interesting but unpublished approach that was suggested was based on the observation that an adenovirus with MLP containing four specific mutations in the upstream promoter element (UPE) coupled with a specific A-to-G transition in the TATA box motif was intrinsically lethal for virus replication, but might be recoverable by complementation with a specific variant of the TATA box-binding protein TFIID, TBP-m3e, from yeast (Young 2003). In this scenario, TBP-m3e exhibits specificity against the altered TATA sequence and can prime transcription from the MLP (Strubin and Struhl 1992). Initially, we attempted to test this approach and found that while the specified mutations in the UPE and TATA element of the MLP were indeed lethal for virus replication, we were unable to recover viable vectors after several attempts

using transient expression of TBP-m3e from plasmids or expression from the adenovirus E1-deleted region under control of the CMV promoter (data not shown).

Temperature-sensitive mutant adenoviruses have been explored for complementing AAV replication with an aim to reduce adenovirus contaminations (Handa, Shiroki, and Shimojo 1975). For example Farson et al showed that adenoviruses with mutations in the virus E2B DNA polymerase or pTP, rendering them less able to replicate at 37°C, were nevertheless able to 'help' rAAV production comparable to the wildtype virus (Farson et al. 2004). Interestingly, while the pTP temperature-sensitive mutant showed no improvement at reducing adenovirus contaminations, use of the E2B-mutant reduced production of replication-competent adenoviruses by 4-fold, to approximately ~2 x 10^8 infectious units/mL. Infection with this temperature-sensitive E2B-mutant also yielded a 2-6 fold increase in rAAV vectors, consistent with our findings using TESSA, and may suggest more cellular resources can be dedicated to rAAV production in the absence of adenovirus replication.

Replication-deficient adenoviruses, such as an Ad protease-deleted (AdDPS) mutant, have also been explored but resulted in lower AAV vector yields compared to wildtype adenoviruses (Merten, Geny-Fiamma, and Douar 2005). Interestingly, Kruger-Haag et al recently developed and evaluated life cycle-defective adenoviruses, deleted of the pTP or 100K coding sequence, for rAAV production in A549-based stable AAV producer cells encoding rep and cap, and the ITR transfer genome. As the pTP and 100K protein is important for initiating adenovirus genome replication and late-phase of the virus life cycle, respectively, viruses deficient of these essential proteins require production from *trans*-complementing cells, which can be laborious and difficult to up-scale production. Interestingly, while the ΔpTP-mutant supported moderately high titre rAAV production from the A549-based stable producer cell line, the Δ100K-mutant was unable to do so despite functioning effectively as a helper virus when the rep-cap genes and the rAAV genome

were provided *in trans* by plasmid transfection (Kruger-Haag et al. 2019). As the L4 100K mRNA is transcribed from the MLP during the late phase of the virus life cycle, its expression from TESSA is likely repressed alongside the L2 and L5 mRNA transcripts, assessed by hexon and fibre-specific qPCR respectively (**Figure 3.9A**) (Hodges et al. 2001). As such, it can be expected that TESSA may be unable to support rAAV production from similar A549 or HeLa-based stable AAV packaging cells in its current configuration. The use of TESSA for the production of rAAV vectors from stable packaging cell lines is further investigated in Chapter 6, while Chapters 4 and 5 explore the use of TESSA to deliver the AAV rep and cap genes, to allow transfection-free, scalable production of rAAV vectors.

3.5 Chapter conclusions

1. Adenovirus vectors with significant alterations to the endogenous MLP via insertion of TetO elements were recovered and shown to be viable.
2. Insertion of TetO site downstream of the adenovirus MLP TATA box and encoding the TetR under transcription control of the MLP enables auto-repression of promoter activity to truncate the adenovirus late life cycle. This inhibition is reversed by the presence of doxycycline
3. This self-repressing adenovirus vector ('TESSA') can provide all the requisite adenovirus 'helper' functions and can also encode the AAV transfer genome, allowing efficient manufacture of rAAV vectors with very little contaminating adenovirus.

Chapter 4

Encoding AAV rep and cap in TESSA to support efficient rAAV manufacture

4.1 Introduction

In the previous chapter we showed the simple TESSA system, wherein pRepCap is introduced via transfection, can deliver adenovirus helper functions and the AAV transfer genome for efficient production of rAAV batches without adenovirus contamination. However, its productivity and potential for scale-up are likely to be limited by the need to transfect cells with a plasmid encoding AAV rep and cap. Transfection steps are hard to scale and can be expensive (Wright 2009). Unexpectedly, we found that TESSA-E1 at its current configuration was unable to support episomal DNA replication of AAV rep and cap genes, and rAAV production, from HelaRC32 AAV packaging cells during MLP repression. We therefore aimed to advance a completely new strategy using TESSA to overcome these limitations, using TESSA vectors to provide all the packaging components and completely removing any reliance on plasmid transfection or stable AAV packaging cell lines.

There have been several attempts to construct Ad vectors encoding AAV genetic elements, although it has proved challenging to produce a robust manufacturing system that circumvents the need for transfection completely. One important issue is that although the rAAV genome can be stably encoded within the E1-deleted region of Ad vectors , and also within TESSA without

affecting virus replication kinetics, encoding the AAV rep and cap genes into an adenovirus vector had yield limited success, as Rep is a potent inhibitor of adenovirus replication (Fisher et al. 1996; Casto, Atchison, and Hammon 1967; Casper et al. 2005).

In attempts to generate E1/E3Δ-Ad vectors encoding AAV rep, the use of tissue-specific promoters, inducible expression systems, and even promoterless constructs aimed at minimizing Rep expression was explored and found to be unsuccessful during recovery in HEK293 cells (Carlson, Shayakhmetov, and Lieber 2002; Fisher et al. 1996). Interestingly, Zhang et al. reported recovery of an E1/E3Δ-Ad encoding the full AAV rep and cap sequence (albeit without AAV ITRs) from HEK293 cells. At early passages, this hybrid virus Ad/RepCap supported the production of rAAV vectors when HEK293 cells were co-infected with another E1/E3Δ-Ad encoding the rAAV transfer genome. However, significant instability was observed as the Ad/RepCap vector showed an over 10-fold decrease in replication and loss of rep coding during serial passage (Zhang et al. 2001).

While it is well documented that Rep proteins inhibit transcription from adenovirus early and late (MLP) promoters, DNA in the AAV p40 promoter region, involved in driving Cap expression and embedded within the rep gene coding sequence, was more recently identified as a potent inhibitor of adenovirus replication *in cis* (Casper et al. 2005; Needham et al. 2006; Sitaraman et al. 2011). Although the mechanism is unclear, it was suggested that transcription from the p40 promoter induced stalling of an RNA polymerase II transcription complex and interference of adenovirus genome replication. Importantly, scrambling of the p40 promoter, and hence the Ad-inhibitory sequence, by synonymous codons exchange of the large Rep78 polypeptide allowed stable propagation within the Ad vector (Weger et al. 2016; Sitaraman et al. 2011).

Similarly, and prior to identification of the *cis* inhibitory sequence within the rep coding sequence, Zhang and Li. developed a three-adenovirus vector system for producing rAAV via reconfiguration

of the AAV rep and cap genes. In this approach, the p40 promoter is deleted and Cap expression is under control of a CMV promoter, while Rep expression is controlled within the Ad vector using a tetracycline-inducible system. rAAV production is induced by the addition of tetracycline and co-infection with two more E1/E3Δ-Ad vectors, encoding the AAV transfer genome and expressing the transactivator rtTA, respectively. While this system is cumbersome and generated a modest yield of AAV with adenovirus contamination, inadvertent ablation of the p40 *cis* inhibitory DNA sequence and controlled Rep expression allowed AAV rep and cap to be stably maintained within the adenovirus during extended passages. This provided proof-of-concept for a complete adenovirus-mediated approach to producing AAV vectors (Zhang and Li 2001).

Encoding all the components required for AAV replication into a single adenovirus vector is likely to be unfeasible due to limitations in the packaging size of an E1/E3-Ad5 vector (Bett, Prevec, and Graham 1993). Such an approach would also raise inherent risks of generating replication-competent AAVs. Accordingly, in this chapter, we aimed to engineer a complete adenovirus-mediated approach for rAAV production using two TESSA vectors. By removing the need for a transfection step and increasing yield, this should provide a lower base cost for manufacturing and quality control of adenovirus vectors at industrial-scale, and allow the production of rAAV economically with significant reduction in contaminating adenoviruses.

To this end, we initially explored integration of an additional inducible gene expression system for repressing Rep expressing during TESSA manufacture. We assessed the use of the Tet-4C5G variation of the tetracycline-inducible system and also the cumate-inducible expression system (Krueger et al. 2007). The Tet-4C5G system is a variation of the TetR inducible expression system, which comprises a mutant Tet repressor 'TetR-E37A-P39K' with recognition specificity for a variant TetO sequence TetO-4C5G. Importantly, the TetR-E37A-P39K repressor does not bind to the canonical TetO sequence, while TetO-4C5G is not recognized by the native TetR, allowing

exclusivity from the MLP-TetO1b – TetR loop encoded in TESSA. Similarly, the cumate-inducible expression system consists of a cumate transactivator protein cTA, composed of a repressor protein CmyR fused to the transactivator domain of VP16 from the herpes simplex virus (Mullick et al. 2006). Gene transcription is induced by binding of the cTA to the inducible promoter CuOx6-minCMV (consists of CmyR binding sites fused to a core minimal CMV promoter). This system also allows exclusivity from the MLP-TetO1b – TetR loop in TESSA.

By limiting Rep expression and scrambling the p40 inhibitory sequence by synonymous codon exchange, we were able to stably propagate it in TESSA vectors alongside the Cap coding sequences. In this chapter we evaluated the development of these vectors, and combined together TESSA vectors encoding the rAAV transfer genome, and rep and cap genes for production of rAAV serotype 2, -5, -6, -8, and -9.

4.2 Chapter aims

1. Evaluate strategies to deplete rep toxicity and engineer TESSA vectors stably encoding AAV rep and cap genes
2. Evaluate production of rAAV vectors using two TESSA vectors to provide all required components
3. Characterisation of physical and biological properties of AAV particles produced using the TESSA two-vector system (TESSA2.0)

4.3 Results

4.3.1 AAV Rep proteins repress MLP activity

AAV Rep protein is known to inhibit transcription from the MLP by binding to regions between the promoter TATA box and initiation element (Inr) via interactions with a cellular TATA-box binding protein (Needham et al. 2006). As the MLP-TetO1b encoded within TESSA was significantly modified by insertion of TetO sequence between the TATA box and Inr, we initially assess whether its basal activity was also inhibited by Rep. EGFP reporter plasmids pMLP-TetO1b-EGFP or pMLP-WT-EGFP was co-transfected into HEK293 cells with either stuffer plasmid (pCMV) or plasmids encoding rep78, rep68, rep52, or rep40 under transcription control of the CMV promoter (plasmids provided by OXGENE). In parallel, cells were also transfected using a promoterless EGFP reporter plasmid (pMCS-EGFP) as a mock-transfection control for background EGFP expression. EGFP expression was analysed by flow cytometry at 72 hpt. As shown in **Figure 4.1A**, repression of both (**i**) MLP-WT and (**ii**) MLP-TetO1b was observed from all Rep proteins compared to the control group, wherein the MLP EGFP plasmids were co-transfected with the stuffer DNA plasmid (pCMV). Rep40 was observed to be the most significant repressor of both MLP-WT and MLP-TetO1b activity, reducing EGFP levels comparable to that observed in cells transfected with the promoterless EGFP plasmid (pMCS-EGFP). This result suggests that in order to encode AAV rep within TESSA, carefully regulating Rep protein expression is important, particularly during the TESSA manufacturing step.

4.3.2 Development of single-switch virus for repression of AAV Rep

In an attempt to further engineer TESSA to stably encode AAV rep, we explored incorporating an additional variation of the TetR inducible expression system within TESSA (distinct from the embedded MLP-TetO1b – TetR negative feedback loop) for inhibiting Rep expression during TESSA vector production.

From rational design, we reasoned that four criteria were required from this alternative TetR inducible expression system –

1) The alternative repressor protein, in its 'on-state', should have no binding affinity to the TetO sequence embedded within the MLP of TESSA, to avoid inadvertently truncating the virus replication cycle during vector production whilst attempting to repress the 'toxic' rep transgene.
2) The TetR expressed from TESSA, in its 'on-state', should have no binding affinity to the variant TetO sequences, to avoid repression of rep transgene during MLP-TetO1b repression.
3) The alternative repressor protein should display a reverse allosteric response (i.e its 'on-state' is activated by doxycycline) from the TetR expressed by TESSA. This would enable 'toxic' transgene repression, such as Rep, in the presence of doxycycline during TESSA production, and manufacture rAAV in the absence of any low molecular weight inducers, important to minimize the requirements for downstream purification.
4) The alternative repression protein should be expressed at high levels rapidly after virus infection, to enable efficient repression of 'toxic' transgene transcription.

4.3.3 Cloning and evaluation of the rTetR-E37A-P39K TetO-4C5G system

Krueger et al. reported the generation of a novel Tet repressor 'TetR-E37A-P39K' with recognition specificity for a variant tetracycline operator sequence TetO-4C5G. Importantly, it was reported that TetR-E37A-P39K exhibited no recognition specificity for the consensus TetO, while the native TetR was unable to induce repression of promoters encoding TetO-4C5G (Krueger et al. 2007). As these characteristics of the TetO-4C5G system fulfilled the first two criteria identified above for an alternative TESSA-compatible gene repression system, we prioritized this approach for further evaluation. Furthermore, to achieve the 3rd criteria for compatibility with TESSA, we attempted to modify the TetR-E37A-P39K by amino acid exchanges to generate a reverse (r)TetR-E37A-P39K, with a reverse allosteric response to the native TetR in the presence doxycycline (i.e gene transcription repressed by addition of doxycycline), as this have not been demonstrated previously for this system.

TetO-4C5G was shown previously to have no specificity for binding by the native TetR, but is instead recognized by TetR-E37A-P39K to enable promoter repression. TetR-E37A-P39K was shown to have no binding specificity to the consensus TetO sequence within MLP-TetO1b of TESSA. To enable TetR-E37A-P39K to bind TetO-4C5G in the presence of doxycycline, the repressor was modified by amino acid exchanges, analogues to the rTetR, to generate a reverse (r)TetR-E37A-P39K (Zhou et al. 2006).

To determine the specificity of rTetR-E37A-P39K to TetO-4C5G and its allosteric response to doxycycline, inducible EGFP expression plasmids encoding the CMV promoter with the consensus TetO (pCMV-TetO2-EGFP) or TetO-4C5G (pCMV-TetO-4C5G-EGFP) element were co-transfected into HEK293 cells with plasmids expressing the native TetR, rTetR, TetR-E37A-P39K or rTetR-E37A-

P39K from a constitutive CMV promoter (pCMV-TetR and pCMV-rTetR provided by OXGENE). Cells were subsequently treated with DMSO or doxycycline. Cells were harvested at 72hpt and EGFP expression determined by flow cytometry. As expected, >5-fold reduction in EGFP expression was observed from cells co-transfected using pCMV-TetO2-EGFP with pCMV-TetR and cultured with DMSO compared to the doxycycline treated group, which alleviated repression from the TetR (**Figure 4.1B)**. Conversely, when cells were co-transfected with the rTetR and pCMV-TetO2-EGFP, the >5-fold reduction in EGFP expression was observed from the doxycycline treated group, indicating reversed allosteric response to doxycycline compare to native TetR. As TetR-E37A-P39K or the rTetR-E37A-P39K is unable to bind the consensus TetO element, no EGFP repression was observed when co-transfected with the pCMV-TetO2-EGFP. Similarly, TetR is unable to bind TetO-4C5G as reduction in EGFP levels were also not observed from cells co-transfected using pCMV-TetR or pCMV-rTetR with pCMV-TetO-4C5G-EGFP, in both the doxycycline and DMSO treated group. Supporting the findings of Kruger et al., in cells co-transfected using pCMV-TetR-E37A-P39K with pCMV-TetO-4C5G-EGFP, and treated with DMSO, a >5-fold reduction in EGFP expression was observed compared to the doxycycline treated group. Crucially, in contrast, cells co-transfected with the reverse repressor rTetR-E37A-P39K with pCMV-TetO-4C5G-EGFP, and treated with doxycycline, resulted in significant EGFP repression. However, in the corresponding DMSO treated group, EGFP expression levels were ~2-fold lower compared to cells co-transfected using pCMV-rTetR-E37A-P39K with pCMV-TetO2-EGFP, indicating that the absence of doxycycline did not fully alleviate the repression activity of rTetR-E37A-P39K. It therefore seems likely that the E37A and P39K amino acids exchange that enables specificity of the repressor for TetO-4C5G impeded reversal of the allosteric response.

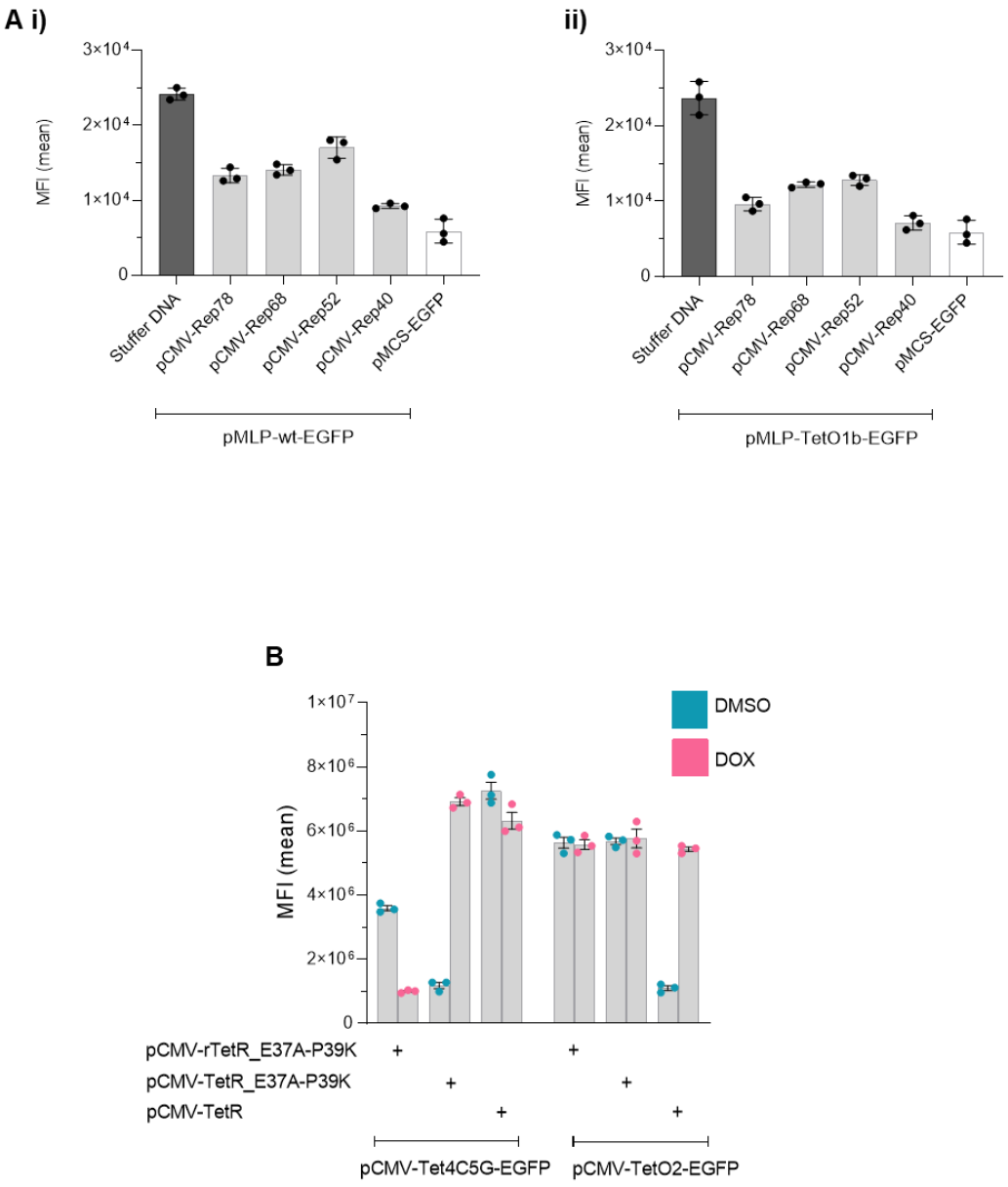


Figure 4.1 AAV Rep inhibits MLP expression and assessment of the Tet-4C5G system A) Repression of adenovirus MLP (i) and MLP-TetO1b (ii) by AAV Rep proteins. HEK293 cells were co-transfected using MLP-EGFP expression plasmids with CMV plasmids expressing AAV Rep. EGFP expression was analyzed by flow cytometry at 72hpt. **B**) Assessment of Tet4C5G repression system. CMV-EGFP expression plasmids encoding the TetO or Tet4C5G sequences were co-transfected into HEK293 cells with CMV-plasmids expressing the TetR, TetR-E37-P39K or the reverse rTetR-E37-P39K. Cells were treated with doxycycline 0.5 µg/mL or DMSO and EGFP expression analyzed by flow cytometry at 72 hpt.

4.3.4 Evaluation of TESSA-DS expressing EGFP from the 4C5G-inducible promoter

Significant repression of the CMV-TetO-4C5G promoter by rTetR-E37A-P39K was achieved in the presence of doxycycline, although this repression of CMV-TetO-4C5G was not fully alleviated in the absence of doxycycline. Nevertheless we reasoned that DNA replication of TESSA, and hence increased copies of rep, might give sufficient expression of Rep to enable efficient AAV replication in the absence of doxycycline. Therefore, we proceeded to further integrate the TetO-4C5G & rTetR-E37A-P39K system into TESSA.

As illustrated in **Figure 4.2A**, the dual-switch TESSA vector (TESSA-DS) exploited the use of a CMV promoter encoding the tetO-4C5G ($CMV^{TetO\text{-}4C5G}$), for modulating transgene expression. Additionally, the reverse repressor rTetR-E37A-P39K is expressed early from a 260bp recombinant micro-CMV promoter (PROM567; provided by OXGENE) and linked to the native TetR via a self-cleaving peptide P2A (Liu et al. 2017). Use of a micro-CMV promoter should enable rapid expression of rTetR-E37A-P39K, for fulfillment of the 4^{th} criteria as disclosed above, whilst ensuring optimal capacity for packaging of transgenes within the TESSA-DS vectors. TESSA-DS constructed to encode transgenes EGFP, BAX, AAV Cap2, AAV Rep, or the bicstronic Cap-EMCV-Rep sequence is also illustrated (Bochkov and Palmenberg 2006).

For initial validation of TESSA-DS, we encoded the EGFP reporter under control of the $CMV^{TetO\text{-}4C5G}$ promoter. The TESSA-DS-$CMV^{TetO\text{-}4C5G}$-EGFP plasmid was linearized to release the vector ITR from the plasmid backbone and transfected into HEK293 cells for vector recovery in the presence of doxycycline or DMSO. As expected, viable vectors were only recovered (12 days post-transfection) in cells cultured with doxycycline, allowing the MLP to TESSA-DS function. TESSA-DS-$CMV^{TetO\text{-}4C5G}$-EGFP viruses were then used for infection of fresh HEK293 cells in the presence

of DMSO or doxycycline, and monitored using brightfield and fluorescent microscopy over 7 days. As shown in **Figure 4.2B**, at day 4 (**i**), viral plaques were observed across the monolayer in cells cultured with doxycycline, while EGFP expression was repressed. In contrast, in the absence of doxycycline, the cell monolayer was absent of observable plaques while EGFP expression was notable from infected cells. Results remained consistent at day 7 (**ii**), with the doxycycline treated cells showing advanced viral CPE and minimal EGFP expression. In the DMSO group, viral spread remained inhibited and EGFP expression is confined to cells from the initial infection. This result confirmed that the dual-switch system within TESSA-DS was capable of enabling EGFP repression in the presence of doxycycline during vector replication, and EGFP expression in the absence of doxycycline during vector repression.

4.3.5 Evaluation of TESSA-DS expressing BAX from the 4C5G-inducible promoter

As proof-of-concept for the use of TESSA-DS to encode toxic transgenes for vector delivery, we inserted a flag-tagged, pro-apoptotic gene, bax under control of the $CMV^{TetO\text{-}4C5G}$ promoter. In parallel, a control virus was constructed wherein the $CMV^{TetO\text{-}4C5G}$-BAX expression cassette was also inserted into an E1-deleted region of an Ad5 vector. Following transfection of vector genomes (TESSA-DS or Ad5 encoding BAX) into HEK293 cells and treatment with doxycycline or DMSO, viral plaques were only observable from the doxycycline group transfected with TESSA-DS-$CMV^{TetO\text{-}4C5G}$-BAX. Vectors were harvested from all cultures at day 14 post-transfection and used for subsequent infection of fresh HEK293 cells, with doxycycline or DMSO added. Cells infected with crude preparations from the Ad5-CMV-BAX showed no viral plaques (data not shown) with an intact cell monolayer comparable to none-infected HEK293 control, confirming that BAX activity

prevented rescue of adenovirus (Arafat et al. 2000). However, from representative brightfield images in **Figure 4.2C**, cells infected with TESSA-DS-CMV$^{TetO\text{-}4C5G}$-BAX and cultured with doxycycline displayed advanced viral CPE at day 7 post-infection, while the DMSO treated group showed significant cytotoxicity and cell death. This suggested there was a high level of BAX expression from TESSA-DS-CMV$^{TetO\text{-}4C5G}$-BAX only in the absence of doxycycline, supporting our proposed activity mechanism.

These results were further validated by western blot (**Figure 4.2D**). Total protein was harvested from cells infected with TESSA-DS-CMV$^{TetO\text{-}4C5G}$-BAX or Ad5-CMV-BAX and equal amounts were probed with (**i**) anti-Ad5 antibody or (**ii**) anti-flag antibody for detection of Ad5 and BAX proteins, respectively, using an automated western blot system. As expected, adenovirus capsid proteins were undetected from cells treated with the Ad5-CMV-BAX samples, confirming the absence of vector replication. Additionally, adenovirus proteins were only present from cells infected with TESSA-DS-CMV$^{TetO\text{-}4C5G}$-BAX in the doxycycline treated group, as in its absence TESSA replication is inhibited. While low levels of BAX expression were detected from TESSA-DS-CMV$^{TetO\text{-}4C5G}$ -BAX in the doxycycline treated cells, suggesting a degree of leaky expression from the TetO-4C5G system, significantly more BAX was observed from cells treated with DMSO. Overall, these results indicate that the TESSA-DS system can be used for repressing and encoding toxic genes, that would otherwise limit production of viable vectors. It is likely that the leaky expression of EGFP and BAX observed from TESSA-DS-CMV$^{TetO\text{-}4C5G}$-EGFP and TESSA-DS-CMV$^{TetO\text{-}4C5G}$-BAX, respectively, may be due to the dynamic interplay between the increasing number of TESSA-DS genomes from DNA replication, and hence transgene templates available for transcription, and the availability of repressor proteins required for silencing transcription.

4.3.6 Design and construction TESSA-DS expressing Rep and Cap from the 4C5G-inducible promoter

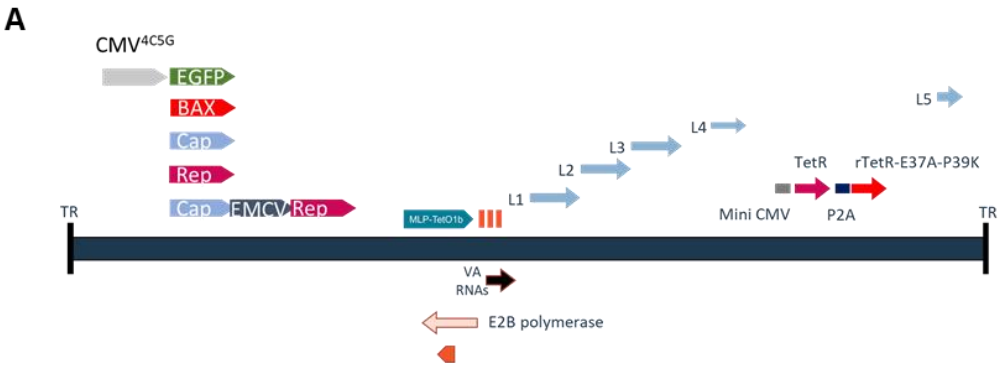
We next assessed whether the TESSA-DS system can enable production of viable adenovirus vectors encoding AAV rep and cap. We showed previously that AAV Rep proteins are potent inhibitors of the modified TESSA MLP (**Figure 4.1)**, consistent with previous reports of its activity against wt MLP (Needham et al. 2006). Additionally, the AAV p40 promoter region, involved in driving transcription of Cap and embedded within the rep gene coding sequence, is known to be a potent inhibitor of adenovirus replication *in cis* (Weger et al. 2016).

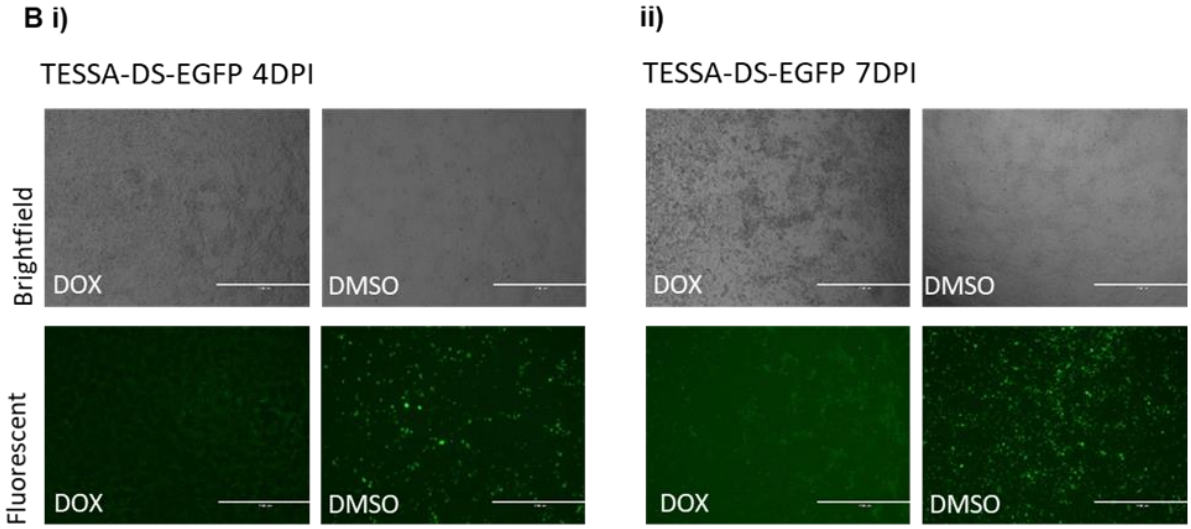
To encode AAV rep and cap within TESSA-DS, a rational combinatorial approach was adopted to alleviate adenoviral repression from Rep proteins and its coding sequences. First, as the two large AAV Rep isoforms 78 and 68 alone was reported to be sufficient for replication of the AAV genome, the AAV p19 promoter TATA element was ablated by synonymous codon exchange, while maintaining the Rep78/68 polypeptides, to prevent expression of Rep52/40 and hence their role in repressing adenoviral replication (Needham et al. 2006; Holscher, Kleinschmidt, and Burkle 1995). Secondly, the AAV p40 promoter region, involved in inhibiting adenoviral replication *in cis*, was scrambled by synonymous codon exchange to maintain Rep78/68 activity without its direct adenovirus inhibitory activity. This repΔp19 sequence configuration, with the ablated p40 promoter, is used throughout this thesis and simply referred as 'Rep' when encoded within a TESSA vector. Lastly, to enable controlled transcription of rep, we constructed two vector variants wherein either the AAV p5 promoter involved in Rep expression was exchanged with the repressible $CMV^{TetO\text{-}4C5G}$ promoter (TESSA-DS-Rep) or alternatively Rep was positioned to be expressed via an EMCV IRES element downstream of AAV5 cap (TESSA-DS-Cap-EMCV-Rep) with transcription of this bicistronic mRNA driven by $CMV^{TetO\text{-}4C5G}$ (Bochkov and Palmenberg 2006). A

TESSA-DS plasmid encoding AAV5 cap (TESSA-DS-Cap) was also constructed by removing the native p40 promoter and placing the cap coding sequence under control of $CMV^{TetO\text{-}4C5G}$.

Plasmid DNA encoding TESSA-DS-Rep, TESSA-DS-Cap-EMCV-Rep, and TESSA-DS-Cap were linearised to release the viral ITRs and transfected into HEK293 cells, and cultured with doxycycline, for vector recovery. However, while viable vectors were recovered from TESSA-DS-Cap with plaques notable at ~6 days post-transfection, cells transfected with TESSA-DS-Rep and TESSA-DS-Cap-EMCV-Rep was absent of plaques up to the observed day ~13, suggesting vectors were non-viable. This was confirmed by subsequent infection of HEK293 cells (in the presence of doxycycline) with cell lysates harvested from these samples. Vector recovery of TESSA-DS-Rep and TESSA-DS-Cap-EMCV-Rep remained unsuccessfully after several attempts (data not shown).

We hypothesized that the failure to recover viable TESSA-DS-Rep and TESSA-DS-cap-EMCV-Rep vectors was likely due to leaky expression of Rep from the TetO-4C5G system, as observed previously with TESSA-DS encoding EGFP and BAX, coupled with the high toxicity of Rep against adenovirus.


A
CMV4C5G
EGFP
BAX
Cap
Rep
Cap
EMCV
Rep
TR
MLP-TetO1b
L1
L2
L3
L4
L5
TetR
rTetR-E37A-P39K
Mini CMV
P2A
TR
VA
RNAs
E2B polymerase


B i)
TESSA-DS-EGFP 4DPI
ii)
TESSA-DS-EGFP 7DPI
Brightfield
Fluorescent
DOX
DMSO
DOX
DMSO
DOX
DMSO
DOX
DMSO

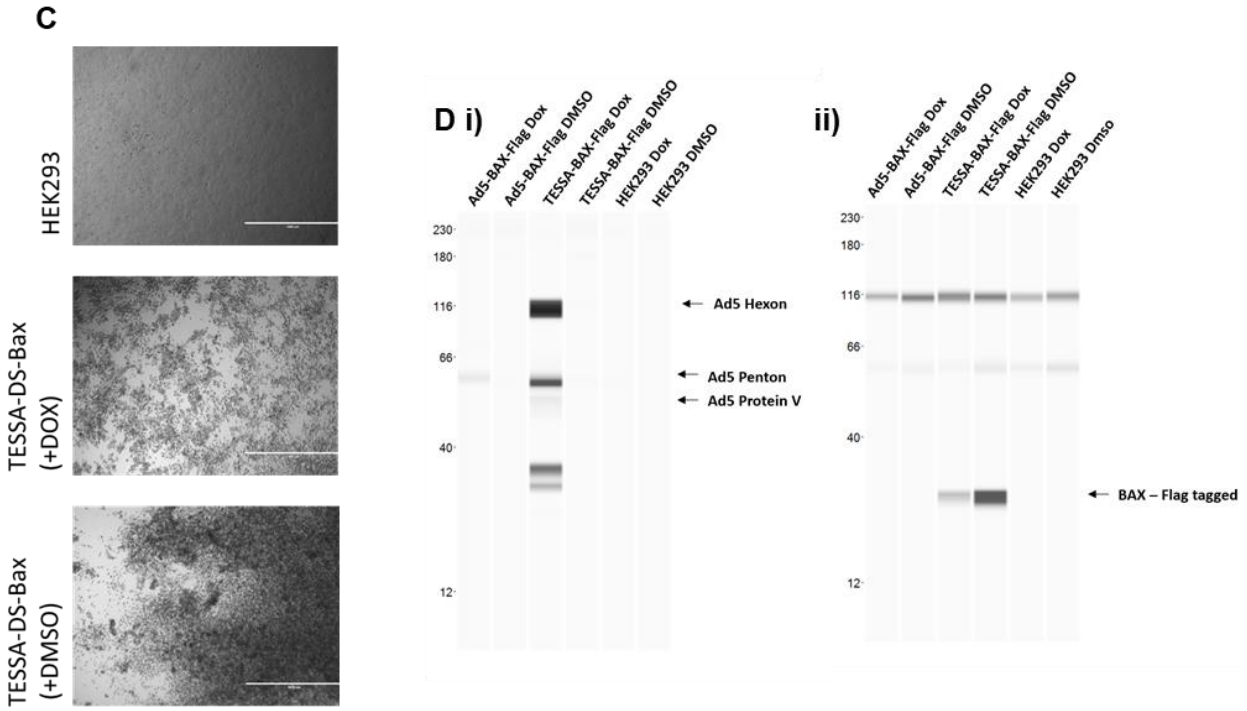

C
HEK293
TESSA-DS-Bax (+DOX)
TESSA-DS-Bax (+DMSO)
D i)
Ad5-BAX-Flag Dox
Ad5-BAX-Flag DMSO
TESSA-BAX-Flag Dox
TESSA-BAX-Flag DMSO
HEK293 Dox
HEK293 DMSO
230
180
116
66
40
12
Ad5 Hexon
Ad5 Penton
Ad5 Protein V
ii)
Ad5-BAX-Flag Dox
Ad5-BAX-Flag DMSO
TESSA-BAX-Flag Dox
TESSA-BAX-Flag DMSO
HEK293 Dox
HEK293 Dmso
230
180
116
66
40
12
BAX – Flag tagged

Figure 4.2 Assessment of the 'dual-switch' TESSA-DS vector for encoding AAV rep and cap genes. A) Schematic genomes of TESSA-DS vectors encoding for EGFP, BAX, AAV Cap2, AAV Rep, and the bicstronic Cap-EMCV-Rep sequence. **B**) Inducible expression of EGFP from TESSA-DS-EGFP vector. HEK293 cells were infected at a 1:100 dilution with crude lysate recovered from cells transfected with plasmid TESSA-DS-EGFP and treated with doxycycline 0.5µg/ml or DMSO. Cells were imaged by brightfield and fluorescent microscopy at day 4 (**i**) and day 7 (**ii**) post infection. **C**) Inducible expression of BAX from TESSA-DS-EGFP vector. HEK293 cells were infected at a 1:100 dilution with crude lysate recovered from cells transfected with plasmid TESSA-DS-EGFP and treated with doxycycline 0.5µg/ml or DMSO. Cells were imaged by brightfield and fluorescent microscopy at day 7 post infection. **D**) Western blot detection of Ad5 and BAX proteins. HEK293 cells infected with crude lysate from cells transfected with pTESSA-DS-EGFP or pAd5-BAX at a 1:100 volume dilution and cultured with doxycycline 0.5 or DMSO. Equal amounts of crude lysates were analysis by automated western blot using (**i**) anti-Ad5 and (**ii**) anti-flag antibodies at day 7 post-infection.

4.3.7 Exploring the Cumate-inducible gene expression system

To explore a more stringent repression strategy that will also be compatible with TESSA, and wherein transgene expression is silent unless induced by the effector molecule, we investigated the cumate-inducible gene expression system.

As discussed, in the cumate-inducible system, transgene expression is under control of the cumate inducible promoter CuOx6-minCMV, composed of cumate operator sites CuO (x6) fused to a core minimal CMV promoter. Transcription of transgene is induced upon binding of the transactivator protein cTA to the CuO sequences. The addition of cumate molecules inhibits DNA binding and hence transactivation by the cTA. As initial validation, HEK293 cells were co-transfected using the inducible expression plasmid pCuOx6-minCMV-EGFP (provided by OXGENE) with a plasmid expressing the cTA (pCMV-CymR-VP16; provided by OXGENE) or stuffer DNA. As expected, EGFP expression was only observed when the cTA is present (**Figure 4.3A**).

4.3.8 Engineering TESSA vectors expressing AAV Rep and Cap from the cumate-inducible system

To incorporate the cumate-inducible system into TESSA, we explored a two-vector strategy. As illustrated in **Figure 4.3B**, in one vector TESSA-AAV-EGFP was further modified to express the transactivator cTA from a constitutive micro-CMV promoter (PROM567; provided by OXGENE) and linked to the native TetR via a self-cleaving peptide P2A (TESSA-AAV-EGFP-cTA). In the other vector TESSA was modified to encode the bicistronic sequence cap5-EMCV-rep, under control of the cumate-inducible promoter CuOx6-minCMV (TESSA-CuOx6-Cap-EMCV-Rep). In this strategy, rAAV production should be induced upon co-infection of the two TESSA vectors, wherein the rAAV transfer genome and the transactivator protein is provided from TESSA-AAV-EGFP-cTA, to induce expression of Rep and Cap for AAV replication.

We first explored the feasibility of this approach by transfection of the inducible pCuOx6-Cap-EMCV-Rep plasmid into HEK293 cells and inducing AAV production using TESSA-AAV-EGFP-cTA which encodes the AAV transfer genome and the cTA. HEK293 cells were either transfected with pCuOx6-Cap-EMCV-Rep, pCuOx6-Cap-EMCV-RepΔp19 (wherein TATA element of the p19 promoter is ablated) or stuffer DNA and infected with TESSA-AAV-EGFP-cTA. Cells were cultured with DMSO or doxycycline after transduction. DNAse resistant particles harvested at 96hpi were quantified by EGFP-specific qPCR. As shown in **Figure 4.3C**, in cells transfected with stuffer DNA and infected TESSA-AAV-EGFP-cTA, ~$5x10^9$ GC/mL of TESSA-AAV-EGFP-cTA were detected by the qPCR in cells treated with doxycycline, while the DMSO treated group showed qPCR background levels. However, in HEK293 cells transfected with pCuOx6-Cap-EMCV-Rep or pCuOx6-Cap-EMCV-RepΔp19, >$2x10^9$ GC/mL of DNAse resistant particles were detected after infection with TESSA-AAV-EGFP-cTA in the DMSO group, indicating successful production of rAAV5-EGFP.

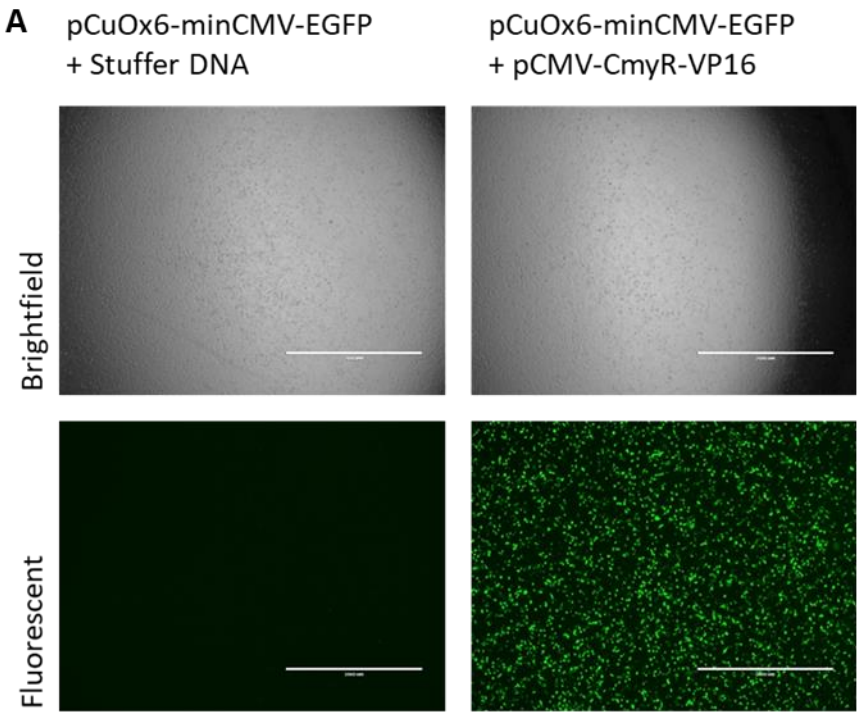
As rAAV5-EGFP titre were comparable between the use of pCuOx6-Cap-EMCV-Rep or pCuOx6-Cap-EMCV-RepΔp19, we opted to insert the CuOx6-Cap-EMCV-RepΔp19 sequence configuration into TESSA. We reasoned that ablation of the p19 TATA box should limit expression of Rep52 and Rep40 and reduce Rep induce toxicity on adenovirus replication.

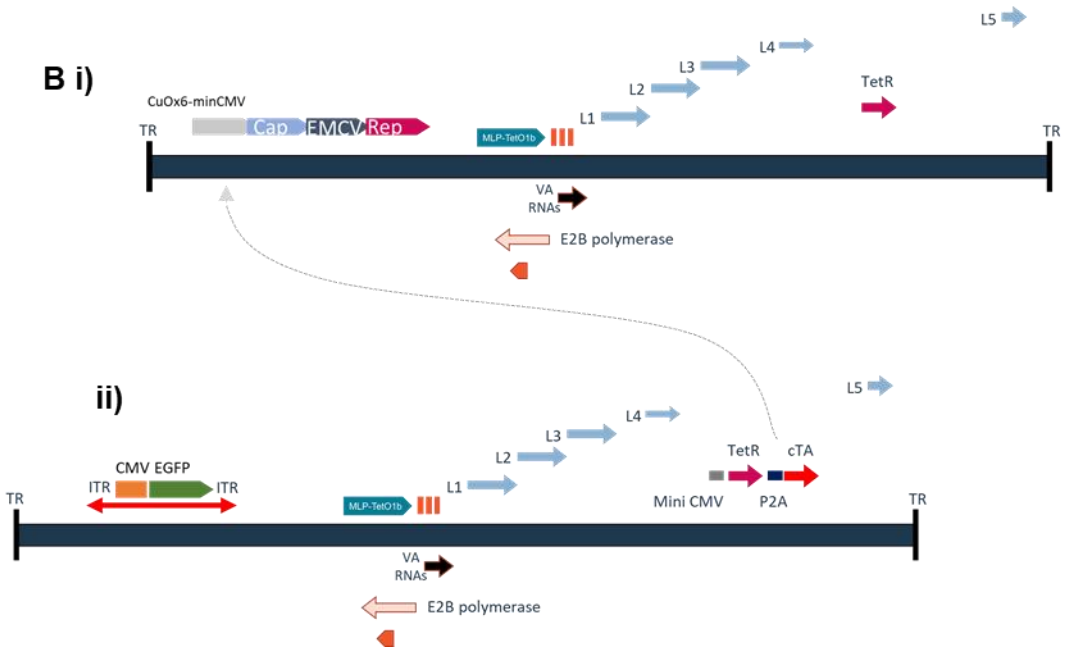
Upon transfection of linearized TESSA genomes and into HEK293 cells and cultured with doxycycline, both TESSA-AAV-EGFP-cTA and TESSA-CuOx6-Cap-EMCV-Rep vectors were recovered without notable hindrance in vector replication. For both vectors, viral plaques were observable on the cell monolayer at ~6 post transfection and vectors were harvested at day 15 upon evidence of advanced CPE.

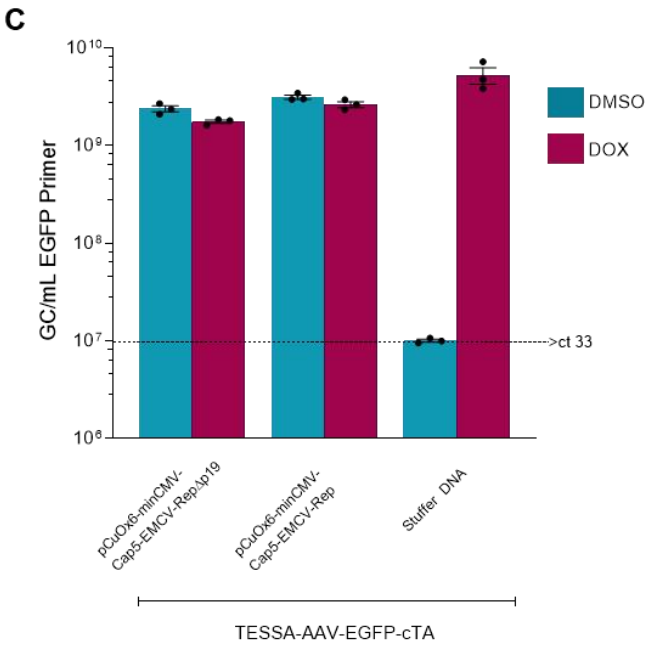
To assess AAV production, HEK293 cells were co-infected using TESSA-CuOx6-cap-EMCV-Rep with TESSA-AAV-EGFP-cTA or TESSA-AAV-EGFP (without the cTA), each at an MOI of 50, and cultured with DMSO or doxycycline. In parallel, cells were infected (MOI50) solely with each of the TESSA vector to control for vector replication and efficiency of DNase treatment. rAAV5 production was compared against the helper-free method. Vectors were harvested at 96hpi and DNAse resistant particles were qPCR directed against the EGFP-specific and adenovirus hexon-specific qPCR. As expected, in HEK293 cells solely infected with TESSA-AAV-EGFP-cTA or TESSA-AAV-EGFP and treated with doxycycline, high levels (>$2x10^9$ GC/mL) of TESSA vectors were detected from the EGFP-specific qPCR, while the DMSO treated group was detected at qPCR background levels. rAAV5-EGFP from the helper-free method was measured at ~$2x10^{10}$ GC/mL. Surprisingly, in both DMSO and doxycycline treated group, cells co-infection of TESSA-CuOx6-Cap-EMCV-Rep with TESSA-AAV-EGFP-cTA showed an absence of DNAse resistant particles (both AAV and TESSA vectors) harboring the CMV-EGFP DNA cassette, by the EGFP-specific qPCR (**Figure 4.3Di**). Similarly, in cells co-infected with the TESSA-CuOx6-Cap-EMCV-Rep with TESSA-AAV-EGFP, intact particles encoding EGFP (both AAV and TESSA) was not detected from the DMSO group, while the

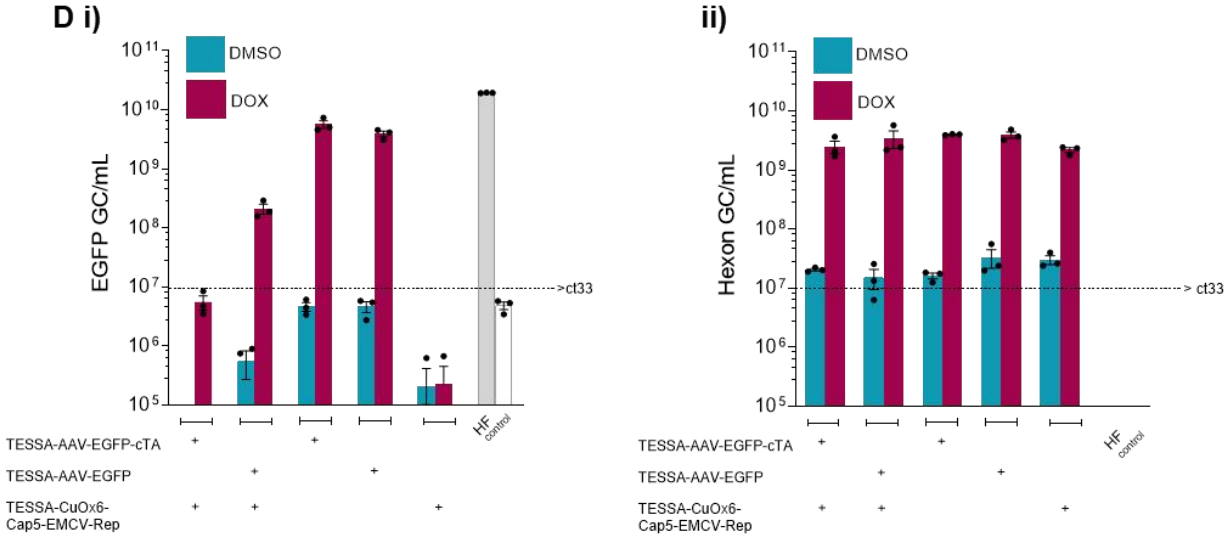
doxycycline treated group (~$2x10^8$ GC/mL) showed a 20-fold reduction in EGFP-containing particles compared to cells solely infected with TESSA-AAV-EGFP. Taken together, these results suggest that while co-infection of TESSA-CuOx6-Cap-EMCV-Rep with TESSA-AAV-EGFP-cTA or TESSA-AAV-EGFP failed to produce rAAV vectors, replication of both TESSA vectors encoding rAAV-EGFP genome was also repressed in the process. As repression of TESSA-AAV-EGFP-cTA was observed to a greater extent compared to TESSA-AAV-EGFP suggest that this effect was due to high transgene expression (presumably Rep) from TESSA-CuOx6-cap-EMCV-Rep. This raises the possibility that even in the absence of the cTA, Rep is expressed at a high level from TESSA-CuOx6-Cap-EMCV-Rep that still mediated an anti-adenovirus effect.

Interestingly, as the TESSA-CuOx6-Cap-EMCV-Rep vector was propagated in HEK293 cells without obvious hindrance in virus replication, we sought to determine whether the anti-adenovirus effect observed was specific to TESSA vectors encoding the rAAV-EGFP transfer genome. Indeed, as shown in **Figure 4.3Dii**, hexon-specific qPCR showed high levels (>$2x10^9$ GC/mL) of TESSA vectors in cells treated with doxycycline, while the DMSO group was at qPCR baseline levels. This confirmed that only TESSA vectors encoding the rAAV-EGFP sequence was repressed when co-infected with the TESSA-CuOx6-Cap-EMCV-Rep vector. As shown in **Figure 4.3E**, upon co-infection with the two TESSA vectors (TESSA-AAV-EGFP-cTA with TESSA-CuOx6-cap-EMCV-Rep) we observed almost complete repression of EGFP under fluorescence microscopy, while EGFP was expressed at high levels when cells were solely infected with TESSA-AAV-EGFP-cTA.


A
pCuOx6-minCMV-EGFP
+ Stuffer DNA
pCuOx6-minCMV-EGFP
+ pCMV-CmyR-VP16
Brightfield
Fluorescent


B i)
CuOx6-minCMV
TR
Cap
EMCV Rep
MLP-TetO1b
L1
L2
L3
L4
L5
TetR
TR
VA
RNAs
E2B polymerase
ii)
CMV EGFP
ITR
ITR
TR
MLP-TetO1b
L1
L2
L3
L4
L5
TetR
cTA
Mini CMV
P2A
TR
VA
RNAs
E2B polymerase


C
GC/mL EGFP Primer
DMSO
DOX
>ct 33
pCuOx6-minCMV-Cap5-EMCV-Rep-Δp19
pCuOx6-minCMV-Cap5-EMCV-Rep
Stuffer DNA
TESSA-AAV-EGFP-cTA


D i)
EGFP GC/mL
DMSO
DOX
>ct33
HF control
TESSA-AAV-EGFP-cTA
TESSA-AAV-EGFP
TESSA-CuOx6-Cap5-EMCV-Rep
ii)
Hexon GC/mL
DMSO
DOX
> ct33
HF control
TESSA-AAV-EGFP-cTA
TESSA-AAV-EGFP
TESSA-CuOx6-Cap5-EMCV-Rep

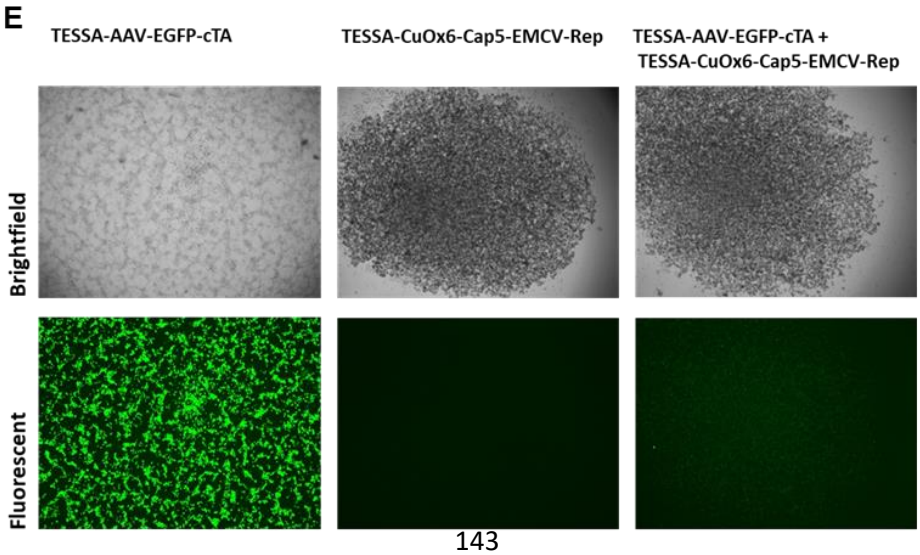

E
TESSA-AAV-EGFP-cTA
TESSA-CuOx6-Cap5-EMCV-Rep
TESSA-AAV-EGFP-cTA + TESSA-CuOx6-Cap5-EMCV-Rep
Brightfield
Fluorescent

Figure 4.3 Evaluation of the Cumate inducible system for production of AAV using TESSA vectors. A) Inducible EGFP reporter expression from the cumate transactivator cTA. HEK293 cells were co-transfected using plasmid expressing EGFP under control of the cumate inducible promoter (CuOx6_minCMV) with pCMV-cTA or stuffer DNA. Cells were imaged by brightfield and fluorescent microscopy 48 hpt. **B**) Production of AAV5 from TESSA using the cumate inducible AAV5 RepCap plasmids. HEK293 cells were infected with TESSA vector encoding the AAV transfer genome and a cTA (TESSA-AAV-EGFP-cTA) at an MOI of 50 and transfected with pCuOx6_minCMV-Cap5-EMCV-Rep, pCuOx6_minCMV-Cap5-EMCV-RepΔp19 (wherein the p19 TATA element is ablated) or stuffer DNA plasmid. Cells were treated DMSO or doxycycline 0.5µg/mL. DNAse resistant vectors harvested at 96hpi were quantified by EGFP-specific qPCR. **C**) Schematic design for production of AAV from two TESSA vectors using the cumate inducible system. Co-infection of TESSA encoding the cumate inducible Cap and Rep expression cassette (i) TESSA-CuOx6-Cap5-Rep with (ii) TESSA-AAV-EGFP-cTA should enable expression of Rep and Cap proteins for replication and encapsidation of AAV genomes. **D**) HEK293 cells were co-infected using TESSA-CuOx6-Cap5-Rep with TESSA-AAV-EGFP-cTA or TESSA-AAV-EGFP (without cTA) at an MOI of 50 and treated with DMSO or doxycycline 0.5µg/mL. AAV5 production was compared to the helper-free method. Vectors were harvested at 96 hpi and encapsidated genomes quantified by (**i**) EGFP-specific and (**ii**) Hexon-specific qPCR. Data as mean±SEM of triple biological replicates. **E**) Representative brightfield and fluorescent images of HEK293 cells infected (MOI50) with TESSA-AAV-EGFP-cTA, TESSA-CuOx6-Cap5-Rep or co-infected together. Cells were imaged at 48hpi.

4.3.9 Construction of TESSA encoding promoterless AAV rep

While viable and high titre vectors were recovered from TESSA-CuOx6-Cap-EMCV-Rep, it failed to induce AAV replication when the rAAV genome was provided by co-infection with TESSA-AAV-EGFP-cTA or TESSA-AAV-EGFP. As transfection of plasmid pCuOx6-Cap-EMCV-Rep enabled high-titre rAAV production from TESSA-AAV-cTA, we reasoned that Rep, known to be detrimental for adenoviral and AAV replication at high levels, is overexpressed from TESSA and involved in silencing production of rAAV from the co-infection experiments (Needham et al. 2006; Chiorini et al. 1996).

In an attempt to effectively ablate Rep expression and to monitor vector replication, we inserted the AAV repΔp19 gene sequence, without its native p5 or any heterologous promoter, into TESSA-AAV that encoded the EGFP expression cassette. Rep was positioned within the E1-deleted region

in a reverse transcription orientation relative to the viral packaging sequence, to avoid transcriptional influence from the AAV or Ad ITRs, wherein the E1A enhancer is embedded within the viral packaging signal, trying to ensure minimal Rep expression (Hearing and Shenk 1983). In parallel, a TESSA-AAV-EGFP vector expressing Cap2 under the constitutive CMV promoter was also constructed for complementation of TESSA-Rep in producing rAAV.

Schematic diagram for insertion of AAV2 Rep and Cap into TESSA-AAV-EGFP is provided in **Figure 4.4 A&C**, respectively. For the construction of TESSA-AAV-EGFP-Rep, the Rep coding sequence was excised from an pE1-shuttle-Rep plasmid (pSU633) and inserted into plasmid pTESSA-AAV-EGFP linearized with PacI. Correct clones screened by restriction enzymes EcoRI and Bstz17I is shown in **Figure 4.4B**. For the construction of pTESSA-AAV-EGFP-Cap2, the CMV-Cap2 expression cassette was excised from an E1-shuttle plasmid pCMV-Cap2 using PacI and inserted into pTESSA-AAV-EGFP linearized with the same enzymes. Correct clones of pTESSA-AAV-EGFP-Cap2 screened by PacI restriction digest is shown in **Figure 4.4D.**

Following transfection of the TESSA genomes into HEK293 cell and treatment with doxycycline, formation of viral plaques was notably delayed from TESSA-AAV-EGFP-Rep, and only observed at ~9 days post-transfection, compared to TESSA-AAV-EGFP-CMV-Cap or the transfection control TESSA-AAV-EGFP which plaqued at day ~5-6. This observation suggested that replication of TESSA-AAV-EGFP-was likely hindered by insertion of rep. To confirm whether the TESSA-AAV-EGFP-Rep vector was viable, fresh HEK293 cells infected (1:1000 volume dilution) with crude lysates from HEK293 cells transfected with pTESSA-AAV-EGFP-Rep or pTESSA-AAV-EGFP showed plaque formation and spread of EGFP across the cell monolayer (**Figure 4.4E**).

To assess whether the rep coding sequence was stably maintained in TESSA-AAV-EGFP-Rep, vectors were harvested at day 16 and serially passaged in HEK293 cells four times in the presence of doxycycline. HEK293 cells were then infected (1:1000 volume dilution) with the passaged

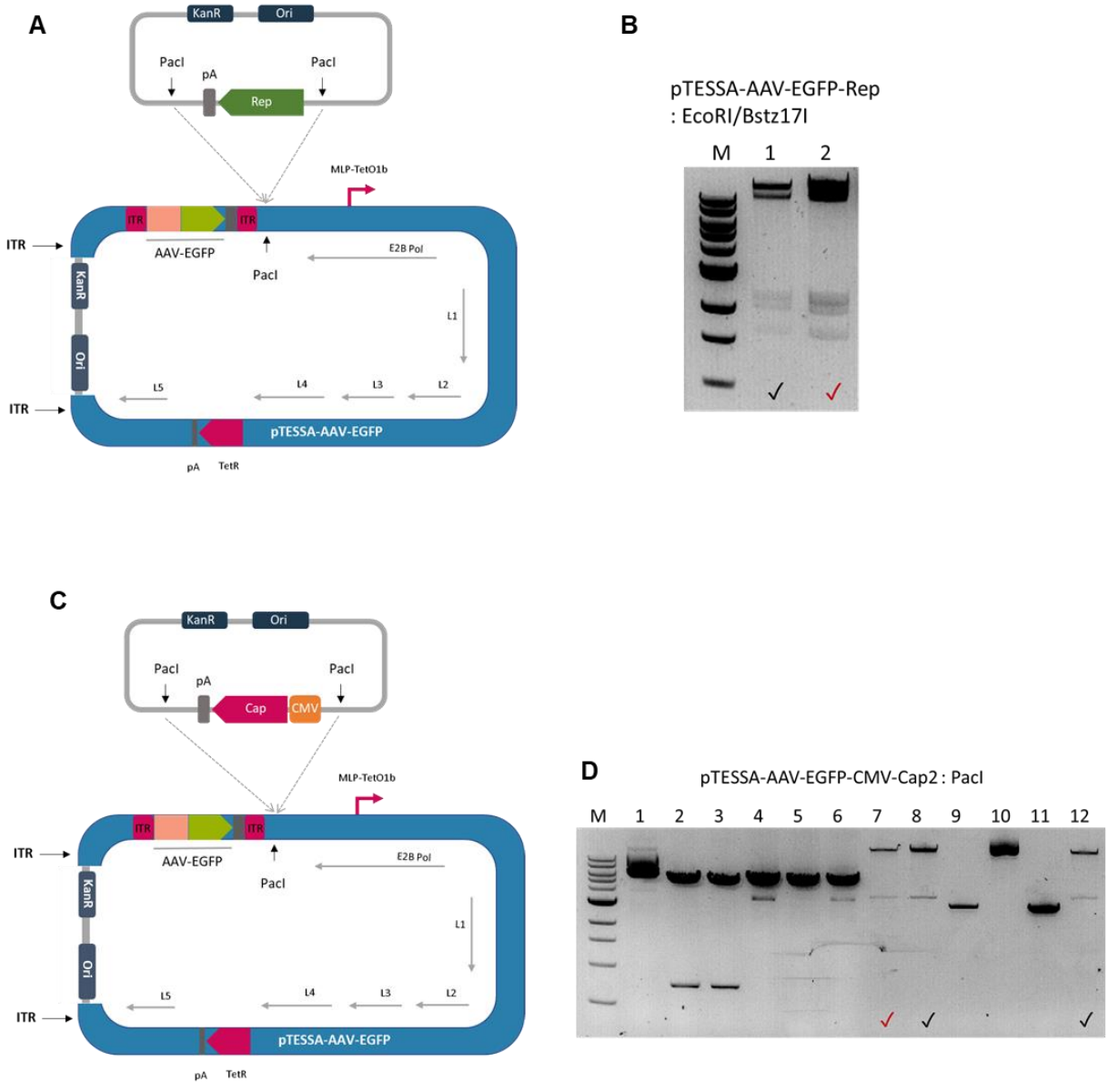
TESSA-AAV-EGFP-CMV-Cap2 or TESSA-AAV-EGFP-Rep and total DNA extracted at 72 hpi. DNA was measured by qPCR using primers and probe directed against EGFP, Rep, and TetR. Rep coding sequence was shown to be equimolar with adenovirus hexon DNA (**Figure 4.4F**), indicating that it was maintained within TESSA. However, a greater than 18-fold increase in EGFP DNA was observed compared to TetR DNA from TESSA-AAV-EGFP-Rep, which was not detected from the TESSA-AAV-EGFP-CMV-Cap2 vector without rep. This confirmed that despite the absence of a heterologous promoter, Rep was sufficiently expressed from TESSA-AAV-EGFP-Rep to enable rescue and replication of the embedded AAV genome. It is likely that simultaneous replication of the recombinant AAV and adenoviral genomes impeded production TESSA-AAV-EGFP-Rep in HEK293 cells, which was typically observed to yield ~10-folds lower in infectious particles compared TESSA-AAV-EGFP-CMV-Cap2 (data not shown).

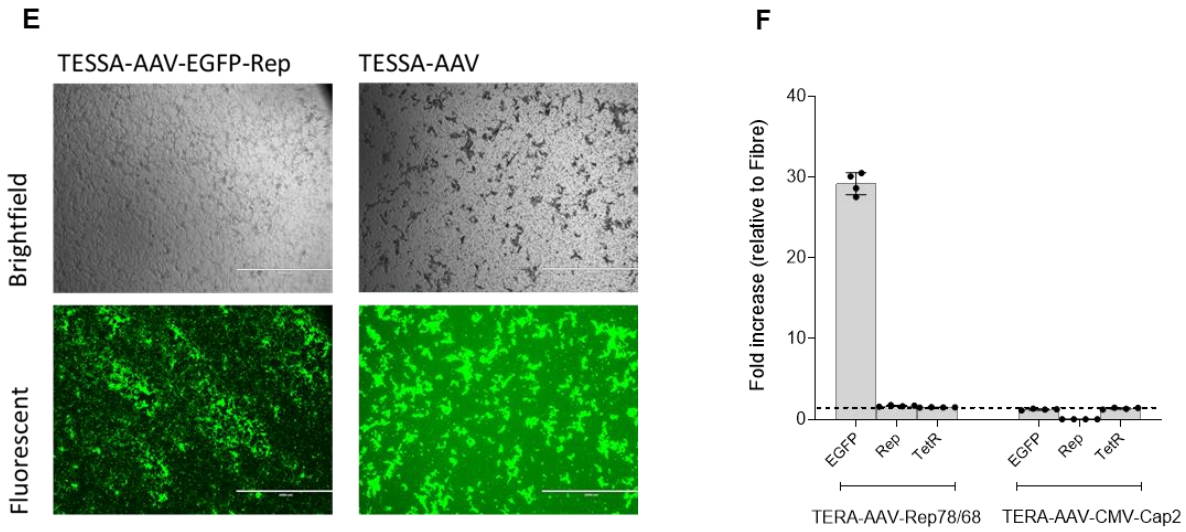
4.3.10 Assessment of rAAV production using TESSA encoding the AAV transfer genome and Rep *in cis*

While rescue of the AAV genome during replication of TESSA vector containing both Rep and the AAV genome in cis is undesirable and suboptimal for large scale manufacture of TESSA vectors, we explored whether this phenomenon could give improvements in rAAV production. HEK293 cells were therefore co-infected using TESSA-AAV-EGFP-Rep with TESSA-AAV-EGFP-CMV-Cap2, and treated with doxycycline or DMSO, or transfected with the helper-free plasmids. Vectors were harvested at 96 hpi and DNase-resistant particles quantified by EGFP-specific and Hexon-specific qPCR. As shown in **Figure 4.4G**, while the helper-free method yielded an average of 4.8 $x10^8$ GC/mL of DNase-resistant rAAV2, a greater than 40-fold increase was observed from co-infection of TESSA which yielded 1.9 $x10^{10}$ and 2.5 $x10^{10}$ GC/mL of rAAV2-EGFP, in the doxycycline

and DMSO treated group, respectively. As expected, adenovirus particles were detected at >2 x10^8 GC/mL from TESSA infected cells that were treated with doxycycline, but absent from the DMSO treatment group or helper-free samples when measured using the Hexon-specific qPCR.

Our results suggest significant improvement in AAV production can be achieved by this complete transfection-free process using two TESSA vectors. However, the low adenovirus yield achieved from production of TESSA-AAV-EGFP-Rep presents significant manufacturing challenges.




E
TESSA-AAV-EGFP-Rep
TESSA-AAV
Brightfield
Fluorescent
F
Fold increase (relative to Fibre)
40
30
20
10
0
EGFP
Rep
TetR
EGFP
Rep
TetR
TERA-AAV-Rep78/68
TERA-AAV-CMV-Cap2

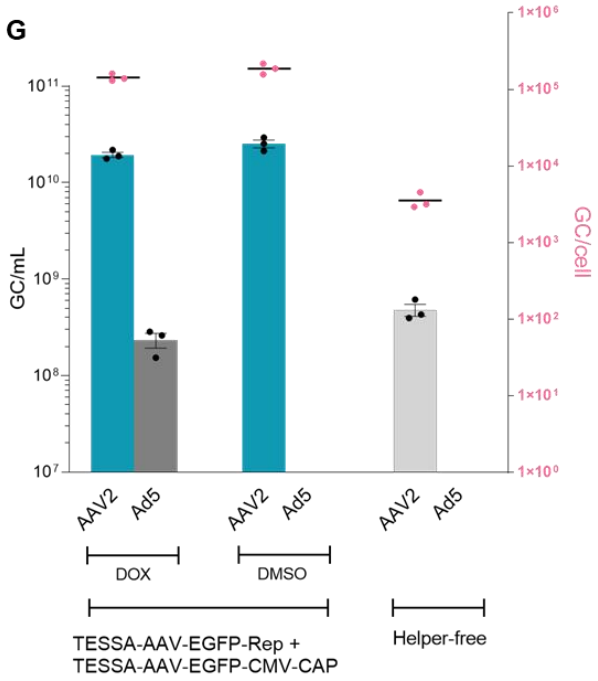

G
GC/mL
GC/cell
AAV2
Ad5
AAV2
Ad5
AAV2
Ad5
DOX
DMSO
TESSA-AAV-EGFP-Rep +
TESSA-AAV-EGFP-CMV-CAP
Helper-free

Figure 4.4 TESSA-AAV-EGFP encoding Rep enables rescue and replication of the AAV transfer genome for high-titre AAV vector production. A) Cloning schematic for insertion of the AAV rep coding sequence into plasmid pTESSA-AAV-CMV-EGFP by restriction cloning and (**B**) restriction digest using EcoRI and Bstz17I for screening correct clones. **C**) Cloning schematic for insertion of the CMV-Cap2 expression cassette into plasmid pTESSA-AAV-CMV-EGFP by restriction cloning and (**D**) restriction digest using PacI for screening correct clones. **E**) Replication of TESSA encoding the AAV transfer genome and AAV rep *in cis.* HEK293 cells were infected at 1:1000 volume dilution using crude lysates from cells transfected with plasmid TESSA-AAV-EGFP-Rep or the control TESSA-AAV-EGFP and cultured doxycycline 0.5 µg/ml. Cells were imaged at day 7 post infection by brightfield and fluorescent microscopy. **F**) AAV transfer genome is rescued and amplified during propagation of the TESSA-AAV-EGFP in HEK293 cells. Cells were infected with TESSA-AAV-EGFP-Rep or TESSA-AAV-EGFP-Cap2 at 1:1000 volume dilution and treated with doxycycline 0.5 µg/ml. Total DNA was extracted at 72hpi for qPCR analysis using primers and probe directed against the EGFP, Rep and TetR coding sequence. Data as mean±SEM of four biological replicates. **G**) Production of AAV using TESSA encoding AAV rep and the transfer genome compared to the helper free method. HEK293 cells were co-infected with TESSA-AAV-EGFP-Rep and TESSA-AAV-EGFP-Cap, each at an MOI of 25, and cultured with doxycycline 0.5 µg/mL or DMSO, or triple transfected with the helper free plasmids. Vectors were harvested 96 hpi and DNAse resistant particles quantified by EGFP and Hexon-specific qPCR, for quantification of AAV and adenovirus particles, respectively. AAV titre (GC/mL) is determined by subtraction of the EGFP-specific qPCR by the amount of adenovirus determined from the Hexon-specific qPCR. Productivity of AAV vectors per cell is shown on the right axis. Data as mean±SEM of triple biological replicates.

4.3.11 rAAV2 production via TESSA^{v1} approach (co-infection of TESSA-Rep with TESSA-AAV-EGFP-Cap2)

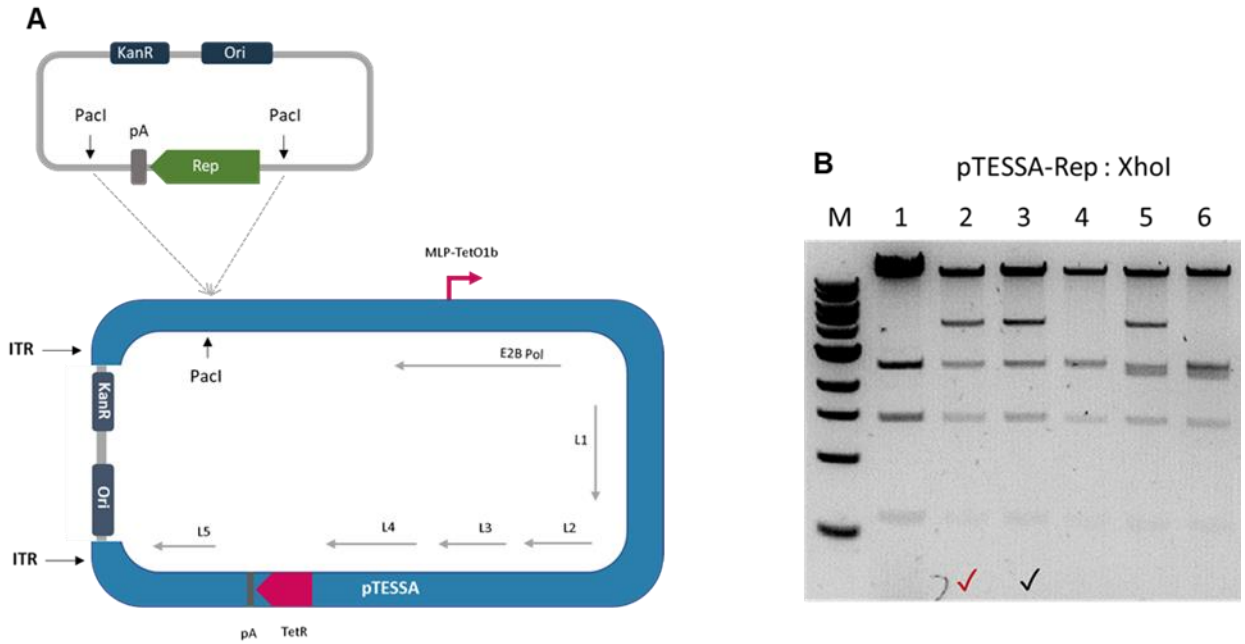
As encoding AAV rep *in cis* with the AAV transfer genome impeded TESSA replication, we inserted the rep, absent of any heterologous promoter and in a reverse transcription orientation relative to the viral packaging sequence, within a TESSA vector without the AAV transfer genome (TESSA-Rep) as shown in **Figure 4.5A**. The rep sequence was excised using PacI from a E1-shuttle plasmid (pSU631) and inserted into pTESSA (pSU390) linearized with the same enzymes. Positive clones isolated and screened by PacI restriction digest is shown in **Figure 4.5B**. TESSA-Rep vectors were recovered in HEK293 cells after transfection of the linearized genome plasmid. Viral plaques were

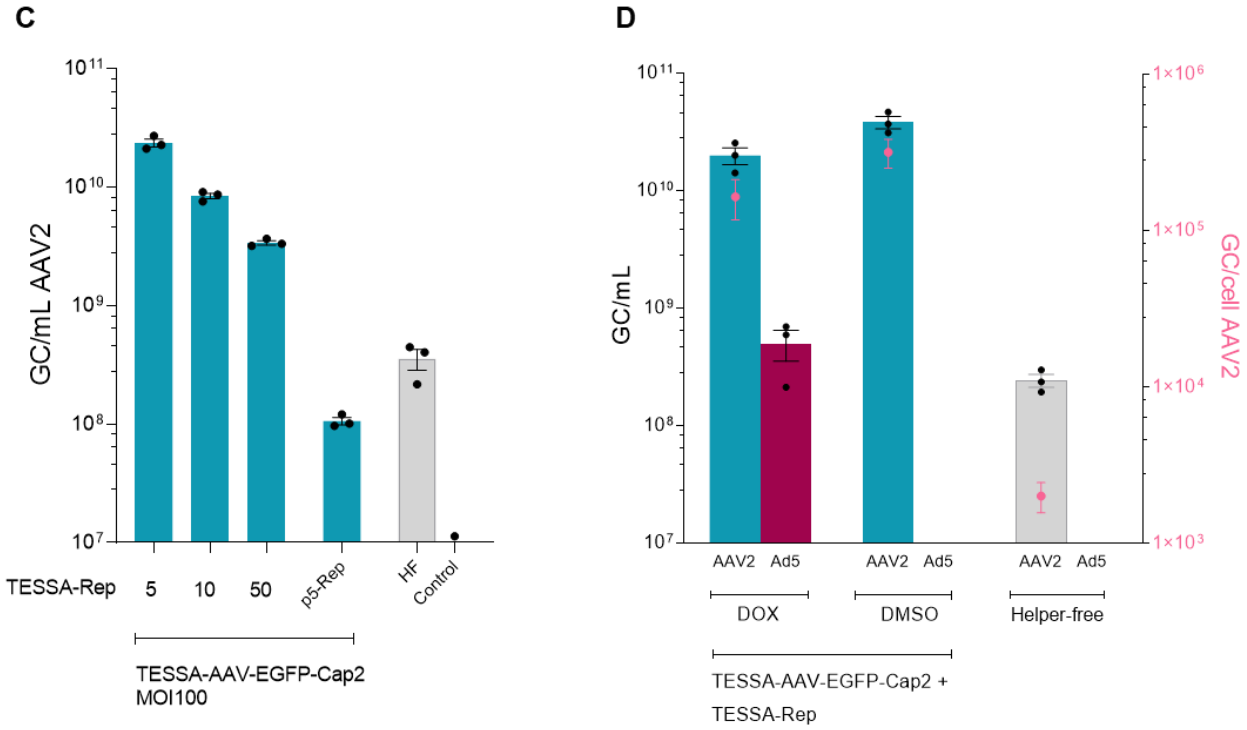
notable on the cell monolayer at the standard ~6-7 days post-transfection and vectors were harvested at day 15.

An initial optimization study was carried out to evaluate the TESSA-Rep. HEK293 cells were co-infected using TESSA vector encoding CMV-Cap2 and the rAAV transfer genome *in cis* (TESSA-AAV-EGFP-Cap2) at an MOI of 100 with increasing MOI of TESSA-Rep or transfected with plasmid encoding the repΔ19 sequence under control of the native AAV p5 promoter. rAAV production via co-infection of TESSA-Rep with TESSA-AAV-EGFP-Cap2 is hereon known as the 'TESSA^{V1}' system. rAAV production was compared to the helper-free method as shown in **Figure 4.5C**. DNAse-resistant particles harvested at 96 hpi, and quantified using EGFP-specific qPCR, showed decreasing levels of rAAV2-EGFP was observed with increasing MOI of TESSA-Rep, consistent with reports that Rep overexpression impedes AAV replication (Li, Samulski, and Xiao 1997). Maximal yield of rAAV2 (2.4 x10^{10} GC/mL) was observed when TESSA-Rep was used at a MOI of 5, and co-infected with vector TESSA-AAV-EGFP-Cap2 (MOI 100), while the helper-free method produced an average of 3.6 x10^{8} GC/mL of AAV2. A low yield of rAAV2 (1.0 x10^{8} GC/mL) was also observed when p5-Rep was provided by transfection suggesting an inherent benefit from delivery of rep using TESSA.

To further evaluate the levels of contaminating adenovirus from the TESSA^{V1} approach, productions in HEK293 cells were also carried out in the presence of DMSO or doxycycline to enable TESSA replication. Vectors produced via TESSA^{v1} or helper-free plasmids were harvested at 96hpi and DNAse-resistant particles quantified by EGFP-specific and Hexon-specific qPCR. As shown in **Figure 4.5D**, while the helper-free method yielded an expected titre of 2.5x10^{8} GC/mL of intact rAAV vectors, cells co-infected using TESSA-Rep with TESSA-AAV-EGFP-Cap2 and treated with DMSO produced 3.8x10^{10} GC/mL of intact rAAV2-EGFP, with the hexon-qPCR measured at baseline levels (ct >35) from these samples. In the doxycycline treated group, co-infection of the

TESSA vectors yielded 2.0x10^{10} GC/mL of intact rAAV2-EGFP, ~50% less compared to treatment with DMSO, which was accompanied with significant amounts (>5x10^{8} GC/mL) of contaminating TESSA vectors measured by the Hexon-specific qPCR. Levels of contaminating infectious adenoviruses from these samples were further confirmed using a TCID50 assay and carried out in HEK293 cells supplemented with doxycycline 0.5 µg/mL to enable replication of any contaminating TESSA vectors. As shown in **Figure 4.5E**, while production of rAAV2-EGFP using TESSA^{V1} in the presence of doxycycline yielded ~2.0x10^{8} TCID50/mL of infectious adenoviruses, less than 10 TCID50/mL were found in the DMSO-treated group. Representative brightfield and fluorescence images of the TCID50 assay taken at day 7 post-infection is shown in **Figure 4.5F**. HEK293 cells infected at 1:10 dilution with rAAV crude lysates derived from the TESSA vectors (DMSO-treated group) showed significant expression of EGFP from rAAV particles, but free of adenovirus plaques and CPE, while plaques were readily detected from the doxycycline-treated group at 1 x 10^{-7} dilution.




C
GC/mL AAV2
TESSA-Rep
5
10
50
p5-Rep
HF
Control
TESSA-AAV-EGFP-Cap2
MOI100
D
GC/mL
GC/cell AAV2
AAV2
Ad5
DOX
DMSO
Helper-free
TESSA-AAV-EGFP-Cap2 +
TESSA-Rep

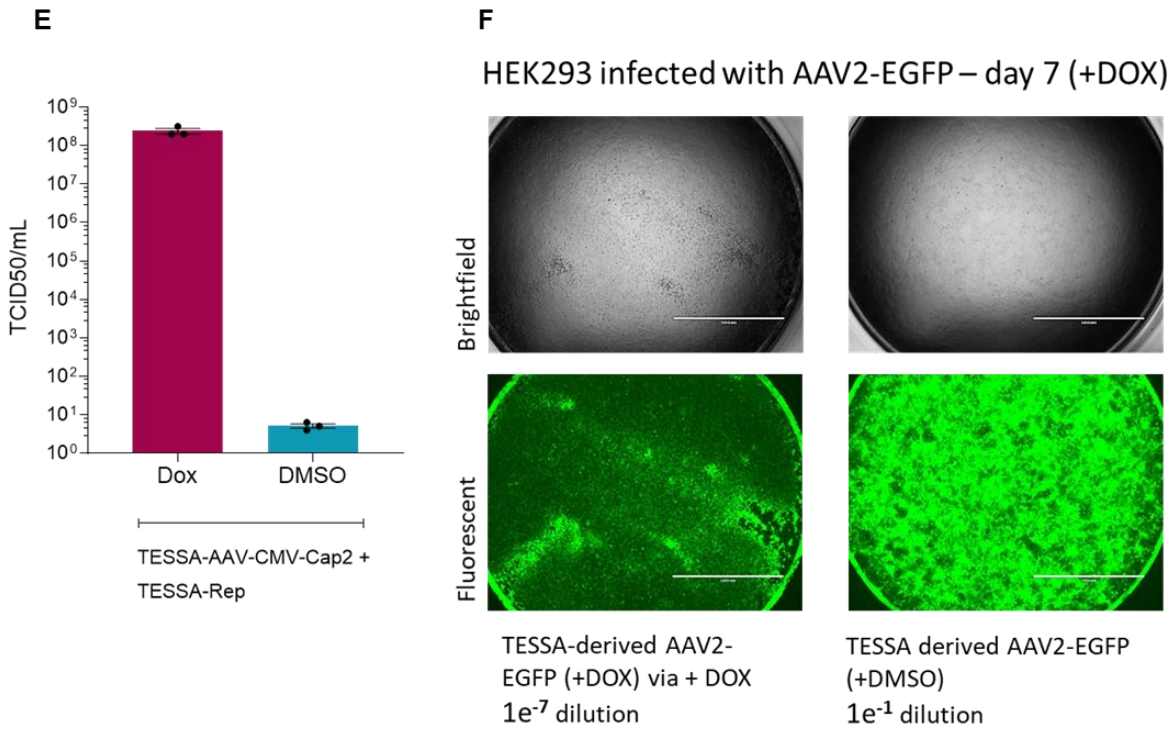

E
TCID50/mL
Dox
DMSO
TESSA-AAV-CMV-Cap2 +
TESSA-Rep
F
HEK293 infected with AAV2-EGFP – day 7 (+DOX)
Brightfield
Fluorescent
TESSA-derived AAV2-EGFP (+DOX) via + DOX
1e-7 dilution
TESSA derived AAV2-EGFP (+DMSO)
1e-1 dilution

Figure 4.5 Production of rAAV2-EGFP via the TESSA^{V1} system. A) Cloning schematic for insertion of the rep coding sequence into plasmid pTESSA by restriction cloning and **B**) XhoI restriction digest for screening correct clones. **C**) HEK293 cells were transfected with the helper-free plasmids or co-infected using TESSA-AAV-EGFP-Cap2 (MOI of 100) with increasing MOI of TESSA-Rep or transfected with plasmid p5-Rep. Samples were harvested 96 hpi and DNAse-resistant AAV quantified by EGFP-specific qPCR. Data as mean±SEM of triple biological replicates. **D**) HEK293 cells were co-infected with TESSA-AAV-EGFP-Cap2 (MOI of 100) and TESSA-Rep (MOI of 5) and treated with doxycycline 0.5 µg/mL or DMSO. AAV production is compared to helper free method. Vectors were harvested 96 hpi and DNAse resistant particles measured by EGFP and Hexon-specific qPCR, for quantification of AAV and adenovirus particles, respectively. AAV titre (GC/mL) is determined by subtraction of the EGFP-specific qPCR by the amount of adenovirus determined from the Hexon-specific qPCR. Productivity of AAV vectors per cell is shown on the right axis. Data as mean±SEM of triple biological replicates. **E**) Quantification of infectious adenovirus using the TCID50 assay. Crude lysates generated from co-infection of TESSA-AAV-EGFP-Cap2 and TESSA-Rep in HEK293 cells and treated DMSO or doxycycline 0.5 µg/ml, were added to fresh HEK293 cells and cultured for a further 10 days in the presence of doxycycline to detect contaminating adenoviruses. Data as mean±SEM of triple biological replicates. **F**) Representative brightfield and fluorescence microscopy imaged at day 7 post infection.

4.3.12 rAAV2 derived from TESSA^{V1} vectors exhibit enhanced cell transduction

To further characterize rAAV2 produced from TESSA^{V1}, we measured transducing of rAAV2-EGFP using a modified TCID50 assay in HEK293 cells. Serial dilutions were prepared using crude rAAV preparations generated from HEK293 cells (cultured in absence of doxycycline) co-infected with the TESSA^{V1} vectors or transfected with the helper-free plasmids. Ten replicates of each dilution were added to individual wells of HEK293 cells seeded in a 96-well plate format. EGFP positive wells were determined using fluorescence microscopy day 6 post-infection.

As shown in **Figure 4.6A**, we observed a low 1.4x10^5 TCID50/mL of rAAV2 produced via the helper-free method, while TESSA^{V1} resulted in significantly higher yields of 1.8x10^8 TCID50/mL of AAV2. These data, when combined with the qPCR quantification for genome numbers results in an extrapolated GC/TCID50 ratio of ~2x10^3 for rAAV2 produced using the helper-free method,

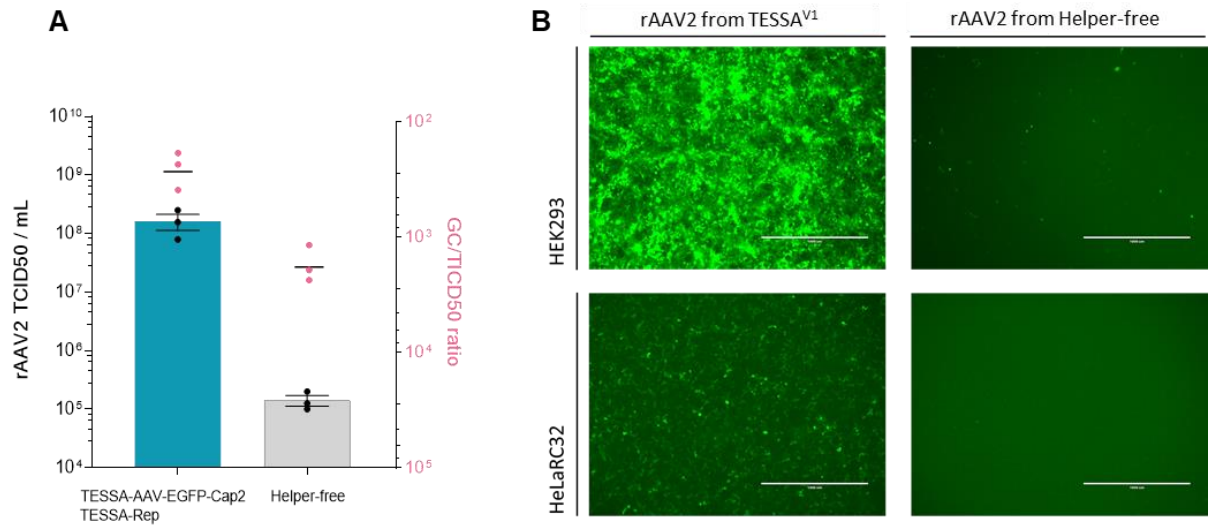
compared to a favorable GC/TCID50 ratio of ~200 for rAAV2 derived from TESSA^{V1} (Figure 4.6A, right axis). This is consistent with previous reported particle to transduction ratio of rAAV2 produced from the helper-free method (Francois et al. 2018; Halbert et al. 1995; Zeltner et al. 2010), indicating that the majority of rAAV2 particles were transduction defective. In contrast, rAAV2 produced from TESSA^{V1} showed a 10-fold increase in transduction efficiency. These results demonstrate a remarkable differential increase of over a 1000-fold (>100-fold particle yield improvement coupled to 10-fold improvement in infectivity per particle) in the production of transduction-competent rAAV2 compared to the helper-free method. This dramatic difference can be easily observable from HEK293 or HeLaRC32 cells infected (at a 1:100 volume dilution) with TESSA-derived or helper-free plasmids-derived crude preparations (**Figure 4.6B**).

4.3.13 Reverse DNA packaging in AAV2 vectors

Packaging of DNA impurities derived from plasmids, helper-virus or cell genome, in rAAV vectors has been extensively reported (Chadeuf et al. 2005). A major source of DNA impurities in AAV vectors, produced via the plasmid transfection process, is derived from inaccurate packaging of the plasmid backbone encoding the rAAV transfer genome, and have been shown to be present at levels ranging from 1-6%. This process is known as 'reverse packaging' (Tai et al. 2018; Penaud-Budloo et al. 2018).

To assess for DNA impurities in rAAV vectors derived from TESSA, DNAse-resistant rAAV2 particles produced TESSA^{V1} were assessed by qPCR directed against the adenovirus packaging signal (approximately 325bp outside the left AAV ITR) or the Cap2 coding sequence (approximately 1717bp outside the right AAV ITR). As shown in **Figure 4.6C**, when compared to the rAAV titre determined by the EGFP-specific qPCR, the adenovirus packaging signal or cap2 sequence was

determined to be present in ~2% of rAAV particles. These levels are comparable to the contamination of plasmid backbone in rAAV particles reported for the helper-free method as discussed above and is further explored in *Section 4.3.20.*



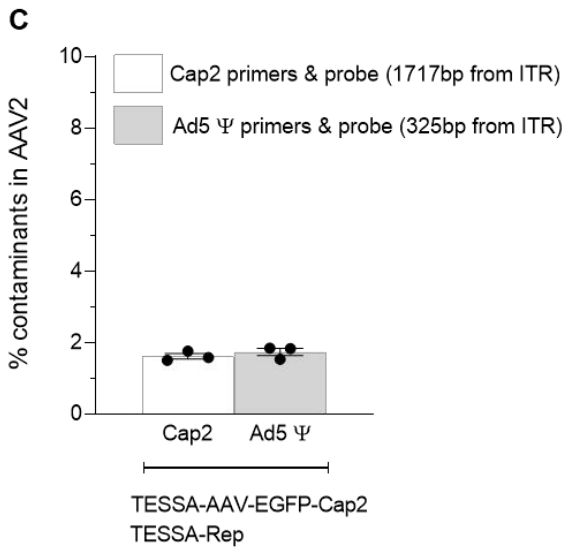


Figure 4.6 rAAV2 produced from the TESSA^{V1} show enhance transduction *in vitro*. A) Transduction efficiency (TCID50 per mL) of rAAV2 vectors produced from the TESSA^{V1} (TESSA-Rep used at MOI5, TESSA-AAV-EGFP-Cap2 used at MOI100) or helper-free plasmids were determined in HEK293 cells using a modified TCID50 assay. GC/TCID50 ratio determined by comparing against intact particles quantified by EGFP-qPCR is shown on the right axis. Data presented as mean ± SEM of triple biological replicates. **B**) Representative fluorescent images of rAAV2-mediated transduction efficiency in HEK293 and HeLa RC32 cells. Cells were infected with rAAV2 crude lysates produced from TESSA^{V1} or helper-free plasmids at a 1 in 100 volume dilution and imaged at 96hpi. Scale bar, 1000 µm. **C**) Quantification of DNA impurities in rAAV derived from TESSA^{V1}. DNAse-resistant rAAV2 particles were quantified by qPCR using primers and probe against the cap2 and adenovirus packaging sequence (Ψ). Data is presented as percentage of DNA contaminants (cap2 or Ψ sequence) in intact rAAV2 particles determined by the EGFP-specific qPCR. Data as mean±SEM of triple biological replicates.

4.3.14 Production of AAV-hFIX vectors using TESSA-Rep

To assess whether improved production of rAAV2 vectors encoding therapeutically relevant transgenes can be achieved from the TESSA^{V1} system, we evaluated the efficiency of production of rAAV2 encoding the human factor IX (hFIX) gene, currently showing great promise in the clinics for the treatment of hemophilia B (Nathwani et al. 2002; Perrin, Herzog, and Markusic 2019). Here, we generated TESSA encoding the rAAV transfer genome containing hFIX and CMV-Cap2 expression cassette *in cis* (TESSA-AAV-hFIX-Cap2).

Schematic diagram for the insertion of the rAAV genome encoding hFIX under control of the liver-specific promoter HCR-hAAT (Nathwani et al. 2002) into plasmid pTESSA-Cap2 (pSU1153) is shown in **Figure 4.7A**. The recombinant AAV transfer genome was excised from plasmid pAAV-hFIX (pSU908) using PacI restriction enzymes and insertion into AsisI linearized pTESSA-Cap2. Positive clones were isolated and screened by EcoRI restriction digest as shown in **Figure 4.7B**.

TESSA-AAV-hFIX-Cap2 vectors were recovered from HEK293 cells by transfection of the plasmid genome. From observation, vector replication was comparable to control E1/E3Δ-Ad5, wherein

vial plaques were observable across the cell monolayer ~6 days post-transfection (not shown) and vectors were harvested at day 15.

For assessment of rAAV2 production, HEK293 cells were co-infected with increasing MOI of TESSA-AAV-hFIX-Cap2 and TESSA-Rep (MOI of 5). rAAV2-hFIX production was compared to the helper-free method using the pAAV-hFIX genome plasmid. In parallel, cells were also infected with TESSA-AAV-hFIX-Cap2 only at the indicated MOI or mock transfected with pAAV-hFIX, pHelper and stuffer DNA (pUC19) to control for efficiency of DNAse treatment. DNAse-resistant vectors were harvested at 96hpi and quantified using hFIX-specific qPCR. While an average yield of 1.0 $x10^8$ GC/mL of AAV2 was observed from the helper-free method, cells co-infected with TESSA-AAV-hFIX-Cap2 and TESSA-Rep produced >100-fold more AAV encoding hFIX (~1 $x10^{10}$ GC/mL). Comparable levels were observed for all three MOI of TESSA-AAV-hFIX-Cap2 that was assessed. Interestingly, productivity of rAAV-hFIX from the helper-free method or $TESSA^{V1}$ were notably lower compared to production of rAAV-EGFP (**Figure 4.5D)**, suggesting an effect of transgene on vector productivity.

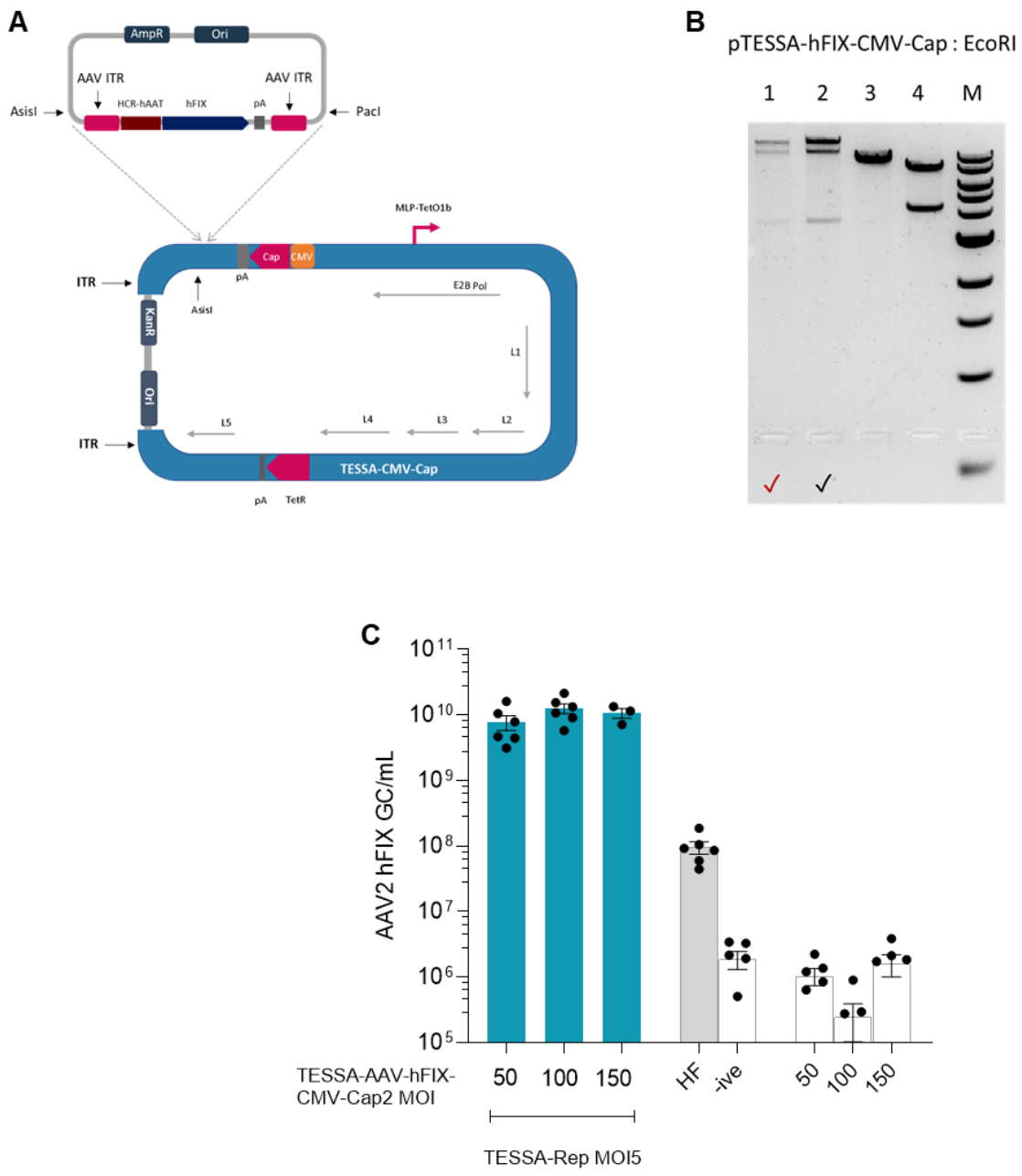


Figure 4.7 Production of rAAV2-hFIX from TESSA^{V1}. A) Cloning schematic for insertion of the rAAV transfer genome encoding hFIX into plasmid pTESSA-Cap2 by restriction cloning and (**B**) PacI restriction digest for screening correct clones. **C**) Production of AAV2-hFIX by co-infection (at the indicated MOI) of TESSA-AAV-hFIX-Cap2 and TESSA-Rep compared to the helper free method. DNAse resistant AAV particles were quantified by hFIX-specific qPCR at 96 hpi. Data as mean±SEM from two independent experiments.

4.3.15 Assessment of AAV9 vector production using TESSA-AAV-EGFP-Cap9

To assess whether the benefit of using TESSA extended to other AAV capsid serotypes, we first assessed production of rAAV9 vectors. Plasmid pTESSA-AAV-EGFP-Cap9 was constructed as per TESSA-AAV-EGFP-Cap2 (**Figure 4.4C**). Cloning and screening of pTESSA-AAV-EGFP-Cap9 was carried out by OXGENE.

TESSA-AAV-EGFP-Cap9 vectors were recovered in HEK293 cells (in presence of doxycycline) by transfection of the SwaI linearized plasmid genome. Viral plaques were observable from around ~7 days post-transfection and without obvious hindrance in replication. TESSA-AAV-EGFP-Cap9 was harvested at 15 days upon display of advanced CPE and subsequently serial passaged for two further rounds in HEK293 cells.

To produce rAAV9-EGFP from the TESSA^{V1} approach, HEK293 cells were co-infected with TESSA-Rep and increasing amounts of TESSA-AAV-EGFP-Cap9 or transfected with the helper-free plasmids. To control for efficiency of DNAse treatment, a mock triple plasmid transfection was included wherein pRepCap was replaced with stuffer DNA, or cells were infected with TESSA-AAV-EGFP-Cap9 (without TESSA-Rep). DNAse-resistant particles harvested at 96hpi were quantified using EGFP-specific qPCR. As shown in **Figure 4.8**, DNAse-resistant vectors harvested at 96 hpi and quantified using EGFP-specific qPCR showed ~4 x10^8 GC/mL of rAAV9-EGFP was obtained from the helper-free method, while a 100-fold increase in productivity was observed TESSA^{V1} approach, which yielded ~4 x10^{10} GC/mL of rAAV9. However, a decrease in productivity of rAAV9-EGFP of ~50% was also observed with increasing MOI (100 or 150) of TESSA-AAV-EGFP-Cap9, possible due to increasing cell toxicity from the high vector dose or an imbalance of Cap9 proteins in relation to Rep required for optimal productivity.

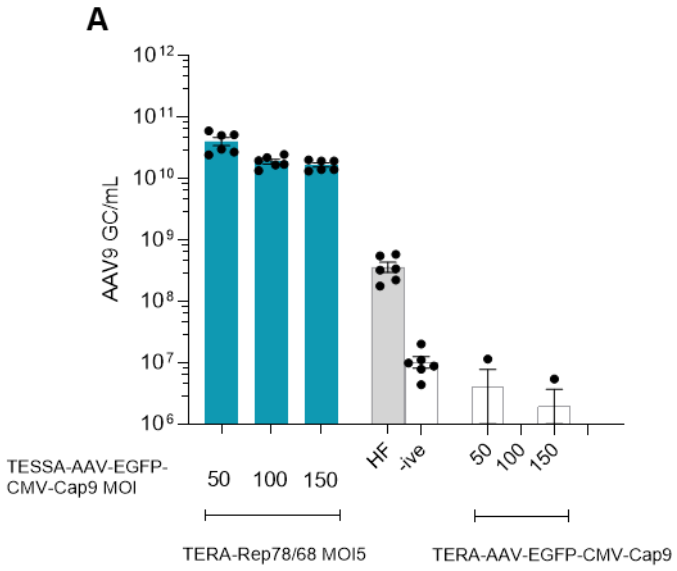


Figure 4.8 TESSA 2-vector approach (TESSA^{V1}) enhances production of AAV9 vectors. HEK293 cells co-infected with TESSA-AAV-Cap9 and TESSA-Rep at the indicated MOI or transfected with the helper-free plasmids. Samples were harvested at 96 hpt and DNAse resistant particles quantified by EGFP-specific qPCR. Data as mean±SEM of triple biological replicates from two independent experiments.

4.3.16 Construction of TESSA-AAV-EGFP-Cap5

AAV5 is the most evolutionally distinctive AAV serotype (Sen et al. 2013). We therefore assessed whether the improvements in rAAV production, observed from rAAV2 and rAAV9, using TESSA^{V1} can be translated to production of rAAV5 vectors.

TESSA-AAV-EGFP-Cap5 plasmid was constructed as per TESSA-AAV-EGFP-Cap2 (**Figure 4.4C**). Positive clones isolated and screened by EcoRI/Bstx17I restriction digest is shown in **Figure 4.9A**.

Replication of TESSA-AAV-EGFP-Cap5 was notably hindered in HEK293 cells as vector recovery from plasmid DNA was unsuccessful from two independent attempts. This was confirmed by adding lysates preparations harvested at 15 days post-transfection to fresh HEK293 cells, and treating with doxycycline, to observe for apparent plaques. At the third attempt, a viral plaque was observed at a day ~10 post-transfection, significantly delayed compared to the control TESSA-

AAV-EGFP vector which plaqued a ~6 days post-transfection. TESSA-AAV-EGFP-Cap5 vectors were harvested at day 18 post-transfection, and subsequently amplified in HEK293 cells. These observations suggest that the CMV-Cap5 expression cassette in TESSA-AAV-EGFP appears relatively toxic either to the cells or selectively to the adenovirus, decreasing recombinant adenovirus activity.

4.3.17 Cap5 coding sequence is lost from TESSA-AAV-EGFP-Cap5 at sequential passages

TESSA-AAV-EGFP-Cap5 showed significant delay in vector recovery from plasmid DNA compared to the control TESSA-AAV-EGFP and TESSA-AAV-EGFP-Cap2 and -9. To further assess replication, HEK293 cells were infected with TESSA-AAV-EGFP-Cap5 or TESSA-AAV-EGFP at a MOI of 5 and treated with doxycycline. Total DNA was extracted at the indicated timepoint and quantified by Hexon-specific qPCR. As shown in **Figure 4.9B**, DNA replication of TESSA-AAV-EGFP-Cap5 was notably delayed at 24hpi compared to the control virus. At 48 and 72 hpi, TESSA-AAV produced ~3-fold more genome compared to TESSA-AAV-EGFP-Cap5.

It can be hypothesized that adenovirus vectors with significantly impaired genome replication will be unstable at sequential passages and loss of the transgene due to selection pressure to enable more efficient growth. To determine whether the cap5 sequence was stably maintained, DNA was extracted from cells infected at an MOI of 5 with TESSA-AAV-EGFP-Cap5 (at passage 3) and quantified by cap5-specific and Hexon-specific qPCR. As expected, an equimolar ratio of Cap5 to Hexon coding sequence was not observed, and up to 83% of TESSA-AAV-EGFP-Cap5 genomes were negative for cap5 (**Figure 4.9C**).

4.3.18 Assessment of AAV5 production via co-infection of TESSA-AAV-EGFP-Cap5 with TESSA-Rep

Despite instability observed from TESSA-AAV-EGFP-Cap5, we used crude lysate preparations to assess whether it was capable of producing rAAV5 vectors. HEK293 cells were transfected with the helper-free plasmids or co-infected with TESSA-Rep with increasing MOI of TESSA-AAV-EGFP-Cap5 (at passage 3), as indicated. or transfected with helper-free plasmids. The helper-free plasmid system yielded ~1 $x10^{10}$ GC/mL of rAAV5-EGFP, and while comparable levels of intact rAAV5 was observed from TESSA-AAV-EGFP-Cap5 used at a MOI 10, a surprising 4-fold increase in rAAV5 yield was achieved when inoculation dose was increased to an MOI of 40 **(Figure 4.9D)**. This result suggests that even though TESSA-AAV-EGFP-Cap5 displayed significant vector instability, significant improvements in rAAV5 yield may also be achievable using TESSA vectors. The maximum MOI of 40 used for assessment of TESSA-AAV-EGFP-Cap5 was due to the difficulty in propagating enough vectors required for testing.

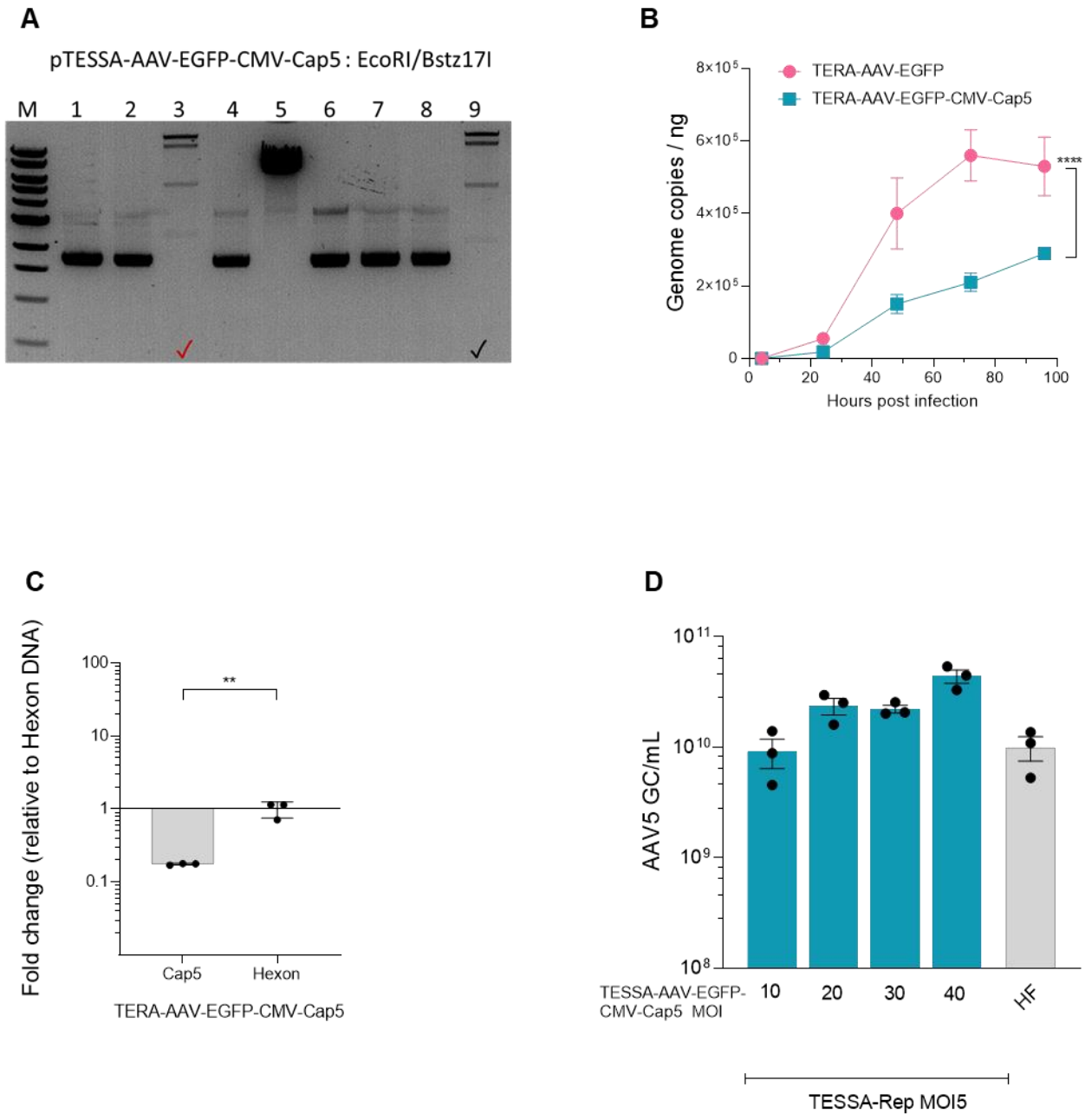


Figure 4.9 TESSA-AAV-EGFP-Cap5 enables high titre AAV5 production but exhibited genetic instability. A) EcoRI and Bstz17I restriction digest for screening correct clones of pTESSA-AAV-EGFP-Cap5. **B**) DNA replication of TESSA-AAV-EGFP-Cap5 compared to control TESSA-AAV-EGFP. HEK293 cells were infected with TESSA-AAV-EGFP-Cap5 or TESSA-AAV-EGFP at an MOI of 5. Total DNA extracted at the indicated timepoint and quantified by Hexon-specific qPCR. Significance determined by two-way ANOVA ****P≤0.0001. **C**) Assessment of TESSA-AAV-EGFP-Cap5 genetic stability by qPCR. TESSA-AAV-EGFP-Cap5 were amplified to passage 4 in HEK293 cells and encapsidated genomes quantified by Hexon and AAV Cap5-specific qPCR. Data presented as fold-change relative to Hexon DNA. **D**) Production of rAAV5 by co-infection of TESSA-AAV-EGFP-Cap5 with TESSA-Rep. HEK293 cells were transfected with the helper-free plasmids or co-infected with the two TESSA vectors at the indicated MOI. DNAse-resistant particles were quantified by EGFP-specific qPCR. Data as mean±SEM of triple biological replicates.

4.3.19 Construction and assessment of TESSA-AAV-EGFP expressing Cap5 from Cumate-inducible promoter

We hypothesized that overexpression of AAV5 capsids from TESSA-AAV-EGFP-Cap5 might contribute to vector instability and impaired replication, as TESSA-CuOx6-Cap5-EMCV-Rep which encodes Cap5 under the inducible CuOx6-minCMV promoter did not show impaired replication (*Section 4.3.8*). Accordingly, we replaced the constitutive CMV promoter in TESSA-AAV-EGFP-Cap5 with an inducible CuOx6-minCMV promoter for driving Cap5 expression. This TESSA vector, entitled TESSA-AAV-EGFP-CuOx6-Cap5, was constructed by insertion of CuOx6-Cap5 expression cassette from an E1-shuttle plasmid (pSU1114) into pTESSA-AAV-EGFP (pSU468) as illustrated in **Figure 4.10A**. Positive clones isolated and screened by SpeI restriction digest is shown in **Figure 4.10B**. During vector recovery in HEK293 cells, viral plaques were observable at ~7 days post-transfection with the genome plasmids and without notable hindrance in replication.

rAAV5 production from TESSA-AAV-EGFP-CuOx6-Cap5 was assessed by providing the cTA protein from a CMV expression plasmid or via co-infection with TESSA-AAV-EGFP-cTA, encoding both cTA and rAAV-EGFP *in cis.* HEK293 cells were triple-infected with using TESSA vectors (TESSA-AAV-EGFP-CuOx6-Cap5, TESSA-AAV-EGFP-cTA and TESSA-Rep) or co-infected with two TESSA vectors (TESSA-AAV-EGFP-CuOx6-Cap5 and TESSA-Rep) and transfected with pCMV-cTA or stuffer DNA. In parallel, cells were transfected with the helper-free plasmids, with a mock transfection group included wherein the pRepCap5 plasmid was replaced with stuffer DNA. As shown in **Figure 4.10C**, samples harvested at 96 hpt showed that the helper-free method yielded 1.7 x10^{10} GC/mL of DNA-resistant rAAV5-EGFP. Comparable yields of rAAV5 (~2x10^{10} GC/mL) were observed from cells infected with the three TESSA vectors (TESSA-AAV-EGFP-CuOx6-Cap5, TESSA-AAV-EGFP-cTA and TESSA-Rep) or when the cTA is provided by plasmid transfection. Surprisingly, co-infection of

TESSA-AAV-EGFP-CuOx6-Cap5 with TESSA-Rep (without the cTA) produced >40% more intact rAAV5-EGFP at 3.6 x10^{10} GC/mL.

This unexpected result suggests that expression of AAV5 capsid was not limited from TESSA-AAV-EGFP-CuOx6-Cap5, and leaky transcription from the inducible CuOx6-minCMV is sufficient for production of high titre rAAV5 vectors. As inducible promoters, usually constructed from a minimal CMV promoter, are not transcriptionally silent and known to leak, it is likely that its low basal transcription activity is exponentially amplified in TESSA due to its inherent genome replication to produce large amount of Cap5 proteins (Chen et al. 2015). With this finding, it then remains unclear why replication was significantly impaired in TESSA expressing Cap5 from the CMV promoter (**Figure 4.9B**) which was not notable from the TESSA-AAV-EGFP-CuOx6-Cap5 vector. It is possible that strong activity of the constitutive CMV promoter produced significantly more AAV5 capsid proteins, and hence exerting a greater degree of toxicity during TESSA replication. Alternatively, as we previously observed enhance transgene expression from TESSA during MLP repression (Chapter 3, Figure 3.10A), it is interesting to speculate that transcription from the CuOx6-minCMV promoter is relatively weak (and hence exerting a lower anti-adenovirus effect) during propagation of TESSA-AAV-EGFP-CuOx6-Cap5 in HEK293 cells with doxycycline, but increases significantly during MLP repression to supply Cap5 proteins for particle assembly. Similarly, increase in intact rAAV5-EGFP observed from co-infection TESSA-AAV-EGFP-CuOx6-Cap5 with TESSA-Rep compared to when the cTA was supplied *in trans* suggest a balance of cellular and viral factors are required for optimal rAAV production. Use of the CuOx6-minCMV promoter provides an alternative approach for rescuing and replication of TESSA vectors encoding transgenes that exhibit instability, such as AAV cap5, and is explored further in this thesis.

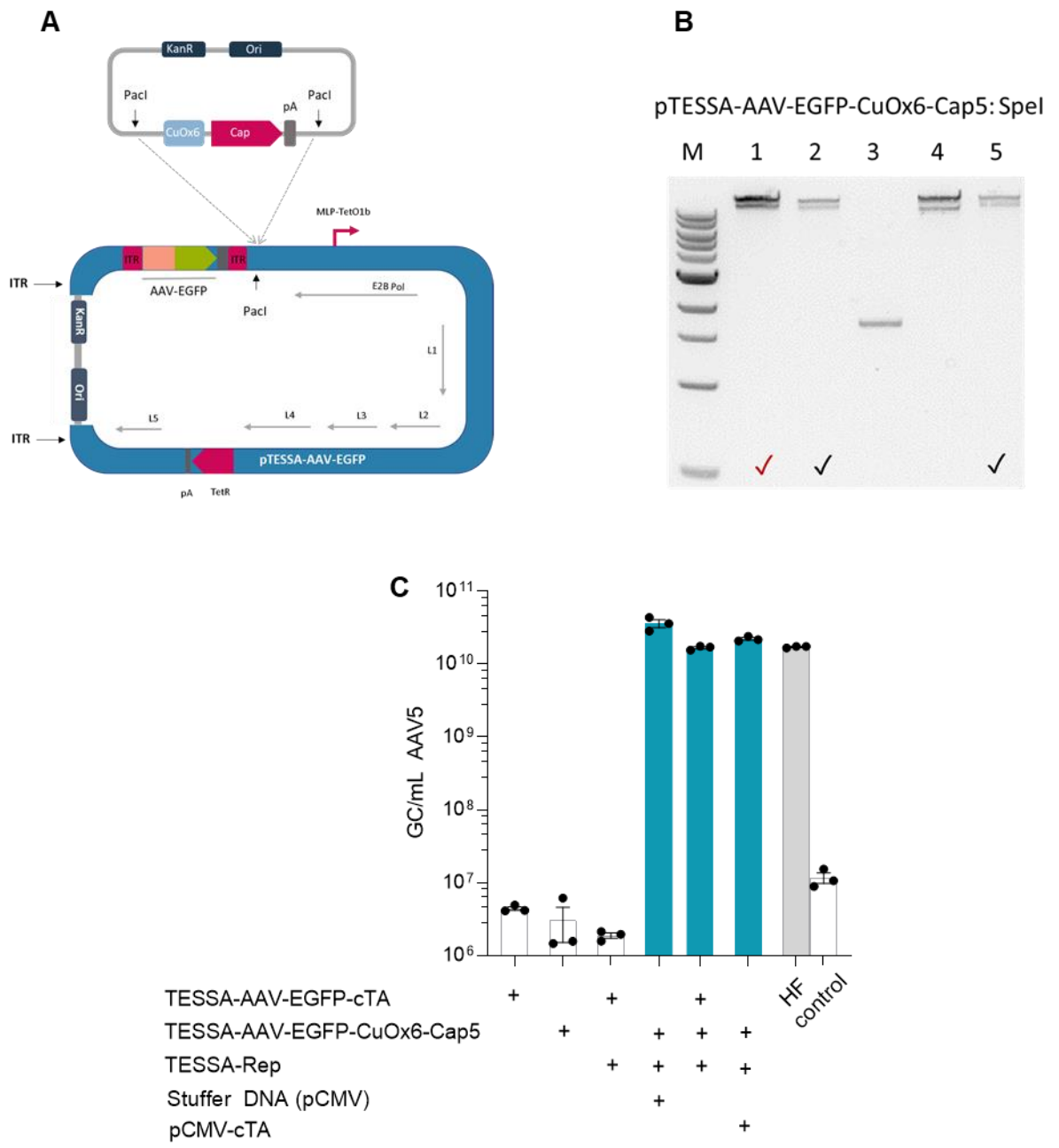


Figure 4.10 Minimal CMV promoter enables high titre rAAV5 production from TESSA. A) Cloning schematic for insertion of CuOx6-Cap5 expression cassette into plasmid pTESSA-AAV-EGFP and (**B**) SpeI restriction digest for screening correct clones. **C**) Production of rAAV5 from HEK293 cells by infection with TESSA vectors, with transfection of stuffer DNA or pCMV-cTA, as indicated. TESSA-AAV-EGFP-cTA and TESSA-AAV-EGCP-cTA used at an MOI100. TESSA-Rep used at an MOI50. Production is compared to helper-free (HF). Control indicates transfection with stuffer DNA in place of pRepCap5. DNAse resistant particles quantified by EGFP-specific qPCR at 96hpt. Data as mean±SEM of triple biological replicates.

4.3.20 Construction of TESSA-RepCap2

A primary concern relating to DNA impurities within encapsidated AAV vectors is the risk of inadvertent packaging and expression of immunogenic proteins or the generation of replication competent (rc) AAV, which may occur by recombination events between the ITR genome and the rep cap coding DNA (Allen et al. 1997). While we observed DNA contaminants mapping to the adenovirus packaging signal (Ψ) and cap sequence in ~2% of intact rAAV2 derived from TESSA-AAV-EGFP-Cap2 (**Figure 4.6C**), it can be postulated that the contaminant cap sequences may exacerbate risk of generating rcAAV or immunogenic peptides. In order to minimize such concerns, TESSA vectors were further modified to encode the AAV rep and cap coding DNA *in trans* to the AAV transfer genome.

As illustrated in **Figure 4.11A**, the CMV-Cap2 expression cassette was excised from an E1-shuttle plasmid (pSU623) using PacI and inserted into pTESSA-Rep (pSU1091) with AsisI. This vector is known as TESSA-RepCap2 from hereon, encoding AAV2 cap under control of a CMV promoter and rep without a heterologous promoter *in cis*, and in a reverse orientation relative to the left ITR. Positive clones isolated and screened by EcoRI restriction digest is shown in **Figure 4.11B**. TESSA-RepCap2 vectors were recovered in HEK293 cells following transfection of the genome plasmid linearized with SwaI. Plaques were notable at day ~7-8 post transfection and vectors were isolated at day 15 upon display of full CPE.

4.3.21 Production and characterisation of rAAV2 particles from TESSA2.0

rAAV production via co-infection of TESSA-RepCap2 and TESSA-AAV-EGFP is hereon known as TESSA2.0. An MOI study was initially carried out to further determine the optimal infectious dose of TESSA2.0 vectors required for efficient rAAV2 production. Here, productivity was compared to multiple production methods that include i) delivery of the rAAV transfer genome by DNA plasmid transfection and infection with TESSA-RepCap2, ii) the helper-free method, or the iii) previous TESSA^{V1} approach (using TESSA-AAV-EGFP-Cap2 & TESSA-Rep). For production using the TESSA2.0 system, HEK293 cells were co-infected using increasing MOI of TESSA-AAV-EGFP with TESSA-RepCap2 at increasing doses. Alternatively, cells were transfected with the pAAV-EGFP transfer plasmid and infected with increasing MOI of TESSA-RepCap, or transfected with the helper-free plasmid, or co-infected with TESSA-AAV-EGFP-Cap2 (at a MOI of 100) and TESSA-Rep (MOI of 5). As a mock infection control, cells were also independently infected with each TESSA vectors used in this experiment. DNAse-resistant rAAV2 particles were harvested at 96 hpi and quantified by EGFP-specific and qPCR. As shown in **Figure 4.11C**, the helper-free process yielded ~1 x10^9 GC/mL of rAAV2, while a modest increase of 2-fold was observed when rAAV is replicated from the ITR transfer plasmid using TESSA-RepCap2. Importantly, while TESSA^{V1} approach yielded >1 x10^{10} GC/mL of rAAV2, comparably high yields were obtained from the TESSA2.0 system (when each vector used at MOI 25) despite ~50% less of input of TESSA vectors.

Interestingly, a decrease in intact rAAV2-EGFP from the TESSA2.0 system was observed when the TESSA-AAV-EGFP vector was used in excess of TESSA-RepCap. Specifically, an 8-fold decrease in rAAV2-EGFP was observed when cells were co-infected with TESSA-AAV-EGFP (MOI 75) and TESSA-RepCap (MOI 5) compared to the use of TESSA-AAV-EGFP at a MOI of 5. This suggest that

a balance of the rAAV transfer genome relative to the Rep and Cap2 coding sequence in TESSA vectors is important for optimal productivity.

To determine the levels of cap sequence impurities in these samples, particles were quantified using AAV2 cap-specific qPCR (**Figure 4.11C, right axis**). When compared to the intact particle titre determined by the EGFP-specific qPCR, ~2% of rAAV produced from TESSA^{V1} method were positive for cap DNA contaminant as expected. Importantly, detection of AAV2 cap DNA was significantly lower in rAAV2 vectors produced via the helper-free method or TESSA2.0 system, which showed average levels of 0.5% and 0.01%, respectively. However, it is likely that these contaminant levels are over-represented due to limitations of DNAse treatment for complete degrading of non-encapsidated DNA, as observed from the baseline detection of EGFP DNA from the mock transfection group by qPCR, despite the absence of rAAV particles.

Levels of contaminating adenovirus during rAAV production from TESSA2.0 was also determined. Crude rAAV lysates produced using TESSA2.0 (TESSA-AAV-EGFP and TESSA-RepCap2 each used at MOI25) in presence of doxycycline 0.5 µg/mL or DMSO, were added to fresh HEK293 cells and supplemented with doxycycline in a TCID50 assay. As shown in **Figure 4.11D**, while $8x10^8$ TCID50/mL of infectious TESSA vectors were detected from the doxycycline treated group, an average of 11 TCID50/mL was detected when rAAV production was carried out in the absence of doxycycline. This represents a 7-log reduction in contaminating adenovirus vectors and confirmed that tight repression of the MLP is maintained in the TESSA2.0 system.

4.3.22 rAAV2 derived from TESSA2.0 exhibit enhance cell entry and transduction

To determine infectivity of rAAV-EGFP, crude preparations derived from the helper-free method, TESSA2.0 (produced at the indicated MOI), or via infection with TESSA-RepCap2 in pAAV-EGFP transfected cells, were added to fresh HEK293 cells at a normalized MOI of 250 GC/cell. As shown in **Figure 4.11Ei**, EGFP expression was significantly higher in cells infected with TESSA-derived rAAV2 compared to helper-free samples. Results were confirmed by flow cytometry and showed that while ~60% of cells were positive after infection with AAV2-derived from the helper-free production, ~100% of cells were EGFP positive after infection with TESSA-derived samples (**ii**). Interestingly, highest expression of EGFP (as determined by the MFI), and 50-fold more than cells infected with helper-free derived rAAV2, was observed from particles produced by TESSA2.0, wherein TESSA-AAV-EGFP and TESSA-RepCap2 was used at a MOI of 25 and 5, respectively. This indicates that particle potency may also be influence by the ratio of the rAAV transfer genome, and the rep and cap genes. The significant increase in EGFP expression of TESSA-derived rAAV2 compared to helper-free samples likely result from increase potency of the particles enabling multiple transduction events within the same cell, and consistent with previous observations (*Chapter 4, Section 4.3.12*).

Transduction activity of rAAV particles produced from the different systems were further quantified using TCID50 assay. Serial dilutions were prepared using rAAV crude preparations from helper-free method, TESSA2.0 (each TESSA vector used at MOI25) and TESSA^{V1} and added to fresh HEK293 cells. As shown in **Figure 4.11F**, the helper-free method yielded an average of 7 x10^5 TCID50/mL of rAAV2 with a GC/TCID50 ratio of ~1.5 x10^3 when compared against the EGFP-specific qPCR titre. TESSA2.0 produced over 1.5 x10^9 TCID50/mL of rAAV2 (with a GC/TCID50 ratio of ~10), representing a 6-fold increase compared to its previous iteration (TESSA^{V1}) which yielded

2.5 x10^8 TCID50/mL (with a GC/TCID50 ratio of ~100), and a 2000-fold increase compared to the helper free system.

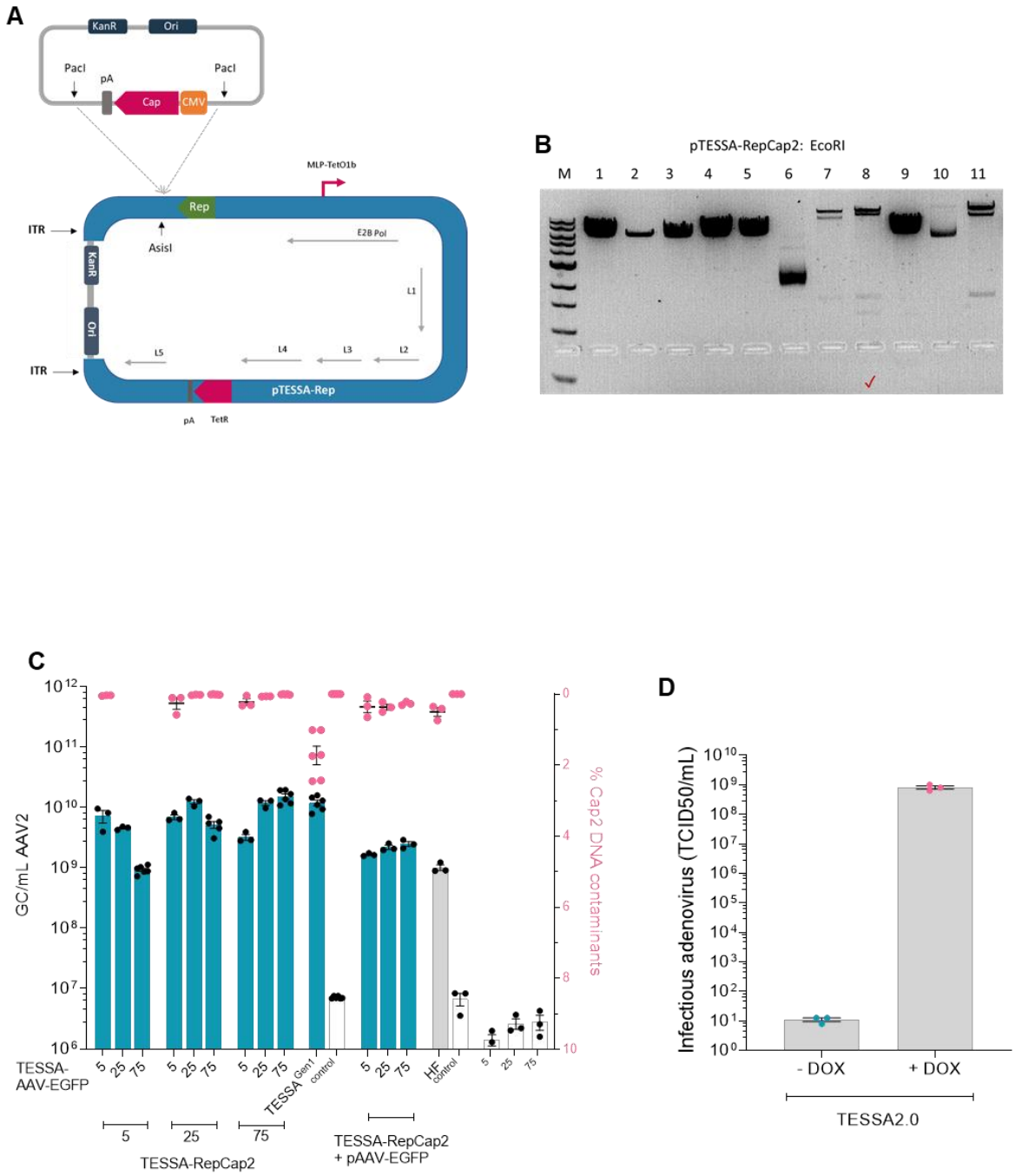
To increase the sensitivity of detecting EGFP expression from a single transduction event, a modified TCID50 assay utilizing TESSA-RepCap2 were also carried out. In this assay, HEK293 cells in 96-well plates are co-infected with replicates of ten-fold serial dilution of rAAV crude preparations in the presence of TESSA-RepCap2 (used at 100 GC/cell). Cells infected with rAAV-EGFP are replicated by TESSA-RepCap2 enabling sensitive detection of EGFP by fluorescence microscopy. As shown in **Figure 4.11G**, rAAV2-EGFP derived from TESSA2.0 was measured at an average of 1.3 x10^{10} TCID50/mL (with a GC/TCID50 ratio of ~1), a 7-fold increase in TCID50/mL compared to assays with TESSA-RepCap2 co-infection. In contrast, rAAV2-EGFP derived from helper-free was measured at 2.6 x10^7 TCID50/mL with a GC/TCID50 ratio of ~50, representing a 37-fold increase in transduction compared to the TCID50 assay without TESSA-RepCap2. It is well documented that adenovirus infections significantly enhances AAV transduction by promoting conversion of the single-stranded viral genomes to transcriptionally competent double-stranded genome (Fisher et al. 1997; Grifman et al. 1999). The increase in transduction observed from rAAV particles (derived from TESSA and helper-free method) in presence TESSA-RepCap2 likely results from increased sensitivity of the assay and effect of the adenovirus helper. However, the more dramatic increase in transduction of helper-free derived rAAV2-EGFP observed in the presence of TESSA-RepCap2 confirmed that the large majority of particles were capable of cellular entry, but transcriptionally silent unless aided by adenovirus infection.

To determine whether the increase transduction observed from TESSA-derived rAAV involved increase cellular uptake, HEK293 cells were infected (50 GC/cell) with crude preparation and AAVX-purified rAAV2-EGFP particles from TESSA2.0 or the helper-free process. At 6 hpi, rAAV-infected cells were trypsinised and extensively washed with PBS before extraction of total DNA.

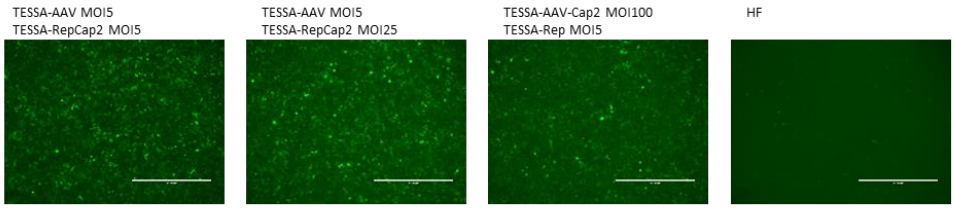
As shown in **Figure 4.11H**, a ~5-fold greater uptake of rAAV2 derived from TESSA2.0 was observed compared to helper-free derived vectors.

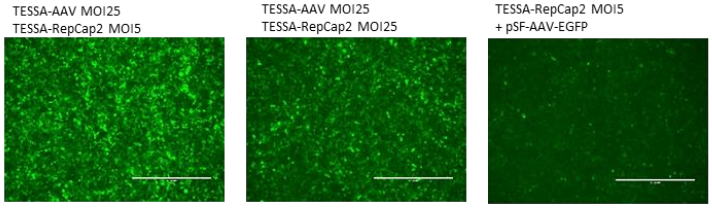
4.3.23 All Rep proteins are expressed from TESSA

Expression of Rep from TESSA-RepCap2 was analysed by western blot. HEK293 cells infected with infected with TESSA-RepCap2 at 25 GC/cell or transfected with pRepCap2 for 24 hours and cell lysates were probed with anti-Rep antibody. Surprisingly, despite attempts to inhibits suppress the expression of Rep52 and Rep40 by ablation of the p19 TATA element via synonymous codons, we found that all four Rep variants (Rep 78/68/52/40) were readily detected with Rep52 and Rep40 expressed in excess compared to Rep78/68 (**Figure 4.11I**). While Rep expression from TESSA was significantly higher than cells transfected with pRepCap2, expression patterns of the Rep isoforms were comparable between the two groups. This unexpected result is consistent with previous findings by and Carter that showed modification of the p19 does not ablate expression of these isoforms (Chejanovsky and Carter 1989). This was particularly encouraging as Rep52 and Rep40 have been suggested to be required for virus production and be involved in DNA encapsidation via helicase activity (King et al. 2001).

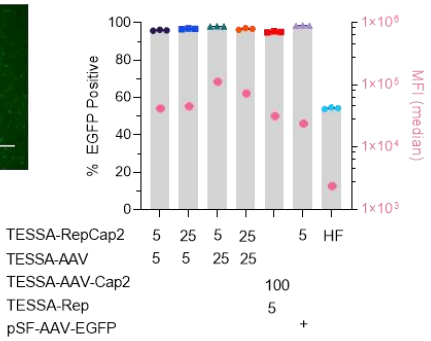

A
KanR
Ori
PacI
pA
PacI
Cap
CMV
MLP-TetO1b
Rep
ITR
AsisI
E2B Pol
KanR
Ori
L1
L5
L4
L3
L2
ITR
pTESSA-Rep
pA
TetR
B
pTESSA-RepCap2: EcoRI
M 1 2 3 4 5 6 7 8 9 10 11
C
GC/mL AAV2
% Cap2 DNA contaminants
TESSA-AAV-EGFP
TESSA Gen1 control
HF control
TESSA-RepCap2
TESSA-RepCap2 + pAAV-EGFP
D
Infectious adenovirus (TCID50/mL)
- DOX
+ DOX
TESSA2.0

E i)

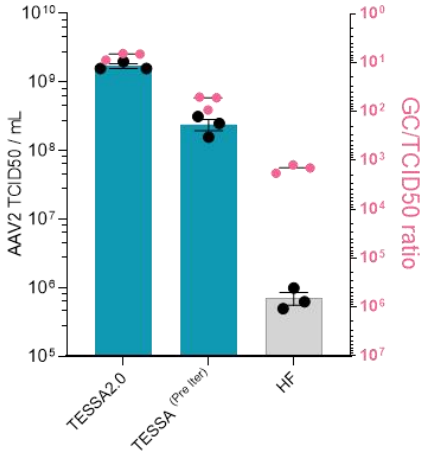

TESSA-AAV MOI5
TESSA-RepCap2 MOI5
TESSA-AAV MOI5
TESSA-RepCap2 MOI25
TESSA-AAV-Cap2 MOI100
TESSA-Rep MOI5
HF


TESSA-AAV MOI25
TESSA-RepCap2 MOI5
TESSA-AAV MOI25
TESSA-RepCap2 MOI25
TESSA-RepCap2 MOI5
+ pSF-AAV-EGFP

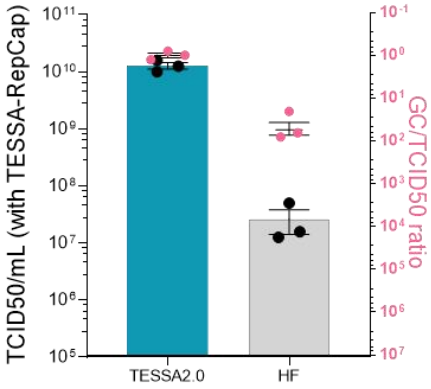
ii)


% EGFP Positive
MFI (median)
TESSA-RepCap2 5 25 5 25 5 HF
TESSA-AAV 5 5 25 25
TESSA-AAV-Cap2 100
TESSA-Rep 5
pSF-AAV-EGFP +

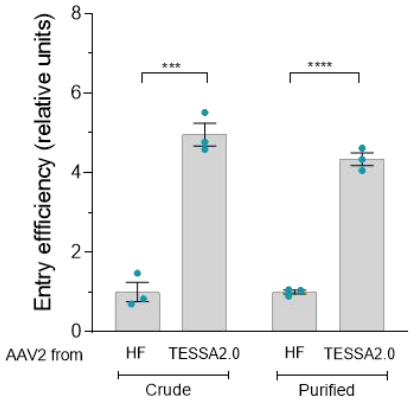
F


AAV2 TCID50 / mL
GC/TCID50 ratio
TESSA2.0
TESSA (Pre Iter)
HF

G


TCID50/mL (with TESSA-RepCap)
GC/TCID50 ratio
TESSA2.0
HF

H


Entry efficiency (relative units)
***
****
AAV2 from
HF
TESSA2.0
HF
TESSA2.0
Crude
Purified

I

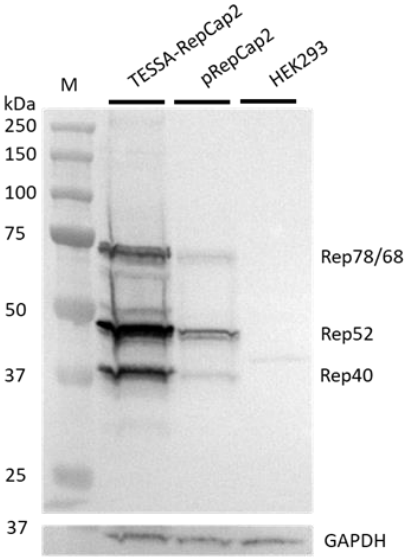

M
TESSA-RepCap2
pRepCap2
HEK293
kDa
250
150
100
75
50
37
25
37
Rep78/68
Rep52
Rep40
GAPDH

Figure 4.11 TESSA2.0 system enhances AAV production with significantly reduction in contaminating AAV capsid DNA. A) Cloning schematic for insertion of the CMV-Cap2 expression cassette into plasmid TESSA-Rep and (**B**) isolation of correct clones by EcoR restriction digest. **C**) Production of AAV2 vectors by the TESSA2.0 approach. HEK293 cells were co-infected with TESSA2.0 vectors (TESSA-RepCap2 and TESSA-AAV-EGFP) at the indicated MOI. AAV production was compared to the TESSA 2-virus (GEN1) approached (co-infection of TESSA-AAV-EGFP-Cap at MOI 100 and TESSA-Rep at MOI of 5), or delivery of the AAV transfer genome by plasmid transfection and infection with TESSA-RepCap2, or the helper-free method. Samples were harvested and DNAse resistant AAV quantified by EGFP-specific qPCR. Contaminating DNA in AAV particles were quantified by Cap2-specific qPCR and presented on the right axis as percentage of DNA contaminants in each preparation. **D**) Quantification of infectious adenovirus in AAV2 crude lysates produced from TESSA2.0 (TESSA-AAV-EGFP MOI25 and TESSA-RepCap MOI5) in the presence or absence of doxycycline 0.5µg/ml. Data as mean±SEM of triple biological replicates. **E**) Assessment of EGFP expression from AAV vectors. Crude AAV preparation derived from the indicated approaches were used to infect fresh HEK293 cells at 250 GC/cell. Cells were imaged at 48 hpi by (**i**) fluorescent microscopy and analyzed by (**ii**) flow cytometry. **F**) Transduction efficiency of AAV2 particle. Crude AAV preparation produced from the TESSA2.0 system (TESSA-AAV-EGFP MOI25 and TESSA-RepCap MOI25), TESSA 2-virus (GEN1; TESSA-AAV-Cap2 MOI100 and TESSA-Rep MOI5), or the helper-free method were quantified in HEK293 cells using a modified TCID50 assay. Ratio of TU/GC determined by comparing against intact particles from the qPCR assay is shown on the right axis. **G**) Assessment of AAV2 transduction in HEK293 cells using TESSA-RepCap2. Crude AAV preparation produced from the TESSA2.0 system or the helper-free method quantified in HEK293 cells infected with TESSA-RepCap2 (100GC/cell) using a modified TCID50 assay. EGFP expression was monitored in each well at 48hpi. Ratio of TU/GC determined by comparing against intact particles from the qPCR assay is shown on the right axis. **H**) Assessment of cell entry of AAV particles made by TESSA2.0 or helper-free. Crude or purified AAV preparations were used to infect HEK293 cells at 50GC/cell. At 6hpi, cells were trypsinised and extensively washed with PBS before extraction of total DNA. AAV-EGFP genomes were quantified by EGFP-specific qPCR and data presented as fold-change relative to cells infected with AAV particles derived from helper-free. Data is N=3 (mean ± SEM). Significance determined by unpaired student's t-test ****p≤0.0001, ***p≤0.005. **I**) Western blot analysis of AAV Rep expressed from TESSA-RepCap2. HEK293 cells infected with TESSA-RepCap2 at 25 GC/cell or transfected with pRepCap2. Cells were harvested at 24 hpt. Equal amounts (25uL) of cellular lysates were analysed by western blot using anti-Rep and anti-GAPDH antibody.

4.3.24 Replication and stability assessment of TESSA-RepCap2

While significant improvements in AAV quality and yield were observed from TESSA2.0 system. During scale-up production of TESSA-RepCap2 in HYPERFlasks, significantly lower titre of ~10-fold were generally observed compared to TESSA-Rep or E1/E3Δ-Ad5 (**Figure 4.12A**). As similar

decrease in vector yield was observed during production of TESSA-AAV-EGFP-Cap2, this suggests that the CMV-Cap2 expression cassette was exerting a degree of hindrance on viral replication, as observed previously for TESSA vectors expression AAV5 cap from the CMV promoter.

To determine DNA replication kinetics, HEK293 cells were infected with TESSA-RepCap2 or the control E1/E3Δ-Ad5 at 10 GC/cell and total DNA was harvested at 4, 48 and 72 hpi, and quantified using hexon-specific qPCR. As shown in **Figure 4.12B**, TESSA-RepCap2 replicated less efficiently compared to the control vector. At 48 and 72 hours, a ~3-fold decrease in TESSA-RepCap2 genomes were observed compared to the E1/E3Δ-Ad5.

As we observed previously with TESSA-AAV-EGFP-Cap5, impaired genome replication may result in genetic stability and a loss of the cap coding sequence (**Figure 4.9C**). To assess genetic stability of TESSA-RepCap2, virus genomes were harvested from cesium chloride purified vectors that were serially passaged to the 4^{th} and 5^{th} passages in HEK293 cells, and the CMV Cap coding sequence amplified by long amplicon PCR and resolved by agarose gel electrophoresis. Binding positions for forward and reverse primers are illustrated in **Figure 4.12Ci**. To control for unspecific binding of primers and amplification, plasmid DNA encoding TESSA-RepCap2 was also amplified by PCR. As the forward and reverse primers flanks the cap DNA sequence, genetic instability and loss of cap transgene within the vectors should be observable by presence of smaller amplicons within the gel. As shown in **Figure 4.12Cii**, expected amplicon fragment size of ~3kb corresponding to the CMV-Cap sequence was confirmed from the TESSA-RepCap2 and plasmid DNA genome. While we also observed smaller amplified fragments present from PCR of the TESSA-RepCap2 vector genome, as these fragments were similar in intensity and size between vector passage 4 and passage 5 suggests they are products of non-specific amplification. This is be supported by the presence of similar fragment patterns from the plasmid DNA control samples.

For a more stringent assessment of genetic stability, TESSA-RepCap2 vectors (at passage 5) was serially passaged for two further rounds, to passages 6 and 7, in HEK293 cells. TESSA vectors were purified by cesium chloride between each passage and genomic DNA extracted from the particles. Genomes from TESSA-RepCap2, at passages 4-7, and the plasmid genome were quantified by qPCR using primers and probe against AAV2 rep and cap, and the Ad5 hexon sequence. As shown in **Figure 4.12D**, AAV2 rep and cap genes are in equimolar to Ad5 hexon from all samples, and confirming stability up to the assessed 7th passage.

4.3.25 siRNA knockdown of cap2 mRNA increase production of TESSA-RepCap2

To enable widespread adaptation of the TESSA2.0 system for use in rAAV production, TESSA vectors must be manufactured to high titre economically. While TESSA-AAV showed replication kinetics and production yield comparable to E1/E3Δ-Ad5 vectors (*Chapter 3, Figure 3.7D*) TESSA-RepCap2 replicated less efficiently.

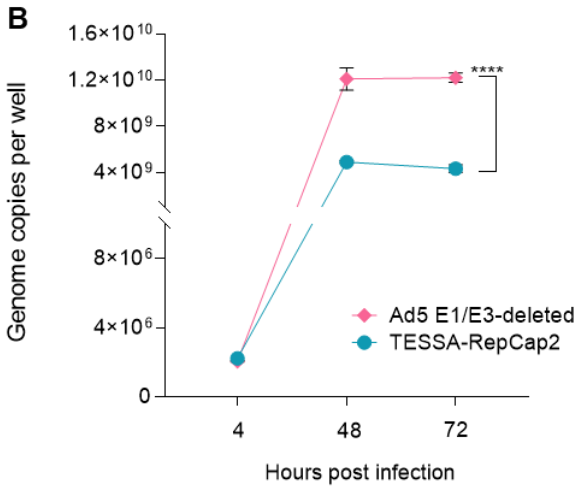
As TESSA solely encoding AAV2 rep did not show significant impairment during vector production (**Figure 4.12A**), we hypothesized that expression of AAV2 capsids to high levels from the CMV promoter was hindering replication of TESSA-RepCap2. To assess whether silencing Cap2 expressing enables more efficient production of TESSA-RepCap2, we designed siRNA targeting the 3' UTR or the Cap2 coding sequence. Genome schematic showing siRNA target position is illustrated in **Figure 4.12Ei**. HEK293 cells were transfected with four siRNA variants or the control scrambled siRNA, and infected with TESSA-RepCap2 or the control E1/E3Δ-Ad5 at 10 GC/cell. Vectors were harvested at 72 hpi and DNAse-resistant particles quantified by Hexon-specific qPCR. As expected, in both non-transfected and scrambled siRNA transfected groups, production

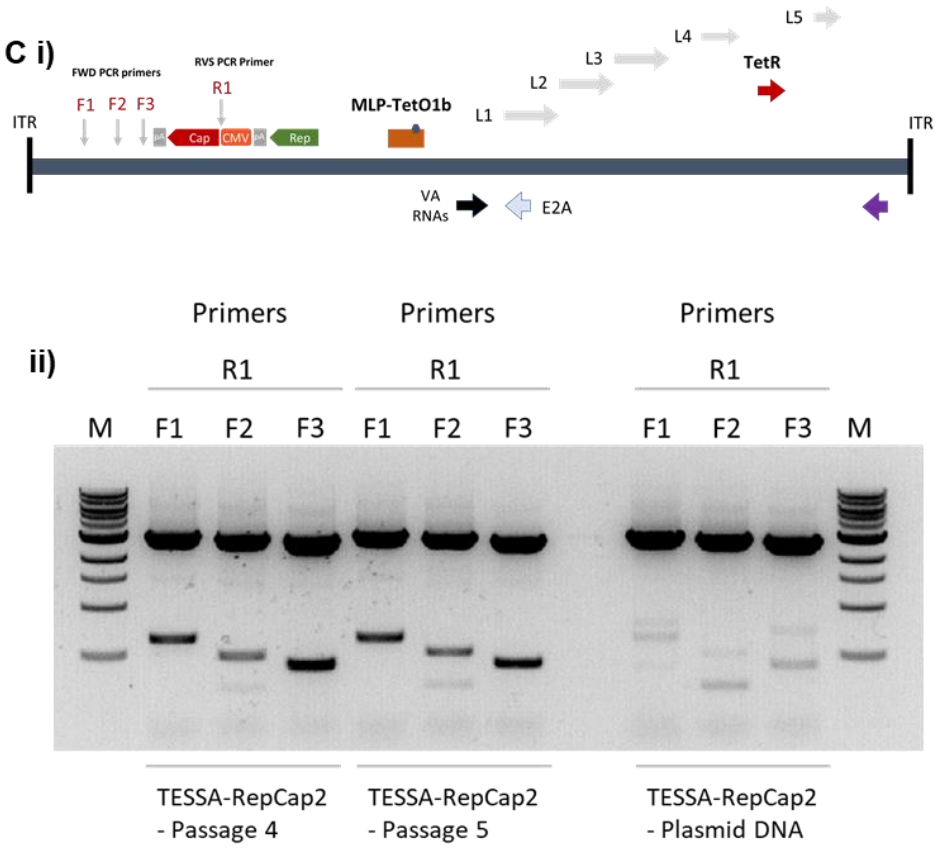
of TESSA-RepCap2 was ~10-fold lower compared to the control vector, which yielded an average of $8x10^9$ GC/mL (**Figure 4.12Eii**). Importantly, cells transfected with siRNA targeting Cap2 expression was able to dramatically improve production of TESSA-RepCap2, with both siRNA targeting the 3' UTR sequence of cap2 recovered TESSA-RepCap2 levels comparable to the control vector. Overall, our results show that while replication of TESSA-RepCap2 is impaired, cap2 and rep coding *in cis* is genetically stable, and vector manufacture can be improved by strategies employing siRNA knockdown of Cap2 expression. Producer cell lines may be engineered to stably express shRNA for suppression of Cap2 for optimal vector production.

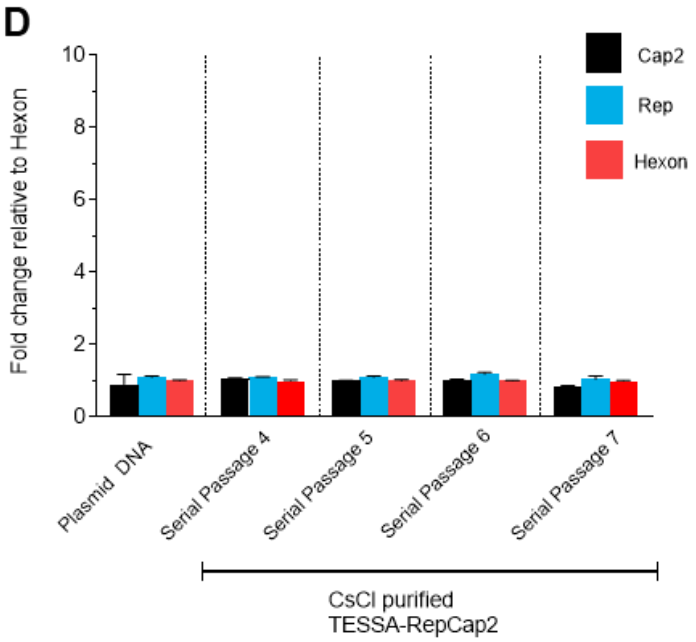
A

	VP/mL	SD
Ad5 E1/E3-deleted	1.82E+12	6.21E+11
TESSA	8.76E+11	2.06E+11
TESSA-AAV-EGFP-Cap2	1.07E+11	2.38E+09
TESSA-Rep	1.20E+12	1.62E+11
TESSA-RepCap2	1.58E+11	5.48E+08

B




C i)
FWD PCR primers
F1 F2 F3
RVS PCR Primer
R1
ITR
Cap
CMV
Rep
MLP-TetO1b
L1
L2
L3
L4
L5
TetR
ITR
VA RNAs
E2A
ii)
Primers
R1
M F1 F2 F3 F1 F2 F3 F1 F2 F3 M
TESSA-RepCap2 - Passage 4
TESSA-RepCap2 - Passage 5
TESSA-RepCap2 - Plasmid DNA


D
Fold change relative to Hexon
10
8
6
4
2
0
Cap2
Rep
Hexon
Plasmid DNA
Serial Passage 4
Serial Passage 5
Serial Passage 6
Serial Passage 7
CsCl purified TESSA-RepCap2

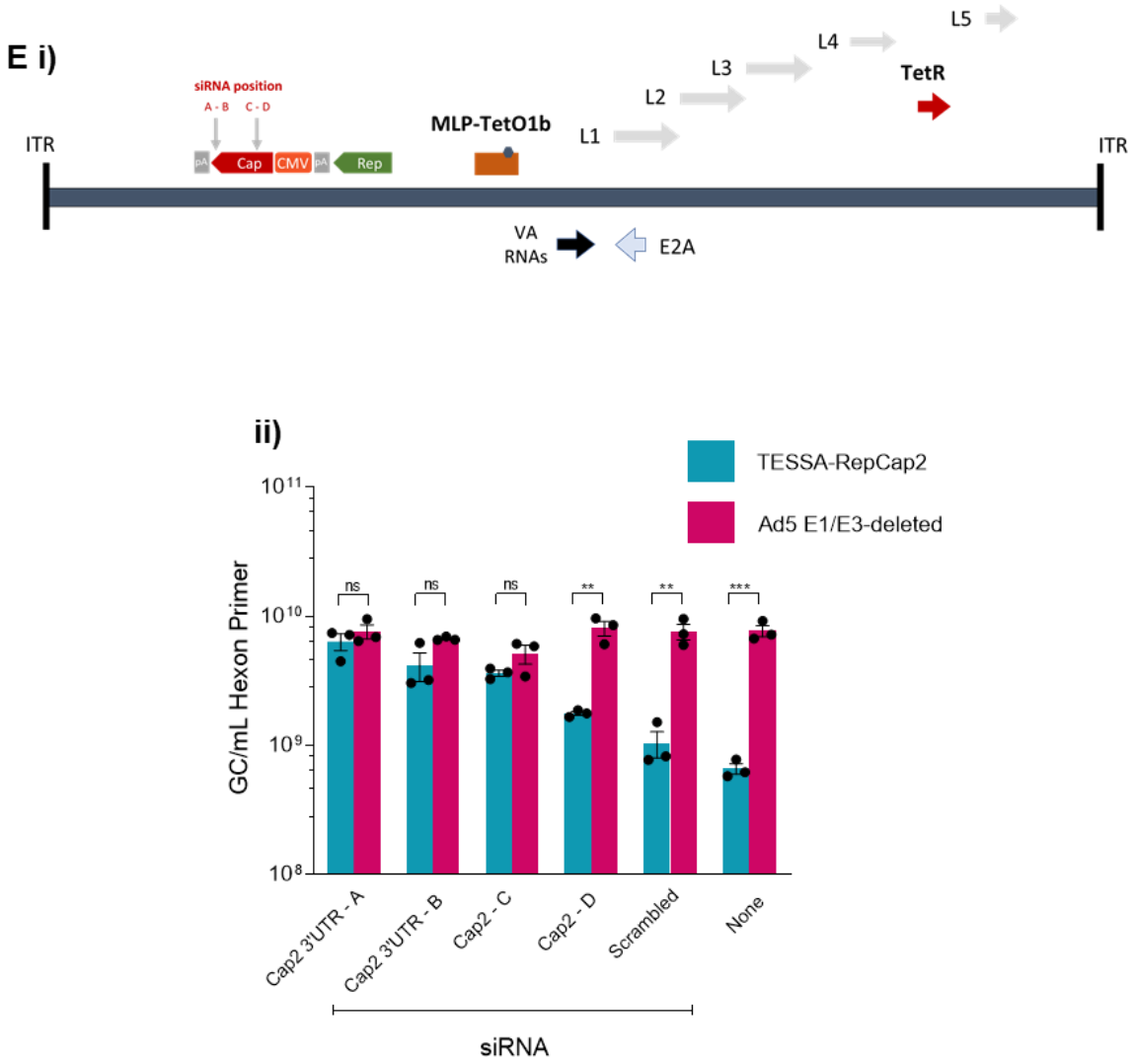


Figure 4.12 TESSA-RepCap2 is genetically stable during serial propagation and can be produced to high titres using an siRNA aided approach. A) Production titre of TESSA vectors compared to the control Ad5 E1/E3-deleted control. Each adenoviral vector batch was amplified from HEK293 cells seeded a HYPERFlask and purified by CsCl gradient banding. Viral particle (VP) per mL determined by the PicoGreen assay. Data as mean±SD of triple technical replicates. **B**) Replication kinetics of TESSA-RepCap2. HEK293 cells were infected with TESSA-RepCap2 or the control E1/E3-deleted Ad5 at a MOI of 10. Total DNA was extracted at the indicated timepoint post infected and quantified by a Hexon-specific qPCR. **C)** Assessment of cap DNA stability within the TESSA-RepCap2 vector by PCR. (**i**) Genome schematic showing the binding position for PCR forward primers (F1-3) and reverse primer (R1) for amplification of the Cap sequence. TESSA-RepCap2 vectors amplified in HEK293 cells to a passage 4 and 5 were purified by CsCl chloride gradient ultracentrifugation. Viral genomes were extracted and amplified by PCR using forward and reverse primers flanking the Cap2 coding sequence. (**ii**) DNA was resolved by gel electrophoresis and amplified DNA fragments compare to the pTESSA-RepCap2 plasmid control. **D**) qPCR analysis of AAV2 rep and cap genes from TESSA-RepCap2 vectors. TESSA-RepCap2 recovered from DNA plasmid was amplified in HEK293 cells to serial passage 3. HEK293 cells were infected (MOI-15) in HYPERFlask cell culture vessel. Vectors were harvested after 3 days and purified by caesium chloride ultracentrifugation to generate serial passage 4. This process was

repeated to create passage 5, 6 and 7. DNA was extracted from purified TESSA-RepCap2 vector at each passage and AAV2 rep and cap, and Ad5 hexon genes quantified by qPCR. Data shows the copy number of AAV2 rep and cap genes relative to Ad5 hexon and compared to DNA plasmid encoding TESSA-RepCap2 (ns, two-way ANOVA). **E**) siRNA knockdown of Cap mRNA increases production of TESSA-RepCap2 in HEK293 cells. HEK293 cells were transfected with various siRNA targeting the AAV2 Cap coding sequence or with the scrambled siRNA control. After 24 hours, cells were infected with TESSA-RepCap2 (and cultured with doxycycline 0.5 µg/ml) or the control Ad5 at 25 GC/cell. Adenovirus vectors were harvested 72hpi and DNAse resistant particles quantified by Hexon-specific qPCR. Data as mean±SEM of triple biological replicates. Significance determined by unpaired t-test **P≤0.01, ***P≤0.001.

4.3.26 Construction of TESSA-RepCap5, -6, -8 and -9 vectors

We next determined whether the significant improvements observed in rAAV2 production using the TESSA2.0 system can be extended to other AAV capsid serotypes. To this end, TESSA vectors encoding the rep (without a heterologous promoter) *in cis* with AAV5, -6 -8 or -9 cap coding sequences were constructed.

We observed previously that TESSA-AAV-EGFP-CMV-Cap5 exhibited genetic instability with loss of the cap5 gene at subsequent passages (**Figure 4.9C**). As this was not observed in TESSA vectors expressing AAV Cap2 from the CMV promoter, we hypothesized that overexpression of Cap5 was detrimental for TESSA replication and stability. In support, TESSA-AAV-EGFP-CuOx6-Cap5, wherein Cap5 is expressed under the inducible CuOx6-minCMV promoter did not show notable hindrance in virus replication but capable of producing high titre rAAV5, even in the absence of the cTA (**Figure 4.10C**). This CuOx6-minCMV promoter configuration was selected for expressing Cap5 from TESSA-RepCap5. Additionally, a TESSA-RepCap8 vector, wherein Cap8 is expressed from the CuOx6-minCMV promoter was also constructed in parallel by OXGENE and is explored in these subsequent studies. For the construction of TESSA-RepCap6 and -9, the constitutive CMV promoter was selected for driving cap gene expression.

Cloning schematic for the construction for the TESSA-RepCap5, -6, and -9 is provided in **Figure 4.13A**. For the construction of TESSA-RepCap5, TESSA-Rep6 and TESSA-RepCap9, the cap expression cassette was excised from shuttle plasmids pSF-CuOx6-minCMV-Cap5 (pSU1114), pSF-CMV-Cap6 (R496) and pSF-CMV-Cap9 (R497), respectively, using PacI and inserted into pTESSA-Rep (pSU1091) linearized with AsisI. Correct clones were isolated and screened by restriction digest for plasmids encoding TESSA-RepCap5 (**Figure 4.13B**), -6 (**Figure 4.13C**), and -9 (**Figure 4.13D**).

Plasmid DNA encoding TESSA-RepCap5 (pSU1257), -6 (pSU1261) and -9 (pSU1249), were linearized using SwaI and transfected into HEK293 cells, and subsequently cultured with doxycycline for vector recovery. For all three TESSA vectors, viral plaques were observable on the cell monolayer ~6-8 days post transfection and vectors were harvested at ~15 day. Vectors were passaged in HEK293 cells for two further rounds before inoculation of HYPERFlasks for vector production and purification by CsCl banding.

4.3.27 Production of rAAV5, rAAV6, rAAV8 and rAAV9 using the TESSA2.0 system

To assess for rAAV5, -6, -8 and -9 vector production using the TESSA2.0 system, HEK293 cells were co-infected using TESSA vector encoding the rAAV transfer genome, TESSA-AAV-EGFP, at an MOI of 25 with increasing amounts of TESSA-RepCap5, -6, -8 or -9 (as indicated). In parallel, cells were also infected with each individual TESSA vector as a mock infection to control for efficiency of DNAse treatment. Productivity of rAAV vectors were compared to yield obtained from the helper-free plasmid transfection process, wherein cells were triple-transfected with pAAV-EGFP and

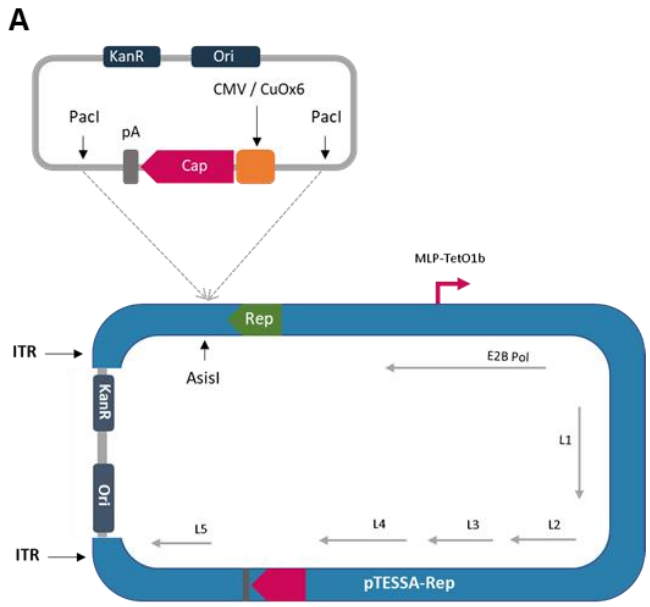
pHelper, and either pRep5, -6,-8, -9 or stuffer DNA (OG10, provided by OXGENE). Samples were harvested at 96 hpi, treated with turbo-DNAse and quantified using an EGFP-specific qPCR.

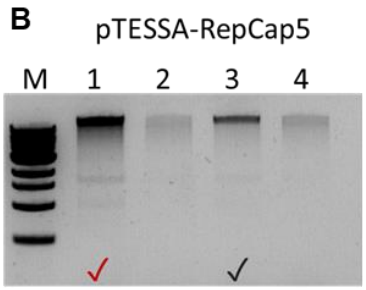
Production of rAAV5 from the helper-free method yielded ~1.5 x10^{10} GC/mL. As shown in **Figure 4.13E**, comparable levels of rAAV5 vectors were observed from the TESSA2.0-AAV5 system, in all three MOI (25, 75, 125 GC/cell) assessed for TESSA-RepCap5, which yielded an average titre of ~2.5 x10^{11} GC/mL. This represented a 16-fold increase in rAAV5 vector productivity compared yields achieved using plasmids.

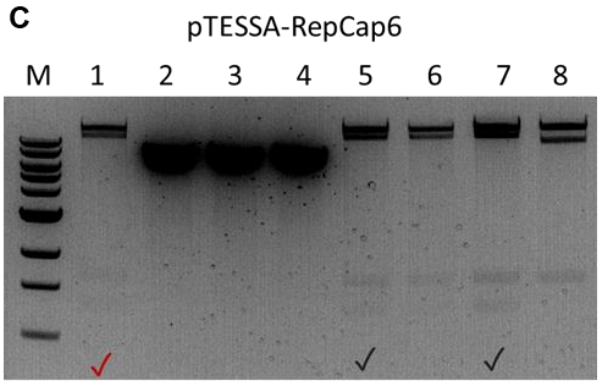
As shown in **Figure 4.13F**, comparable yields were measured from TESSA2.0-AAV6 in all three assessed MOI of TESSA-RepCap6, which produced ~3.3 x10^{10} GC/mL of intact rAAV6 particles. The helper-free process yielded 1.9 x10^{9} GC/mL, 18-fold lower than levels observed from TESSA2.0-AAV6.

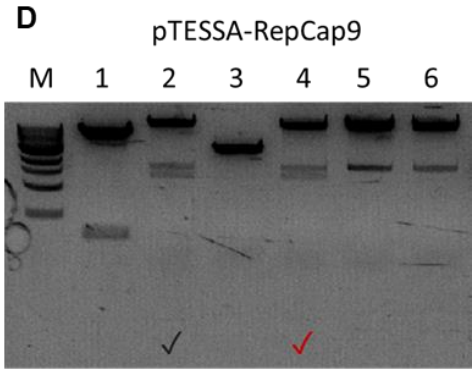
TESSA2.0-AAV8 system yielded ~1.0 x10^{11} GC/mL of rAAV8 vectors when TESSA-RepCap8 was used at both MOI of 25 and 125 GC/cell, as shown in **Figure 4.13G**. This productivity represents a 20-fold increase in rAAV8 vectors compared to the helper free system which yielded ~1.0 x10^{9} GC/mL of AAV8-EGFP.

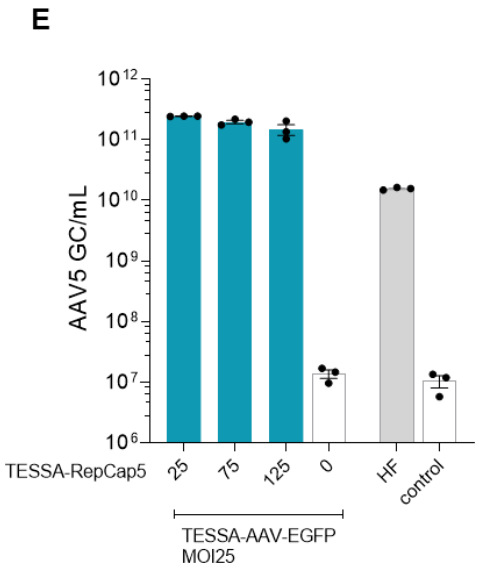
For TESSA2.0-AAV9, optimal levels (2.0 x10^{10} GC/mL) were observed when TESSA-RepCap9 was used at 50 GC/cell, with a ~50% decrease in productivity when the input TESSA was increased to 100 GC/cell, as shown in **Figure 4.13H**. Results were consistent with previous observations from TESSA vector encoding the AAV transfer genome and cap9 expression cassette *in cis*, wherein a 2-fold decrease in AAV9 yield was observed as MOI of the input vector doubled. Production from the helper-free method yielded ~2.5x10^{9} GC/mL, representing an 8-fold decrease compared to yield achieved using TESSA2.0-AAV9. Overall, these results showed remarkable increase in rAAV productivity across different serotypes can be achieved using the TESSA2.0 vectors.

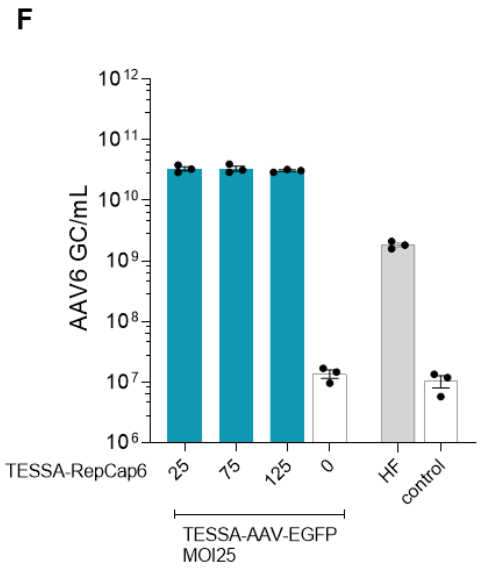

A
KanR
Ori
CMV / CuOx6
PacI
pA
PacI
Cap
MLP-TetO1b
Rep
ITR
AsisI
E2B Pol
KanR
L1
Ori
L5
L4
L3
L2
ITR
pTESSA-Rep


B
pTESSA-RepCap5
M 1 2 3 4


C
pTESSA-RepCap6
M 1 2 3 4 5 6 7 8


D
pTESSA-RepCap9
M 1 2 3 4 5 6


E
AAV5 GC/mL
TESSA-RepCap5
25
75
125
0
HF
control
TESSA-AAV-EGFP
MOI25


F
AAV6 GC/mL
TESSA-RepCap6
25
75
125
0
HF
control
TESSA-AAV-EGFP
MOI25

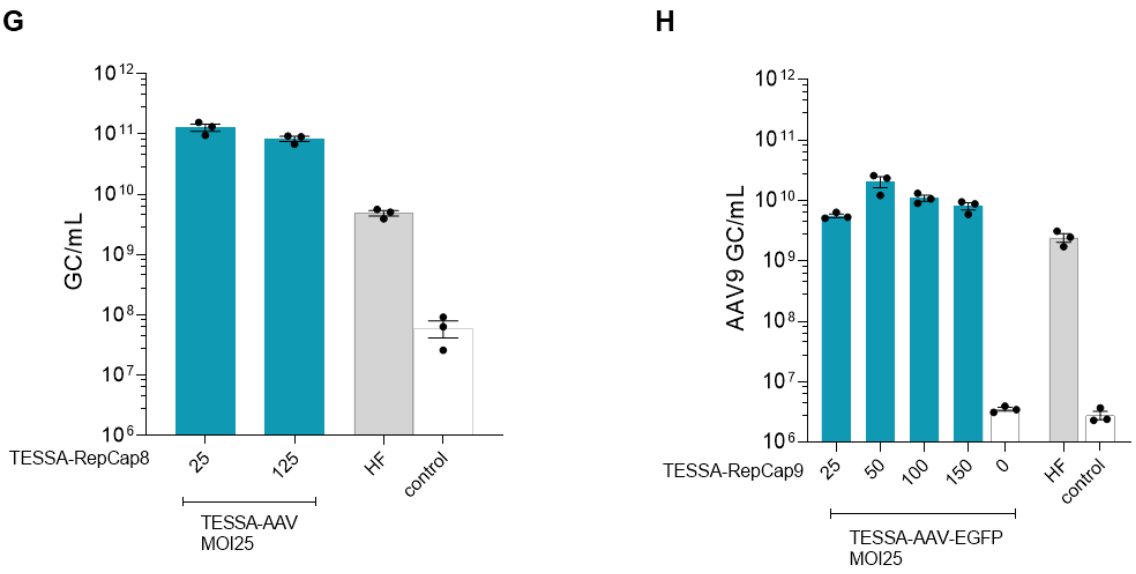


Figure 4.13 TESSA2.0 system significantly enhanced production of AAV5, AAV6, AAV8 and AAV9 vectors. A) Cloning schematic for insertion of the Cap expression cassettes into plasmid pTESSA-Rep by restriction cloning. PacI restriction digest for screening correct clones for plasmid (**B**) TESSA-RepCap5, (**C**) TESSA-RepCap6, and (**D**) TESSA-RepCap9. TESSA vectors encoding Rep and Cap were assessed for the production of (**E**) rAAV5, (**F**) rAAV6, (**G**) rAAV8 and (**H**) AAV9 in HEK293 cells by co-infection with TESSA-AAV-EGFP at the indicated MOI. Vectors were harvested at 96hpi, treated with turbo DNAse and quantified by EGFP-Specific qPCR. AAV productivity was compared to HEK293 cells transfected with the helper free plasmids. Data as mean±SEM of triple biological replicates.

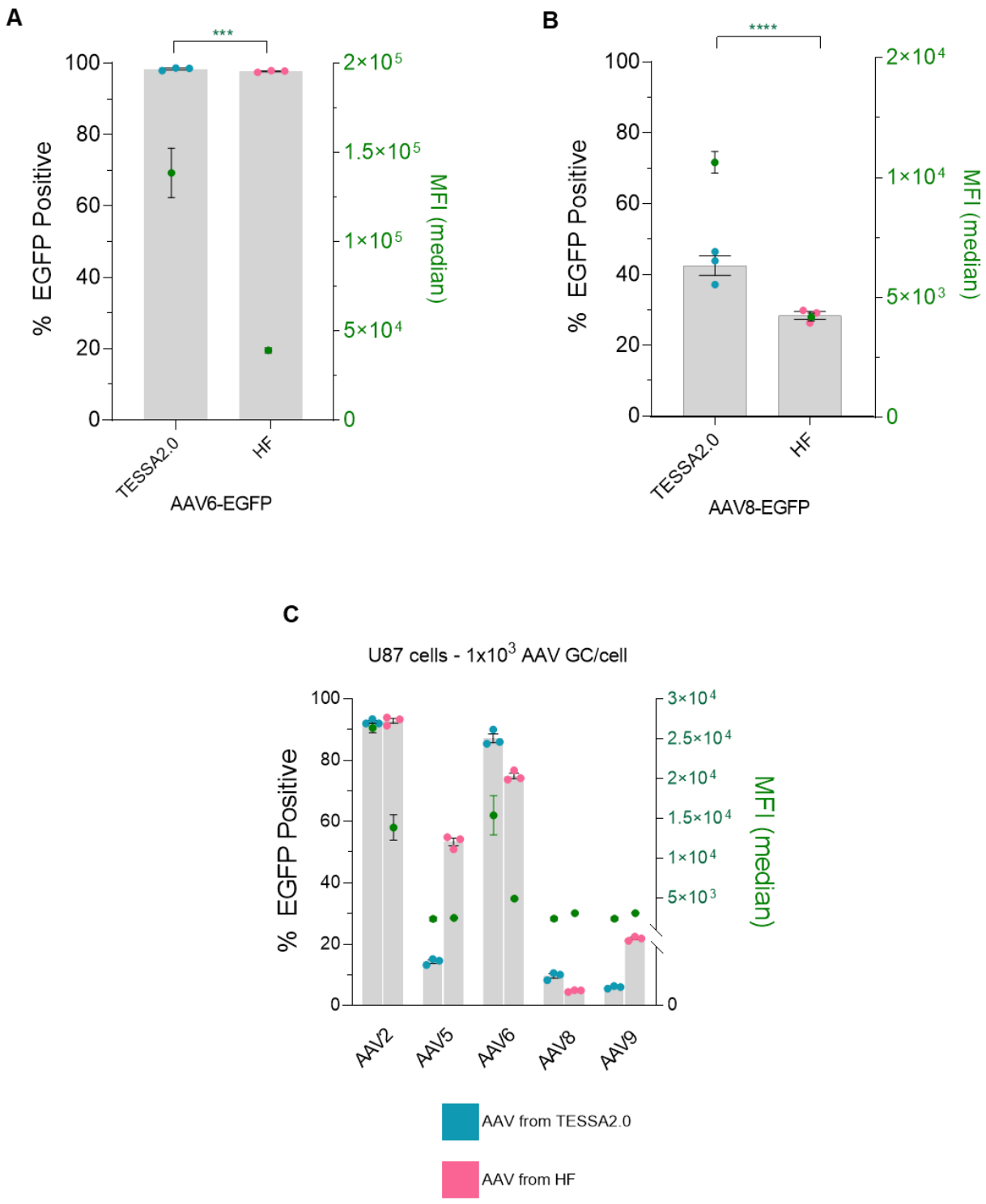
4.3.28 Assessment of rAAV5, rAAV6, rAAV8 and rAAV9 transduction *in vitro*

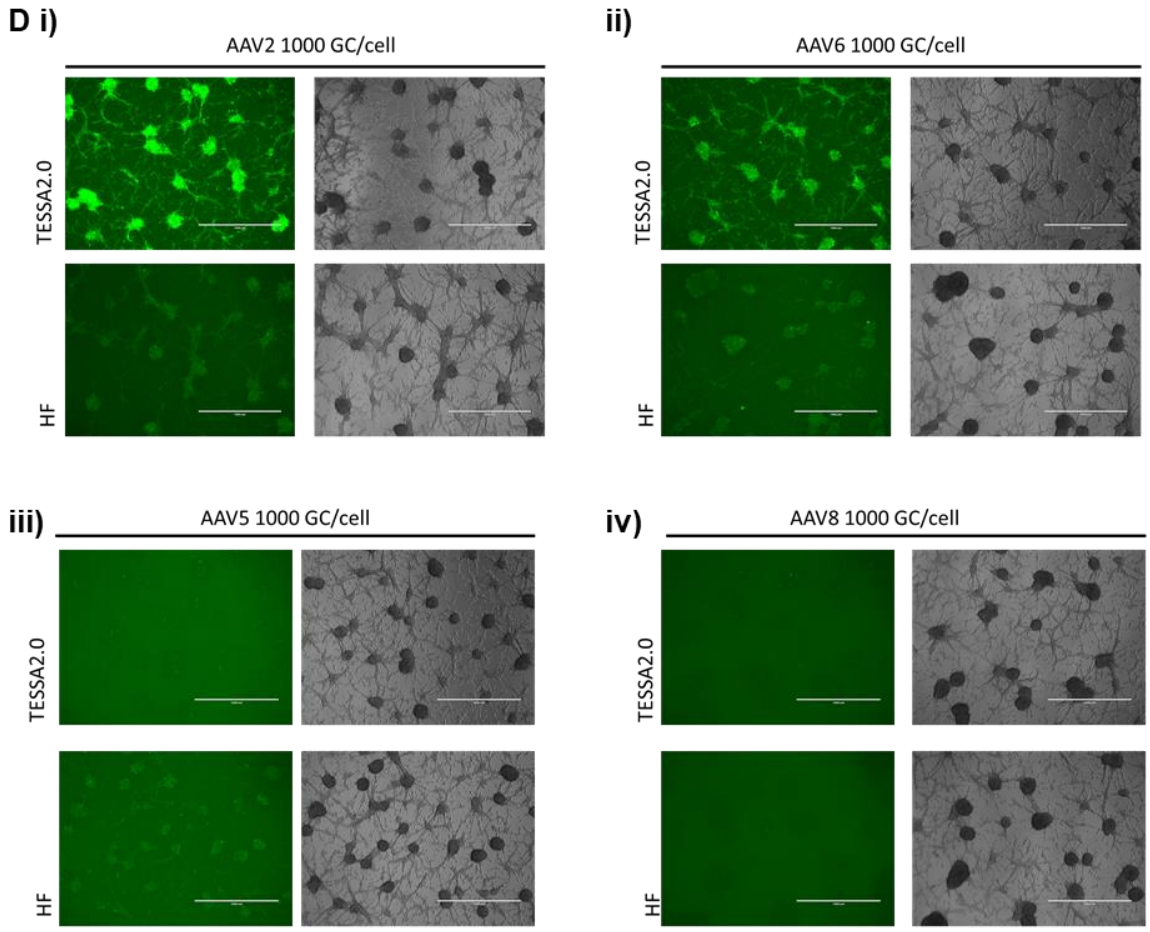
As rAAV6 and rAAV8 were shown to transduce HEK293 cells at varying extent, we initially assess infectivity of the particles derived from the TESSA2.0 system and compared to the helper-free method. rAAV6-EGFP and rAAV8-EGFP derived from TESSA2.0 (TESSA-RepCap used at 125GC/cell and TESSA-AAV-EGFP used at an MOI25) or helper-free method were used to infect HEK293 cells at a normalized 1000 GC/cell and EGFP measured by flow cytometry at 72hpi. As shown in **Figure 4.14A**, while ~100% of cells were positive for EGFP after infection with AAV6-EGFP derived from both TESSA2.0 or helper-free method, particles from TESSA2.0 showed a 3.5-fold increase in EGFP

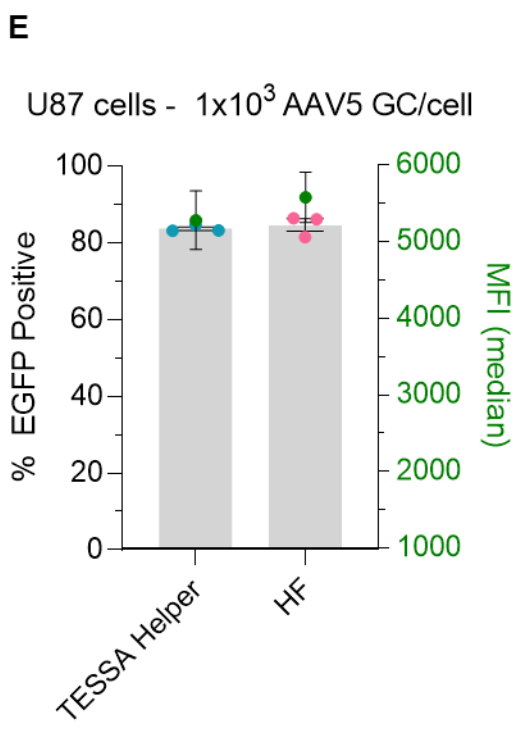
expression (as determined by MFI). Consistent with previous reports, HEK293 cells are less permissive to rAAV8 compared to rAAV6 particles (Ellis et al. 2013). While ~30% of cells were EGFP positive after infection (1000 GC/cell) with rAAV8-EGFP derived from helper-free, infections with particles derived from TESSA2.0 yielded ~40% EGFP positive cells with a 2-fold increase in MFI (**Figure 4.14B**). These results showed AAV6 and AAV8 particles derived from TESSA2.0 also exhibited enhanced transduction in HEK293 cells.

U87, a human primary glioblastoma cell line, was used for assessment of transduction from various rAAV vector serotypes. In this study, crude preparations of rAAV2, rAAV5, rAAV6, rAAV8 and rAAV9-EGFP derived from helper-free or TESSA2.0 were used to infect U87 cells at a normalized MOI of 1000 GC/cell. Cells were analysised for EGFP expression by flow cytometry 72hpi (**Figure 4.14C**). As expected, rAAV2, rAAV6 and rAAV8 particles derived from TESSA2.0 showed enhanced transduction compared to helper-free method. While infection with rAAV2-EGFP derived from TESSA2.0 and helper-free resulted in >90% of cells positive for EGFP expression, a 50% increase in MFI was observed from cells infected with rAAV2-EGFP derived from TESSA2.0 compared to helper-free samples. Similarly, infection with rAAV6-EGFP derived from TESSA2.0 resulted in 10% increase in EGFP positive cells and a 3-fold increase in MFI compared to helper-free derived particles. While U87 cells were least permissive to rAAV8, infection with particles derived from TESSA2.0 resulted in ~10% EGFP positive cells, a 50% increase above the helper-free derived samples. Surprisingly, for both rAAV5 and rAAV9, particles derived from TESSA2.0 exhibited reduced transduction in U87 cells compared to helper-free derived vectors. While EGFP expression (determined by MFI) in U87 cells infected with rAAV5 and rAAV9 particles derived from TESSA2.0 or helper-free were comparable, ~4-fold reduction in EGFP positive cells were observed in cells infected with TESSA-derived AAVs. Representative images of U87 cells transduced with rAAV2, rAAV5, rAAV6 and rAAV8-EGFP derived from TESSA2.0 or helper-free method are presented in **Figure 4.14D**.

The reduced transduction of TESSA2.0-derived rAAV5 and rAAV9 contrasted the increase potency of rAAV2, rAAV6 and rAAV8 vectors derived from TESSA2.0 we observed compared to the helper-free derived particles. To explore whether the reduced potency of rAAV5 and rAAV9 from TESSA2.0 was due to the intrinsic helper functions of TESSA, particles were produced by infection (MOI125) with TESSA helper in HEK293 transfected with the pRepCap (5 or 9) and the AAV transfer genome pAAV-EGFP. rAAV5 and rAAV9 particles produced from TESSA helper or the helper-free method were harvested at 96hpi and used to infect U87 cells at 1000 GC/cell. Cells were analysised by flow cytometry at 72hpi and showed comparable transduction efficiency (~80% EGFP positive cells) for rAAV5 derived from TESSA helper and helper-free method (**Figure 4.14E**), while a 10% increase in EGFP positive cells were observed from cells infected with rAAV9 derived from helper-free compared to TESSA (**Figure 4.14F**). These results confirmed rAAV5 and rAAV9 particles produce from TESSA helper were potent when the pRepCap plasmid was supplied *in trans*. Therefore, the reduce potency of rAAV5 and rAAV9 derived from TESSA2.0 was not due to an intrinsic helper effect of TESSA but likely from the configuration of the Cap5/9 coding sequence or its expression directly from TESSA vector.


A
***
% EGFP Positive
MFI (median)
100
80
60
40
20
0
2×10^5
1.5×10^5
1×10^5
5×10^4
0
TESSA2.0
HF
AAV6-EGFP
B
****
% EGFP Positive
MFI (median)
2×10^4
1×10^4
5×10^3
0
TESSA2.0
HF
AAV8-EGFP
C
U87 cells - 1x10^3 AAV GC/cell
% EGFP Positive
MFI (median)
3×10^4
2.5×10^4
2×10^4
1.5×10^4
1×10^4
5×10^3
AAV2
AAV5
AAV6
AAV8
AAV9
AAV from TESSA2.0
AAV from HF


D i)
AAV2 1000 GC/cell
TESSA2.0
HF
ii)
AAV6 1000 GC/cell
TESSA2.0
HF
iii)
AAV5 1000 GC/cell
TESSA2.0
HF
iv)
AAV8 1000 GC/cell
TESSA2.0
HF


E
U87 cells - 1x10^3 AAV5 GC/cell
% EGFP Positive
MFI (median)
0
20
40
60
80
100
1000
2000
3000
4000
5000
6000
TESSA Helper
HF

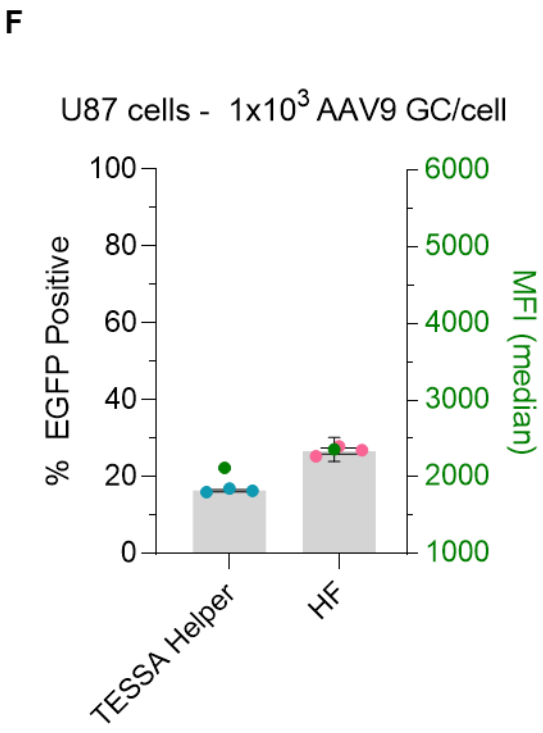

F
U87 cells - 1x10^3 AAV9 GC/cell
% EGFP Positive
MFI (median)
0
20
40
60
80
100
1000
2000
3000
4000
5000
6000
TESSA Helper
HF

Figure 4.14 Assessment of rAAV5, -6, -8 and -9 transduction *in vitro*. Crude preparations containing (**A**) rAAV6-EGFP and (**B**) rAAV8-EGFP vectors produced from the helper free plasmids or via TESSA2.0 approach (TESSA-AAV-EGFP MOI25 and TESSA-RepCap5/8 at 25GC per cell) were used to infect HEK293 cells at $1x10^3$ GC per cell. Cells were analyzed by flow cytometry at 72hpi. **C**) Infection of U87 cells using rAAV2, rAAV5, rAAV6, rAAV8, and rAAV9 encoding EGFP. Cells were infected at $1x10^3$ GC per cell with AAV crude preparations derived from TESSA2.0 or helper-free and analysed by flow cytometry at 72hpi. **D**) Representative brightfield and fluorescent images of U87 cells infected with (**i**) rAAV2, (**ii**) rAAV6, (**iii**) rAAV5, and (**iv**) rAAV8 vectors derived from TESSA2.0 or helper free. Infection of U87 cells using (**E**) rAAV5-EGFP and (**F**) rAAV9-EGFP derived from the use of TESSA as a helper virus. AAV5 and AAV9 vectors were produced in HEK293 cells by the helper-free method or via co-transfection with the AAV genome and pRepCap into HEK293 cells infected with TESSA helper (MOI of 125). U87 cells were infected with crude AAV preparations at $1x10^3$ GC per cell and analysed by flow cytometry at 72 hpi. Data as mean±SEM of triple biological replicates.

4.3.29 Stability assessment of TESSA-RepCap5, -6, -8 and -9 vectors

To assess genetic stability of vectors TESSA-RepCap5, -6, -8 and -9, vectors were serially passaged in HEK293 cells and genomic DNA was extracted from TESSA particles at the indicated passages. The cap coding sequences were measured using cap5, -6, -8 or -9 specific qPCR and compared against hexon-specific qPCR. Plasmid DNA encoding the TESSA-RepCap genomes, isolated from a single bacterial colony, were included as positive control to ensure equimolar ratio of cap and hexon coding sequences. As shown in **Figure 4.15**, while cap5 (**A**), cap8 (**C**) and cap9 (**D**) coding in TESSA were confirmed to be stable up to the assessed 7^{th} passage (purification of TESSA-RepCap8, and the 6^{th} and 7^{th} passages of TESSA-RepCap5 and -9 carried out by OXGENE), ~50% of TESSA-RepCap6 vectors appeared to have lost the cap6 coding DNA at passage 3, which was subsequently increased by 6-fold from vectors at passage 4 (**Figure 4.15B**). Genetic instability observed from TESSA-RepCap6 was in line with challenges observed during production and passage of the vector (data not shown).

Production of TESSA-RepCap5 and TESSA-RepCap9 was assessed against the control E1/E3Δ-Ad5. TESSA-RepCap6 was omitted from this study as re-configuration of the vector was required to

address issues of genetic instability. HEK293 cells were infected with the TESSA vectors or control Ad5 and supplemented with doxycycline. DNAse-resistant vectors harvested at 72hpi and quantified by Hexon-specific qPCR showed comparable yields between TESSA-RepCap9 and the control Ad5 (**Figure 4.15E**). However, a 4-fold lower titre was observed from TESSA-RepCap5 compared to the control vector. As siRNA knockdown of Cap2 was shown to enhance titre of TESSA-RepCap2 from HEK293 cells (**Figure 4.12E**), a similar strategy may be adopted to maximize production of TESSA-RepCap5 if required. To note, as the 3' UTR of the Cap coding sequence is shared between the TESSA-RepCap vectors, a single siRNA target design may be applicable across multiple vectors to increase productivity and will be explored in the future.

Genetic instability of the AAV cap sequence appears to be serotype dependent, as loss of cap coding from TESSA-RepCap2 and TESSA-RepCap9 was not observed at passage 7. We hypothesise that the genetic stability and production yield of TESSA vectors encoding cap6 (amongst other serotypes) can be enhanced by adopting the minimal CMV (CuOx6-minCMV) configuration. The use of TESSA vector expressing Cap6 under the minimal CMV configuration is explored further in Chapter 5.

Importantly, while we also observed >80% of TESSA-AAV-EGFP-CMV-Cap5 deficient of the cap5 coding sequence at passage 4, TESSA-RepCap5 wherein the cap5 transcription is driven by the weak minimal CMV promoter was still maintained at the equimolar ratio with hexon at passage 7, and fully capable producing high titre rAAV5 particles. Similarly, TESSA-RepCap8 which adopted the minimal CMV (CuOx6-minCMV) for driving Cap8 expression produced >20-fold increase in intact rAAV8 vectors compared to the helper-free method (**Figure 4.13G**) and the Cap8 DNA was stably maintained up to the 7^{th} assessed passage.

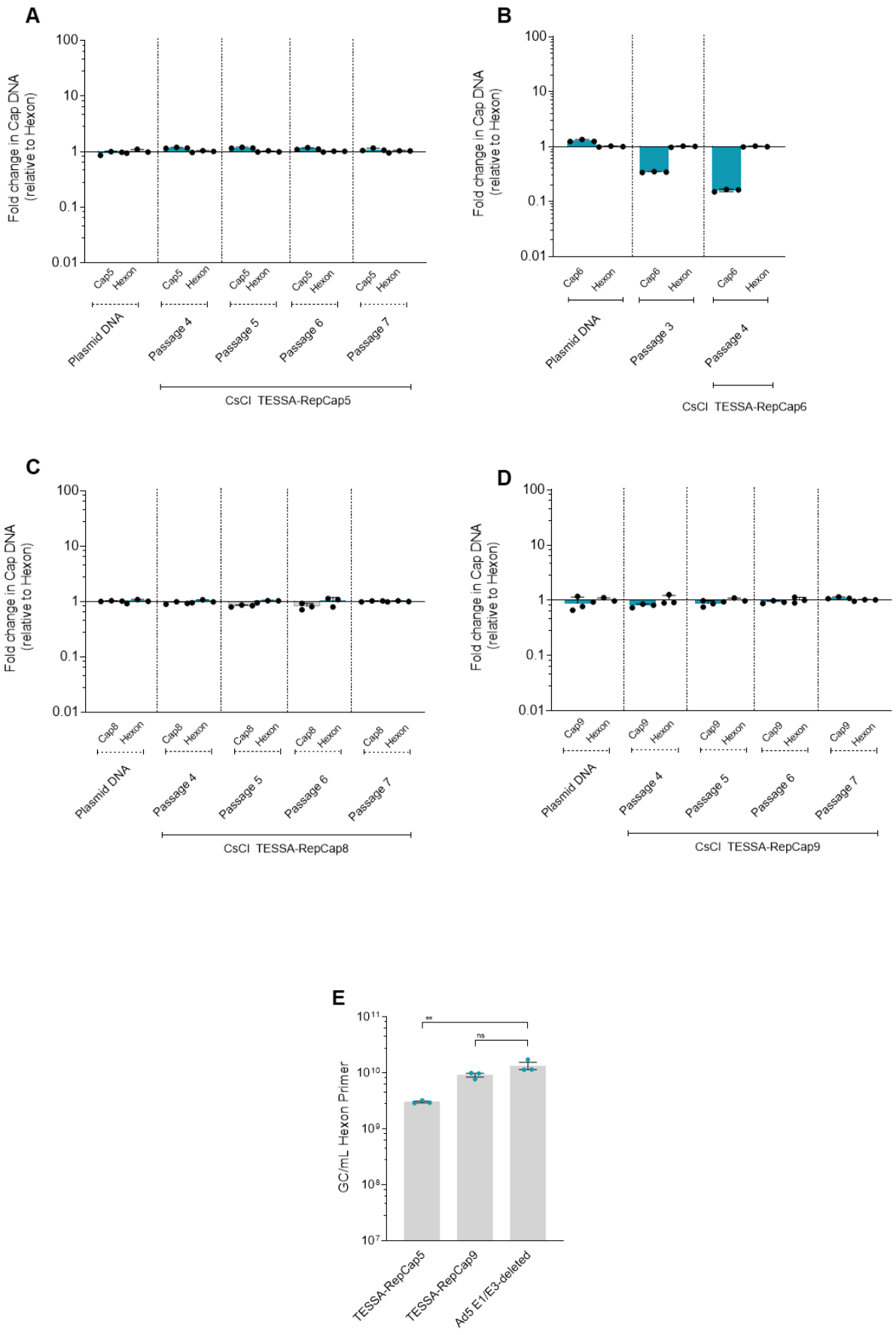

A
Fold change in Cap DNA (relative to Hexon)
100
10
1
0.1
0.01
Cap5
Hexon
Plasmid DNA
Passage 4
Passage 5
Passage 6
Passage 7
CsCl TESSA-RepCap5
B
Fold change in Cap DNA (relative to Hexon)
Cap6
Hexon
Plasmid DNA
Passage 3
Passage 4
CsCl TESSA-RepCap6
C
Fold change in Cap DNA (relative to Hexon)
Cap8
Hexon
Plasmid DNA
Passage 4
Passage 5
Passage 6
Passage 7
CsCl TESSA-RepCap8
D
Fold change in Cap DNA (relative to Hexon)
Cap9
Hexon
Plasmid DNA
Passage 4
Passage 5
Passage 6
Passage 7
CsCl TESSA-RepCap9
E
GC/mL Hexon Primer
10^{11}
10^{10}
10^{9}
10^{8}
10^{7}
**
ns
TESSA-RepCap5
TESSA-RepCap9
Ad5 E1/E3-deleted

Figure 4.15 Stability assessment of TESSA-RepCap5, -6, and -9 vectors. qPCR analysis of AAV cap genes in (**A**) TESSA-RepCap5, (**B**) TESSA-RepCap6, (**C**) TESSA-RepCap8 (**D**) TESSA-RepCap9. TESSA-RepCap vectors were recovered and sequentially passaged in HEK293 cells. HEK293 cells were infected (MOI-15) in HYPERFlask cell culture vessel using inoculating seed stock at passage 3. Vectors were harvested after 3 days and purified by caesium chloride ultracentrifugation to generate serial passage 4. This process was repeated to generate the indicated TESSA vector passages. DNA was extracted TESSA vector at the indicated passage and quantified by hexon and cap5, cap6, cap8 or cap9-specific qPCR. Data shows the copy number of the cap genes relative to Ad5 hexon, and compared to DNA plasmid encoding the TESSA-RepCap vectors. (**E**) Production of TESSA-RepCap5, TESSA-RepCap9 and E1/E3Δ-Ad5. HEK293 cells were infected with the TESSA vectors or control Ad5 at 25GC/cell and supplemented with doxycycline 0.5µg/mL. DNAse-resistant vectors harvested at 72hpi were quantified by hexon-specific qPCR. Data as mean±SEM of triple biological replicates. Significance determined by Student's t-test **P≤0.01.

4.4 Chapter discussion

In this chapter, we aimed to develop a transfection-free and scalable approach for producing rAAV vectors using TESSA. We show for the first time the engineering of a self-repressing adenovirus 'helper' that stably encodes both AAV rep and cap. By providing the rAAV transfer genome *in trans* using another TESSA vector, the 2-virus TESSA system (TESSA2.0) yielded a significant increase in rAAV2, -5, -6, -8, -9 vectors, with rAAV2, rAAV6, and rAAV8 particles displaying significant increase in transduction activity.

AAV Rep and its DNA coding sequences were shown to inhibit adenovirus replication when encoded *in cis* within the adenovirus genome (Sitaraman et al. 2011; Weger et al. 2016). Initially, we attempted to address AAV rep toxicity by exploring a combinatorial approach that included scrambling of the 'adeno-toxic' p40 *cis* inhibitory sequence by synonymous codon exchange, and repressing Rep expression to allow its propagation within TESSA. In addition, as Rep78 or 68 alone was previously shown to be sufficient for AAV replication, we attempted to reduce the expression of Rep52 and Rep40 proteins, and hence their anti-adenovirus effect, by synonymous codon of

the P19 promoter TATA element (Holscher, Kleinschmidt, and Burkle 1995). However, while the use of the Tet-4C5G repression system enabled recovery of a TESSA vector encoding 'toxic' proteins such as the pro-apoptotic protein BAX (**Figure 4.2 C&D**), which otherwise would induce cell death to limit adenovirus replication, it was unsuccessful at the recovery of vectors encoding rep, despite the extensive modifications discussed above (Arafat et al. 2000).

More interestingly, we were successful at producing a TESSA vector (TESSA-CuOx6-Cap5-Rep) by re-configuring the repΔp19 and cap sequence and controlling their expression using the cumate-inducible promoter. However, upon co-infection with the TESSA vector encoding the rAAV transfer genome and the cTA, we were unable to detect rAAV5 production (using EGFP-specific qPCR), but also selective silencing of the TESSA vector encoding the rAAV genome. Surprisingly, replication silencing of TESSA-AAV-EGFP-cTA was accompanied by repression of EGFP transcribed from the constitutive CMV promoter (**Figure 4.3 D&E**). While the mechanism of this selective repression on TESSA-AAV-EGFP-cTA remains unclear, it likely involved interaction of Rep and the AAV ITR sequence elements within the TESSA vector as overexpression of Rep was shown to induce an inhibitory effect on both rAAV and adenoviruses replication (Li, Samulski, and Xiao 1997; Needham et al. 2006).

Previous attempts to integrate AAV rep and cap coding sequences into E1/E3Δ-Ad vectors have been challenging and resulted in genetic instability and loss of transgene expression after sequential passages (Zhang et al. 2001; Fisher et al. 1996). Consistent with these previous observations, we were also unable to recover adenoviral vectors containing the native Rep coding sequence. Surprisingly, by scrambling of the p40 cis inhibitory sequence through synonymous codon exchange and inserting the repΔp19 sequence, in the reverse orientation relative to the adenovirus right ITR sequence, and without a heterologous promoter enabled *in cis* rescue and replication of the rAAV transfer genome from TESSA (**Figure 4.4F**). This result suggested sufficient

levels of Rep were produced in this configuration to allow AAV replication. Indeed, when assessed for production of rAAV, this TESSA-AAV-EGFP-Rep vector was shown to produce over 40-fold more intact rAAV than the plasmid transfection approach (**Figure 4.4G**). While we have not identified the viral transcription elements responsible for Rep expression from TESSA, adenoviral promoters can act in an orientation independent manner and influence transcription of genes several kilobases away from the RNA start site (Steinwaerder and Lieber 2000; Imperiale, Hart, and Nevins 1985; Imperiale and Nevins 1984). Candidate promoter elements that are potentially able to influence Rep expression from TESSA include the E1A enhancer, adjacent to the viral ITR, the pIX, E2, or E4 promoters (Donovan-Banfield et al. 2020).

However replication of the TESSA vector encoding both rep and the AAV transfer genome *in cis* was severely compromised, perhaps reflecting conflict caused by simultaneous replication of the rAAV and adenoviral genomes. Importantly, replication of the TESSA vector solely encoding rep was not impaired and fully capable of enabling rAAV replication over multiple passages. Similarly, re-coding of the entire rep78 by synonymous codon exchange and controlling its expression by a Tet-inducible promoter was previously shown to allow replication *in cis* within adenovirus vectors without hinder, suggesting that the Rep coding sequence was well tolerated after scrambling of the p40 cis inhibitory sequence (Sitaraman et al. 2011). However, by insertion of the CMV-Cap2 expression cassette into the TESSA-Rep vector, we observed slower replication kinetics, approximately ~3-fold lower in DNA replication and 10-fold lower in particle production, compared to the E1/E3Δ-Ad5 control (**Figure 4.12A**). Importantly, assessment of genetic stability found that the coding for rep and cap to be stable and intact at an equimolar ratio with the virus hexon after seven sequential passages (**Figure 4.12D**). In attempts to increase manufacturing yields of the TESSA-RepCap2 vector, we showed the use of siRNAs targeting the Cap mRNA transcript was able to recover production levels comparable to the control vector (**Figure 4.12E**).

Future work will explore the generation of stable cell lines expressing shRNAs targeting the AAV cap sequences to facilitate the efficient production of TESSA-RepCap vectors.

The instability of AAV capsid genes within adenovirus vectors is likely serotype dependent. While the TESSA vectors encoding Cap5 or Cap6 under control of the CMV promoter cassette showed replication impediment and loss of the cap coding at sequential passages, we did not observe this effect from the equivalent TESSA vector encoding the CMV-Cap9 or CMV-Cap2. Additionally, the TESSA-RepCap9 vector showed similar growth kinetics compared to the control Ad5 vector (**Figure 4.15E**). Importantly, via exchange of the constitutive CMV in place of the core minimal CMV (CuOx6_minCMV) stability of TESSA vector encoding Cap5 was maintained and capable of producing rAAV5 vectors at levels of 16-fold higher than the helper-free approach. Similarly, TESSA-RepCap8 which adopted the CuOx6_minCMV configuration for expression of Cap8 was shown to be stable at sequential passages and also capable of producing high-titre rAAV particles. The use of the CuOx6_minCMV configuration for driving Cap6 expression from TESSA vectors in attempts to improve stability is further explored in Chapter 5.

Although we attempted to reduce Rep52 and Rep40 expression by synonymous codon exchange of the P19 TATA motif, we found that this modification had little effect as the small Rep isoforms were detected at significantly higher amounts compared to Rep78/68 by western blot and exhibited a Rep expression pattern comparable to cells transfected with pRepCap2 (**Figure 4.11I**). Consistent with our findings, ablation of the P19 promoter TATA box was also previously attempted to inhibit expression of the Rep52 and Rep40 but found to not affect their synthesis (Chejanovsky and Carter 1989). Possibly, the expression profile of the Rep isoforms from TESSA may occur from transcription activity of the P19 promoter in producing high levels of Rep52/40 and weak transcriptional readthrough from an adenoviral promoter to supply Rep78/68. The significantly high amounts of Rep52/40 and relatively low levels of Rep78/68 expressed from

TESSA vectors provides an intriguing explanation for the dramatic increase in rAAV productivity, as the small Rep isoforms have been suggested to be involved in the accumulation of the AAV ssDNA genome and DNA encapsidation via helicase activity (King et al. 2001). Indeed, several groups have shown that improved rAAV yields and particle transduction were achieved by downregulation of Rep78/68 (as discussed previously at *Introduction, section 1.2.8*). The pRepCap plasmids employed (provided by OXGENE) in this thesis have also been optimised to improve viral production yields and based upon a similar strategy to the AAVpro Helper Free System, TAKARA (Natsoulis 1995). Sequence alignment of the pRepCap plasmid against the wt AAV genome shows that while expression of Rep52/40 from pRepCap is driven from the native p19 promoter, the TATA box motif of the p5 promoter was ablated and repositioned over 1Kb upstream from the translation start codon for Rep78/68 (appendix 3) . However, rAAV yields achieved from the helper-free system are consistently lower compared to the TESSA2.0 system suggests an inherent benefit from the delivery of the rep and cap genes, and the rAAV transfer genome using TESSA.

Surprisingly, we found that while rAA2, -6 and -8 vectors derived from TESSA2.0 showed enhance transduction *in vitro,* rAAV5 and rAAV9 particles derived from TESSA were less potent. The reason(s) for the reduced potency of rAAV5 and -9 remains unclear, however, it is likely due to the expression of the Cap and Rep proteins from TESSA as supplying these genes *in trans* by transfection with pRepCap recovered particle potency (**Figure 4.14 F&G**).

After exploring different configurations of TESSA vectors encoding the rAAV transfer genome, the cap and rep genes *in cis* or *trans*, the TESSA2.0 system described in this chapter offers several advantages over its previous iterations. Encoding the AAV transfer genome *in trans* of the rep and cap genes reduced encapsulation of cap sequences into AAV particles (via reverse packaging process), which can elicit immunological responses, but also decrease the likelihood of recombination and generation of replication-competent AAVs. The flexibility of encoding AAV cap

and rep within a single TESSA allows for the simple construction of a panel of TESSA vectors expressing the different natural AAV capsid serotypes and novel capsids. We showed the TESSA2.0 approach significantly enhanced the production of intact rAAV2, -5, -6, -8, and 9 vectors compared to the helper-free method. As the overall similarities between the AAV serotypes 1-9, at the amino acid level, is ~45%, with AAV5 representing the most divergent serotype, we hypothesis that similar improvements in yield from TESSA can be extended to all serotypes (Zincarelli et al. 2008).

4.5 Chapter conclusions

1. By scrambling the p40 cis inhibitory sequence via synonymous codon exchange and limiting expression from the absence of a heterologous promoter, AAV rep can be stably encoded in TESSA for AAV production.
2. By using two TESSA vectors, the TESSA2.0 system, significant improvements in yields of rAAV vectors 2, -5, -6, -8, and -9 were achieved. Dependent on the capsid serotype and transgene expression cassette, up to 10 or 100-fold increase was observed compared to the helper-free method.
3. rAAV vectors produced using TESSA2.0 were largely free of infectious adenoviruses (~10 TCID50/mL) but also exhibited significantly enhanced transduction *in vitro.*

Chapter 5

Production of rAAV via propagation and capsid-exchange using TESSA

5.1 Introduction

We showed in the previous chapter that the TESSA2.0 system enables rAAV2 vector production, with significant improvements in titre and transduction competent particles compared to the traditional plasmids transfection process. As the process is completely free of plasmid transfection, the TESSA2.0 platform should enable scalable production of rAAV vectors. The benefit of the TESSA2.0 system was also translated to the production of other AAV capsid serotypes that included rAAV5, -6, -8 and -9.

An apparent bottleneck of the TESSA2.0 system includes the engineering of TESSA vectors encoding the rAAV transfer genomes for different transgene expression cassettes. While the TESSA genome can be readily manipulated with simple molecular cloning tools and know-how, the timescale from the construction of the TESSA genome plasmid to the manufacture of stock vectors for *in vitro* assessment can take up to a few weeks due to the innate biology of the adenovirus (Luo et al. 2007).

In addition, a risk remains concerning DNA impurities from reverse packaging *in cis* DNA sequences that directly flank the AAV ITRs of the transfer genome. We showed in the previous chapter that these DNA contaminants, inherent to all rAAV vector manufacturing platforms to

date, was also detectable from particles produced using TESSA (Clement and Grieger 2016). While it is quite feasible to reduce risks, genotoxicity and immunotoxicity, associated with these DNA impure particles by the inclusion of stuffer DNA sequences or silencing elements to flank the AAV ITRs (Hauck et al. 2009; Gray and Zolotukhin 2011); here we explore a novel approach using the TESSA vectors encoding the AAV rep and cap genes, to eliminate these contaminant particles, by directly propagating rAAV vectors from particle seed-stocks. This approach also bypasses requirements for the construction of TESSA vectors encoding the rAAV transfer genome or supplying it *in trans* via plasmid transfection.

To our knowledge, the use of rAAV particles as direct inoculation seed-stock for further vector propagation has not yet been reported. Presumably, for this approach to be economically viable, seed-stock rAAV vectors should be manufactured at low-cost and display high infectivity to the packaging or producer cells; and wherein the rep and cap genes, and 'helper' functions to induce AAV replication are also efficiently introduced into the process. While rAAV2 vectors display the highest efficiency for *in vitro* transduction of cell lines that are typically used for rAAV production, including A549, Hela and HEK293-based cells, their efficiencies are generally reported in the range of 1000 – 10,000 particles per transduction event, dependent on the production method and cell lines used for assessment of infectivity (Huang et al. 2013). It is likely that this relatively low transduction efficiency, coupled with requirements for delivering/inducing helper functions, and Rep and Cap expression, hindered exploration of this rAAV propagation approach. We hypothesize that the criteria required to allow efficient rAAV production via propagation can be fulfilled by the use of the TESSA vector system. We showed previously in Chapter 4, rAAV vectors are efficiently produced from TESSA2.0 and showed enhance transduction *in vitro*. In addition, by encoding rep and cap genes, TESSA should provide a simple solution for the delivery of these genes and helper functions to manufacture rAAV vectors economically.

Ideally, we envision an approach wherein rAAV vector stocks can be used concurrently with TESSA-RepCap vectors, from a selected range of AAV capsid serotypes, and in a straightforward co-infection process for amplification to high-titre and improving the quality of the AAV particles. However, while AAV2 and AAV6 capsid serotypes are relatively infectious in HEK293 cells, the majority of other capsid serotypes, including AAV5, AAV8, and AAV9, infects 293 cells poorly. To solve this, we explored further in this Chapter the feasibility of propagation rAAV vector via a capsid exchange strategy, wherein rAAV2 vectors are used as inoculation seed-stock for the generation of rAAV5, rAAV6, rAAV8, and rAAV9 vectors using TESSA-RepCap5, -6, -8, and -9, respectively.

5.2 Chapter aims

1. Assess the feasibility of producing rAAV2 vectors via propagation using TESSA-RepCap
2. Assess the feasibility of producing rAAV5, -6, -8 and -9 vectors via capsid exchange of rAAV2
3. Characterisation of production yield, potency, and impurities of rAAV produced via the propagation/capsid exchange method using TESSA

5.3 Results

5.3.1 Propagation of AAV2 using TESSA-RepCap2

To assess whether TESSA-RepCap2 could propagate rAAV particles directly, we infected fresh HEK293 cells with rAAV2-EGFP (50 GC/cell) that were produced by TESSA2.0, TESSA-RepCap2 wherein pAAV-EGFP was delivered by transfection, or via the helper-free method. Interestingly while EGFP expression is almost undetectable by fluorescence microscopy when cells were infected with rAAV produced by the helper-free approach (**Figure 5.1A, top images**), yet when TESSA-RepCap2 is added to these cells almost every cell becomes EGFP positive (**Figure 5.1A, lower images**). This suggests that at least one rAAV genome must have been present in these cells to act as a template for replication by TESSA-RepCap2. This finding is consistent with results from the previous assessment of rAAV2-EGFP infectivity using TESSA-RepCap2 via TCID50 assay, which showed that rAAV2 derived from helper-free exhibits a GC to infectivity ratio of ~50 (*Chapter 4, Figure 4.11G*).

rAAV productivity from the propagation approach using TESSA-RepCap2 was compared to yield achieved from TESSA2.0 or helper-free system. As shown in **Figure 5.1B**, DNAse-resistant particles harvested at 96 hpi were undetectable by EGFP-specific qPCR from cells solely infected with rAAV2 vectors (produced via the different sources). Upon co-infection of TESSA-RepCap2 with rAAV2 (derived from the different sources), comparable yields of rAAV2-EGFP and above $2x10^{10}$ GC/mL were observed, which is marginally higher than was achieved using TESSA2.0 ($1.5 x10^{10}$ GC/mL), but approximately 50-fold higher than the helper-free system. This finding confirmed that high productivity of intact rAAV2 can be achieved by the propagation of existing rAAV vector stocks using TESSA-RepCap2.

5.3.2 Assessment of transduction

The infectious activity of rAAV produced from the different approaches was assessed visually. Crude lysate preparations were added to fresh HEK293 cells at a 1:100 dilution and imaged using brightfield and fluorescent microscopy. rAAV vectors produced via the propagation approach, wherein the inoculating rAAV2 was derived from TESSA-RepCap2 with the transfection of pAAV-EGFP, was not further assessed as it was not anticipated to be biologically distinct from the other rAAV vectors propagated using TESSA-ReCap2. As expected, dramatic differences in EGFP expression can be observed between TESSA-derived and helper-free derived rAAV (**Figure 5.1C**). Transducing units were also measured using the TCID50 assay in HEK293 cells (without the aid of TESSA vectors). The highest yields (9.7 $x10^8$ TCID50/mL) were obtained from particles derived from the TESSA2.0 approach, whereas rAAV propagated using TESSA-RepCap2 with rAAV stocks produced slightly less at approximately 4.0$x10^8$ TCID50/mL. The helper-free approach produced considerably fewer rAAV infectious units (~1.0 $x10^6$ TCID50/mL) in comparison to the two TESSA approaches (**Figure 5.1D**). Additionally, when compared against the qPCR titre, rAAV2-EGFP derived from helper-free exhibit a GC to infectivity ratio of ~1000, while a more favourable ratio of under ~100 was observed from TESSA-derived rAAV particles.

5.3.3 Assessment of contaminating adenoviruses

The level of contaminating adenoviruses from these samples was also measured using the TCID50 assay. Here, crude lysate preparations were serially diluted before adding to fresh HEK293 cells and cultured with doxycycline over 12 days to monitor adenovirus plaques. As expected, the levels of contaminant adenovirus were low in each preparation, which was measured to be less than 10 infectious adenovirus vectors per mL (**Figure 5.1E**).

5.3.4 Assessment of capsid composition

To determine the expression of capsid proteins from TESSA-RepCap2, crude preparations were separated by SDS-PAGE and analysed by western blot using anti-AAV VP1/2/3 antibody. As shown in **Figure 5.1F**, expression of the capsid proteins VP1, 2 and 3 is similar to that observed in ATCC reference standard AAV2 particles (ATCC VR-1616), showing approximately 1:1:10 ratio in the absence of doxycycline for TESSA2.0, TESSA-RepCap2 and also for cells infected with TESSA-RepCap2 alongside rAAV2. In the presence of doxycycline, when the MLP is active, the TESSA2.0 system produced significantly less VP1, 2 and 3. As expected, AAV capsids were undetected from control samples infected with AAV2 or TESSA encoding the rAAV transfer vector.

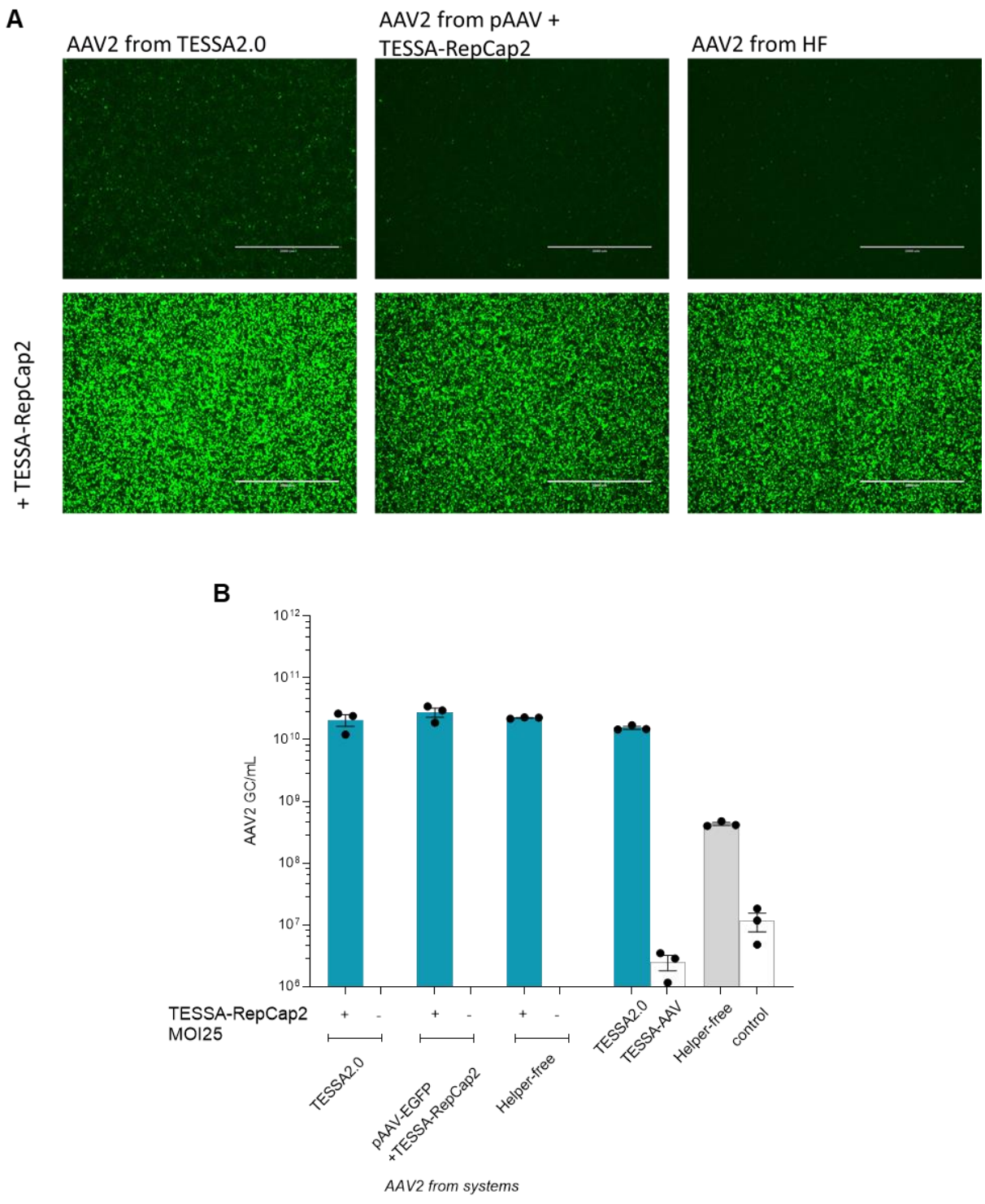
5.3.5 Assessment of contaminant DNA

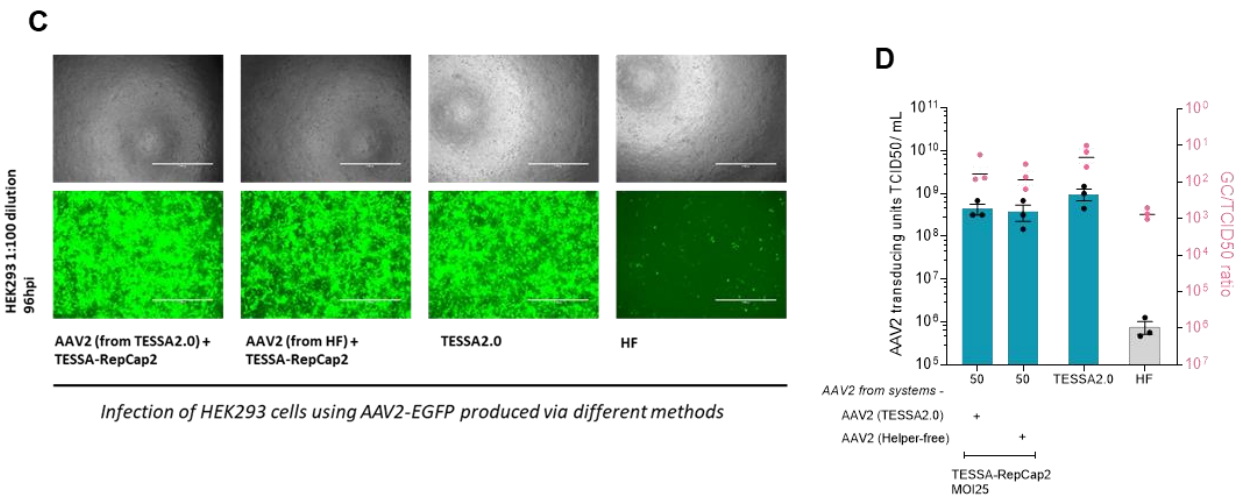
To determine DNA impurities from reverse packaging of DNA sequences adjacent to the AAV ITRs, we measured the incorporation of adenovirus DNA or plasmid backbone DNA into AAV2 particles produce via TESSA or the helper-free approach, respectively. rAAV-EGFP vectors were produced in HEK293 cells via TESS2.0, helper-free method or propagated using escalating doses of rAAV2 vectors. This inoculating rAAV2 stock used for propagation was derived from the TESSA2.0 approach with TESSA-RepCap2. As shown in **Figure 5.1G,** qPCR against the adenovirus packaging signal (approximately 325 bases from the left AAV ITR) showed that approximately 2.5% of AAV particles produced using TESSA2.0 contain DNA sequences mapping to the adenovirus packaging signal. As expected, rAAV derived from the helper-free approach showed 2.8% of particles containing the Ampicillin resistance gene sequences. This level is within the expected range of 1-6% reported in the literature (Chadeuf et al. 2005; Penaud-Budloo et al. 2018). Given that the adenovirus packaging signal DNA would not contain both terminal AAV ITR sequences, and would

likely not replicate as normal, a single passage of rAAV2 (used at 50 GC/cell) in conjunction with TESSA-Rep-Cap2 reduced DNA contaminant levels to 0.05%. We also observed a slight decrease in AAV vector yield and an increase in contaminant DNA with increasing input of AAV2 vector. Specifically, infection with rAAV2-EGFP at 1500 GC/cell, vector yield was 1.7-fold less than the lowest assess MOI, with the adenovirus packaging signal detected in 0.4% of particles. This result suggests that optimal rAAV productivity and reduced contaminant DNA is achieved with minimal rAAV vector input.

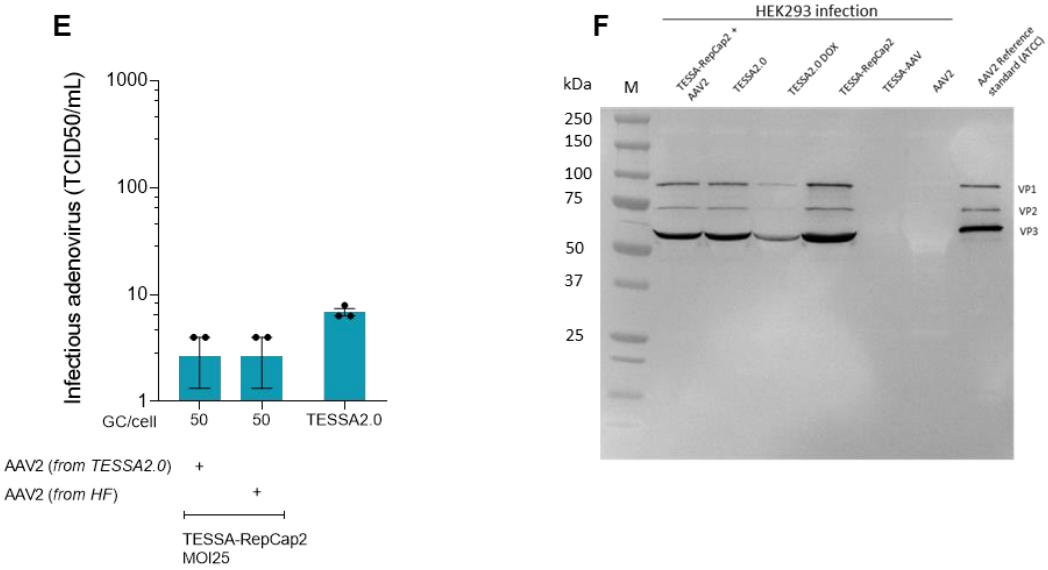
5.3.6 Assessment of AAV2 particles by TEM

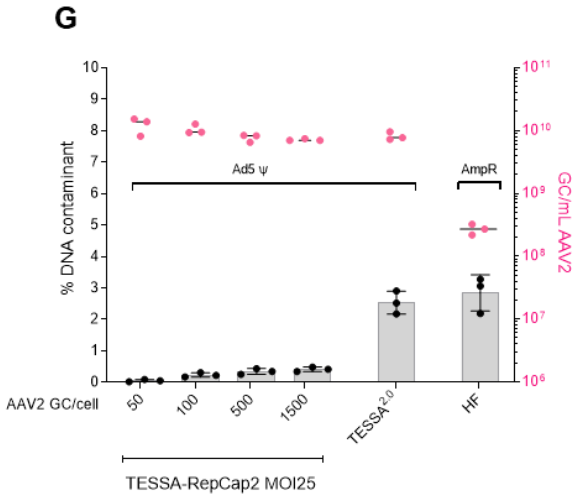
Purified (using AAVX affinity resin) rAAV2 particles from TESSA (derived from TESSA2.0 or the propagation strategy using TESSA-RepCap2) were prepared with 2% uranyl acetate and imaged using a transmission electron microscope (carried out by Dr Errin Johnson, Sir William Dunn School of Pathology, University of Oxford). Particles morphology and empty/full nature were compared to rAAV2 (as positive control) produced by helper-free method (samples provided by OXGENE, produced in suspension HEK293 cells from a 10L stirred-tank bioreactor and purified using AAVX affinity resin). Representative images are shown in **Figure 5.1H**. AAV particles derived from TESSA or the helper-free method appeared indistinguishable. As empty capsids are identified by an electron-dense circle at the centre of the capsid, full particle counts were estimated from a panel of image sets (Fu et al. 2019). While the helper-free samples showed approximately 60% of particles containing the genome, levels were consistently higher from TESSA-derived particles wherein 70-80% of capsids were observed to contain a genome. However, these levels are significantly higher than reported in the literature, wherein full capsids for rAAV2 vectors are reported at a range of 1-18% full by ELISA (Penaud-Budloo et al. 2018).


A
AAV2 from TESSA2.0
AAV2 from pAAV +
TESSA-RepCap2
AAV2 from HF
+ TESSA-RepCap2
B
AAV2 GC/mL
TESSA-RepCap2
MOI25
TESSA2.0
pAAV-EGFP
+TESSA-RepCap2
Helper-free
TESSA2.0
TESSA-AAV
Helper-free
control
AAV2 from systems



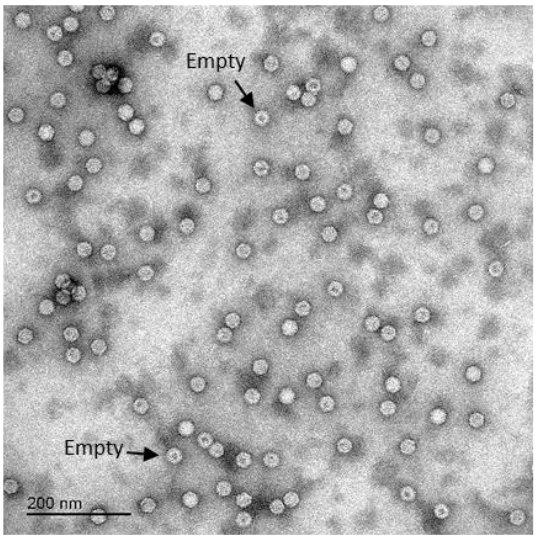
Infection of HEK293 cells using AAV2-EGFP produced via different methods





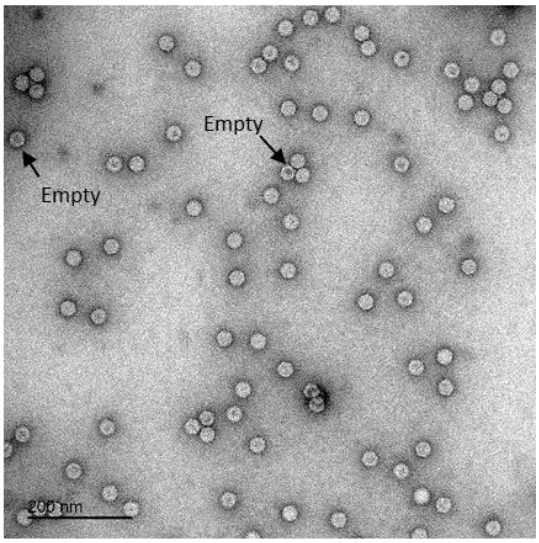
H

i) TESSA-RepCap2 + AAV2 (from HF)



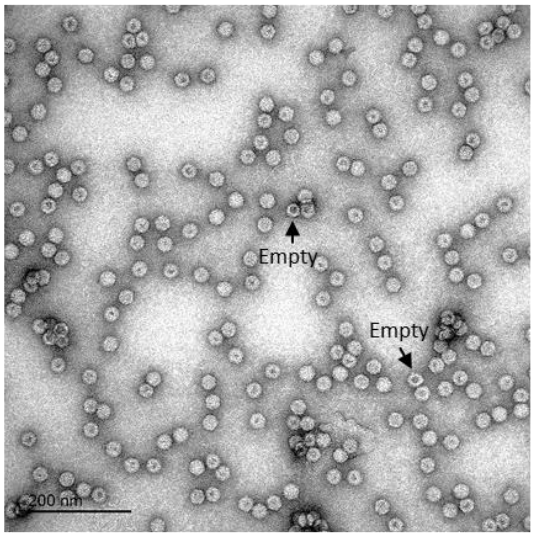
83.1% full

ii) TESSA-RepCap2 + AAV2 (from TESSA2.0)



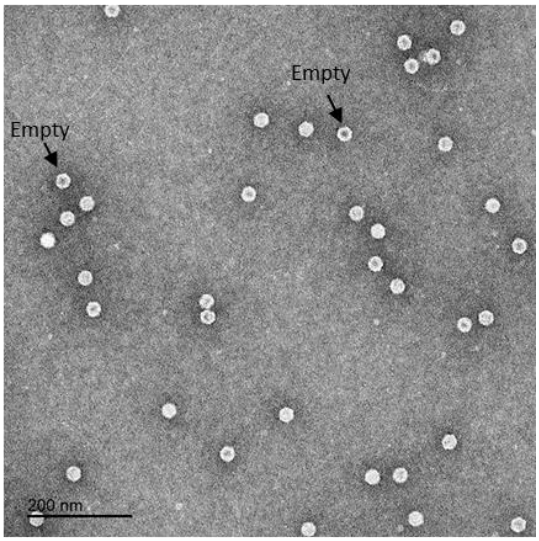
74.1% full

iii) TESSA2.0



76.36% full

iv) Helper-free



63% full

Figure 5.1 Propagation of AAV2 in HEK293 cell using TESSA-RepCap2. A) Fluorescent images of cells infected with AAV2-EGFP (50 GC/cell) derived from TESSA2.0, TESSA-RepCap2 with transfection of pAAV-EGFP genome, or the helper-free method. Crude AAV2 prepartions were added to HEK293 cells in the absence (**i**) or presence of TESSA-RepCap2 at an MOI of 25 (**ii**) and imaged at 48hpi. Scale bar, 2000 µm. Vectors were harvested at 96hpi and encapsidated particles quantified by EGFP-specific qPCR. AAV2 productivity was compared to the TESSA2.0 and helper-free approach. Data as mean±SEM of triple biological replicates. Crude lysates derived via propagation of AAV2 using TESSA-RepCap, TESSA2.0 or helper-free method were added to fresh HEK293 cells at 1:100 volume dilution and imaged (**C**) by fluorescent microscopy at 96hpi. **D**) Transducing units of AAV2 vectors were determined by measuring GFP-expressing cells 6 days post-infection. Ratio of encapsulated AAV2 GC to TU is shown on the right axis. N=3, mean ± SEM. **E**) Adenoviral contamination in AAV2 produced using TESSA2.0, or via passage of AAV using TESSARepCap2, determined by TCID50 assay. **F**) Western blot of AAV2 capsid proteins from particles produced using TESSA2.0 (+/- doxycycline 0.5 µg/mL), or via co-infection of AAV2 particles (produced from TESSA2.0) at 50 GC/cell with TESSA-RepCap2 (MOI-25). Samples were harvested at 96 hpi. Cell lysate (25uL) was probed with anti-AAV VP1/2/3 antibody. AAV2 standard (ATCC VR-1616) is also shown. (**G**) DNA contaminants were determined in AAV2 vectors produced via TESSA2.0, HF transfection, or co-infection of TESSA-RepCap2 (MOI-25) with escalating AAV2 vector (produced using TESSA2.0) doses. Samples were harvested 96 hpi DNA, impurities were determined in DNAse-resistant AAV2 by qPCR against the adenovirus packaging signal Ψ (for TESSA2.0 derived AAV) or AmpR (for HF derived AAV). Data is percentage of adenovirus or AmpR DNA compared to EGFP. Titre of AAV2 vectors shown on the right axis. Data presented as mean ± SEM of triple biological replicates. **H**) Transmission electron microscopy imaging of negatively stained AAVX-purified AAV2 particles produced via TESSA2.0, propagation using TESSA-RepCap2 or helper-free method.

5.3.7 Capsid-exchange for the propagation of rAAV5, -6 and -9

We next explored whether the propagation approach using TESSA-RepCap can translate to produce rAAV vectors with different capsid serotypes. However, infectivity of HEK293 cells differs dramatically between different serotypes (Ellis et al. 2013). As exemplified in **Figure 5.2A**, infection of HEK293 cells using rAAV2, rAAV5, rAAV6 and rAAV9 vectors (derived from the helper-free process) encoding EGFP results in a few EGFP positive cells from the rAAV2-EGFP group, but absent from the other serotypes. While co-infection with TESSA-RepCap2 should result in replication of rAAV from any successful infection events, hence, increase EGFP expression, significant differences were still observable from cells infected with different capsid serotypes.

We therefore explored a strategy of capsid-exchange for the production of different rAAV vector serotypes. Accordingly, we infected HEK293 cells with rAAV2-EGFP (helper-free derived) at 50 GC/cell alongside TESSA-RepCap5, TESSA-RepCap6 or TESSA-RepCap9 (**Figure 5.2B**). To note, while we previously observed genetic instability associated with TESSA-RepCap6 (**Figure 4.15B**), the use of this vector was explored for validation of the capsid-exchange strategy. In each case, ~100% of the cells showed EGFP positivity at as early as 48 hpi with the different TESSA-RepCap vectors, confirming significant rAAV replication in these cells after infection with the rAAV2-EGFP vectors.

As rAAV9 infects HEK293 cells poorly, we initially compared productivity by propagation using TESSA-RepCap9 with high doses of rAAV9-EGFP, or low doses of rAAV2-EGFP particles, for delivery of the rAAV transfer genome. At 250 GC/cell, rAAV9-EGFP used in conjunction with TESSA-RepCap9 produced rAAV9 yields comparable to the helper-free method of ~2 $x10^9$ GC/mL, and a modest 1.5-fold increase was observed when input rAAV9-EGFP was increased to 750 GC/cell (**Figure 5.2C**). Conversely, at 50 GC/cell, rAAV2-EGFP used in conjunction with TESSA-RepCap9 increased titre 7-fold compared to yield achieved using helper-free plasmids. This result confirmed that AAV2 particles provide a more efficient strategy than AAV9 for delivery of the rAAV transfer genome for propagating rAAV9 vectors using TESSA-RepCap9.

Similarly, high productivity was observed for rAAV6 and rAAV5 serotype vectors using the capsid-switch strategy. As showing in **Figure 5.2 D-E**, production using the helper-free method yielded 8.5 $x10^8$ GC/mL and 7 $x10^9$ GC/mL of rAAV6 and rAAV5, respectively. However, yields above 1.5 $x10^{10}$ GC/mL of rAAV6 and 1.2 $x10^{11}$ GC/mL of rAAV5 were achieved with the capsid-exchange method using rAAV2 as seed vector. This represented over 15-fold more intact particles than the helper-method approach.

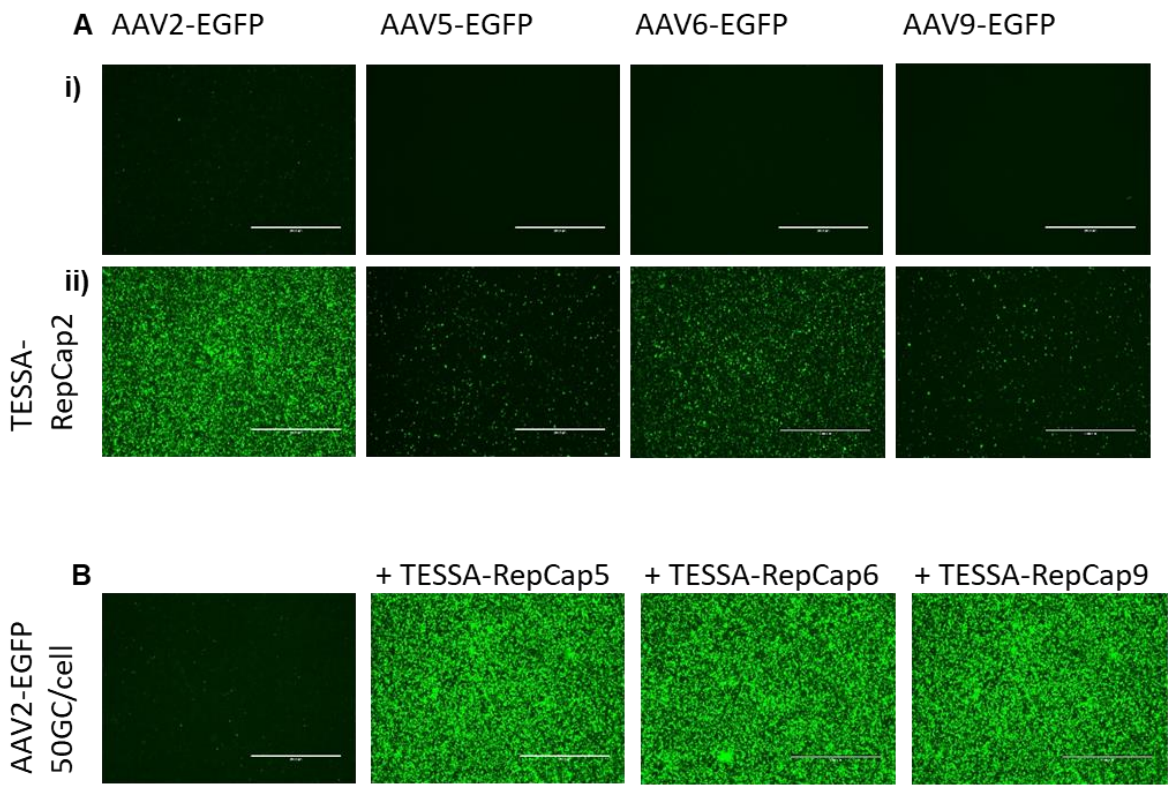
5.3.8 Analysis of rAAV5, -6 and -9 derived from the capsid-exchange method

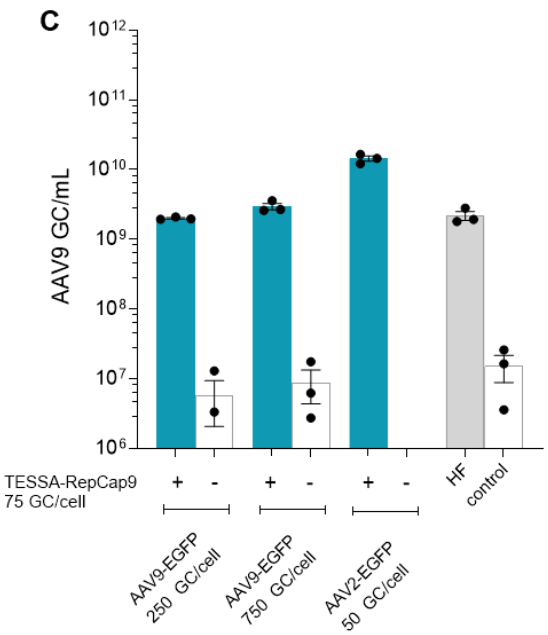
To determine infectivity of rAAV5, -6 and -9 derived from the capsid-exchange method using TESSA-RepCap, crude preparations were used to infect HeLaRC32 cells in the presence of an Ad5-E1 helper virus and infectious titre determine by the TCID50 assay. The HeLaRC32 cells stably encodes the AAV rep-cap genes (devoid of the ITR sequences) and are commonly used for infectious titration of rAAV vectors. In these assays, co-infection of rAAV with the wt adenovirus induced high expression of Rep and Cap to enable replication of the rAAV for sensitive detection by reporter transgene or qPCR detection (Zen et al. 2004). As expected in the TCID50 assay, rAAV5 and rAAV9 derived from TESSA-RepCap5 and -9 also showed reduced infectivity compared to the helper-free derived samples (**Figure 5.2F**), consistent with the low potency observed from these serotypes in the TESSA2.0 approach (*Chapter 4, Figure 4.14*). Specifically, while rAAV5 and rAAV9 derived from helper-free exhibit a particle to infectious ratio of approximately $5x10^4$ and $2x10^5$ GC/TCID50, respectively, rAAV5 and rAAV9 particles derived TESSA were unfavourable higher by 10- and 3-fold compare to helper-free samples. In contrast, rAAV6 derived from TESSA was measured at $1.4x10^8$ TCID50/mL, an approximately 120-fold increase in infectious particles compared to the helper-free samples ($1.2x10^6$ TCID50/mL). rAAV6 particles derived from TESSA exhibited a particle to infectivity ratio of 180:1, while a ratio of 750:1 GC/TCID50 was observed from helper-free derived samples.

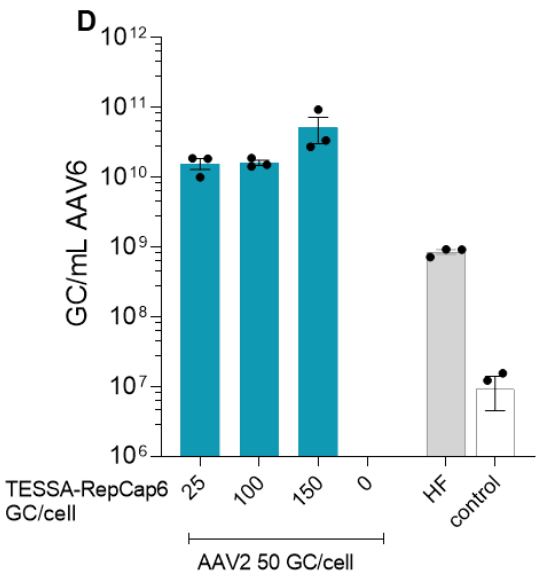
rAAV vectors were analysed by western blot to assess capsid proteins using anti-AAV VP1/2/3 antibody. An equal amount of lysate preparations from TESSA-derived rAAV9, rAAV6 and rAAV5 using the capsid-exchange strategy were compared against helper-free derived vectors. As expected, significantly more AAV9, -6 and -5 capsid proteins were observed from TESSA-RepCap derived samples and also showing comparably composition of VP1, 2 and 3 to the helper-free

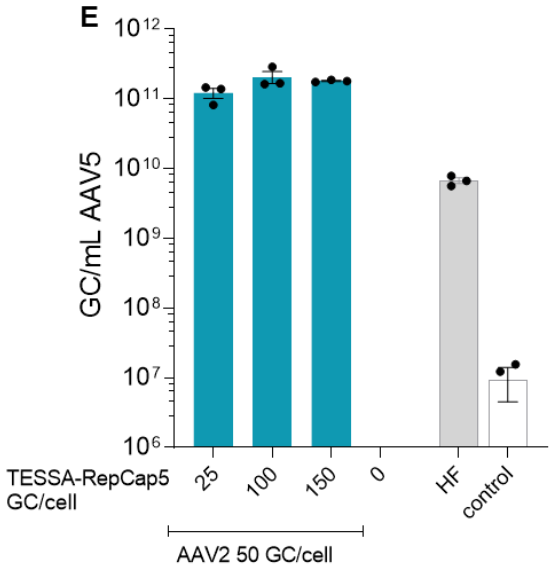
derived particles (**Figure 5.2G**). rAAV6 derived from the helper-free process was faintly detected from the blot likely due to a low titre in these samples as confirmed by the EGFP-specific qPCR (**Figure 5.2D**). The band (denoted asterisk*) above VP2 of AAV5 particles, previously reported from production in HEK293 cells, were also observably from both TESSA and helper-free samples (Kondratov et al. 2017).

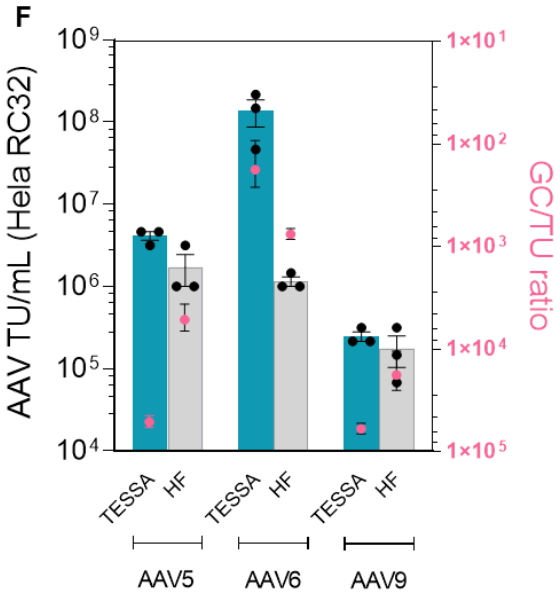
As particles derived from TESSA-RepCap5 were significantly less potent than the helper-free samples, further analysis was carried out to determine the balance of the VP1, VP2 and VP3 subunits within purified vectors. rAAV5 encoding the firefly Luciferase reporter (Fluc) were produced in HEK293 cells, from the helper-free method or via capsid-exchange using rAAV2-Fluc with TESSA-RepCap5, and purified using AAVX affinity resin. rAAV5-Fluc particles (5 $x10^{11}$ and 1 $x10^{11}$ VP) were analysed by western blot using anti-AAV VP1/2/3 antibody. As shown in **Figure 5.2Hi**, while levels of VP3 were comparable between TESSA and helper-free derived particles, incorporation of VP1 and VP2 were significantly lower in rAAV5 from TESSA. This was further confirmed by (**ii**) densitometry analysis of the VP bands using the Image Lab 6.0 software. Whereas particles derived from the helper-free method showed a VP1, 2, and 3 proportion similar to the consensus 1:1:10, a ratio of 1:2:35 was observed from the TESSA-derived particles. While unclear, this result suggests that the low potency of rAAV5 derived from TESSA-RepCap5 is likely due to low incorporation of VP1 and VP2 within the capsid or an over-expression of VP3 proteins from the TESSA vector.

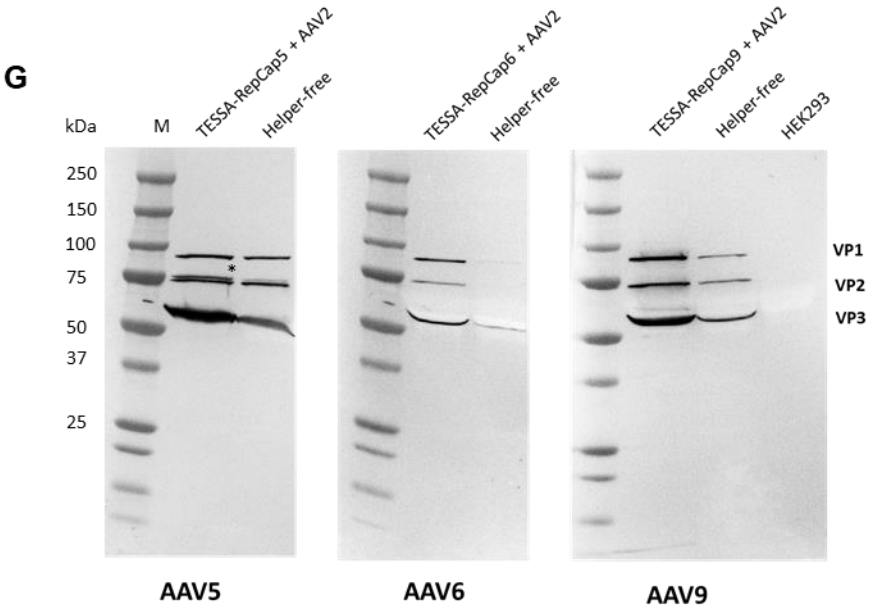

A
AAV2-EGFP
AAV5-EGFP
AAV6-EGFP
AAV9-EGFP
i)
ii)
TESSA-RepCap2
B
+ TESSA-RepCap5
+ TESSA-RepCap6
+ TESSA-RepCap9
AAV2-EGFP 50GC/cell

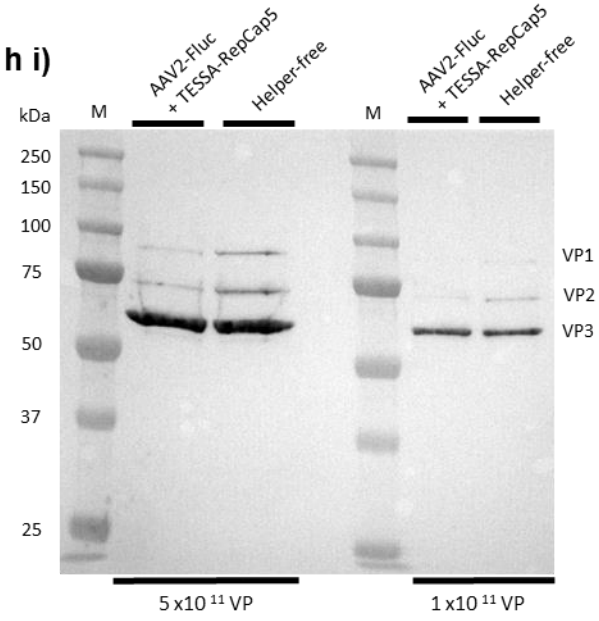

C
AAV9 GC/mL
TESSA-RepCap9
75 GC/cell
HF
control
AAV9-EGFP
250 GC/cell
AAV9-EGFP
750 GC/cell
AAV2-EGFP
50 GC/cell


D
GC/mL AAV6
TESSA-RepCap6
GC/cell
25
100
150
0
HF
control
AAV2 50 GC/cell


E
GC/mL AAV5
TESSA-RepCap5
GC/cell
25
100
150
0
HF
control
AAV2 50 GC/cell


F
AAV TU/mL (Hela RC32)
GC/TU ratio
TESSA
HF
AAV5
AAV6
AAV9


G
kDa
M
TESSA-RepCap5 + AAV2
Helper-free
TESSA-RepCap6 + AAV2
Helper-free
TESSA-RepCap9 + AAV2
Helper-free
HEK293
250
150
100
75
50
37
25
VP1
VP2
VP3
AAV5
AAV6
AAV9


h i)
kDa
M
AAV2-Fluc + TESSA-RepCap5
Helper-free
M
AAV2-Fluc + TESSA-RepCap5
Helper-free
250
150
100
75
50
37
25
VP1
VP2
VP3
5 x10 11 VP
1 x10 11 VP

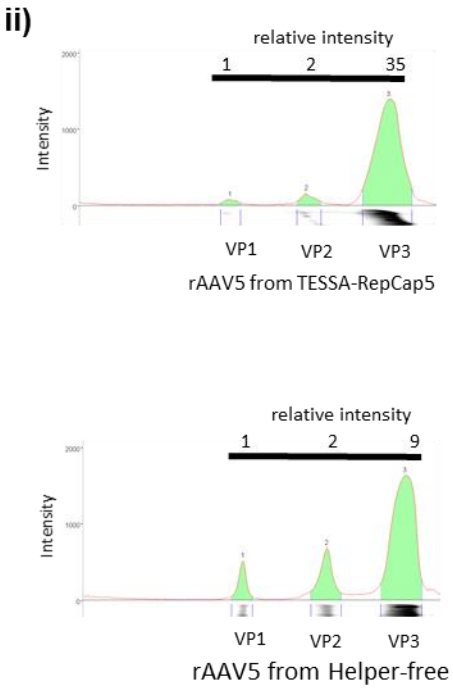

ii)
relative intensity
1
2
35
Intensity
VP1
VP2
VP3
rAAV5 from TESSA-RepCap5
relative intensity
1
2
9
Intensity
VP1
VP2
VP3
rAAV5 from Helper-free

Figure 5.2 Propagation of AAV5, AAV6 and AAV9 via capsid-exchange using TESSA-RepCap. A) Representative fluorescent images of HEK293 cells transduced with (**i**) AAV2, -5, -6 and -9 vectors encoding the EGFP reporter, (**ii**) or the same with TESSARepCap2. Cells were infected (at 50 GC/cell) with AAV2, -5, -6 and -9 crude lysates (produced via helper-free method), or co-infected with TESSA-RepCap2 (MOI-25), and imaged at 48hpi. Scale bar, 2000 µm. **B**) Representative fluorescent images of HEK293 cells infected (at 50 GC/cell) with AAV2 vectors encoding the EGFP reporter (produced via helperfree method) or co-infected with TESSA-RepCap5 (at 100GC/cell), TESSA-RepCap6 (at 100GC/cell), or TESSA-RepCap9 (at 75GC/cell). Cells were imaged at 48hpi. Scale bar, 2000 µm. **C)** Production of AAV9 via capsid-exchange using TESSA-RepCap9. HEK293 cells were co-infected using TESSA-RepCap9 with AAV9 or AAV2 at the indicated MOI. Production of rAAV6 (**D**) and rAAV5 (**E**) via c-infected with AAV2 and TESSA-RepCap6 or TESSA-RepCap5, respectively. rAAV production is compared to the helper-free method. Vectors were harvested 96hpi and DNAse resistant particles quantified by EGFP-specific qPCR. N=3, mean ± SEM. **F**) Transduction of rAAV5, -6, and -9 determined by the TCID50 assay in HeLaRC32 cells. Serial dilutions were prepared using crude rAAV lysates derived from TESSA-RepCap or the helper-free samples with Ad5-E1 (used at an MOI of 50) before infection of HeLaRC32 cells in the TCID50 assay. EGFP expression from each well was monitored by fluorescent microscopy at 72 hpi. **G**) Western blot of (**i**) AAV5, (**ii**) AAV6 and (**iii**) AAV9 capsid proteins from particles produced using AAV2 capsid-exchange or helper-free method. Equal amounts of crude preparations (25uL) containing rAAV5, rAAV6 and rAAV9-EGFP produced via helper-free method or via co-infection of rAAV2 (50 GC/cell) with TESSA-RepCap5 (100 GC/cell), TESSA-RepCap6 (100 GC/cell), TESSA-RepCap9 (75 GC/cell) were probed with anti-AAV VP1/2/3 antibody for western blot detection. **H**) Purified rAAV5-Fluc particles (5x 10^{11} and 1x 10^{11}) derived from helper-free transfection or via capsid-exchange, using rAAV2-Fluc with TESSA-RepCap5, were probed with anti-AAV VP1/2/3 antibody for (**i**) western blot detection. **ii**) Densitometry analysis of the VP bands from the 5 x10^{11} VP lane samples using the Image Lab 6.0 software.

5.3.9 Production of AAV8 via capsid-exchange using TESSA-RepCap8

Production of rAAV8 vectors by capsid-exchange using AAV2 particles and TESSA-RepCap8 was also explored. As shown in **Figure 5.3A**, HEK293 cells co-infected with rAAV2-EGFP and TESSA-RepCap8 (used at 25 or 125 GC/cell) yield approximately 2.5x10^{11} GC/mL of DNAase resistant particles. This represented a 19-fold increase in intact particles compared to the helper-free process which yielded 1.3x10^{10} GC/mL.

Infectivity of the particles was confirmed in HEK293 cells. Crude preparations at 1:100 volume dilution was used to infect HEK293 cells and EGFP expression analyzed by flow cytometry at 72 hpi. As shown in **Figure 5.3B**, approximately 20% of cells were positive for EGFP expression after

infected with rAAV8-EGFP derived from TESSA-RepCap8 (used at 25GC/cell) compared to ~2% observed from helper-free samples. Interestingly, a decrease in AAV8-EGFP potency was also observed when TESSA-RepCap8 was used at a high 125 GC/cell, suggesting a balance of Rep and Cap proteins is required for particle infectivity. Alternatively, infection with an increased dose of TESSA vector may also be exerting a higher degree of cellular stress and toxicity that is suboptimal for AAV maturation.

rAAV8-EGFP vectors were analysed by western blot using anti-AAV VP1/2/3 antibody. An equal amount of crude lysate preparations from production using TESSA2.0, capsid-exchange with rAAV-2-EGFP and TESSA-RepCap8, and the helper-free method were probed using anti-AAV VP1/2/3 antibody. As expected, significantly more capsid proteins were observed from TESSA-derived samples compared to the helper-free production (**Figure 5.3C**). Additionally, the proportion were VP1, VP2 and VP3 between TESSA and helper-free derived vectors were observed to be comparable.

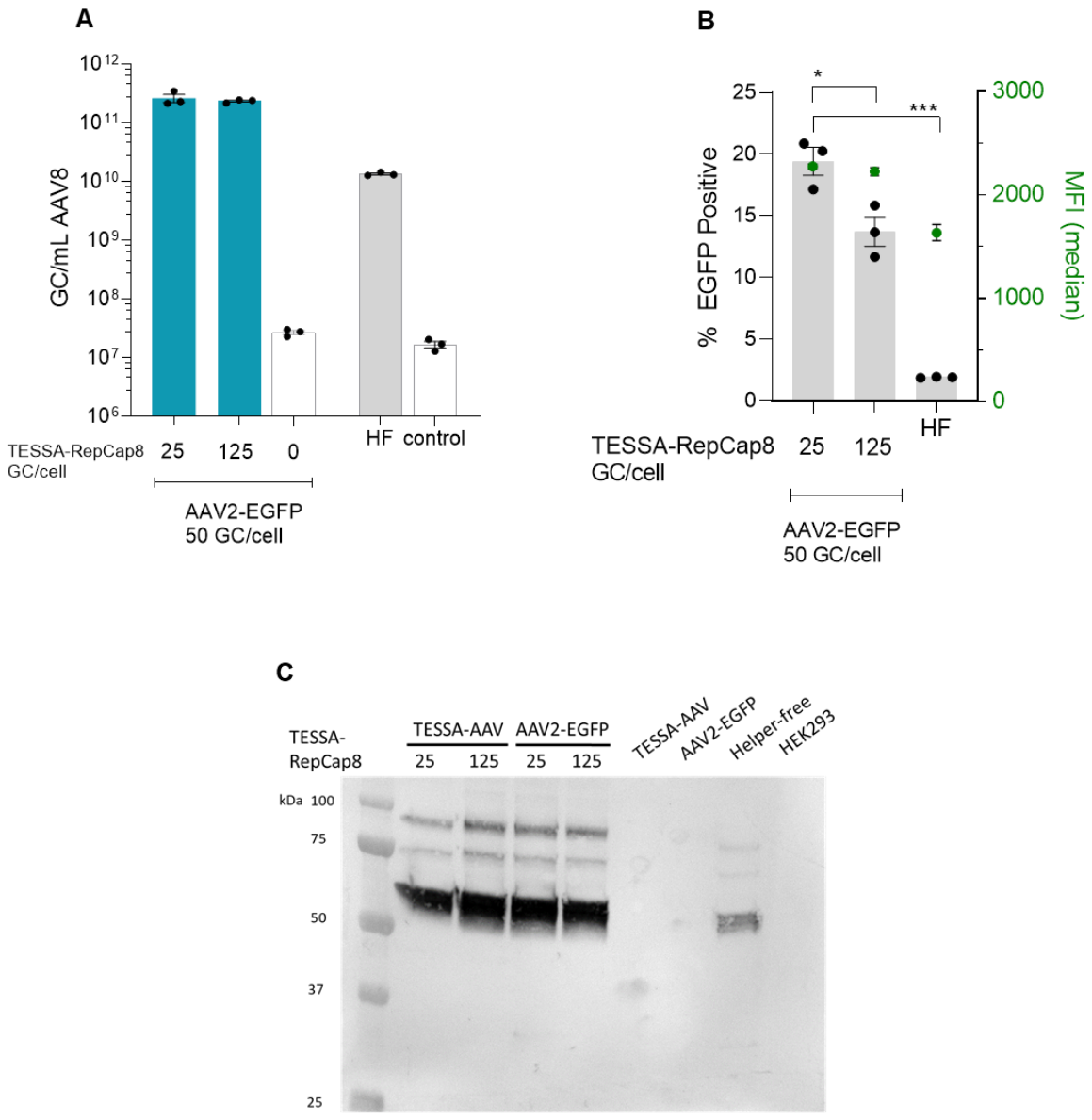


Figure 5.3 Production of rAAV8 vectors via Capside-exchange using TESSA-RepCap8. A) HEK293 cells were co-infected using AAV2-EGFP (derived from helper-free method) at 50GC/cell and TESSA-RepCap8 at the indicated MOI. Productivity is compared to the helper-free process. DNAse resistant particles harvested at 96hpt were quantified by EGFP-specific qPCR. **B**) Infection (at 1:100 volume dilution) of HEK293 cell using rAAV8-EGFP crude preparations. EGFP expression analysed by flow cytometry at 72 hpi. MFI of EGFP positive cells shown on the right axis. Data as N=3, mean ± SEM. Significance determined by the Student's t-test *P≤0.05, ***P≤0.001. **C**) Western blot of AAV8 capsid proteins. Equal amounts of crude preparations (25uL) containing rAAV8-EGFP produced via helper-free method, or co-infection of rAAV2-EGFP (50 GC/cell) or TESSA-AAV-EGFP (25 GC/cell) with TESSA-RepCap8 at the indicated MOI were probed with anti-AAV VP1/2/3 antibody for western blot detection.

5.3.10 Production of rAAV using TESSA-RepCap6-v2

We showed previously that TESSA-RepCap6, wherein Cap6 is expressed from a CMV promoter, exhibited genetic instability at subsequent passages of the vector and eventual loss of cap6 DNA (*Chapter4, Figure 4.15B*). To improve vector stability, TESSA-RepCap6 was reconfigured by the exchange of the CMV promoter for minimal CMV (CuOx6-minCMV) to drive Cap6 expression. This new TESSA-RepCap vector entitled 'TESSA-RepCap6-v2' was constructed and purified by OXGENE.

rAAV6 production from TESSA-RepCap6-v2 was evaluated by co-infection with TESSA-AAV-EGFP (TESSA2.0-AAV6-v2) or rAA2-EGFP particles (capsid-exchange). As shown in **Figure 5.4A**, the helper-free method yielded $5x10^9$ GC/mL of intact rAAV6, while a 20-fold increase in titre was observed from the TESSA2.0 approach which yielded ~$1x10^{11}$ GC/mL. Similarly, high yields were also observed using the capsid-exchange process. Co-infection of rAAV2-EGFP (50 GC/cell) with TESSA-RepCap6-v2, at an MOI of 25 or 125 GC/cell, yielded ~$1x10^{11}$ and $2x10^{11}$ GC/mL of intact rAAV6, respectively. Transduction of rAAV6-EGFP vectors were also assessed in HEK293 cells using crude preparations at a 1:100 volution dilution. As shown in **Figure 5.4B**, analysis of EGFP expression at 72 hpi showed that ~90% of cells were EGFP positive after infection with particles derived from TESSA-RepCap6-v2, while 15% of cells were EGFP positive after infection with sample derived from the helper-free process.

Genetically stability of the cap6 coding sequence within TESSA-RepCap6-v2 was assessed by qPCR. As shown in **Figure 5.4C**, genomic DNA was extracted from purified TESSA-RepCap6-v2 at the indicated serial passages and measured by Cap6 and Hexon-specific qPCR. Cap6 DNA was detected at an equimolar ratio to the virus Hexon coding sequence up to the assessed 7^{th} passage. This result confirmed that while genetic instability was observed from TESSA-RepCap6 (Cap6 is driven from the CMV promoter) from an early 3^{rd} passage, exchange of the CMV for the minimal CMV promoter enables cap6 to be stably maintained in TESSA-RepCap6-v2.

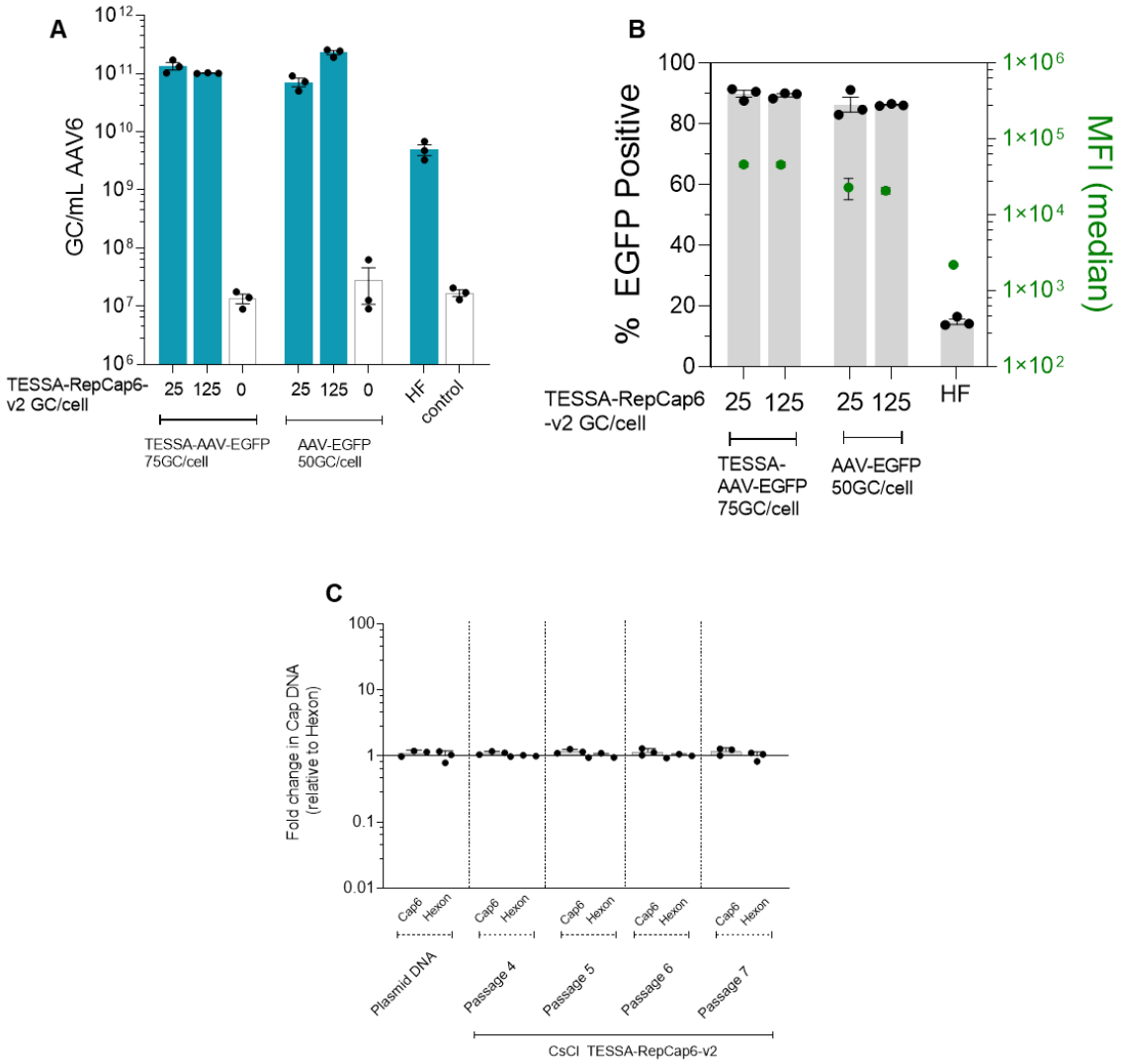


Figure 5.4 Production of AAV6 vectors via TESSA2.0-AAV6 and capsid-exchange method using TESSA-RepCap-v2. A) HEK293 cells were co-infected using TESSA-AAV-EGFP (75 GC/cell) or rAAV2-EGFP (50 GC/cell) with TESSA-RepCap6-v2 at the indicated dose. Productivity is compared to the helper-free process. DNAse resistant particles harvested at 96 hpt were quantified by EGFP-specific qPCR. **B**) Infection (at 1:100 volume dilution) of HEK293 cell using rAAV6-EGFP crude preparations. EGFP expression analysed by flow cytometry at 72hpi. MFI of EGFP positive cells shown on the right axis. Data as N=3, mean ± SEM. **C**) Assessment of Cap6 genetic stability by qPCR. Plasmid DNA or TESSA-RepCap6-v2 vector genomes, amplified to the indicated passages in HEK293 cells and purified using CsCl banding, were quatified using Cap6 and Hexon-specific qPCR. Data presented as fold-change relative to Hexon DNA.

5.4 Chapter discussion

In this chapter, as a proof-of-concept, we explored the propagation of rAAV vectors from particle seed-stock using TESSA-RepCap to create a simple and scalable approach to rAAV manufacture. We found that rAAV2 seed-particles generated from the three different approaches, that include TESSA2.0, TESSA-RepCap2 plus transfection of the pAAV-EGFP genome, or the commonly used helper-free method, were comparably sufficient at delivering the rAAV transfer genome into HEK293 cells for further amplification using TESSA-RepCap. This should enable pre-existing rAAV2 particles to be used as inoculation seed-stocks for further amplification, or seed vectors can be generated at small-scale by helper-free method, or via transfection of the rAAV genome into TESSA-RepCap infected cells, for inoculation of large vessels. A significant advantage of this approach is the relatively low infectious dose of rAAV2 vectors required for inoculation. We showed that at an inoculating dose of rAAV2 at 50 GC/cell, vectors were amplified over 3000-fold per cell using TESSA-RepCap2. Using this capsid-exchange method, we were able to produce $>3x10^{14}$ GC of intact rAAV2 vectors from a 1L stir-tank bioreactor process using suspension HEK293 cells (unpublished data provided by OXGENE).

It is well known that rAAV vectors encapsulate not only the transfer genome, but also contaminant DNA derived from the cell or medium, such as plasmid DNA or helper viruses, that was used in the production process. To reduce oncogenic, immunogenic and infectious risk associated with DNA impurities, guidelines provided by the US Food and Drug Administration (FDA) recommends that residual cellular DNA should be ≤10 ng per vector dose and a median DNA fragment size of <200 bp ("FDA Briefing Document Vaccines and Related Biological Products Advisory Committee Meeting 2012"). In rAAV stocks produced from HEK293 or HeLa-base cells, contaminant DNA mapping to the rep, cap and helper genes, were reported to be present at levels ranging from 0.01% to 0.4% relative to the vector genomes (Martin et al. 2013). However, a more

significant proportion of contaminant DNA is derived from the vector plasmid via reverse packaging, with levels ranging from 2-6% aligning to the antibiotic resistance gene or bacterial origin (Chadeuf et al. 2005). Similar levels of DNA contaminants were also reported from AAV vector stocks derived from the dual-baculovirus/Sf9 cells system (Penaud-Budloo et al. 2017). Several strategies have been explored to reduce the risks associated with reverse packaged DNA contaminants, which include the use of DNA minicircle technology to remove the bacterial backbone from the AAV transfer genome, or by redesigning the vector plasmid to increase its overall size and via insertion of stuffer DNA adjacent to the ITRs (Hauck et al. 2009; Schnodt et al. 2016).

In rAAV production processes using helper adenoviruses (wt or E1/E3-deleted), encapsidation of adenoviral DNA in rAAV particles has not been reported in any literature published to date, to our knowledge. It was suggest that, perhaps, due to the presence of terminal proteins covalently linked to the adenovirus ITRs, incorporation of adenovirus DNA into AAV capsids is expected to occur at low frequencies (Penaud-Budloo et al. 2018). However, by encoding the recombinant AAV genome within TESSA, we observed reverse packaging of adenovirus DNA within AAV particles from our qPCR assays. rAAV vectors derived from TESSA2.0 showed contaminant DNA from the adenovirus packaging sequence at levels of 2-3% relative to the AAV vector genome. Interestingly, by propagating AAV vectors from a single passage using TESSA-RepCap, a significant reduction in contaminant DNA to 0.05% that aligned to the adenovirus packaging signal was observed. It is likely that these contaminant sequences would not contain both terminal AAV ITR sequences, and would likely not replicate as normal during the production process to enable cleaner rAAV stocks.

To extend the AAV propagation approach in producing AAV capsid serotype 5, 6, 8 and 9 we adapted a novel capsid-exchange strategy, as these serotypes infected HEK293 cells less

efficiently than rAAV2 particles. Here, the rAAV transfer genome is first encapsidated in an AAV2 particle, and use alongside TESSA-RepCap5, TESSA-RepCap6, TESSA-RepCap8 or TESSA-RepCap9. While we observed a significant increase in vector yield comparable to the TESSA2.0 system, it can be expected that rAAV2 particles, that failed at cell entry, may be present in the rAAV5, 6, 8 and -9 vector preparations. It remains to be determined the risks associated with these rAAV2 particle remnants, their level will likely be dependent on the quality of the rAAV2 seed-stock used for propagation, such as infectivity and the proportion of empty capsids. For rAAV2 produced using TESSA-RepCap, we observed an almost perfect vector genome to infectivity ratio and ~20% empty particle as determined by TEM imaging. Based upon this assumption, a 3000-fold amplification per rAAV2 vector input would result in less than 0.005% of seed contaminants in output vector preparations.

Possibly, rAAV2 particle contaminants may be further reduced by using AAV serotype-specific affinity resins for purification of the target vector serotype, such as the POROS AAV9 and AAV8 CaptureSelect Affinity matrices (Mietzsch et al. 2020). Further work will explore this, and also the use of AAV2 titration ELISA for accurate quantification rAAV2 particle remnants within AAV5, AAV6 and AAV9 preparations (Grimm et al. 1999). Alternatively, as different AAV serotypes were shown to differ in susceptibility to proteases, fragmentation with various proteases should provide unique patters to enable capsid validation (Van Vliet et al. 2006). Overall, our result suggests that the propagation of AAV strategy using TESSA-RepCap vectors provides a simple and unique approach to manufacture rAAV vectors at scale, but also aid to eliminate DNA contaminants from rAAV vectors, and therefore warrants further exploration.

5.5 Chapter conclusions

1. Propagation of rAAV vectors produced yield and quality of particles comparable to the TESSA2.0 system.
2. Capsid exchange strategy using TESSA-RepCap provides a convenient method for the production of rAAV5, -6, and -9 vectors from rAAV2 particles.
3. rAAV vectors produced from the propagation method using TESSA-RepCap showed reduced DNA contaminants from the reverse packaging process.

Chapter 6

Production of rAAV from stable AAV packaging cell line using TESSA

6.1 Introduction

The AAV replicative life cycle requires the presence of a helper virus, such as adenovirus, to provide essential factors for regulating AAV gene expression and DNA replication (Samulski et al. 1982; Grieger, Soltys, and Samulski 2016). rAAV vectors are derived from the removal of the rep and cap genes in the AAV genome, essential for viral DNA replication and capsid formation, and replacing these with sequences encoding a transgene expression cassette. Only the viral inverted terminal repeats (ITRs) are retained in the transfer vector. These are palindromic sequences that confer a DNA hairpin structure and are required *in cis* for replication and encapsidation of the single-stranded viral genome (Goncalves 2005). While the helper-free method has the crucial advantage of producing rAAV vectors free of contaminating adenovirus particles, important for clinical grade vectors, it is limited by scalability and manufacturing costs (Farson et al. 2004; Xiao, Li, and Samulski 1998). Alternatively, the development of stable packaging/producer cell lines has been explored extensive as a scalable system for high rAAV productivity. In this approach, the rep and cap genes (devoid of viral ITRs) are integrated in the cell's chromosome, typically HeLa and A549-based cell lines, which may contain additional integrations such as the transfer genome (Gao, Lu, et al. 2002; Zhang et al. 2009). Alternatively the transfer vector is delivered by plasmid

transfection or infection with a hybrid Ad-AAV vector, and rAAV production is induced by infection with wt adenoviruses (Fisher et al. 1997). One popular stable packaging cell line is HeLaRC32 cells (Chadeuf et al. 2000; Favre et al. 2001).

Major disadvantages of the mammalian-stable cell line approach for rAAV production include the labour and time requirements to establish and screen high producing packaging/producer clones, and the intricate processes for removal of any adventitious virus (Clark 2002). However, this approach, remains attractive as it offers easy scalability for rAAV production at an industrial level (200-2000 L scale) and is widely pursued. Notably, an AAV1 vector, AAV1-SERCA2a, manufactured from a HeLa-based stable producer cell line was used in phase 2 clinical trials for advanced heart failure (Hulot et al. 2017; Greenberg et al. 2014).

Despite few (~2) integrated copies of AAV rep-cap genes, these stable packaging cells support high titre rAAV production. While the mechanism remains unclear, upon infection with the wt adenovirus the integrated rep and cap genes undergo exponential DNA amplification episomally, with levels reported ranging from 100-1000 copies per cell (Chadeuf et al. 2000). This is thought to be required to express sufficient rep and cap proteins for efficient rAAV production. This episomal amplification effect is crucially dependent on a *cis*-acting replication element (CARE), mapped to the P5 promoter of the rep gene, and requires DNA binding protein (DBP) from adenovirus alongside the Rep protein (Tessier et al. 2001). However, transfection of the Ad genome into these stable packaging cells is unable to induce CARE-dependent amplification, and other adenovirus proteins that play a role in mobilizing the CARE element have never been fully defined (Nony et al. 2001; Clark 2002; Liu et al. 2000).

In this chapter, we explored the use of TESSA as a self-silencing helper virus for the contaminant-free manufacture of rAAV from stable packaging cell line, HeLaRC32. These cells have been used widely for rAAV production and titration of infectious AAV particles. They are stably integrated

with AAV2 rep and cap genes, under transcriptional control of their native p5/p19 and p40 promoters, respectively, but lacks the *cis*-acting left and right AAV ITR sequences. rAAV replication can be achieved in this cell line by providing the rAAV genome *in trans,* via plasmid transfections or infection with intact AAV particles or E1/E3Δ- Ad5 encoding the AAV genome, and infection with a wildtype adenovirus to provide to helper functions, such as the E1A protein to induce AAV gene expression.

As shown in the previous chapters, the TESSA platform enables efficient production of rAAV with minimal Ad vector contaminants, when the AAV rep and cap genes are delivered in HEK293 cells by plasmid transfection or encoded within the TESSA vectors. However, as discussed previously (*Chapter 3, Discussion*), indirect evidence from evaluation of a 100KΔ-mutant Ad helper by Kruger-Haag et al. suggest that this (late) protein may be important for CARE-dependent amplification of AAV genes from these cells, implying that TESSA is likely be unable to induce rAAV production from stable packaging cells except in the presence of doxycycline (Kruger-Haag et al. 2019).

6.2 Chapter aims

1. Construction of a TESSA virus encoding E1 and explore its utility in rAAV production from HeLaRC32 AAV packaging cells
2. Define adenovirus proteins required for mobilizing amplification of AAV rep-cap DNA from HeLaRC32 cells

6.3 Results

6.3.1 Expression from the adenovirus MLP is required for rAAV production from HeLaRC32 stable AAV packaging cell line

To enable rAAV production from HeLaRC32 cells using TESSA or E1/E3Δ-Ad5, we engineered adenovirus E1, required for transactivation of AAV p5 promoter, back into these Ad vectors to create TESSA-E1 and Ad5-E1, respectively. While the E3 genes are still absent from TESSA-E1, the presence of the E1 genes should enable the virus to replicate in non-E1 containing cell lines in the presence of doxycycline. For the construction of TESSA-E1 (schematic shown on **Figure 6.1A**) and the control Ad5-E1, the Ad5 E1 coding sequence was amplified by PCR (primers: appendix 2.4) from plasmid encoding the wildtype Ad5 genome (provided by OXGENE) and inserted into the TESSA and Ad5-E1/E3Δ-Ad5 plasmid linearized with PacI via Snapfast assembly reagent (provided by OXGENE). Positive clones were isolated and screened by restriction digest (**Figure 6.1B**) and used for virus recovery in HEK293 cells. For the recovery and amplification of TESSA-E1 in HEK293 cells, growth media was supplemented with doxycycline 0.5 µg/mL.

To assess rAAV production, HeLaRC32 cells were transfected with the plasmid (pAAV-EGFP) encoding the rAAV transfer genome, and infected with TESSA-E1 or Ad5-E1 at increasing MOI (**Figure 6.1C**). Vectors were harvested 96 hpi and DNAse-resistant particles quantified by EGFP-specific qPCR. While Ad5-E1 (MOI 25 and 50) enabled rAAV production at a range of ~$1x10^9$ GC/mL, with 80% reduction in intact particles when used at a MOI 500, TESSA-E1 failed to support rAAV production with qPCR-background levels comparable to the control HeLaRC32 cells transfected with pAAV-EGFP only. Addition of doxycycline to TESSA-E1 during AAV production in

HELARC32 packaging cells completely restored the rAAV yield, achieving similar levels to those shown using wild type Ad5 helper virus (**Figure 6.1D**). These data suggest that an adenovirus factor(s) that is expressed under transcriptional control of the MLP was necessary for efficient rAAV production from the HeLaRC32 cells.

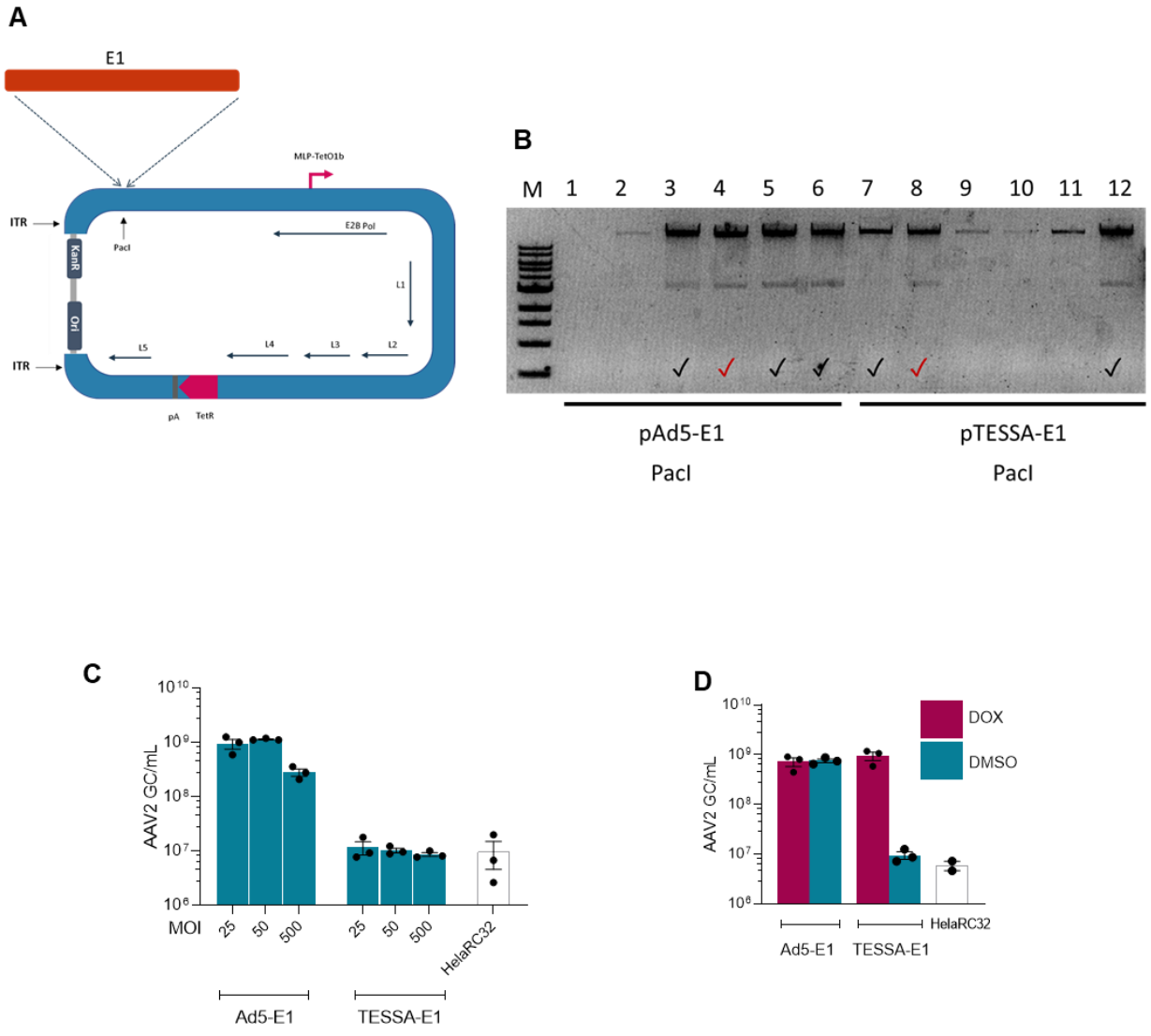


Figure 6.1 Expression from the adenovirus MLP is required to induce AAV production from stable producer cells HeLaRC32. A) cloning schematic for insertion of the E1 sequence into the PacI position of pTESSA. **B**) PacI restriction digest for screening positive clones of pAd5-E1 and pTESSA-E1. **C**) Production of AAV2-EGFP from HeLaRC32 cells. Cells were transfected with the plasmid pAAV-EGFP and infected with Ad5-E1 or TESSA-E1 at the indicated MOI. Vectors were harvested 96 hpi and DNAse-resistant particles quantified by EGFP-specific qPCR. A control for efficiency of DNAse treatment was included wherein cells were transfected with pAAV-EGFP only. **D**) Production of AAV2-EGFP using Ad5-E1 or TESSA-E1 from HeLaRC32 cells cultured with DMSO or doxycycline. HeLaRC32 cells transfected with pAAV-EGFP was infected with Ad5-E1 or TESSA-E1 at an MOI50, and cultured with DMSO or doxycycline 0.5µg/mL. Vectors were harvested and quantified at 96 hpi by EGFP-specific qPCR. Data presented as mean ± SD of triple biological replicates.

6.3.2 Expression from the adenovirus MLP is required to maintain AAV rep and cap DNA amplification from HeLaRC32 AAV packaging cells

As mentioned previously, infection with wt helper adenoviruses in stable AAV packaging cells, including HeLaRC32 cells, was shown to promote 100-1000 fold amplification of the integrated AAV rep-cap genes. We next explored whether the beneficial effect of MLP activation on rAAV production using TESSA-E1 in HeLaRC32 cells was accompanied by episomal amplification of the integrated rep cap gene. HeLaRC32 cells transfected with pAAV-EGFP and infected at an MOI of 50 with Ad5-E1 or TESSA-E1. Cells infected with TESSA-E1 were either supplemented with DMSO or doxycycline, or doxycycline for 16hpi. Total DNA was harvested at 96 hpi and amplified by endpoint PCR (20 cycles) using primers against AAV2 rep and cap. As shown in **Figure 6.2A**, TESSA-E1 in the absence of doxycycline (where the MLP is turned off) there was only a very weak PCR signal detected for both AAV rep (i) and cap (ii), but when doxycycline was added (and the MLP activated) a strong PCR band, for both rep and cap, was detectable and comparable to cells infected with the control Ad5-E1. Furthermore, in TESSA-E1 infected cells and treated with doxycycline for 16 hours, PCR rep and cap bands of intermediate intensity can be observed

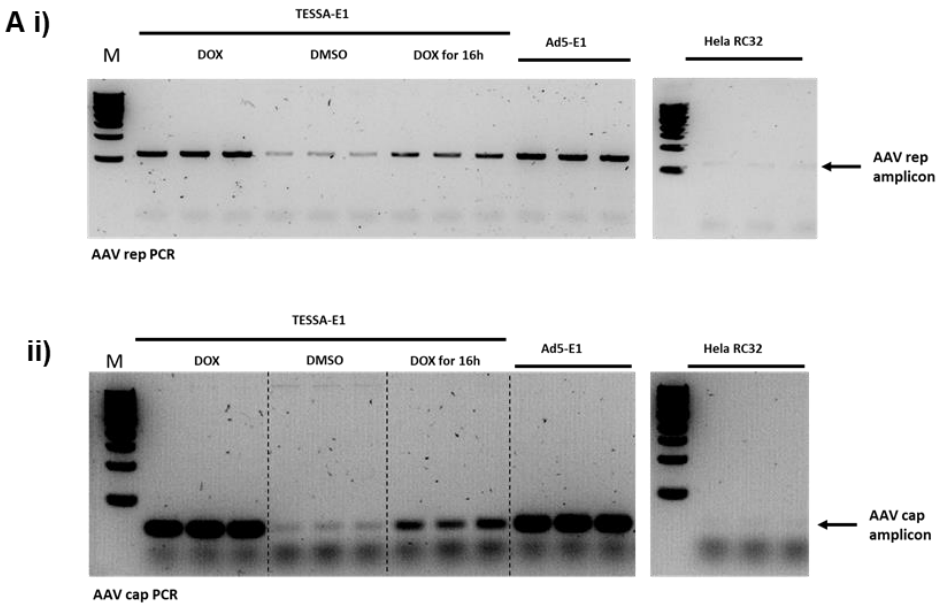
suggesting sustained transcription from the MLP is essential for maintaining cap DNA amplification. These results were confirmed by AAV2 rep and cap specific qPCR (**Figure 6.2B**), which showed over 200-fold amplification of integrated rep (i) and cap (ii) DNA from HeLaRC32 cells following infection with TESSA-E1 in the presence of doxycycline. In the DMSO treated samples, a 2-4 fold increase in rep and cap DNA was observed above none-infected HeLaRC32 cells.

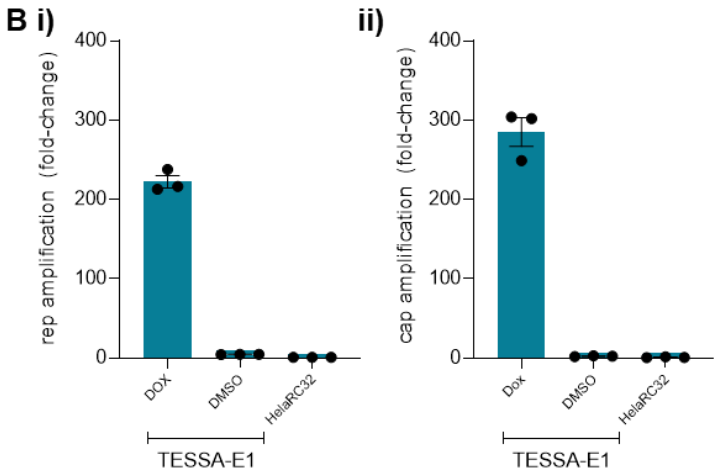
To determine whether the factor(s) restricting the ability of TESSA-E1 to produce rAAV with its MLP repressed in HELARC32 cells were dominant or recessive, different ratios of Ad5-E1 and TESSA-E1 were added for infection of HELARC32 cells at a total MOI of 50. Cells were subsequently transfected with pAAV-EGFP and cultured with DMSO or doxycycline. In the doxycycline group, cells co-infected with Ad5-E1 and TESSA-E1 produced comparable amounts of rAAV2 compared to the Ad5-E1 control as expected (**Figure 6.2C**). However, while cells infected with TESSA-E1 failed to support rAAV production in the absence of doxycycline, production was recovered via co-infection with Ad5-E1, with increasing rAAV2 levels observed by increasing MOI of Ad5-E1. This result suggests that repression of the MLP by TESSA-E1 was not exerting a dominant negative effect on rAAV production from the HeLaRC32 cells.

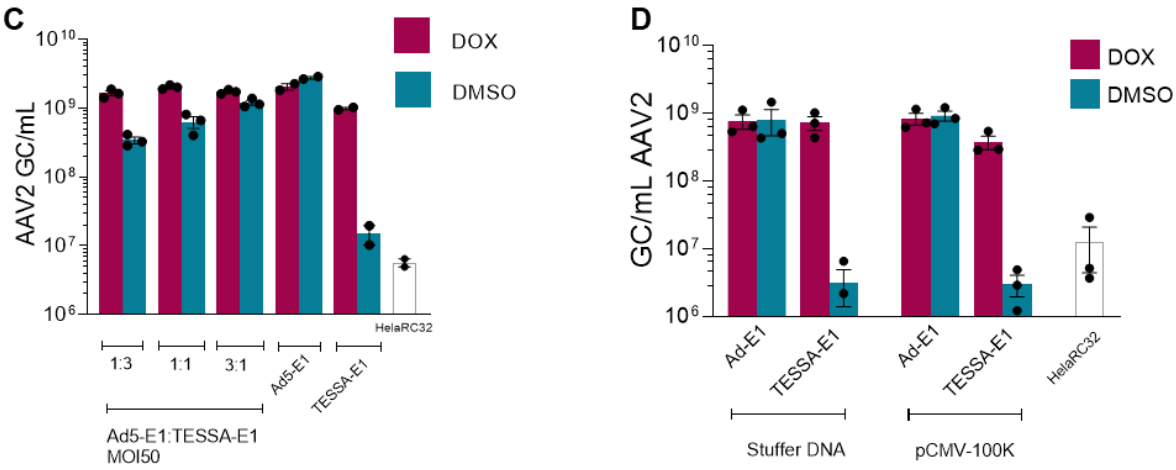
As discussed previously, adenovirus deleted of 810 bp within the 100K gene was unable to efficiently promote amplification of the stably integrated rep-cap genes, and high titre rAAV production from an A549-based stable AAV packaging cell line (Kruger-Haag et al. 2019). As the 100K protein is expressed from the MLP, we assessed whether it comprises the missing 'late' adenovirus protein from TESSA-E1, during MLP repression, that is required to facilitate rep and cap DNA amplification.

To test this, HeLaRC32 cells were co-transfected with pAAV-EGFP and a plasmid expressing the 100K from a CMV promoter or stuffer DNA, and infected with TESSA-E1 or Ad5-E1 at an MOI of

50. As shown in **Figure 6.2D**, transfection with the 100K expression plasmid was unable to recover AAV production from TESSA-E1 in the DMSO treated group. Additionally, this was confirmed by AAV rep and cap-specific qPCR assay which showed that the 100K plasmid was unable to recover rep and cap DNA amplification (**Figure 6.2E i-ii**) using TESSA-E1 in the absence of doxycycline. This suggests that 100K is either not necessary or other factor(s) are required from the MLP to support episomal amplification of AAV rep and cap, and rAAV production from stable AAV packaging cells.




B i)
rep amplification (fold-change)
400
300
200
100
0
DOX
DMSO
HelaRC32
TESSA-E1
ii)
cap amplification (fold-change)
400
300
200
100
0
Dox
DMSO
HelaRC32
TESSA-E1


C
AAV2 GC/mL
10^{10}
10^{9}
10^{8}
10^{7}
10^{6}
DOX
DMSO
HelaRC32
1:3
1:1
3:1
Ad5-E1
TESSA-E1
Ad5-E1:TESSA-E1
MOI50
D
GC/mL AAV2
10^{10}
10^{9}
10^{8}
10^{7}
10^{6}
DOX
DMSO
Ad-E1
TESSA-E1
Ad-E1
TESSA-E1
HelaRC32
Stuffer DNA
pCMV-100K

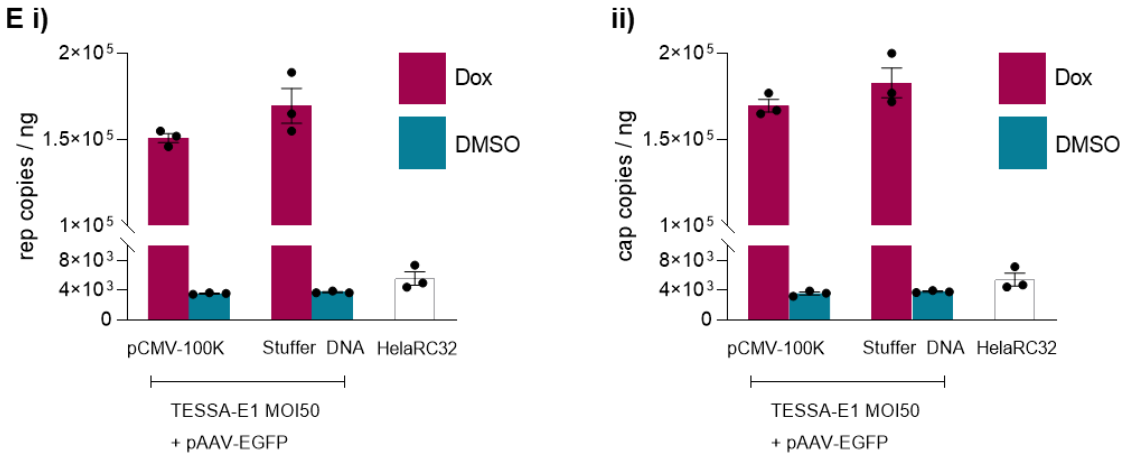

E i)
rep copies / ng
2×10^5
1.5×10^5
1×10^5
8×10^3
4×10^3
0
Dox
DMSO
pCMV-100K
Stuffer DNA
HelaRC32
TESSA-E1 MOI50
+ pAAV-EGFP
ii)
cap copies / ng
2×10^5
1.5×10^5
1×10^5
8×10^3
4×10^3
0
Dox
DMSO
pCMV-100K
Stuffer DNA
HelaRC32
TESSA-E1 MOI50
+ pAAV-EGFP

Figure 6.2 Expression from the adenovirus MLP is required to maintain rep and cap DNA amplification from HeLaRC32 cells. A) Episomal DNA amplification of AAV rep and cap in HeLaRC32 cells. Cells were infected (MOI50) with Ad5-E1 or TESSA-E1 and cultured with DMSO, doxycycline 0.5µg/mL, or doxycycline for 16hpi. Total DNA was extracted 96hpi and used for endpoint PCR (20 cycles) with primers directed against AAV2 rep and cap. Equal amounts of PCR reactions were resolved by gel electrophoresis. Data presented as n=3. **B**) Quantification of AAV rep and cap DNA by qPCR. DNA from HeLaRC32 cells infected (MOI50) with TESSA-E1 and cultured with DMSO or doxycycline 0.5µg/mL were quantified by rep or cap-specific qPCR. Data presented as fold change above none-infected HeLaRC32 cells. Data presented as mean ± SD of triple biological replicates. **C**) Production of rAAV2-EGFP via co-infection of TESSA-E1 with Ad5-E1. HeLaRC32 cells were transfected with pAAV-EGFP and infected (total MOI50) with Ad5-E1, TESSA, or co-infected at the indicated ratio. Cells were supplemented with DMSO or doxycycline 0.5µg/mL and vectors harvested at 96hpi. DNAse resistant particles determined by EGFP-specific qPCR. **D**) Production of rAAV2-EGFP in HeLaRC32 cells transfected with 100K expression plasmid. Cells were co-transfected using pAAV-EGFP with pCMV-100K or stuffer DNA and infected with TESSA-E1 or the control Ad5-E1. DNAse resistant particles were quantified at 96hpi by EGFP-specific qPCR. **E**) Quantification of AAV2 rep and cap in TESSA-E1 infected (MOI50) HeLaRC32 cells that were transfected with the pCMV-100K or stuffer DNA. Total DNA was extracted at 96 hpi and quantified by (i) rep or (ii) cap-specific qPCR. Data presented as copies per ng of DNA. Data presented as mean ± SD of triple biological replicates.

6.3.3 siRNA knockdown of Ad5 E2B recovered rep and cap amplification in TESSA-E1-infected HeLaRC32 cells during MLP repression

As shown previously, adenovirus deleted for the pTP gene is incapable of DNA replication and shows undetectable levels of late mRNAs (Schaack, Guo, and Langer 1996). Specifically, the pTP is essential for initiation of adenovirus genome replication, a prerequisite for activation of the MLP and expression of late virus genes, including the 100K protein. It is therefore intriguing that, while their Ad5-Δ100K was unable to support rep and cap DNA amplification, Kruger-Haag et al. showed that a helper-Ad5 deleted of the pTP (Ad5-ΔpTP) was capable of inducing rep amplification and rAAV production from the stable packaging cells at levels comparable to the wt adenovirus. As the Ad5-ΔpTP virus is unable to induce late infection, these findings are in stark

contrast to our results which suggested a factor(s) expressed from the MLP and the author's Ad5-Δ100K mutant that showed involvement of the 100K protein in this process.

To reconcile this discrepancy, an obvious biological difference between the Ad5-ΔpTP and TESSA-E1 (in the absence of doxycycline) or the Ad5-Δ100K in an ongoing infection in rAAV producer cell lines is the inability of the Ad5-ΔpTP mutant to replicate its DNA. This led us to hypothesize that, perhaps, factor(s) embedded within the major late transcription unit, required for rep and cap DNA amplification in HeLaRC32 cells, may be also expressed at early infection (non-MLP transcribed) but titrated away by binding to the replicating TESSA-E1 or Ad5-Δ100K genomes. In line with this hypothesis, it is possible that repression of the MLP or absence of the 100K protein in TESSA-E1 and Ad5-Δ100K, respectively, resulted in insufficient production of this factor(s) to reach the levels required for supporting CARE-dependent DNA amplification from these rAAV stable packaging cells.

To test this hypothesis, we employed an siRNA strategy to reduce DNA replication of TESSA-E1 by knockdown of the E2B transcription unit which codes for the virus DNA polymerase and pTP (Kneidinger et al. 2012). This should reduce DNA replication of the adenoviral genomes and, if our hypothesis is correct, enable recovery of AAV rep-cap DNA amplification. In this assay, HeLaRC32 cells were transfected with siRNA targeting E2B or non-complementing (NC) scrambled siRNA for 24 hours before transfection with the pAAV-EGFP plasmid and infection with TESSA-E1 or the control Ad5-E1. Cells were subsequently treated with doxycycline or DMSO and total DNA harvested at 72 hpt for qPCR quantification. As expected, up to 4-fold more genomes were detected by Hexon-specific qPCR from cells infected with TESSA-E1 and treated with DMSO compared to the doxycycline-group (**Figure 6.3A**). In both DMSO and doxycycline-group, transfection with the siRNA E2B resulted in a 10-fold reduction in Ad5-E1 genomes compared to NC-siRNA or the none-siRNA control. Significantly reduction in TESSA-E1 genomes were also

achieved from knockdown with E2B siRNA compared to the NC siRNA, with 10- and 30-fold reduction in total genomes in the DMSO and doxycycline-group, respectively. As expected, TESSA-E1 was unable to induce DNA amplification of rep-cap during MLP repressing (DMSO group) in cells transfected with NC-siRNA or in the none-siRNA group, while treatment with doxycycline resulted in over 80-fold increase in rep and cap DNA. Importantly, when measuring amplification of AAV DNA, knockdown with the E2B siRNA resulted in up to 30-fold more rep (**Figure 6.3B**) and cap (**Figure 6.3C**) DNA in HeLaRC32 cells compared to NC- or the non-siRNA group after infection with TESSA-E1 (DMSO-group). While surprising, this finding supports the hypothesis and confirmed that reduction in TESSA-E1 genomes via siRNA knockdown of E2B enabled recovery of CARE-dependent DNA amplification in HeLaRC32 cells. Interestingly, knockdown with E2B siRNA also promoted a 3-fold increase in rep and cap DNA in cells infected with the control Ad5-E1 compare to the NC- or non-siRNA group, suggesting a balance in adenovirus 'helper' functions and genome replication is optimal for amplification of AAV rep and cap DNA.

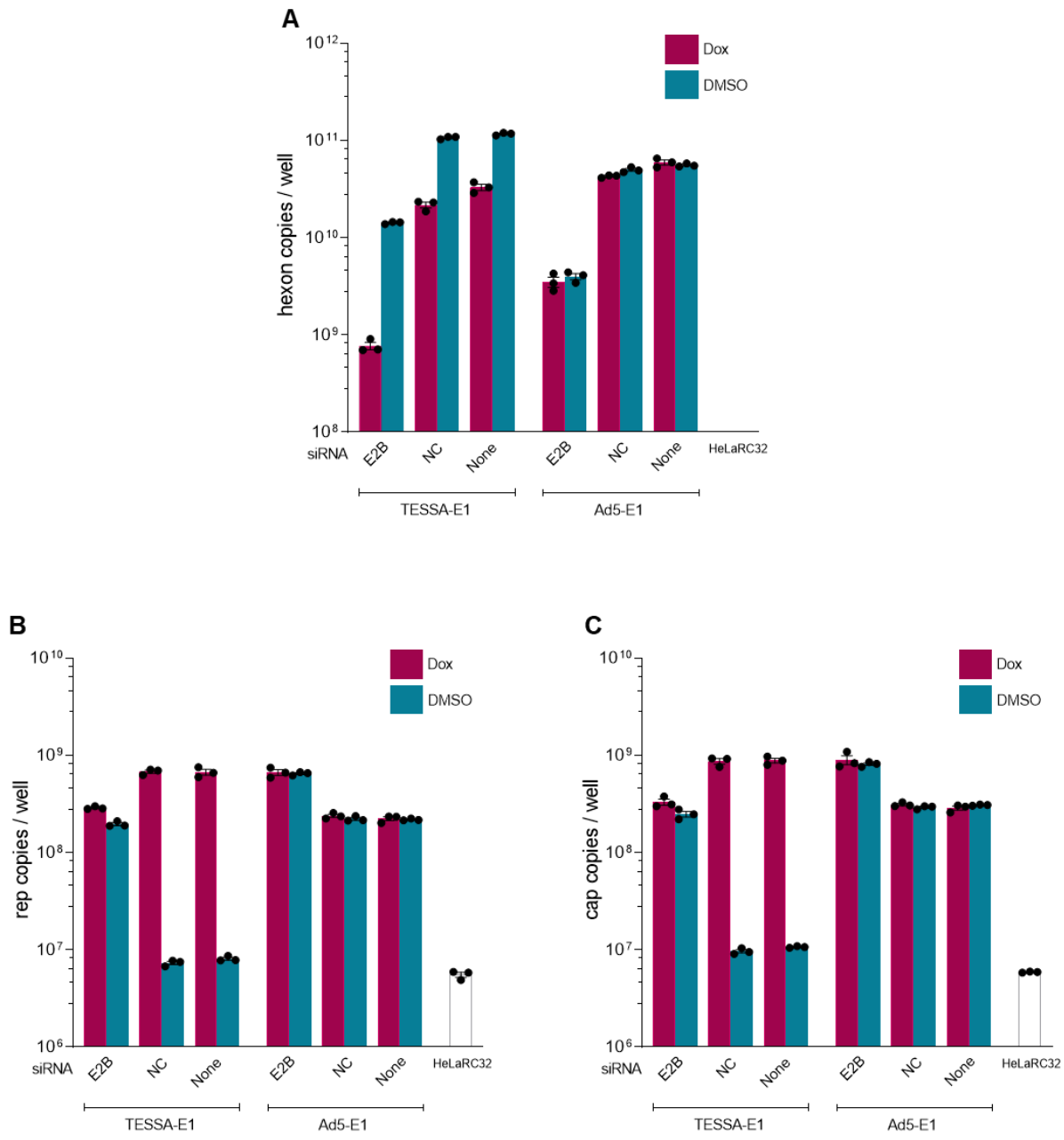


Figure 6.3 siRNA knockdown of Ad5 E2B transcription unit recovered rep and cap amplification in HeLaRC32 cells during MLP repression from TESSA-E1. HeLaRC32 cells transfected with siRNA targeting Ad5 E2B unit, scrambled siRNA (NC) or mock transfection for 24 h, were infected with TESSA-E1 or Ad5-E1 at an MOI of 50 and transfected pAAV-EGFP. Cells were subsequently treated with doxycycline 0.5µg/mL or DMSO. Total DNA was extracted at 72 hpt and quantified by (**A**) hexon, (**B**) AAV2 rep, and (**C**) AAV2 cap-specific qPCR. Data as mean ± SD of triple biological replicates.

6.3.4 Expression of the intermediate & late L4 22/33K unit is required for rAAV production from HelaRC32 cells

Overall, our results indicate that factor(s) embedded in the major late transcription unit, that is expressed both early/intermediate (non-MLP controlled) and late (MLP controlled), was required for rAAV production from HeLaRC32 cells using TESSA-E1. In an attempt to identify this 'CARE-induction' factor(s), we focused on the non-structural 22K and 33K proteins, encoded with the L4 transcription unit, as they are known to be expressed from an intermediate-phase promoter, and also from the MLP at late-phase of infection (Morris, Scott, and Leppard 2010).

To assess involvement of the L4-22K and -33K, we employed a siRNA strategy for knockdown of the different L4 mRNA transcripts. As shown in **Figure 6.4A**, siRNAs were designed for specific targeting of the L4 100K mRNA ('100K A' & '100K B'), an siRNA that targets the mRNA sequences shared between L4-100K, -22K and -33K ('22/33K'), or an siRNA that targets all L4 transcripts including L4 pVIII ('L4 A' and 'L4 B'). HeLaRC32 cells were transfected with NC-siRNA or siRNAs targeting the L4 transcripts for 24 hours before transfection with the pAAV-EGFP genome and infection with TESSA-E1. Cells were subsequently cultured with doxycycline to enable transcription from the MLP and rAAV production. At 72 hpi, total DNA was extracted and quantified by AAV2 rep and cap-specific qPCR. As shown in **Figure 6.4B**, transfection with both siRNA solely targeting the 100K mRNA did not affect amplification of (**i**) rep or (**ii**) cap from the HeLaRC32 cells, with levels comparable to the no siRNA control (~3 $x10^8$ copies per well). In contrast, an over 20-fold decrease in rep and cap DNA was observed from cells transfected with the 22/33K targeting siRNA and infected with TESSA-E1 in presence of doxycycline. Similarly, an approximately 10-fold decrease in AAV DNA was also observed from cells transfected with siRNA L4 A and -B. Several conclusions may be drawn from this strategic siRNA knockdown assay. As both siRNAs targeting the 100K mRNA did not affect the amplification of AAV DNA in the

HeLaRC32 cells, this suggest that the 100K protein may not be essential in this CARE-dependent amplification process. Additionally, as the 22/33K siRNA which targets the sequence shared between the L4-100K, -22K and, -33K mRNA significantly inhibited CARE-dependent amplification, this suggests that the last L4 transcript, L4-pVIII, was not also not involved in this process. L4-22K and/or -33K is likely important for rAAV production from HeLaRC32 cells, as its coding sequence was targeted by 22/33K and the L4 siRNAs, and in each case significantly reducing the amplification of AAV rep-cap DNA.

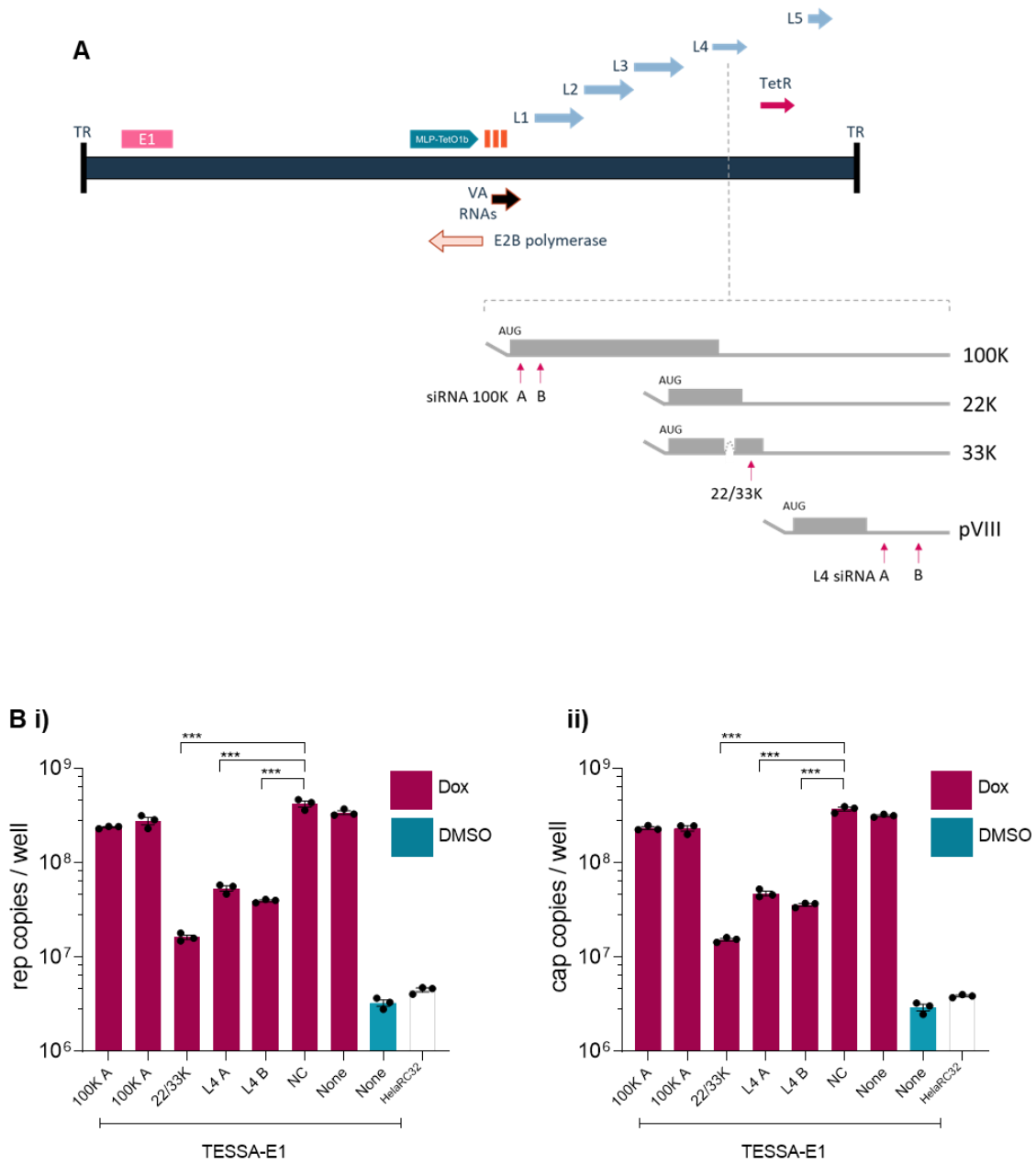


Figure 6.4 Transcription from the L4 unit is important for rAAV production from HelaRC32 cells. A) Genome schematic of TESSA-E1 illustrating the L4 mRNA transcripts and complementary positions for siRNAs 100K A&B, 22/33K, and L4 A&B. Diagram not drawn to scale. **B**) HeLaRC32 cells transfected with the indicated siRNAs for 24 h, were infected with TESSA-E1 at an MOI of 50 and transfected pAAV-EGFP. Cells were subsequently treated with doxycycline 0.5µg/mL or DMSO as indicated. Total DNA was extracted at 72 hpi and quantified by rep and cap-specific qPCR. Data as mean ± SD of triple biological replicates.

6.4 Chapter discussion

While TESSA was fully capable of providing helper functions to enable rAAV production when the rep and cap genes were provided *in trans* via plasmid transfection or from a TESSA vector encoding these genes, we found that during MLP repression, TESSA-E1 was unable to support rep-cap DNA amplification and rAAV production from AAV packaging HeLaRC32 cells. In evaluating life cycle-defective adenoviruses for rAAV production from A549-based stable AAV packaging cells, Kruger-Haag et al showed that while the Ad5-Δ100K was unable to support rAAV production, the Ad5-ΔpTP mutant promoted AAV rep DNA amplification, despite the Ad virus itself unable to undergo DNA replication. As DNA replication of the adenovirus genome is a prerequisite for activation of the MLP and expressing of late viral genes, including the 100K protein, this apparent discrepancy in 'helper' ability between Ad5-ΔpTP and Ad5-Δ100K or TESSA-E1 (during MLP repression) led us to hypothesise that, perhaps, it is the replication of the adenovirus genomes in the latter viruses that hindered CARE-dependent amplification of rep-cap from the HeLaRC32 cells. Indeed, upon siRNA knockdown of the E2B transcription unit, encoding for the virus DNA polymerase and pTP, we were able to recover rep-cap DNA amplification using TESSA-E1. This result, while surprising, confirmed our initial hypothesis and observations that the CARE-induction factor(s), important for this AAV DNA amplification process, was produced both at the early/intermediate and late-infection phases, with the late-phases expressed from the MLP at high levels to support adenovirus and rAAV replication. To elucidate this factor(s), we focused on the L4 unit encoding the 22K and 33K none-structural proteins, as they are reported to be expressed late from the MLP but also from an independent intermediate-phase promoter. We showed by a series of siRNA targeting the L4 mRNAs that the 22K/33K was important, as siRNA targeting these transcripts repressed rep and cap DNA amplification in HeLaRC32 cells by over 20-fold. However, it remains unknown the role of the 22K/33K proteins or how their coding

sequences are involved in amplification of AAV rep-cap from stable producer cells. The L4-22K and -33K proteins, both sharing the first 105 amino acids but differs at the C-terminus, are multifunctional and involved in regulating the expression of early and late adenoviral genes, RNA splicing and the genome encapsidation process (Biasiotto and Akusjarvi 2015). While the L4-22K protein was shown to bind A repeats in the adenovirus packaging signal at a conserved TTTG motif, L4-33K interacts with the IVa2 protein that associates with the packaging domain of the Ad genome and functions as DNA packaging ATPase (Ostapchuk et al. 2006). Interestingly, it was also shown by co-immunoprecipitation assays and confocal-microscopy that the L4-33K protein also co-localizes with adenovirus DBP, which was reported to be essential for rep-cap DNA amplification from AAV packaging cells (Ahi et al. 2015; Tessier et al. 2001).

Taken together, our results suggest a model wherein the L4-22K or/and 33K proteins are important for rep-cap amplification and rAAV production from HeLaRC32 cells but can be titrated away by DNA replication of the adenovirus genomes. Possibly, in the Ad5-ΔpTP virus developed by Kruger-Haag et al, L4-22K/33K proteins are expressed at sufficient levels from its endogenous promoter to support this rAAV production process. However, in the TESSA-E1 and Ad5-Δ100K viruses, replication of the viral genomes coupled with repression of the MLP, and absence of the 100K protein, respectively, results in limited availability of L4-22K/33K at late-infection phase required to support AAV rep-cap amplification.

Further work will explore whether this effect was universal to rAAV stable packaging cells, including those that are based on the A549 cell lines, and whether both L4-22K and 33K are involved by supplying these proteins in *trans*-complementing assays or selective ablation of their expression from TESSA-E1. To enable the use of TESSA-E1 for rAAV production from stable AAV packaging cells, further work will also explore feasibility of repressing DNA replication of the adenovirus by employing shRNA for the E2B transcriptional unit. As mentioned previously a small

RNA, MLP-TSS-sRNA, expressed from the MLP was shown to repress adenovirus DNA replication. Expression of the MLP-TSS-sRNA independently from MLP-TetO1b in TESSA-E1, and using a heterologous promoter, may also provide an alternative strategy for repressing adenoviral genome replication in attempts to recover CARE-dependent amplification.

6.5 Chapter conclusions

1. TESSA-E1 (DMSO) is unable to support rAAV production from HeLaRC32 cells as expression from the MLP is required for episomal amplification of AAV rep-cap
2. siRNA knockdown of the virus E2B transcription unit recovered CARE-dependent amplification of rep-cap from HeLaRC32 cells, suggesting titration of CARE-dependent factor(s) by the adenovirus genomes
3. Adenovirus 100K protein is unlikely to be directly involved, but the CARE-dependent factor(s) may be encoded within the L4 22/33K unit.

Chapter 7

Final Discussion

7.1 Overview of the thesis

AAV is the vector of choice for *in vivo* gene therapy, with two products Luxturna and Zolgensma gaining FDA approval. Additionally, very promising therapies are in advanced development for the treatment of important diseases such as haemophilia A and B, as well as devastating rare genetic disorders such as lysosomal storage diseases (Perrin, Herzog, and Markusic 2019; Li and Samulski 2020). Since many of these treatments are given intravenously the dose requirements for rAAV vectors can be large, this provides a significant hurdle for the cost-effective manufacture of agents for widespread deployment (Bowles et al. 2012; van der Loo and Wright 2016; Miesbach et al. 2018). Recent observations of severe toxicity associated with high-dose rAAV to treat myotubular myopathy and muscular degenerations have also highlighted the need for improving vector potency and free of impurities ('High-dose AAV gene therapy deaths' 2020).

Since its initial development in the late 1990s, the helper-free plasmid transfection method remains the predominant approach for the production of clinical/pre-clinical rAAV vectors (Xiao, Li, and Samulski 1998). However, this system is costly and challenging to scale up. Advancements in rAAV manufacturing platforms have been intermittent. Most notably, mammalian cell lines stably expressing the AAV packaging components and the Baculovirus/Sf9 approach remain actively pursued strategies for scalable production of rAAV (Mietzsch et al. 2017; Martin et al.

2013). Although attractive, each approaches bearing unique advantages as discussed (*Introduction 1.2.6*), significant concerns over contaminants of adventitious viruses and genotoxic impurities from using transformed mammalian cell lines, and particle tropism and transduction efficacies are some of the issues limiting the widespread utility of the stable packaging cell line and Baculovirus/Sf9 approaches, respectively (Penaud-Budloo et al. 2018; Clement and Grieger 2016).

In this thesis, we set out to use rational adenovirus engineering to develop a more efficient method to manufacture rAAV vectors in HEK293 cells that completely avoids the use of plasmid transfection and also avoids adenovirus contamination during this process. We achieved this by inserting a tetracycline TetO site into the adenovirus MLP and encoding TetR under its transcriptional control, creating the TESSA adenoviral vectors in which the MLP is capable of self-repression. We further extended the TESSA platform by encoding both AAV rep and cap. This is the first demonstration of a stable adenovirus expressing both of these genes and required that the rep gene (known to be toxic to adenovirus had no heterologous promoter (Weger et al. 2016; Zhang et al. 2001). We also encoded the rAAV genome within a second TESSA virus, which when combined with TESSA-RepCap, created the TESSA2.0 system. In all cases, the TESSA2.0 platform was shown to yield significant increases in intact rAAV2, -5, -6, -8, -9 vectors of approximately 10-30 fold over the standard helper-free transfection approach. While rAAV5 and rAAV9 display reduced potency, rAAV2 and rAAV6 particles showed over 10-100 fold increase in transduction activity compared to the helper-free derived particles. To reduce manufacturing complexity associated with creating TESSA vectors encoding different rAAV-transgene genomes, we also explored a unique approach to manufacture rAAV vectors by propagating rAAV particles using TESSA-RepCap vectors, including a *trans*-pseudotyping method to generate rAAV-5, -6, -8, and -9 particles from rAAV2. We demonstrated that this approach leads to high yields that are

comparable to the TESSA2.0 system, but has the additional benefit of reducing 'reverse-packaged' illegitimate DNA within rAAV particles.

7.2 Repression of the MLP

TESSA was engineered to contain a negative feedback loop that self-inhibits its own MLP, preventing structural gene expression in the absence of doxycycline. Surprisingly, despite a tendency for transcriptional leakage from TetR regulated systems (Ramos et al. 2005; Chen et al. 2015), encoding the TetR under the MLP gave a self-limiting feedback mechanism that dramatically improves gene expression control. While unclear, it may be that significant repression was achieved by dynamic linking of MLP activity to the level of the TetR transcripts. The more the MLP is active, the more it represses itself. Alternatively, transcription from the MLP is complex and temporally regulated, it may be that binding of the TetR induced a conformational change to the MLP or occluded transcription activators required for full promoter activity. Crucially, the TESSA platform produces extraordinarily low levels of infectious adenovirus contamination during rAAV manufacture, typically 2-15 infectious TESSA particles per mL of total cell lysate. Affinity chromatography commonly employed for purification of rAAV vectors should eliminate any adventitious viruses that may result from the production run or residual particles from the inoculation step, and is currently being explored further in our laboratory (Mietzsch et al. 2020).

As adenovirus capsid proteins are highly immunogenic, their effective removal is essential for cGMP manufacturing (Chirmule et al. 1999). Guidelines for viral vector manufacture and purity specifications are issued in the International Conference on Harmonization (ICH) Q5A report ("Guidance for Industry Q5A Viral Safety Evaluation of Biotechnology Products Derived From Cell

Lines of Human or Animal Origin"). This usually requires a well-characterised inactivation step and, stepwise, orthogonal additive separation step for removal of the relevant virus. In a process established for manufacturing of a clinical-grade rAAV1 product using wt Ad5, clearance of the adventitious virus was ensured by a series of steps that included the capture of the wt Ad5 by ion-exchange chromatography (IEX) from clarified lysates, column capture of the rAAV1 and followed by heat-inactivation of the residual Ad particles. Subsequent steps to purify the rAAV and removal of the wt Ad5 involved further column-chromatography, nanofiltration, and polishing (Thorne et al. 2008). The use of TESSA may circumvent these requirements but remain to be determined, as this strategy enables the production of high-titre rAAV vectors with an unprecedented absence of contaminating adenovirus. TESSA, therefore, has the potential to provide a scalable and cost-effective solution for cGMP manufacture of rAAV.

7.3 Packaging of illegitimate DNA into rAAV

Encapsidation of contaminant DNA in AAV particles during vector production is universal to all production platforms to date (Penaud-Budloo et al. 2018). Genomic DNA fragments from mammalian producer cells detected in purified intact rAAV vectors have been reported at up to 1% of total DNA. However, a substantial portion of DNA contaminants in rAAV particles is derived from sequences directly adjacent to the virus ITR elements and arise from a 'reverse packaging' process (Ayuso et al. 2010). In line with other manufacturing platforms, we found that ~2% of intact rAAV vectors produced from the TESSA2.0 process were shown to contain contaminating DNA sequences mapping to the adenovirus packaging signal, adjacent to the left AAV ITR sequence. These levels were comparable to the amounts of antibiotic sequences in rAAV derived from the helper-free method or mammalian stable cell lines processes which were reported at a

range of 1-6% (Chadeuf et al. 2005; Martin et al. 2013). Similar 2.1% of rAAV derived from of dual-baculovirus/Sf9 platform were also shown to be harbour baculovirus DNA (Penaud-Budloo et al. 2017).

Quality controls assays to determine the level of potential high-risk DNA contaminants, such as antibiotic sequence, are required for AAV-based gene therapy products and risks associated with encapsidation of adenovirus DNA in AAV particles remain to be determined. More recently, a DNA production technology, termed Doggybone^{TM} DNA, that generates covalently closed linear double-stranded DNA constructs using Phi29 DNA polymerase and protelomerase was shown to be capable of producing functional lentiviral vectors from 293 cells (Karda et al. 2019). While it remains to be demonstrated, potentially, Doggybone^{TM} DNA harbouring AAV components may be used for transfection of mammalian cells to generate rAAV vectors free of bacterial DNA sequences. We showed for the first time, to our knowledge, that propagation of rAAV vectors using TESSA-RepCap reduced contaminating Ad DNA to unprecedented levels of ~0.05% of intact vectors. It is likely that TESSA-RepCap vectors can be used to significantly reduce DNA impurities from rAAV stocks, including antibiotic resistance DNA in helper-free derived rAAV, and warrants further exploration. However, a question remains over genetic stability of the rAAV-transgene expression cassette, and compromise of vector potency, at serial passages of the rAAV. Further work will confirm whether errors in viral genome replication and incorporation of truncated or rearranged genomes are increased as a result of rAAV propagation using TESSA-RepCap or from the TESSA2.0 approach. Next-generation sequencing techniques, which include Single-Stranded DNA Virus Sequencing (SSV-seq) and AAV-genome population sequencing (AAV-GPseq) can be used for addressing these issues, but also for characterising DNA impurities within AAV particles (Lecomte et al. 2019; Tai et al. 2018).

7.4 The potency of rAAV from TESSA

AAV infectivity is largely dependent on the capsid composition. VP3 alone is sufficient to form capsomers while the incorporation of VP1 is essential for infectivity. Also, VP2 was shown to be non-essential for AAV infection, and insertion of peptide sequences at its N-terminus has widely been explored in attempts to retarget viral tropism. Surprisingly, whereas rAAV2, -6, and -8 vectors produced from the TESSA2.0 approach or via propagation using TESSA-RepCap showed enhance transduction above the helper-free method, rAAV5 and -9 were less potent. Further work is required to resolve these discrepancies, but in particular, we found that rAAV5 particles derived from TESSA-RepCap5 were shown to have low incorporation of VP1 and VP2 which suggested an imbalance of VP1/VP2/VP3 stoichiometry that hindered particle transduction. Similar challenges in producing highly infectious AAV5 particles, with the canonical 1:1:10 ratio of VP1/VP2/VP3, compared to other AAV capsid serotypes have also been documented for the baculovirus system (Urabe et al. 2006; Mietzsch, Grasse, et al. 2014). More recently, Bosma et al. were able to generate a potent rAAV5 vector from insect cells after extensively screening a library of baculovirus expression vectors encoding AAV5 cap with modulations in the translation-start region of VP1 (Bosma et al. 2018). Possibly, the reduced potency of rAAV5 and rAAV9 produced from TESSA-RepCap may be due to transcription of the cap gene from the CMV promoter or the genetic context surrounding the transcriptional start site, resulting in inaccurate splicing of the Cap mRNA. This is supported by our previous experiments wherein transfection with pRepCap plasmid enabled the production of infectious particles from the TESSA helper, indicating that the low infectivity of rAAV5 and -9 was not the result of insufficient adenovirus helper functions. Future work may involve reconfiguration of the Cap transcription unit relative to the CMV transcription start site or exploration of alternative heterologous promoters. More recently, direct liquid chromatography/mass spectrometry (LC/MS) approaches have been developed for

evaluating the VP ratios at greater resolution, but also for the assessment of post-translational modifications (Jin et al. 2017; Mary et al. 2019). These analytic approaches can be useful to further characterise rAAV produced from TESSA and compare alongside particles derived the helper-free processes.

7.5 Potential applications to TESSA encoding AAV rep and cap

During the evaluation of the TESSA-RepCap vectors, several potential utilities were hypothesised but beyond the scope of this thesis, including the development of a TESSA-based rAAV infectious titration platform and the use of TESSA vectors for the generation of novel AAV capsid libraries. Both of these platforms are currently under investigation in our laboratory.

The first potential use of TESSA relates to accurate titration of infectious rAAV vectors, an analytical criterion essential to determine particle potency and efficacy of AAV-based gene therapy products (Clement and Grieger 2016). Infectivity of rAAV is most commonly determined using the TCID50 assay in HeLa-based stable AAV packaging cell lines, such as HeLaRC32 cells (Zen et al. 2004). Use of replication centre assays (RCA) employing wt Ad and wt AAVs to supply essential genes for inducing replication of the rAAV vectors and detection by DNA probes have also been reported (Francois et al. 2018). While rAAV vector titration by RCA is generally compounded by lack of reproducibility due to the required balance of the two wt viruses AAV and Ad, the TCID50 assay is dependent on a cell line harbouring the AAV rep-cap genes and, therefore, only applicable to AAV capsid serotypes capable of infecting these cells. As wt Ad5 can infect and replicate in numerous tissue types, a TESSA virus (with the E1 genes intact) encoding AAV rep

should provide a valuable tool to induce rAAV replication and quantification of infectious rAAV titres in targeted cells. Co-infection of the rAAV with a TESSA virus expressing AAV rep (as described in this thesis) in a chosen cell line/primary cells should induce amplification of the rAAV genome to enable sensitive detection by qPCR, hybridization with DNA probes, or measurement of transgene expression. Similarly, an rAAV infectivity titration assay utilising a replication-defective Herpes simplex virus (HSV) vector expressing AAV Rep and Cap was described, however, utility of this assay was limited to cells efficiently permissive to HSV infection (Mohiuddin et al. 2005).

The second potential use of TESSA relates to the generation of pooled AAV capsid libraries, a robust methodology for the selection of novel AAV capsids for gene delivery. Commonly, pooled AAV capsid libraries are produced by transfection of a plasmid library of rAAV-genomes encoding rep-cap variants into HEK293 cells. AAV capsid libraries are then purified and subjected to a screening process, *in vivo* or *in vitro,* for the selection of the desired variants. This process may involve multiple rounds of enrichment to select for the desired characteristics that include tissue-specific tropism and antibody neutralization. Such approaches have aided in the generation of numerous novel capsids, including AAVDJ and AAV-PHP.eB that exhibited superior transduction of the liver and central nervous system, respectively, over its parental counterparts (Grimm et al. 2008; Deverman et al. 2016; Colella, Ronzitti, and Mingozzi 2018). However, the quality of AAV capsid libraries is largely dependent on the diversity of variants, lack of capsid mosaicism, and crucially, on the genotype-phenotype linkage of each variant i.e, an rAAV-cap genome is packaged within its' encoded capsid. Capsid mosaicism and loss of genotype-phenotype linkage (termed 'genome cross-packaging') within pooled AAV capsid libraries are commonly reported, hindering the capsid selection process (Schmit et al. 2020; Nonnenmacher et al. 2015). To reduce these occurrences, HEK293 cells are usually transfected with a limited quantity (typically 10 ng per 150 mm dish) of ITR-containing rep-cap plasmid to avoid internalisation of multiple plasmids per cell,

and decreasing the likelihood of multiple capsid variants being expressing within a single cell. However, this approach can still be confounded by cross-packaging and mosaicism, and the generation of a high-titre and diverse library is limited, owing to the inefficiency of transfecting low amounts of plasmid DNA. More recently, efforts to obtain AAV capsids with the desired properties have focused on high-throughput screening via Illumina NGS of barcoded AAV variants (Pekrun et al. 2019). TESSA vectors encoding AAV rep and cap may provide a niche advantage for the generation and screening of AAV capsid libraries. We hypothesised that capsid mosaicism and genome cross-packaging can be eliminated, and a high-diversity AAV library obtained by a 2-step capsid-pseudotyping method using TESSA-RepCap2. In this approach, rAAV genomes encoding cap variants under an inducible promoter, such as cumate-inducible, are first packaged within AAV2 capsids using TESSA-RepCap2. Subsequently, this AAV2 particle library is used to infect HEK293 cells at a low MOI, to ensure that each cell is infected with one genome particle, alongside a TESSA vector expressing Rep and the cTA to enable AAV capsid expression from each rAAV genome. This process should ensure that one library clone per cell is produced if the cap variant is capable of particle formation and genome encapsidation. While this approach is more labour intensive due to the requirements of first generating a library within AAV2 capsids, AAV2 particles derived from TESSA-Repcap2 should enable efficient cell transduction and ensure a highly diverse library with minimal cross-packaging and capsid mosaicism. Possible, TESSA virus expressing AAV rep may also be employed in the capsid selection process, *in vitro* or *in vivo,* to induce rAAV-cap genome replication and aid identification by PCR or NGS. Exploration of this approach in combination with machine learning to design highly diverse AAV capsids is currently being undertaken in our laboratory.

Concluding remarks

The TESSA system offers a superior and scalable strategy for the manufacture of rAAV. The quality of individual AAV particles is similar to those obtained with regular adenovirus helper systems, however, the yields are appreciably higher, possibly reflecting no depletion of cellular resources for production of adenovirus structural proteins. Finally, adenovirus contamination is decreased to trace levels, and even that contaminant is doubly attenuated. TESSA2.0 and the unique capsid-exchange method, therefore, have the potential to provide a scalable and cost-effective solution for the manufacture of AAV vectors for gene transfer.

References

Adam, S. A., and G. Dreyfuss. 1987. 'Adenovirus proteins associated with mRNA and hnRNA in infected HeLa cells', *J Virol*, 61: 3276-83.

Afione, S. A., J. Wang, S. Walsh, W. B. Guggino, and T. R. Flotte. 1999. 'Delayed expression of adeno-associated virus vector DNA', *Intervirology*, 42: 213-20.

Ahi, Y. S., and S. K. Mittal. 2016. 'Components of Adenovirus Genome Packaging', *Front Microbiol*, 7: 1503.

Ahi, Y. S., S. V. Vemula, A. O. Hassan, G. Costakes, C. Stauffacher, and S. K. Mittal. 2015. 'Adenoviral L4 33K forms ring-like oligomers and stimulates ATPase activity of IVa2: implications in viral genome packaging', *Front Microbiol*, 6: 318.

Al-Dosari, M. S., and X. Gao. 2009. 'Nonviral gene delivery: principle, limitations, and recent progress', *AAPS J*, 11: 671-81.

Alazard-Dany, N., A. Nicolas, A. Ploquin, R. Strasser, A. Greco, A. L. Epstein, C. Fraefel, and A. Salvetti. 2009. 'Definition of herpes simplex virus type 1 helper activities for adeno-associated virus early replication events', *PLoS Pathog*, 5: e1000340.

Alba, R., A. Bosch, and M. Chillon. 2005. 'Gutless adenovirus: last-generation adenovirus for gene therapy', *Gene Ther*, 12 Suppl 1: S18-27.

AlDallal, S. M. 2020. 'Yescarta: A New Era for Non-Hodgkin Lymphoma Patients', *Cureus*, 12: e11504.

Ali, S., R. Kjeken, C. Niederlaender, G. Markey, T. S. Saunders, M. Opsata, K. Moltu, B. Bremnes, E. Gronevik, M. Muusse, G. D. Hakonsen, V. Skibeli, M. E. Kalland, I. Wang, I. Buajordet, A. Urbaniak, J. Johnston, K. Rantell, E. Kerwash, M. Schuessler-Lenz, T. Salmonson, J. Bergh, C. Gisselbrecht, K. Tzogani, I. Papadouli, and F. Pignatti. 2020. 'The European Medicines Agency Review of Kymriah (Tisagenlecleucel) for the Treatment of Acute Lymphoblastic Leukemia and Diffuse Large B-Cell Lymphoma', *Oncologist*, 25: e321-e27.

Allen, J. M., D. J. Debelak, T. C. Reynolds, and A. D. Miller. 1997. 'Identification and elimination of replication-competent adeno-associated virus (AAV) that can arise by nonhomologous recombination during AAV vector production', *J Virol*, 71: 6816-22.

Allen, J. M., C. L. Halbert, and A. D. Miller. 2000. 'Improved adeno-associated virus vector production with transfection of a single helper adenovirus gene, E4orf6', *Mol Ther*, 1: 88-95.

Anguela, X. M., and K. A. High. 2019. 'Entering the Modern Era of Gene Therapy', *Annu Rev Med*, 70: 273-88.

Arafat, W. O., J. Gomez-Navarro, J. Xiang, M. N. Barnes, P. Mahasreshti, R. D. Alvarez, G. P. Siegal, A. O. Badib, D. Buchsbaum, D. T. Curiel, and M. A. Stackhouse. 2000. 'An adenovirus encoding proapoptotic Bax induces apoptosis and enhances the radiation effect in human ovarian cancer', *Mol Ther*, 1: 545-54.

Atchison, R. W., B. C. Casto, and W. M. Hammon. 1965. 'Adenovirus-Associated Defective Virus Particles', *Science*, 149: 754-6.

Ayuso, E., F. Mingozzi, J. Montane, X. Leon, X. M. Anguela, V. Haurigot, S. A. Edmonson, L. Africa, S. Zhou, K. A. High, F. Bosch, and J. F. Wright. 2010. 'High AAV vector purity results in serotype- and tissue-independent enhancement of transduction efficiency', *Gene Ther*, 17: 503-10.

Bartlett, J. S., R. Wilcher, and R. J. Samulski. 2000. 'Infectious entry pathway of adeno-associated virus and adeno-associated virus vectors', *J Virol*, 74: 2777-85.

Berk, A. J. 2016. 'Discovery of RNA splicing and genes in pieces', *Proc Natl Acad Sci U S A*, 113: 801-5.

Berkner, K. L., and P. A. Sharp. 1985. 'Effect of the tripartite leader on synthesis of a non-viral protein in an adenovirus 5 recombinant', *Nucleic Acids Res*, 13: 841-57.

Bertram, R., and W. Hillen. 2008. 'The application of Tet repressor in prokaryotic gene regulation and expression', *Microb Biotechnol*, 1: 2-16.

Bett, A. J., L. Prevec, and F. L. Graham. 1993. 'Packaging capacity and stability of human adenovirus type 5 vectors', *J Virol*, 67: 5911-21.

Biasiotto, R., and G. Akusjarvi. 2015. 'Regulation of human adenovirus alternative RNA splicing by the adenoviral L4-33K and L4-22K proteins', *Int J Mol Sci*, 16: 2893-912.

Blaese, R. M., K. W. Culver, A. D. Miller, C. S. Carter, T. Fleisher, M. Clerici, G. Shearer, L. Chang, Y. Chiang, P. Tolstoshev, J. J. Greenblatt, S. A. Rosenberg, H. Klein, M. Berger, C. A. Mullen, W. J. Ramsey, L. Muul, R. A. Morgan, and W. F. Anderson. 1995. 'T lymphocyte-directed gene therapy for ADA- SCID: initial trial results after 4 years', *Science*, 270: 475-80.

Blessing, D., N. Deglon, and B. L. Schneider. 2018. 'Scalable Production and Purification of Adeno-Associated Viral Vectors (AAV)', *Methods Mol Biol*, 1850: 259-74.

Bochkov, Y. A., and A. C. Palmenberg. 2006. 'Translational efficiency of EMCV IRES in bicistronic vectors is dependent upon IRES sequence and gene location', *Biotechniques*, 41: 283-4, 86, 88 passim.

Booth, M. J., A. Mistry, X. Li, A. Thrasher, and R. S. Coffin. 2004. 'Transfection-free and scalable recombinant AAV vector production using HSV/AAV hybrids', *Gene Ther*, 11: 829-37.

Bosma, B., F. du Plessis, E. Ehlert, B. Nijmeijer, M. de Haan, H. Petry, and J. Lubelski. 2018. 'Optimization of viral protein ratios for production of rAAV serotype 5 in the baculovirus system', *Gene Ther*, 25: 415-24.

Boulaiz, H., J. A. Marchal, J. Prados, C. Melguizo, and A. Aranega. 2005. 'Non-viral and viral vectors for gene therapy', *Cell Mol Biol (Noisy-le-grand)*, 51: 3-22.

Boutin, S., V. Monteilhet, P. Veron, C. Leborgne, O. Benveniste, M. F. Montus, and C. Masurier. 2010. 'Prevalence of serum IgG and neutralizing factors against adeno-associated virus (AAV) types 1, 2, 5, 6, 8, and 9 in the healthy population: implications for gene therapy using AAV vectors', *Hum Gene Ther*, 21: 704-12.

Bowles, D. E., S. W. McPhee, C. Li, S. J. Gray, J. J. Samulski, A. S. Camp, J. Li, B. Wang, P. E. Monahan, J. E. Rabinowitz, J. C. Grieger, L. Govindasamy, M. Agbandje-McKenna, X. Xiao, and R. J. Samulski. 2012. 'Phase 1 gene therapy for Duchenne muscular dystrophy using a translational optimized AAV vector', *Mol Ther*, 20: 443-55.

Brenkman, A. B., E. C. Breure, and P. C. van der Vliet. 2002. 'Molecular architecture of adenovirus DNA polymerase and location of the protein primer', *J Virol*, 76: 8200-7.

Brunet, L. J., L. E. Babiss, C. S. Young, and D. R. Mills. 1987. 'Mutations in the adenovirus major late promoter: effects on viability and transcription during infection', *Mol Cell Biol*, 7: 1091-100.

Bryant, L. M., D. M. Christopher, A. R. Giles, C. Hinderer, J. L. Rodriguez, J. B. Smith, E. A. Traxler, J. Tycko, A. P. Wojno, and J. M. Wilson. 2013. 'Lessons learned from the clinical development and market authorization of Glybera', *Hum Gene Ther Clin Dev*, 24: 55-64.

Bulaklak, K., and C. A. Gersbach. 2020. 'The once and future gene therapy', *Nat Commun*, 11: 5820.

Bulcha, J. T., Y. Wang, H. Ma, P. W. L. Tai, and G. Gao. 2021. 'Viral vector platforms within the gene therapy landscape', *Signal Transduct Target Ther*, 6: 53.

Buller, R. E., M. S. Shahin, J. A. Horowitz, I. B. Runnebaum, V. Mahavni, S. Petrauskas, R. Kreienberg, B. Karlan, D. Slamon, and M. Pegram. 2002. 'Long term follow-up of patients with recurrent ovarian cancer after Ad p53 gene replacement with SCH 58500', *Cancer Gene Ther*, 9: 567-72.

Capella, C., M. J. Beltejar, C. Brown, V. Fong, W. Daddacha, B. Kim, and S. Dewhurst. 2012. 'Selective modification of adenovirus replication can be achieved through rational mutagenesis of the adenovirus type 5 DNA polymerase', *J Virol*, 86: 10484-93.

Caravokyri, C., and K. N. Leppard. 1996. 'Human adenovirus type 5 variants with sequence alterations flanking the E2A gene: effects on E2 expression and DNA replication', *Virus Genes*, 12: 65-75.

Carlson, C. A., D. M. Shayakhmetov, and A. Lieber. 2002. 'An adenoviral expression system for AAV rep78 using homologous recombination', *Mol Ther*, 6: 91-8.

Carter, T. H., and H. S. Ginsberg. 1976. 'Viral transcription in KB cells infected by temperature-sensitive "early" mutants of adenovirus type 5', *J Virol*, 18: 156-66.

Casper, J. M., J. M. Timpe, J. D. Dignam, and J. P. Trempe. 2005. 'Identification of an adeno-associated virus Rep protein binding site in the adenovirus E2a promoter', *J Virol*, 79: 28-38.
Casto, B. C., R. W. Atchison, and W. M. Hammon. 1967. 'Studies on the relationship between adeno-associated virus type I (AAV-1) and adenoviruses. I. Replication of AAV-1 in certain cell cultures and its effect on helper adenovirus', *Virology*, 32: 52-9.
Cawood, R., H. H. Chen, F. Carroll, M. Bazan-Peregrino, N. van Rooijen, and L. W. Seymour. 2009. 'Use of tissue-specific microRNA to control pathology of wild-type adenovirus without attenuation of its ability to kill cancer cells', *PLoS Pathog*, 5: e1000440.
Cervelli, T., A. Backovic, and A. Galli. 2011. 'Formation of AAV single stranded DNA genome from a circular plasmid in Saccharomyces cerevisiae', *PLoS One*, 6: e23474.
Chadeuf, G., C. Ciron, P. Moullier, and A. Salvetti. 2005. 'Evidence for encapsidation of prokaryotic sequences during recombinant adeno-associated virus production and their in vivo persistence after vector delivery', *Mol Ther*, 12: 744-53.
Chadeuf, G., D. Favre, J. Tessier, N. Provost, P. Nony, J. Kleinschmidt, P. Moullier, and A. Salvetti. 2000. 'Efficient recombinant adeno-associated virus production by a stable rep-cap HeLa cell line correlates with adenovirus-induced amplification of the integrated rep-cap genome', *J Gene Med*, 2: 260-8.
Chang, L. S., and T. Shenk. 1990. 'The adenovirus DNA-binding protein stimulates the rate of transcription directed by adenovirus and adeno-associated virus promoters', *J Virol*, 64: 2103-9.
Chao, R., Y. Yuan, and H. Zhao. 2015. 'Recent advances in DNA assembly technologies', *FEMS Yeast Res*, 15: 1-9.
Chejanovsky, N., and B. J. Carter. 1989. 'Mutagenesis of an AUG codon in the adeno-associated virus rep gene: effects on viral DNA replication', *Virology*, 173: 120-8.
Chen, H., D. Wang, R. Xia, Q. Mao, and H. Xia. 2015. 'A novel adenoviral vector carrying an all-in-one Tet-On system with an autoregulatory loop for tight, inducible transgene expression', *BMC Biotechnol*, 15: 4.
Chiorini, J. A., F. Kim, L. Yang, and R. M. Kotin. 1999. 'Cloning and characterization of adeno-associated virus type 5', *J Virol*, 73: 1309-19.
Chiorini, J. A., S. M. Wiener, L. Yang, R. H. Smith, B. Safer, N. P. Kilcoin, Y. Liu, E. Urcelay, and R. M. Kotin. 1996. 'The roles of AAV Rep proteins in gene expression and targeted integration', *Curr Top Microbiol Immunol*, 218: 25-33.
Chiorini, J. A., L. Yang, Y. Liu, B. Safer, and R. M. Kotin. 1997. 'Cloning of adeno-associated virus type 4 (AAV4) and generation of recombinant AAV4 particles', *J Virol*, 71: 6823-33.
Chirmule, N., K. Propert, S. Magosin, Y. Qian, R. Qian, and J. Wilson. 1999. 'Immune responses to adenovirus and adeno-associated virus in humans', *Gene Ther*, 6: 1574-83.
Choudhry, A., J. Mathena, J. D. Albano, M. Yacovone, and L. Collins. 2016. 'Safety evaluation of adenovirus type 4 and type 7 vaccine live, oral in military recruits', *Vaccine*, 34: 4558-64.
Clark, K. R. 2002. 'Recent advances in recombinant adeno-associated virus vector production', *Kidney Int*, 61: S9-15.
Clark, K. R., F. Voulgaropoulou, D. M. Fraley, and P. R. Johnson. 1995. 'Cell lines for the production of recombinant adeno-associated virus', *Hum Gene Ther*, 6: 1329-41.
Clement, N., and J. C. Grieger. 2016. 'Manufacturing of recombinant adeno-associated viral vectors for clinical trials', *Mol Ther Methods Clin Dev*, 3: 16002.
Cohen, C. J., J. T. Shieh, R. J. Pickles, T. Okegawa, J. T. Hsieh, and J. M. Bergelson. 2001. 'The coxsackievirus and adenovirus receptor is a transmembrane component of the tight junction', *Proc Natl Acad Sci U S A*, 98: 15191-6.
Colella, P., G. Ronzitti, and F. Mingozzi. 2018. 'Emerging Issues in AAV-Mediated In Vivo Gene Therapy', *Mol Ther Methods Clin Dev*, 8: 87-104.

Condezo, G. N., R. Marabini, S. Ayora, J. M. Carazo, R. Alba, M. Chillon, and C. San Martin. 2015. 'Structures of Adenovirus Incomplete Particles Clarify Capsid Architecture and Show Maturation Changes of Packaging Protein L1 52/55k', *J Virol*, 89: 9653-64.

Conway, J. E., C. M. Rhys, I. Zolotukhin, S. Zolotukhin, N. Muzyczka, G. S. Hayward, and B. J. Byrne. 1999. 'High-titer recombinant adeno-associated virus production utilizing a recombinant herpes simplex virus type I vector expressing AAV-2 Rep and Cap', *Gene Ther*, 6: 986-93.

Cournoyer, D., and C. T. Caskey. 1990. 'Gene transfer into humans: a first step', *N Engl J Med*, 323: 601-3.

Culver, K. W., W. F. Anderson, and R. M. Blaese. 1991. 'Lymphocyte gene therapy', *Hum Gene Ther*, 2: 107-9.

Danthinne, X., and M. J. Imperiale. 2000. 'Production of first generation adenovirus vectors: a review', *Gene Ther*, 7: 1707-14.

Das, A. T., L. Tenenbaum, and B. Berkhout. 2016. 'Tet-On Systems For Doxycycline-inducible Gene Expression', *Curr Gene Ther*, 16: 156-67.

Daya, S., and K. I. Berns. 2008. 'Gene therapy using adeno-associated virus vectors', *Clin Microbiol Rev*, 21: 583-93.

Daya, S., N. Cortez, and K. I. Berns. 2009. 'Adeno-associated virus site-specific integration is mediated by proteins of the nonhomologous end-joining pathway', *J Virol*, 83: 11655-64.

de Jong, R. N., P. C. van der Vliet, and A. B. Brenkman. 2003. 'Adenovirus DNA replication: protein priming, jumping back and the role of the DNA binding protein DBP', *Curr Top Microbiol Immunol*, 272: 187-211.

de Oliveira, A. P., and C. Fraefel. 2010. 'Herpes simplex virus type 1/adeno-associated virus hybrid vectors', *Open Virol J*, 4: 109-22.

Deuschle, U., W. K. Meyer, and H. J. Thiesen. 1995. 'Tetracycline-reversible silencing of eukaryotic promoters', *Mol Cell Biol*, 15: 1907-14.

Deverman, B. E., P. L. Pravdo, B. P. Simpson, S. R. Kumar, K. Y. Chan, A. Banerjee, W. L. Wu, B. Yang, N. Huber, S. P. Pasca, and V. Gradinaru. 2016. 'Cre-dependent selection yields AAV variants for widespread gene transfer to the adult brain', *Nat Biotechnol*, 34: 204-9.

Di Pasquale, G., and J. A. Chiorini. 2006. 'AAV transcytosis through barrier epithelia and endothelium', *Mol Ther*, 13: 506-16.

Di Pasquale, G., B. L. Davidson, C. S. Stein, I. Martins, D. Scudiero, A. Monks, and J. A. Chiorini. 2003. 'Identification of PDGFR as a receptor for AAV-5 transduction', *Nat Med*, 9: 1306-12.

Dingermann, T., U. Frank-Stoll, H. Werner, A. Wissmann, W. Hillen, M. Jacquet, and R. Marschalek. 1992. 'RNA polymerase III catalysed transcription can be regulated in Saccharomyces cerevisiae by the bacterial tetracycline repressor-operator system', *EMBO J*, 11: 1487-92.

Donovan-Banfield, I., A. S. Turnell, J. A. Hiscox, K. N. Leppard, and D. A. Matthews. 2020. 'Deep splicing plasticity of the human adenovirus type 5 transcriptome drives virus evolution', *Commun Biol*, 3: 124.

Douar, A. M., K. Poulard, D. Stockholm, and O. Danos. 2001. 'Intracellular trafficking of adeno-associated virus vectors: routing to the late endosomal compartment and proteasome degradation', *J Virol*, 75: 1824-33.

Duan, D., Q. Li, A. W. Kao, Y. Yue, J. E. Pessin, and J. F. Engelhardt. 1999. 'Dynamin is required for recombinant adeno-associated virus type 2 infection', *J Virol*, 73: 10371-6.

Dudek, A. M., S. Pillay, A. S. Puschnik, C. M. Nagamine, F. Cheng, J. Qiu, J. E. Carette, and L. H. Vandenberghe. 2018. 'An Alternate Route for Adeno-associated Virus (AAV) Entry Independent of AAV Receptor', *J Virol*, 92.

Eaton, R. W. 1997. 'p-Cymene catabolic pathway in Pseudomonas putida F1: cloning and characterization of DNA encoding conversion of p-cymene to p-cumate', *J Bacteriol*, 179: 3171-80.

Ellis, B. L., M. L. Hirsch, J. C. Barker, J. P. Connelly, R. J. Steininger, 3rd, and M. H. Porteus. 2013. 'A survey of ex vivo/in vitro transduction efficiency of mammalian primary cells and cell lines

with Nine natural adeno-associated virus (AAV1-9) and one engineered adeno-associated virus serotype', *Virol J*, 10: 74.
Emmerling, V. V., A. Pegel, E. G. Milian, A. Venereo-Sanchez, M. Kunz, J. Wegele, A. A. Kamen, S. Kochanek, and M. Hoerer. 2016. 'Rational plasmid design and bioprocess optimization to enhance recombinant adeno-associated virus (AAV) productivity in mammalian cells', *Biotechnol J*, 11: 290-7.
Enomoto, T., J. H. Lichy, J. E. Ikeda, and J. Hurwitz. 1981. 'Adenovirus DNA replication in vitro: purification of the terminal protein in a functional form', *Proc Natl Acad Sci U S A*, 78: 6779-83.
Erles, K., P. Sebokova, and J. R. Schlehofer. 1999. 'Update on the prevalence of serum antibodies (IgG and IgM) to adeno-associated virus (AAV)', *J Med Virol*, 59: 406-11.
Evans, J. D., and P. Hearing. 2003. 'Distinct roles of the Adenovirus E4 ORF3 protein in viral DNA replication and inhibition of genome concatenation', *J Virol*, 77: 5295-304.
Farley, D. C., J. L. Brown, and K. N. Leppard. 2004. 'Activation of the early-late switch in adenovirus type 5 major late transcription unit expression by L4 gene products', *J Virol*, 78: 1782-91.
Farson, D., T. C. Harding, L. Tao, J. Liu, S. Powell, V. Vimal, S. Yendluri, K. Koprivnikar, K. Ho, C. Twitty, P. Husak, A. Lin, R. O. Snyder, and B. A. Donahue. 2004. 'Development and characterization of a cell line for large-scale, serum-free production of recombinant adeno-associated viral vectors', *J Gene Med*, 6: 1369-81.
Favre, D., N. Provost, V. Blouin, G. Blancho, Y. Cherel, A. Salvetti, and P. Moullier. 2001. 'Immediate and long-term safety of recombinant adeno-associated virus injection into the nonhuman primate muscle', *Mol Ther*, 4: 559-66.
"FDA Briefing Document Vaccines and Related Biological Products Advisory Committee Meeting 2012." In., 30.
Fessler, S. P., and C. S. Young. 1998. 'Control of adenovirus early gene expression during the late phase of infection', *J Virol*, 72: 4049-56.
Finer, M., and J. Glorioso. 2017. 'A brief account of viral vectors and their promise for gene therapy', *Gene Ther*, 24: 1-2.
Fisher, K. J., K. Jooss, J. Alston, Y. Yang, S. E. Haecker, K. High, R. Pathak, S. E. Raper, and J. M. Wilson. 1997. 'Recombinant adeno-associated virus for muscle directed gene therapy', *Nat Med*, 3: 306-12.
Fisher, K. J., W. M. Kelley, J. F. Burda, and J. M. Wilson. 1996. 'A novel adenovirus-adeno-associated virus hybrid vector that displays efficient rescue and delivery of the AAV genome', *Hum Gene Ther*, 7: 2079-87.
Flotte, T. R., and K. I. Berns. 2005. 'Adeno-associated virus: a ubiquitous commensal of mammals', *Hum Gene Ther*, 16: 401-7.
Francois, A., M. Bouzelha, E. Lecomte, F. Broucque, M. Penaud-Budloo, O. Adjali, P. Moullier, V. Blouin, and E. Ayuso. 2018. 'Accurate Titration of Infectious AAV Particles Requires Measurement of Biologically Active Vector Genomes and Suitable Controls', *Mol Ther Methods Clin Dev*, 10: 223-36.
Friedmann, T. 1992. 'A brief history of gene therapy', *Nat Genet*, 2: 93-8.
Frohberg, C., L. Heins, and C. Gatz. 1991. 'Characterization of the interaction of plant transcription factors using a bacterial repressor protein', *Proc Natl Acad Sci U S A*, 88: 10470-4.
Fu, X., W. C. Chen, C. Argento, P. Clarner, V. Bhatt, R. Dickerson, G. Bou-Assaf, M. Bakhshayeshi, X. Lu, S. Bergelson, and J. Pieracci. 2019. 'Analytical Strategies for Quantification of Adeno-Associated Virus Empty Capsids to Support Process Development', *Hum Gene Ther Methods*, 30: 144-52.
Gaggar, A., D. M. Shayakhmetov, and A. Lieber. 2003. 'CD46 is a cellular receptor for group B adenoviruses', *Nat Med*, 9: 1408-12.
Gallimore, P. H., and A. S. Turnell. 2001. 'Adenovirus E1A: remodelling the host cell, a life or death experience', *Oncogene*, 20: 7824-35.

Gao, G. P., M. R. Alvira, L. Wang, R. Calcedo, J. Johnston, and J. M. Wilson. 2002. 'Novel adeno-associated viruses from rhesus monkeys as vectors for human gene therapy', *Proc Natl Acad Sci U S A*, 99: 11854-9.

Gao, G. P., F. Lu, J. C. Sanmiguel, P. T. Tran, Z. Abbas, K. S. Lynd, J. Marsh, N. B. Spinner, and J. M. Wilson. 2002. 'Rep/Cap gene amplification and high-yield production of AAV in an A549 cell line expressing Rep/Cap', *Mol Ther*, 5: 644-9.

Gao, G. P., Y. Yang, and J. M. Wilson. 1996. 'Biology of adenovirus vectors with E1 and E4 deletions for liver-directed gene therapy', *J Virol*, 70: 8934-43.

Gatz, C., and P. H. Quail. 1988. 'Tn10-encoded tet repressor can regulate an operator-containing plant promoter', *Proc Natl Acad Sci U S A*, 85: 1394-7.

Gaydos, C. A., and J. C. Gaydos. 1995. 'Adenovirus vaccines in the U.S. military', *Mil Med*, 160: 300-4.

Ghebremedhin, B. 2014. 'Human adenovirus: Viral pathogen with increasing importance', *Eur J Microbiol Immunol (Bp)*, 4: 26-33.

Goncalves, G. A. R., and R. M. A. Paiva. 2017. 'Gene therapy: advances, challenges and perspectives', *Einstein (Sao Paulo)*, 15: 369-75.

Goncalves, M. A. 2005. 'Adeno-associated virus: from defective virus to effective vector', *Virol J*, 2: 43.

Gossen, M., and H. Bujard. 1992. 'Tight control of gene expression in mammalian cells by tetracycline-responsive promoters', *Proc Natl Acad Sci U S A*, 89: 5547-51.

Goverdhana, S., M. Puntel, W. Xiong, J. M. Zirger, C. Barcia, J. F. Curtin, E. B. Soffer, S. Mondkar, G. D. King, J. Hu, S. A. Sciascia, M. Candolfi, D. S. Greengold, P. R. Lowenstein, and M. G. Castro. 2005. 'Regulatable gene expression systems for gene therapy applications: progress and future challenges', *Mol Ther*, 12: 189-211.

Gowing, G., S. Svendsen, and C. N. Svendsen. 2017. 'Ex vivo gene therapy for the treatment of neurological disorders', *Prog Brain Res*, 230: 99-132.

Gray, J. T., and S. Zolotukhin. 2011. 'Design and construction of functional AAV vectors', *Methods Mol Biol*, 807: 25-46.

Greber, U. F. 2020. 'Adenoviruses - Infection, pathogenesis and therapy', *FEBS Lett*, 594: 1818-27.

Greenberg, B., A. Yaroshinsky, K. M. Zsebo, J. Butler, G. M. Felker, A. A. Voors, J. J. Rudy, K. Wagner, and R. J. Hajjar. 2014. 'Design of a phase 2b trial of intracoronary administration of AAV1/SERCA2a in patients with advanced heart failure: the CUPID 2 trial (calcium up-regulation by percutaneous administration of gene therapy in cardiac disease phase 2b)', *JACC Heart Fail*, 2: 84-92.

Grieger, J. C., S. M. Soltys, and R. J. Samulski. 2016. 'Production of Recombinant Adeno-associated Virus Vectors Using Suspension HEK293 Cells and Continuous Harvest of Vector From the Culture Media for GMP FIX and FLT1 Clinical Vector', *Mol Ther*, 24: 287-97.

Grifman, M., N. N. Chen, G. P. Gao, T. Cathomen, J. M. Wilson, and M. D. Weitzman. 1999. 'Overexpression of cyclin A inhibits augmentation of recombinant adeno-associated virus transduction by the adenovirus E4orf6 protein', *J Virol*, 73: 10010-9.

Grimm, D., M. A. Kay, and J. A. Kleinschmidt. 2003. 'Helper virus-free, optically controllable, and two-plasmid-based production of adeno-associated virus vectors of serotypes 1 to 6', *Mol Ther*, 7: 839-50.

Grimm, D., A. Kern, M. Pawlita, F. Ferrari, R. Samulski, and J. Kleinschmidt. 1999. 'Titration of AAV-2 particles via a novel capsid ELISA: packaging of genomes can limit production of recombinant AAV-2', *Gene Ther*, 6: 1322-30.

Grimm, D., A. Kern, K. Rittner, and J. A. Kleinschmidt. 1998. 'Novel tools for production and purification of recombinant adenoassociated virus vectors', *Hum Gene Ther*, 9: 2745-60.

Grimm, D., J. S. Lee, L. Wang, T. Desai, B. Akache, T. A. Storm, and M. A. Kay. 2008. 'In vitro and in vivo gene therapy vector evolution via multispecies interbreeding and retargeting of adeno-associated viruses', *J Virol*, 82: 5887-911.

"Guidance for Industry Q5A Viral Safety Evaluation of Biotechnology Products Derived From Cell Lines of Human or Animal Origin." In., 33.
Halbert, C. L., I. E. Alexander, G. M. Wolgamot, and A. D. Miller. 1995. 'Adeno-associated virus vectors transduce primary cells much less efficiently than immortalized cells', *J Virol*, 69: 1473-9.
Handa, H., K. Shiroki, and H. Shimojo. 1975. 'Complementation of adeno-associated virus growth with temperature-sensitive mutants of human adenovirus types 12 and 5', *J Gen Virol*, 29: 239-42.
Hansen, J., K. Qing, H. J. Kwon, C. Mah, and A. Srivastava. 2000. 'Impaired intracellular trafficking of adeno-associated virus type 2 vectors limits efficient transduction of murine fibroblasts', *J Virol*, 74: 992-6.
Hauck, B., S. L. Murphy, P. H. Smith, G. Qu, X. Liu, O. Zelenaia, F. Mingozzi, J. M. Sommer, K. A. High, and J. F. Wright. 2009. 'Undetectable transcription of cap in a clinical AAV vector: implications for preformed capsid in immune responses', *Mol Ther*, 17: 144-52.
Hearing, P., R. J. Samulski, W. L. Wishart, and T. Shenk. 1987. 'Identification of a repeated sequence element required for efficient encapsidation of the adenovirus type 5 chromosome', *J Virol*, 61: 2555-8.
Hearing, P., and T. Shenk. 1983. 'The adenovirus type 5 E1A transcriptional control region contains a duplicated enhancer element', *Cell*, 33: 695-703.
Hermonat, P. L., and N. Muzyczka. 1984. 'Use of adeno-associated virus as a mammalian DNA cloning vector: transduction of neomycin resistance into mammalian tissue culture cells', *Proc Natl Acad Sci U S A*, 81: 6466-70.
Herold, B. C., D. Marcellino, G. Marcelin, P. Wilson, C. Burrow, and L. M. Satlin. 2002. 'Herpes simplex virus as a model vector system for gene therapy in renal disease', *Kidney Int*, 61: S3-8.
Herzog, R. W., O. Cao, and A. Srivastava. 2010. 'Two decades of clinical gene therapy--success is finally mounting', *Discov Med*, 9: 105-11.
Hess, M., A. Cuzange, R. W. Ruigrok, J. Chroboczek, and B. Jacrot. 1995. 'The avian adenovirus penton: two fibres and one base', *J Mol Biol*, 252: 379-85.
Hidalgo, P., W. H. Ip, T. Dobner, and R. A. Gonzalez. 2019. 'The biology of the adenovirus E1B 55K protein', *FEBS Lett*, 593: 3504-17.
'High-dose AAV gene therapy deaths'. 2020. *Nat Biotechnol*, 38: 910.
Hodges, B. L., H. K. Evans, R. S. Everett, E. Y. Ding, D. Serra, and A. Amalfitano. 2001. 'Adenovirus vectors with the 100K gene deleted and their potential for multiple gene therapy applications', *J Virol*, 75: 5913-20.
Hoeben, R. C., and T. G. Uil. 2013. 'Adenovirus DNA replication', *Cold Spring Harb Perspect Biol*, 5: a013003.
Hofmann, A., G. P. Nolan, and H. M. Blau. 1996. 'Rapid retroviral delivery of tetracycline-inducible genes in a single autoregulatory cassette', *Proc Natl Acad Sci U S A*, 93: 5185-90.
Holscher, C., J. A. Kleinschmidt, and A. Burkle. 1995. 'High-level expression of adeno-associated virus (AAV) Rep78 or Rep68 protein is sufficient for infectious-particle formation by a rep-negative AAV mutant', *J Virol*, 69: 6880-5.
Houri, N., K. C. Huang, and J. Nalbantoglu. 2013. 'The Coxsackievirus and Adenovirus Receptor (CAR) undergoes ectodomain shedding and regulated intramembrane proteolysis (RIP)', *PLoS One*, 8: e73296.
Huang, X., A. V. Hartley, Y. Yin, J. H. Herskowitz, J. J. Lah, and K. J. Ressler. 2013. 'AAV2 production with optimized N/P ratio and PEI-mediated transfection results in low toxicity and high titer for in vitro and in vivo applications', *J Virol Methods*, 193: 270-7.
Hulot, J. S., J. E. Salem, A. Redheuil, J. P. Collet, S. Varnous, P. Jourdain, D. Logeart, E. Gandjbakhch, C. Bernard, S. N. Hatem, R. Isnard, P. Cluzel, C. Le Feuvre, P. Leprince, N. Hammoudi, F. M. Lemoine, D. Klatzmann, E. Vicaut, M. Komajda, G. Montalescot, A. M. Lompre, R. J. Hajjar, and Agent-Hf Investigators. 2017. 'Effect of intracoronary administration of AAV1/SERCA2a

on ventricular remodelling in patients with advanced systolic heart failure: results from the AGENT-HF randomized phase 2 trial', *Eur J Heart Fail*, 19: 1534-41.

Imperiale, M. J., R. P. Hart, and J. R. Nevins. 1985. 'An enhancer-like element in the adenovirus E2 promoter contains sequences essential for uninduced and E1A-induced transcription', *Proc Natl Acad Sci U S A*, 82: 381-5.

Imperiale, M. J., and J. R. Nevins. 1984. 'Adenovirus 5 E2 transcription unit: an E1A-inducible promoter with an essential element that functions independently of position or orientation', *Mol Cell Biol*, 4: 875-82.

Jiang, H., E. J. White, C. I. Rios-Vicil, J. Xu, C. Gomez-Manzano, and J. Fueyo. 2011. 'Human adenovirus type 5 induces cell lysis through autophagy and autophagy-triggered caspase activity', *J Virol*, 85: 4720-9.

Jin, X., L. Liu, S. Nass, C. O'Riordan, E. Pastor, and X. K. Zhang. 2017. 'Direct Liquid Chromatography/Mass Spectrometry Analysis for Complete Characterization of Recombinant Adeno-Associated Virus Capsid Proteins', *Hum Gene Ther Methods*, 28: 255-67.

Johnson, F. B., H. L. Ozer, and M. D. Hoggan. 1971. 'Structural proteins of adenovirus-associated virus type 3', *J Virol*, 8: 860-63.

Johnson, J. S., C. Li, N. DiPrimio, M. S. Weinberg, T. J. McCown, and R. J. Samulski. 2010. 'Mutagenesis of adeno-associated virus type 2 capsid protein VP1 uncovers new roles for basic amino acids in trafficking and cell-specific transduction', *J Virol*, 84: 8888-902.

Johnson, J. S., and R. J. Samulski. 2009. 'Enhancement of adeno-associated virus infection by mobilizing capsids into and out of the nucleolus', *J Virol*, 83: 2632-44.

Kamel, W., and G. Akusjarvi. 2017. 'An Ago2-associated capped transcriptional start site small RNA suppresses adenovirus DNA replication', *RNA*, 23: 1700-11.

Kang, W., L. Wang, H. Harrell, J. Liu, D. L. Thomas, T. L. Mayfield, M. M. Scotti, G. J. Ye, G. Veres, and D. R. Knop. 2009. 'An efficient rHSV-based complementation system for the production of multiple rAAV vector serotypes', *Gene Ther*, 16: 229-39.

Kapranov, P., L. Chen, D. Dederich, B. Dong, J. He, K. E. Steinmann, A. R. Moore, J. F. Thompson, P. M. Milos, and W. Xiao. 2012. 'Native molecular state of adeno-associated viral vectors revealed by single-molecule sequencing', *Hum Gene Ther*, 23: 46-55.

Karda, R., J. R. Counsell, K. Karbowniczek, L. J. Caproni, J. P. Tite, and S. N. Waddington. 2019. 'Production of lentiviral vectors using novel, enzymatically produced, linear DNA', *Gene Ther*, 26: 86-92.

Kim, H. J., C. Gatz, W. Hillen, and T. R. Jones. 1995. 'Tetracycline repressor-regulated gene repression in recombinant human cytomegalovirus', *J Virol*, 69: 2565-73.

King, J. A., R. Dubielzig, D. Grimm, and J. A. Kleinschmidt. 2001. 'DNA helicase-mediated packaging of adeno-associated virus type 2 genomes into preformed capsids', *EMBO J*, 20: 3282-91.

Kneidinger, D., M. Ibrisimovic, T. Lion, and R. Klein. 2012. 'Inhibition of adenovirus multiplication by short interfering RNAs directly or indirectly targeting the viral DNA replication machinery', *Antiviral Res*, 94: 195-207.

Knight, S., M. Collins, and Y. Takeuchi. 2013. 'Insertional mutagenesis by retroviral vectors: current concepts and methods of analysis', *Curr Gene Ther*, 13: 211-27.

Kohn, D. B., M. Sadelain, and J. C. Glorioso. 2003. 'Occurrence of leukaemia following gene therapy of X-linked SCID', *Nat Rev Cancer*, 3: 477-88.

Kondratov, O., D. Marsic, S. M. Crosson, H. R. Mendez-Gomez, O. Moskalenko, M. Mietzsch, R. Heilbronn, J. R. Allison, K. B. Green, M. Agbandje-McKenna, and S. Zolotukhin. 2017. 'Direct Head-to-Head Evaluation of Recombinant Adeno-associated Viral Vectors Manufactured in Human versus Insect Cells', *Mol Ther*, 25: 2661-75.

Kotin, R. M., M. Siniscalco, R. J. Samulski, X. D. Zhu, L. Hunter, C. A. Laughlin, S. McLaughlin, N. Muzyczka, M. Rocchi, and K. I. Berns. 1990. 'Site-specific integration by adeno-associated virus', *Proc Natl Acad Sci U S A*, 87: 2211-5.

Kotin, R. M., and R. O. Snyder. 2017. 'Manufacturing Clinical Grade Recombinant Adeno-Associated Virus Using Invertebrate Cell Lines', *Hum Gene Ther*, 28: 350-60.
Kotterman, M. A., T. W. Chalberg, and D. V. Schaffer. 2015. 'Viral Vectors for Gene Therapy: Translational and Clinical Outlook', *Annu Rev Biomed Eng*, 17: 63-89.
Kovesdi, I., and S. J. Hedley. 2010. 'Adenoviral producer cells', *Viruses*, 2: 1681-703.
Kronenberg, S., B. Bottcher, C. W. von der Lieth, S. Bleker, and J. A. Kleinschmidt. 2005. 'A conformational change in the adeno-associated virus type 2 capsid leads to the exposure of hidden VP1 N termini', *J Virol*, 79: 5296-303.
Krueger, M., O. Scholz, S. Wisshak, and W. Hillen. 2007. 'Engineered Tet repressors with recognition specificity for the tetO-4C5G operator variant', *Gene*, 404: 93-100.
Kruger-Haag, A., C. Lehmann, E. Schmidt, F. Sonntag, M. Horer, and S. Kochanek. 2019. 'Evaluation of life cycle defective adenovirus mutants for production of adeno-associated virus vectors', *J Gene Med*, 21: e3094.
Kumar, S. R., D. M. Markusic, M. Biswas, K. A. High, and R. W. Herzog. 2016. 'Clinical development of gene therapy: results and lessons from recent successes', *Mol Ther Methods Clin Dev*, 3: 16034.
Lai, T., Y. Yang, and S. K. Ng. 2013. 'Advances in Mammalian cell line development technologies for recombinant protein production', *Pharmaceuticals (Basel)*, 6: 579-603.
Lan, S., W. Kamel, T. Punga, and G. Akusjarvi. 2017. 'The adenovirus L4-22K protein regulates transcription and RNA splicing via a sequence-specific single-stranded RNA binding', *Nucleic Acids Res*, 45: 1731-42.
Lapteva, L., T. Purohit-Sheth, M. Serabian, and R. K. Puri. 2020. 'Clinical Development of Gene Therapies: The First Three Decades and Counting', *Mol Ther Methods Clin Dev*, 19: 387-97.
Laughlin, C. A., J. D. Tratschin, H. Coon, and B. J. Carter. 1983. 'Cloning of infectious adeno-associated virus genomes in bacterial plasmids', *Gene*, 23: 65-73.
Lebkowski, J. S., M. M. McNally, T. B. Okarma, and L. B. Lerch. 1988. 'Adeno-associated virus: a vector system for efficient introduction and integration of DNA into a variety of mammalian cell types', *Mol Cell Biol*, 8: 3988-96.
Lecomte, E., A. Leger, M. Penaud-Budloo, and E. Ayuso. 2019. 'Single-Stranded DNA Virus Sequencing (SSV-Seq) for Characterization of Residual DNA and AAV Vector Genomes', *Methods Mol Biol*, 1950: 85-106.
Lee, C. S., E. S. Bishop, R. Zhang, X. Yu, E. M. Farina, S. Yan, C. Zhao, Z. Zheng, Y. Shu, X. Wu, J. Lei, Y. Li, W. Zhang, C. Yang, K. Wu, Y. Wu, S. Ho, A. Athiviraham, M. J. Lee, J. M. Wolf, R. R. Reid, and T. C. He. 2017. 'Adenovirus-Mediated Gene Delivery: Potential Applications for Gene and Cell-Based Therapies in the New Era of Personalized Medicine', *Genes Dis*, 4: 43-63.
Leopold, P. L., and R. G. Crystal. 2007. 'Intracellular trafficking of adenovirus: many means to many ends', *Adv Drug Deliv Rev*, 59: 810-21.
Li, C., and R. J. Samulski. 2020. 'Engineering adeno-associated virus vectors for gene therapy', *Nat Rev Genet*, 21: 255-72.
Li, J., R. J. Samulski, and X. Xiao. 1997. 'Role for highly regulated rep gene expression in adeno-associated virus vector production', *J Virol*, 71: 5236-43.
Li, S., and L. Huang. 2000. 'Nonviral gene therapy: promises and challenges', *Gene Ther*, 7: 31-4.
Li, X., Y. P. Zhang, H. S. Kim, K. H. Bae, K. M. Stantz, S. J. Lee, C. Jung, J. A. Jimenez, T. A. Gardner, M. H. Jeng, and C. Kao. 2005. 'Gene therapy for prostate cancer by controlling adenovirus E1a and E4 gene expression with PSES enhancer', *Cancer Res*, 65: 1941-51.
Lichtenstein, D. L., K. Toth, K. Doronin, A. E. Tollefson, and W. S. Wold. 2004. 'Functions and mechanisms of action of the adenovirus E3 proteins', *Int Rev Immunol*, 23: 75-111.
Ling, C., Y. Wang, Y. Lu, L. Wang, G. R. Jayandharan, G. V. Aslanidi, B. Li, B. Cheng, W. Ma, T. Lentz, C. Ling, X. Xiao, R. J. Samulski, N. Muzyczka, and A. Srivastava. 2015. 'The Adeno-Associated Virus Genome Packaging Puzzle', *J Mol Genet Med*, 9.

Lion, T. 2014. 'Adenovirus infections in immunocompetent and immunocompromised patients', *Clin Microbiol Rev*, 27: 441-62.
Liu, H., J. H. Naismith, and R. T. Hay. 2000. 'Identification of conserved residues contributing to the activities of adenovirus DNA polymerase', *J Virol*, 74: 11681-9.
Liu, X. L., K. R. Clark, and P. R. Johnson. 1999. 'Production of recombinant adeno-associated virus vectors using a packaging cell line and a hybrid recombinant adenovirus', *Gene Ther*, 6: 293-9.
Liu, X., F. Voulgaropoulou, R. Chen, P. R. Johnson, and K. R. Clark. 2000. 'Selective Rep-Cap gene amplification as a mechanism for high-titer recombinant AAV production from stable cell lines', *Mol Ther*, 2: 394-403.
Liu, Z., O. Chen, J. B. J. Wall, M. Zheng, Y. Zhou, L. Wang, H. R. Vaseghi, L. Qian, and J. Liu. 2017. 'Systematic comparison of 2A peptides for cloning multi-genes in a polycistronic vector', *Sci Rep*, 7: 2193.
Logan, J. S., and T. Shenk. 1982. 'Transcriptional and translational control of adenovirus gene expression', *Microbiol Rev*, 46: 377-83.
Logan, J., and T. Shenk. 1984. 'Adenovirus tripartite leader sequence enhances translation of mRNAs late after infection', *Proc Natl Acad Sci U S A*, 81: 3655-9.
Lu, H., M. D. Reach, E. Minaya, and C. S. Young. 1997. 'The initiator element of the adenovirus major late promoter has an important role in transcription initiation in vivo', *J Virol*, 71: 102-9.
Lundstrom, K. 2018. 'Viral Vectors in Gene Therapy', *Diseases*, 6.
Luo, J., Z. L. Deng, X. Luo, N. Tang, W. X. Song, J. Chen, K. A. Sharff, H. H. Luu, R. C. Haydon, K. W. Kinzler, B. Vogelstein, and T. C. He. 2007. 'A protocol for rapid generation of recombinant adenoviruses using the AdEasy system', *Nat Protoc*, 2: 1236-47.
Lyle, C., and F. McCormick. 2010. 'Integrin alphavbeta5 is a primary receptor for adenovirus in CAR-negative cells', *Virol J*, 7: 148.
Lynch, J. P., 3rd, and A. E. Kajon. 2016. 'Adenovirus: Epidemiology, Global Spread of Novel Serotypes, and Advances in Treatment and Prevention', *Semin Respir Crit Care Med*, 37: 586-602.
Ma, Y., and M. B. Mathews. 1996. 'Structure, function, and evolution of adenovirus-associated RNA: a phylogenetic approach', *J Virol*, 70: 5083-99.
Macpherson, J. L., and J. E. Rasko. 2014. 'Clinical potential of gene therapy: towards meeting the demand', *Intern Med J*, 44: 224-33.
Madigan, V. J., and A. Asokan. 2016. 'Engineering AAV receptor footprints for gene therapy', *Curr Opin Virol*, 18: 89-96.
Maldonado, R., S. Jalil, and K. Wartiovaara. 2020. 'Curative gene therapies for rare diseases', *J Community Genet*.
Mali, S. 2013. 'Delivery systems for gene therapy', *Indian J Hum Genet*, 19: 3-8.
Mangel, W. F., and C. San Martin. 2014. 'Structure, function and dynamics in adenovirus maturation', *Viruses*, 6: 4536-70.
Martin-Gonzalez, N., M. Hernando-Perez, G. N. Condezo, M. Perez-Illana, A. Siber, D. Reguera, P. Ostapchuk, P. Hearing, C. San Martin, and P. J. de Pablo. 2019. 'Adenovirus major core protein condenses DNA in clusters and bundles, modulating genome release and capsid internal pressure', *Nucleic Acids Res*, 47: 9231-42.
Martin, J., A. Frederick, Y. Luo, R. Jackson, M. Joubert, B. Sol, F. Poulin, E. Pastor, D. Armentano, S. Wadsworth, and K. Vincent. 2013. 'Generation and characterization of adeno-associated virus producer cell lines for research and preclinical vector production', *Hum Gene Ther Methods*, 24: 253-69.
Mary, B., S. Maurya, S. Arumugam, V. Kumar, and G. R. Jayandharan. 2019. 'Post-translational modifications in capsid proteins of recombinant adeno-associated virus (AAV) 1-rh10 serotypes', *FEBS J*, 286: 4964-81.

Matsushita, T., S. Elliger, C. Elliger, G. Podsakoff, L. Villarreal, G. J. Kurtzman, Y. Iwaki, and P. Colosi. 1998. 'Adeno-associated virus vectors can be efficiently produced without helper virus', *Gene Ther*, 5: 938-45.

Maunder, H. E., J. Wright, B. R. Kolli, C. R. Vieira, T. T. Mkandawire, S. Tatoris, V. Kennedy, S. Iqball, G. Devarajan, S. Ellis, Y. Lad, N. G. Clarkson, K. A. Mitrophanous, and D. C. Farley. 2017. 'Enhancing titres of therapeutic viral vectors using the transgene repression in vector production (TRiP) system', *Nat Commun*, 8: 14834.

Maurer, A. C., S. Pacouret, A. K. Cepeda Diaz, J. Blake, E. Andres-Mateos, and L. H. Vandenberghe. 2018. 'The Assembly-Activating Protein Promotes Stability and Interactions between AAV's Viral Proteins to Nucleate Capsid Assembly', *Cell Rep*, 23: 1817-30.

Mayo, K. E., R. Warren, and R. D. Palmiter. 1982. 'The mouse metallothionein-I gene is transcriptionally regulated by cadmium following transfection into human or mouse cells', *Cell*, 29: 99-108.

McCarty, D. M. 2008. 'Self-complementary AAV vectors; advances and applications', *Mol Ther*, 16: 1648-56.

McCarty, D. M., M. Christensen, and N. Muzyczka. 1991. 'Sequences required for coordinate induction of adeno-associated virus p19 and p40 promoters by Rep protein', *J Virol*, 65: 2936-45.

McCarty, D. M., P. E. Monahan, and R. J. Samulski. 2001. 'Self-complementary recombinant adeno-associated virus (scAAV) vectors promote efficient transduction independently of DNA synthesis', *Gene Ther*, 8: 1248-54.

McPherson, R. A., L. J. Rosenthal, and J. A. Rose. 1985. 'Human cytomegalovirus completely helps adeno-associated virus replication', *Virology*, 147: 217-22.

Mei, Y. F., J. Skog, K. Lindman, and G. Wadell. 2003. 'Comparative analysis of the genome organization of human adenovirus 11, a member of the human adenovirus species B, and the commonly used human adenovirus 5 vector, a member of species C', *J Gen Virol*, 84: 2061-71.

Meier, A. F., C. Fraefel, and M. Seyffert. 2020. 'The Interplay between Adeno-Associated Virus and its Helper Viruses', *Viruses*, 12.

Meier, O., and U. F. Greber. 2004. 'Adenovirus endocytosis', *J Gene Med*, 6 Suppl 1: S152-63.

Mejia-Toiber, J., C. G. Castillo, and M. Giordano. 2011. 'Strategies for the development of cell lines for ex vivo gene therapy in the central nervous system', *Cell Transplant*, 20: 983-1001.

Merten, O. W., C. Geny-Fiamma, and A. M. Douar. 2005. 'Current issues in adeno-associated viral vector production', *Gene Ther*, 12 Suppl 1: S51-61.

Miesbach, W., K. Meijer, M. Coppens, P. Kampmann, R. Klamroth, R. Schutgens, M. Tangelder, G. Castaman, J. Schwable, H. Bonig, E. Seifried, F. Cattaneo, C. Meyer, and F. W. G. Leebeek. 2018. 'Gene therapy with adeno-associated virus vector 5-human factor IX in adults with hemophilia B', *Blood*, 131: 1022-31.

Mietzsch, M., F. Broecker, A. Reinhardt, P. H. Seeberger, and R. Heilbronn. 2014. 'Differential adeno-associated virus serotype-specific interaction patterns with synthetic heparins and other glycans', *J Virol*, 88: 2991-3003.

Mietzsch, M., S. Grasse, C. Zurawski, S. Weger, A. Bennett, M. Agbandje-McKenna, N. Muzyczka, S. Zolotukhin, and R. Heilbronn. 2014. 'OneBac: platform for scalable and high-titer production of adeno-associated virus serotype 1-12 vectors for gene therapy', *Hum Gene Ther*, 25: 212-22.

Mietzsch, M., H. Hering, E. M. Hammer, M. Agbandje-McKenna, S. Zolotukhin, and R. Heilbronn. 2017. 'OneBac 2.0: Sf9 Cell Lines for Production of AAV1, AAV2, and AAV8 Vectors with Minimal Encapsidation of Foreign DNA', *Hum Gene Ther Methods*, 28: 15-22.

Mietzsch, M., J. K. Smith, J. C. Yu, V. Banala, S. N. Emmanuel, A. Jose, P. Chipman, N. Bhattacharya, R. McKenna, and M. Agbandje-McKenna. 2020. 'Characterization of AAV-Specific Affinity

Ligands: Consequences for Vector Purification and Development Strategies', *Mol Ther Methods Clin Dev*, 19: 362-73.
Milone, M. C., and U. O'Doherty. 2018. 'Clinical use of lentiviral vectors', *Leukemia*, 32: 1529-41.
Mohiuddin, I., S. Loiler, I. Zolotukhin, B. J. Byrne, T. R. Flotte, and R. O. Snyder. 2005. 'Herpesvirus-based infectious titering of recombinant adeno-associated viral vectors', *Mol Ther*, 11: 320-6.
Moore, A., M. Ling, A. Bucko, V. Manna, and M. J. Rueda. 2015. 'Efficacy and Safety of Subantimicrobial Dose, Modified-Release Doxycycline 40 mg Versus Doxycycline 100 mg Versus Placebo for the treatment of Inflammatory Lesions in Moderate and Severe Acne: A Randomized, Double-Blinded, Controlled Study', *J Drugs Dermatol*, 14: 581-6.
Moore, A. R., B. Dong, L. Chen, and W. Xiao. 2015. 'Vaccinia virus as a subhelper for AAV replication and packaging', *Mol Ther Methods Clin Dev*, 2: 15044.
Morris, S. J., G. E. Scott, and K. N. Leppard. 2010. 'Adenovirus late-phase infection is controlled by a novel L4 promoter', *J Virol*, 84: 7096-104.
Mul, Y. M., C. P. Verrijzer, and P. C. van der Vliet. 1990. 'Transcription factors NFI and NFIII/oct-1 function independently, employing different mechanisms to enhance adenovirus DNA replication', *J Virol*, 64: 5510-8.
Mullick, A., Y. Xu, R. Warren, M. Koutroumanis, C. Guilbault, S. Broussau, F. Malenfant, L. Bourget, L. Lamoureux, R. Lo, A. W. Caron, A. Pilotte, and B. Massie. 2006. 'The cumate gene-switch: a system for regulated expression in mammalian cells', *BMC Biotechnol*, 6: 43.
Murakami, P., and M. T. McCaman. 1999. 'Quantitation of adenovirus DNA and virus particles with the PicoGreen fluorescent Dye', *Anal Biochem*, 274: 283-8.
Mysiak, M. E., M. H. Bleijenberg, C. Wyman, P. E. Holthuizen, and P. C. van der Vliet. 2004. 'Bending of adenovirus origin DNA by nuclear factor I as shown by scanning force microscopy is required for optimal DNA replication', *J Virol*, 78: 1928-35.
Naidoo, J., and D. Young. 2012. 'Gene regulation systems for gene therapy applications in the central nervous system', *Neurol Res Int*, 2012: 595410.
Nakamura, S., R. Nakamura, K. Shibata, M. Kobayashi, N. Sahara, K. Shigeno, K. Shinjo, K. Naito, K. Ohnishi, N. Kasahara, and Y. Iwaki. 2004. 'Development of packaging cell lines for generation of adeno-associated virus vectors by lentiviral gene transfer of trans-complementary components', *Eur J Haematol*, 73: 285-94.
Nakano, M. Y., K. Boucke, M. Suomalainen, R. P. Stidwill, and U. F. Greber. 2000. 'The first step of adenovirus type 2 disassembly occurs at the cell surface, independently of endocytosis and escape to the cytosol', *J Virol*, 74: 7085-95.
Naldini, L. 2011. 'Ex vivo gene transfer and correction for cell-based therapies', *Nat Rev Genet*, 12: 301-15.
Nash, K., W. Chen, W. F. McDonald, X. Zhou, and N. Muzyczka. 2007. 'Purification of host cell enzymes involved in adeno-associated virus DNA replication', *J Virol*, 81: 5777-87.
Nash, K., W. Chen, and N. Muzyczka. 2008. 'Complete in vitro reconstitution of adeno-associated virus DNA replication requires the minichromosome maintenance complex proteins', *J Virol*, 82: 1458-64.
Nathwani, A. C., A. M. Davidoff, H. Hanawa, Y. Hu, F. A. Hoffer, A. Nikanorov, C. Slaughter, C. Y. Ng, J. Zhou, J. N. Lozier, T. D. Mandrell, E. F. Vanin, and A. W. Nienhuis. 2002. 'Sustained high-level expression of human factor IX (hFIX) after liver-targeted delivery of recombinant adeno-associated virus encoding the hFIX gene in rhesus macaques', *Blood*, 100: 1662-9.
Natsoulis, Georges. 1995. "High efficiency helper system for AAV vector production." In. USA.
Nayak, R., and D. J. Pintel. 2007. 'Positive and negative effects of adenovirus type 5 helper functions on adeno-associated virus type 5 (AAV5) protein accumulation govern AAV5 virus production', *J Virol*, 81: 2205-12.

Needham, P. G., J. M. Casper, V. Kalman-Maltese, K. Verrill, J. D. Dignam, and J. P. Trempe. 2006. 'Adeno-associated virus rep protein-mediated inhibition of transcription of the adenovirus major late promoter in vitro', *J Virol*, 80: 6207-17.
Nemerow, G., and J. Flint. 2019. 'Lessons learned from adenovirus (1970-2019)', *FEBS Lett*, 593: 3395-418.
Nevins, J. R. 1981. 'Mechanism of activation of early viral transcription by the adenovirus E1A gene product', *Cell*, 26: 213-20.
Nguyen, L. T., K. Atobe, J. M. Barichello, T. Ishida, and H. Kiwada. 2007. 'Complex formation with plasmid DNA increases the cytotoxicity of cationic liposomes', *Biol Pharm Bull*, 30: 751-7.
Ni, T. H., W. F. McDonald, I. Zolotukhin, T. Melendy, S. Waga, B. Stillman, and N. Muzyczka. 1998. 'Cellular proteins required for adeno-associated virus DNA replication in the absence of adenovirus coinfection', *J Virol*, 72: 2777-87.
Nonnenmacher, M., H. van Bakel, R. J. Hajjar, and T. Weber. 2015. 'High capsid-genome correlation facilitates creation of AAV libraries for directed evolution', *Mol Ther*, 23: 675-82.
Nonnenmacher, M., and T. Weber. 2011. 'Adeno-associated virus 2 infection requires endocytosis through the CLIC/GEEC pathway', *Cell Host Microbe*, 10: 563-76.
———. 2012. 'Intracellular transport of recombinant adeno-associated virus vectors', *Gene Ther*, 19: 649-58.
Nony, P., J. Tessier, G. Chadeuf, P. Ward, A. Giraud, M. Dugast, R. M. Linden, P. Moullier, and A. Salvetti. 2001. 'Novel cis-acting replication element in the adeno-associated virus type 2 genome is involved in amplification of integrated rep-cap sequences', *J Virol*, 75: 9991-4.
O'Donnell, J., K. A. Taylor, and M. S. Chapman. 2009. 'Adeno-associated virus-2 and its primary cellular receptor--Cryo-EM structure of a heparin complex', *Virology*, 385: 434-43.
Ogden, P. J., E. D. Kelsic, S. Sinai, and G. M. Church. 2019. 'Comprehensive AAV capsid fitness landscape reveals a viral gene and enables machine-guided design', *Science*, 366: 1139-43.
Ostapchuk, P., M. E. Anderson, S. Chandrasekhar, and P. Hearing. 2006. 'The L4 22-kilodalton protein plays a role in packaging of the adenovirus genome', *J Virol*, 80: 6973-81.
Ostapchuk, P., and P. Hearing. 2003. 'Regulation of adenovirus packaging', *Curr Top Microbiol Immunol*, 272: 165-85.
———. 2005. 'Control of adenovirus packaging', *J Cell Biochem*, 96: 25-35.
Pardo-Mateos, A., and C. S. Young. 2004. 'Adenovirus IVa2 protein plays an important role in transcription from the major late promoter in vivo', *Virology*, 327: 50-9.
Parks, C. L., and T. Shenk. 1997. 'Activation of the adenovirus major late promoter by transcription factors MAZ and Sp1', *J Virol*, 71: 9600-7.
Pegoraro, G., A. Marcello, M. P. Myers, and M. Giacca. 2006. 'Regulation of adeno-associated virus DNA replication by the cellular TAF-I/set complex', *J Virol*, 80: 6855-64.
Pekrun, K., G. De Alencastro, Q. J. Luo, J. Liu, Y. Kim, S. Nygaard, F. Galivo, F. Zhang, R. Song, M. R. Tiffany, J. Xu, M. Hebrok, M. Grompe, and M. A. Kay. 2019. 'Using a barcoded AAV capsid library to select for clinically relevant gene therapy vectors', *JCI Insight*, 4.
Penaud-Budloo, M., A. Francois, N. Clement, and E. Ayuso. 2018. 'Pharmacology of Recombinant Adeno-associated Virus Production', *Mol Ther Methods Clin Dev*, 8: 166-80.
Penaud-Budloo, M., E. Lecomte, A. Guy-Duche, S. Saleun, A. Roulet, C. Lopez-Roques, B. Tournaire, B. Cogne, A. Leger, V. Blouin, P. Lindenbaum, P. Moullier, and E. Ayuso. 2017. 'Accurate Identification and Quantification of DNA Species by Next-Generation Sequencing in Adeno-Associated Viral Vectors Produced in Insect Cells', *Hum Gene Ther Methods*, 28: 148-62.
Penzes, J. J., R. Menendez-Conejero, G. N. Condezo, I. Ball, T. Papp, A. Doszpoly, A. Paradela, A. J. Perez-Berna, M. Lopez-Sanz, T. H. Nguyen, M. J. van Raaij, R. E. Marschang, B. Harrach, M. Benko, and C. San Martin. 2014. 'Molecular characterization of a lizard adenovirus reveals the first atadenovirus with two fiber genes and the first adenovirus with either one short or three long fibers per penton', *J Virol*, 88: 11304-14.

Perez-Berna, A. J., R. Marabini, S. H. Scheres, R. Menendez-Conejero, I. P. Dmitriev, D. T. Curiel, W. F. Mangel, S. J. Flint, and C. San Martin. 2009. 'Structure and uncoating of immature adenovirus', *J Mol Biol*, 392: 547-57.

Perrin, G. Q., R. W. Herzog, and D. M. Markusic. 2019. 'Update on clinical gene therapy for hemophilia', *Blood*, 133: 407-14.

Philpott, N. J., C. Giraud-Wali, C. Dupuis, J. Gomos, H. Hamilton, K. I. Berns, and E. Falck-Pedersen. 2002. 'Efficient integration of recombinant adeno-associated virus DNA vectors requires a p5-rep sequence in cis', *J Virol*, 76: 5411-21.

Philpott, N. J., J. Gomos, K. I. Berns, and E. Falck-Pedersen. 2002. 'A p5 integration efficiency element mediates Rep-dependent integration into AAVS1 at chromosome 19', *Proc Natl Acad Sci U S A*, 99: 12381-5.

Pilankatta, R., T. Chawla, N. Khanna, and S. Swaminathan. 2010. 'The prevalence of antibodies to adenovirus serotype 5 in an adult Indian population and implications for adenovirus vector vaccines', *J Med Virol*, 82: 407-14.

Pillay, S., and J. E. Carette. 2017. 'Host determinants of adeno-associated viral vector entry', *Curr Opin Virol*, 24: 124-31.

Pillay, S., N. L. Meyer, A. S. Puschnik, O. Davulcu, J. Diep, Y. Ishikawa, L. T. Jae, J. E. Wosen, C. M. Nagamine, M. S. Chapman, and J. E. Carette. 2016. 'An essential receptor for adeno-associated virus infection', *Nature*, 530: 108-12.

Pillay, S., W. Zou, F. Cheng, A. S. Puschnik, N. L. Meyer, S. S. Ganaie, X. Deng, J. E. Wosen, O. Davulcu, Z. Yan, J. F. Engelhardt, K. E. Brown, M. S. Chapman, J. Qiu, and J. E. Carette. 2017. 'Adeno-associated Virus (AAV) Serotypes Have Distinctive Interactions with Domains of the Cellular AAV Receptor', *J Virol*, 91.

Pronk, R., and P. C. van der Vliet. 1993. 'The adenovirus terminal protein influences binding of replication proteins and changes the origin structure', *Nucleic Acids Res*, 21: 2293-300.

Qiao, C., J. Li, A. Skold, X. Zhang, and X. Xiao. 2002. 'Feasibility of generating adeno-associated virus packaging cell lines containing inducible adenovirus helper genes', *J Virol*, 76: 1904-13.

Rabinowitz, J. E., F. Rolling, C. Li, H. Conrath, W. Xiao, X. Xiao, and R. J. Samulski. 2002. 'Cross-packaging of a single adeno-associated virus (AAV) type 2 vector genome into multiple AAV serotypes enables transduction with broad specificity', *J Virol*, 76: 791-801.

Radko, S., R. Jung, O. Olanubi, and P. Pelka. 2015. 'Effects of Adenovirus Type 5 E1A Isoforms on Viral Replication in Arrested Human Cells', *PLoS One*, 10: e0140124.

Ramke, M., J. Y. Lee, D. W. Dyer, D. Seto, J. Rajaiya, and J. Chodosh. 2017. 'The 5'UTR in human adenoviruses: leader diversity in late gene expression', *Sci Rep*, 7: 618.

Ramos, J. L., M. Martinez-Bueno, A. J. Molina-Henares, W. Teran, K. Watanabe, X. Zhang, M. T. Gallegos, R. Brennan, and R. Tobes. 2005. 'The TetR family of transcriptional repressors', *Microbiol Mol Biol Rev*, 69: 326-56.

Raper, S. E., N. Chirmule, F. S. Lee, N. A. Wivel, A. Bagg, G. P. Gao, J. M. Wilson, and M. L. Batshaw. 2003. 'Fatal systemic inflammatory response syndrome in a ornithine transcarbamylase deficient patient following adenoviral gene transfer', *Mol Genet Metab*, 80: 148-58.

Rawlins, D. R., P. J. Rosenfeld, R. J. Wides, M. D. Challberg, and T. J. Kelly, Jr. 1984. 'Structure and function of the adenovirus origin of replication', *Cell*, 37: 309-19.

Reach, M., L. X. Xu, and C. S. Young. 1991. 'Transcription from the adenovirus major late promoter uses redundant activating elements', *EMBO J*, 10: 3439-46.

Rebetz, J., M. Na, C. Su, B. Holmqvist, A. Edqvist, C. Nyberg, B. Widegren, L. G. Salford, H. O. Sjogren, N. Arnberg, Q. Qian, and X. Fan. 2009. 'Fiber mediated receptor masking in non-infected bystander cells restricts adenovirus cell killing effect but promotes adenovirus host co-existence', *PLoS One*, 4: e8484.

Reddy, P. S., N. Idamakanti, A. N. Zakhartchouk, M. K. Baxi, J. B. Lee, C. Pyne, L. A. Babiuk, and S. K. Tikoo. 1998. 'Nucleotide sequence, genome organization, and transcription map of bovine adenovirus type 3', *J Virol*, 72: 1394-402.

Reddy, V. S., and G. R. Nemerow. 2014. 'Structures and organization of adenovirus cement proteins provide insights into the role of capsid maturation in virus entry and infection', *Proc Natl Acad Sci U S A*, 111: 11715-20.

Reichel, R., S. D. Neill, I. Kovesdi, M. C. Simon, P. Raychaudhuri, and J. R. Nevins. 1989. 'The adenovirus E4 gene, in addition to the E1A gene, is important for trans-activation of E2 transcription and for E2F activation', *J Virol*, 63: 3643-50.

Riley, D., and S. J. Flint. 1993. 'RNA-binding properties of a translational activator, the adenovirus L4 100-kilodalton protein', *J Virol*, 67: 3586-95.

Risso-Ballester, J., J. M. Cuevas, and R. Sanjuan. 2016. 'Genome-Wide Estimation of the Spontaneous Mutation Rate of Human Adenovirus 5 by High-Fidelity Deep Sequencing', *PLoS Pathog*, 12: e1006013.

Riviere, C., O. Danos, and A. M. Douar. 2006. 'Long-term expression and repeated administration of AAV type 1, 2 and 5 vectors in skeletal muscle of immunocompetent adult mice', *Gene Ther*, 13: 1300-8.

Rodriguez-Estevez, L., P. Asokan, and T. Borras. 2020. 'Transduction optimization of AAV vectors for human gene therapy of glaucoma and their reversed cell entry characteristics', *Gene Ther*, 27: 127-42.

Rowe, W. P., R. J. Huebner, L. K. Gilmore, R. H. Parrott, and T. G. Ward. 1953. 'Isolation of a cytopathogenic agent from human adenoids undergoing spontaneous degeneration in tissue culture', *Proc Soc Exp Biol Med*, 84: 570-3.

Rutledge, E. A., C. L. Halbert, and D. W. Russell. 1998. 'Infectious clones and vectors derived from adeno-associated virus (AAV) serotypes other than AAV type 2', *J Virol*, 72: 309-19.

Rux, J. J., and R. M. Burnett. 2004. 'Adenovirus structure', *Hum Gene Ther*, 15: 1167-76.

Ryals, J., P. Dierks, H. Ragg, and C. Weissmann. 1985. 'A 46-nucleotide promoter segment from an IFN-alpha gene renders an unrelated promoter inducible by virus', *Cell*, 41: 497-507.

Saha, B., C. M. Wong, and R. J. Parks. 2014. 'The adenovirus genome contributes to the structural stability of the virion', *Viruses*, 6: 3563-83.

Sakhuja, K., P. S. Reddy, S. Ganesh, F. Cantaniag, S. Pattison, P. Limbach, D. B. Kayda, M. J. Kadan, M. Kaleko, and S. Connelly. 2003. 'Optimization of the generation and propagation of gutless adenoviral vectors', *Hum Gene Ther*, 14: 243-54.

Samulski, R. J., K. I. Berns, M. Tan, and N. Muzyczka. 1982. 'Cloning of adeno-associated virus into pBR322: rescue of intact virus from the recombinant plasmid in human cells', *Proc Natl Acad Sci U S A*, 79: 2077-81.

Samulski, R. J., L. S. Chang, and T. Shenk. 1989. 'Helper-free stocks of recombinant adeno-associated viruses: normal integration does not require viral gene expression', *J Virol*, 63: 3822-8.

San Martin, C. 2012. 'Latest insights on adenovirus structure and assembly', *Viruses*, 4: 847-77.

Sarantis, H., G. Johnson, M. Brown, M. Petric, and R. Tellier. 2004. 'Comprehensive detection and serotyping of human adenoviruses by PCR and sequencing', *J Clin Microbiol*, 42: 3963-9.

Schaack, J., X. Guo, and S. J. Langer. 1996. 'Characterization of a replication-incompetent adenovirus type 5 mutant deleted for the preterminal protein gene', *Proc Natl Acad Sci U S A*, 93: 14686-91.

Schmit, P. F., S. Pacouret, E. Zinn, E. Telford, F. Nicolaou, F. Broucque, E. Andres-Mateos, R. Xiao, M. Penaud-Budloo, M. Bouzelha, N. Jaulin, O. Adjali, E. Ayuso, and L. H. Vandenberghe. 2020. 'Cross-Packaging and Capsid Mosaic Formation in Multiplexed AAV Libraries', *Mol Ther Methods Clin Dev*, 17: 107-21.

Schneider, R. J. 1995. 'Cap-independent translation in adenovirus infected cells', *Curr Top Microbiol Immunol*, 203: 117-29.

Schnepp, B. C., K. R. Clark, D. L. Klemanski, C. A. Pacak, and P. R. Johnson. 2003. 'Genetic fate of recombinant adeno-associated virus vector genomes in muscle', *J Virol*, 77: 3495-504.

Schnodt, M., M. Schmeer, B. Kracher, C. Krusemann, L. E. Espinosa, A. Grunert, T. Fuchsluger, A. Rischmuller, M. Schleef, and H. Buning. 2016. 'DNA Minicircle Technology Improves Purity of Adeno-associated Viral Vector Preparations', *Mol Ther Nucleic Acids*, 5: e355.

Sen, D., B. Balakrishnan, N. Gabriel, P. Agrawal, V. Roshini, R. Samuel, A. Srivastava, and G. R. Jayandharan. 2013. 'Improved adeno-associated virus (AAV) serotype 1 and 5 vectors for gene therapy', *Sci Rep*, 3: 1832.

Shen, S., K. D. Bryant, J. Sun, S. M. Brown, A. Troupes, N. Pulicherla, and A. Asokan. 2012. 'Glycan binding avidity determines the systemic fate of adeno-associated virus type 9', *J Virol*, 86: 10408-17.

Shirley, J. L., Y. P. de Jong, C. Terhorst, and R. W. Herzog. 2020. 'Immune Responses to Viral Gene Therapy Vectors', *Mol Ther*, 28: 709-22.

Sitaraman, V., P. Hearing, C. B. Ward, D. V. Gnatenko, E. Wimmer, S. Mueller, S. Skiena, and W. F. Bahou. 2011. 'Computationally designed adeno-associated virus (AAV) Rep 78 is efficiently maintained within an adenovirus vector', *Proc Natl Acad Sci U S A*, 108: 14294-9.

Sollerbrant, K., J. Elmen, C. Wahlestedt, J. Acker, H. Leblois-Prehaud, M. Latta-Mahieu, P. Yeh, and M. Perricaudet. 2001. 'A novel method using baculovirus-mediated gene transfer for production of recombinant adeno-associated virus vectors', *J Gen Virol*, 82: 2051-60.

Song, B., and C. S. Young. 1997. 'Functional characterization of the major late promoter of mouse adenovirus type 1', *Virology*, 235: 109-17.

Sonntag, F., S. Bleker, B. Leuchs, R. Fischer, and J. A. Kleinschmidt. 2006. 'Adeno-associated virus type 2 capsids with externalized VP1/VP2 trafficking domains are generated prior to passage through the cytoplasm and are maintained until uncoating occurs in the nucleus', *J Virol*, 80: 11040-54.

Sonntag, F., K. Schmidt, and J. A. Kleinschmidt. 2010. 'A viral assembly factor promotes AAV2 capsid formation in the nucleolus', *Proc Natl Acad Sci U S A*, 107: 10220-5.

Srivastava, A., E. W. Lusby, and K. I. Berns. 1983. 'Nucleotide sequence and organization of the adeno-associated virus 2 genome', *J Virol*, 45: 555-64.

Steinwaerder, D. S., and A. Lieber. 2000. 'Insulation from viral transcriptional regulatory elements improves inducible transgene expression from adenovirus vectors in vitro and in vivo', *Gene Ther*, 7: 556-67.

Stillman, B. W. 1983. 'The replication of adenovirus DNA with purified proteins', *Cell*, 35: 7-9.

Strubin, M., and K. Struhl. 1992. 'Yeast and human TFIID with altered DNA-binding specificity for TATA elements', *Cell*, 68: 721-30.

Strunze, S., M. F. Engelke, I. H. Wang, D. Puntener, K. Boucke, S. Schleich, M. Way, P. Schoenenberger, C. J. Burckhardt, and U. F. Greber. 2011. 'Kinesin-1-mediated capsid disassembly and disruption of the nuclear pore complex promote virus infection', *Cell Host Microbe*, 10: 210-23.

Stutika, C., A. Gogol-Doring, L. Botschen, M. Mietzsch, S. Weger, M. Feldkamp, W. Chen, and R. Heilbronn. 2016. 'A Comprehensive RNA Sequencing Analysis of the Adeno-Associated Virus (AAV) Type 2 Transcriptome Reveals Novel AAV Transcripts, Splice Variants, and Derived Proteins', *J Virol*, 90: 1278-89.

Summerford, C., and R. J. Samulski. 1998. 'Membrane-associated heparan sulfate proteoglycan is a receptor for adeno-associated virus type 2 virions', *J Virol*, 72: 1438-45.

Sun, B., Y. T. Chen, A. Bird, F. Xu, Y. X. Hou, A. Amalfitano, and D. D. Koeberl. 2003. 'Packaging of an AAV vector encoding human acid alpha-glucosidase for gene therapy in glycogen storage disease type II with a modified hybrid adenovirus-AAV vector', *Mol Ther*, 7: 467-77.

Sun, C., Y. Zhang, L. Feng, W. Pan, M. Zhang, Z. Hong, X. Ma, X. Chen, and L. Chen. 2011. 'Epidemiology of adenovirus type 5 neutralizing antibodies in healthy people and AIDS patients in Guangzhou, southern China', *Vaccine*, 29: 3837-41.

Swaminathan, S., and B. Thimmapaya. 1995. 'Regulation of adenovirus E2 transcription unit', *Curr Top Microbiol Immunol*, 199 (Pt 3): 177-94.

Szybalska, E. H., and W. Szybalski. 1962. 'Genetics of human cell line. IV. DNA-mediated heritable transformation of a biochemical trait', *Proc Natl Acad Sci U S A*, 48: 2026-34.

Tai, P. W. L., J. Xie, K. Fong, M. Seetin, C. Heiner, Q. Su, M. Weiand, D. Wilmot, M. L. Zapp, and G. Gao. 2018. 'Adeno-associated Virus Genome Population Sequencing Achieves Full Vector Genome Resolution and Reveals Human-Vector Chimeras', *Mol Ther Methods Clin Dev*, 9: 130-41.

Tamayose, K., Y. Hirai, and T. Shimada. 1996. 'A new strategy for large-scale preparation of high-titer recombinant adeno-associated virus vectors by using packaging cell lines and sulfonated cellulose column chromatography', *Hum Gene Ther*, 7: 507-13.

Tessier, J., G. Chadeuf, P. Nony, H. Avet-Loiseau, P. Moullier, and A. Salvetti. 2001. 'Characterization of adenovirus-induced inverted terminal repeat-independent amplification of integrated adeno-associated virus rep-cap sequences', *J Virol*, 75: 375-83.

Thomas, C. E., T. A. Storm, Z. Huang, and M. A. Kay. 2004. 'Rapid uncoating of vector genomes is the key to efficient liver transduction with pseudotyped adeno-associated virus vectors', *J Virol*, 78: 3110-22.

Thomas, G. P., and M. B. Mathews. 1980. 'DNA replication and the early to late transition in adenovirus infection', *Cell*, 22: 523-33.

Thorne, B. A., P. Quigley, G. Nichols, C. Moore, E. Pastor, D. Price, J. W. Ament, R. K. Takeya, and R. W. Peluso. 2008. 'Characterizing clearance of helper adenovirus by a clinical rAAV1 manufacturing process', *Biologicals*, 36: 7-18.

Thorne, B. A., R. K. Takeya, and R. W. Peluso. 2009. 'Manufacturing recombinant adeno-associated viral vectors from producer cell clones', *Hum Gene Ther*, 20: 707-14.

Timpe, J. M., K. C. Verrill, and J. P. Trempe. 2006. 'Effects of adeno-associated virus on adenovirus replication and gene expression during coinfection', *J Virol*, 80: 7807-15.

Tobiasch, E., T. Burguete, P. Klein-Bauernschmitt, R. Heilbronn, and J. R. Schlehofer. 1998. 'Discrimination between different types of human adeno-associated viruses in clinical samples by PCR', *J Virol Methods*, 71: 17-25.

Toniatti, C., H. Bujard, R. Cortese, and G. Ciliberto. 2004. 'Gene therapy progress and prospects: transcription regulatory systems', *Gene Ther*, 11: 649-57.

Tratschin, J. D., I. L. Miller, M. G. Smith, and B. J. Carter. 1985. 'Adeno-associated virus vector for high-frequency integration, expression, and rescue of genes in mammalian cells', *Mol Cell Biol*, 5: 3251-60.

Tratschin, J. D., M. H. West, T. Sandbank, and B. J. Carter. 1984. 'A human parvovirus, adeno-associated virus, as a eucaryotic vector: transient expression and encapsidation of the procaryotic gene for chloramphenicol acetyltransferase', *Mol Cell Biol*, 4: 2072-81.

Trempe, J. P., and B. J. Carter. 1988. 'Alternate mRNA splicing is required for synthesis of adeno-associated virus VP1 capsid protein', *J Virol*, 62: 3356-63.

Uil, T. G., J. Vellinga, J. de Vrij, S. K. van den Hengel, M. J. Rabelink, S. J. Cramer, J. J. Eekels, Y. Ariyurek, M. van Galen, and R. C. Hoeben. 2011. 'Directed adenovirus evolution using engineered mutator viral polymerases', *Nucleic Acids Res*, 39: e30.

Urabe, M., C. Ding, and R. M. Kotin. 2002. 'Insect cells as a factory to produce adeno-associated virus type 2 vectors', *Hum Gene Ther*, 13: 1935-43.

Urabe, M., T. Nakakura, K. Q. Xin, Y. Obara, H. Mizukami, A. Kume, R. M. Kotin, and K. Ozawa. 2006. 'Scalable generation of high-titer recombinant adeno-associated virus type 5 in insect cells', *J Virol*, 80: 1874-85.

Urlinger, S., U. Baron, M. Thellmann, M. T. Hasan, H. Bujard, and W. Hillen. 2000. 'Exploring the sequence space for tetracycline-dependent transcriptional activators: novel mutations yield expanded range and sensitivity', *Proc Natl Acad Sci U S A*, 97: 7963-8.

Vachon, V. K., and G. L. Conn. 2016. 'Adenovirus VA RNA: An essential pro-viral non-coding RNA', *Virus Res*, 212: 39-52.

Vales, L. D., and J. E. Darnell, Jr. 1989. 'Promoter occlusion prevents transcription of adenovirus polypeptide IX mRNA until after DNA replication', *Genes Dev*, 3: 49-59.
van der Loo, J. C., and J. F. Wright. 2016. 'Progress and challenges in viral vector manufacturing', *Hum Mol Genet*, 25: R42-52.
van der Vliet, P. C., D. van Dam, and M. M. Kwant. 1984. 'Adenovirus DNA replication in vitro is stimulated by RNA from uninfected HeLa cells', *FEBS Lett*, 171: 5-8.
Van Vliet, K., V. Blouin, M. Agbandje-McKenna, and R. O. Snyder. 2006. 'Proteolytic mapping of the adeno-associated virus capsid', *Mol Ther*, 14: 809-21.
Vincent, K. A., S. T. Piraino, and S. C. Wadsworth. 1997. 'Analysis of recombinant adeno-associated virus packaging and requirements for rep and cap gene products', *J Virol*, 71: 1897-905.
Waehler, R., S. J. Russell, and D. T. Curiel. 2007. 'Engineering targeted viral vectors for gene therapy', *Nat Rev Genet*, 8: 573-87.
Wang, Q., and M. H. Finer. 1996. 'Second-generation adenovirus vectors', *Nat Med*, 2: 714-6.
Ward, P., P. Elias, and R. M. Linden. 2003. 'Rescue of the adeno-associated virus genome from a plasmid vector: evidence for rescue by replication', *J Virol*, 77: 11480-90.
Ward, P., M. Falkenberg, P. Elias, M. Weitzman, and R. M. Linden. 2001. 'Rep-dependent initiation of adeno-associated virus type 2 DNA replication by a herpes simplex virus type 1 replication complex in a reconstituted system', *J Virol*, 75: 10250-8.
Weger, S., E. Hammer, M. Gonsior, C. Stutika, and R. Heilbronn. 2016. 'A Regulatory Element Near the 3' End of the Adeno-Associated Virus rep Gene Inhibits Adenovirus Replication in cis by Means of p40 Promoter-Associated Short Transcripts', *J Virol*, 90: 3981-93.
Weger, S., A. Wistuba, D. Grimm, and J. A. Kleinschmidt. 1997. 'Control of adeno-associated virus type 2 cap gene expression: relative influence of helper virus, terminal repeats, and Rep proteins', *J Virol*, 71: 8437-47.
Weinberg, M. S., S. Nicolson, A. P. Bhatt, M. McLendon, C. Li, and R. J. Samulski. 2014. 'Recombinant adeno-associated virus utilizes cell-specific infectious entry mechanisms', *J Virol*, 88: 12472-84.
Weindler, F. W., and R. Heilbronn. 1991. 'A subset of herpes simplex virus replication genes provides helper functions for productive adeno-associated virus replication', *J Virol*, 65: 2476-83.
Wells, K. D., J. A. Foster, K. Moore, V. G. Pursel, and R. J. Wall. 1999. 'Codon optimization, genetic insulation, and an rtTA reporter improve performance of the tetracycline switch', *Transgenic Res*, 8: 371-81.
Wiethoff, C. M., H. Wodrich, L. Gerace, and G. R. Nemerow. 2005. 'Adenovirus protein VI mediates membrane disruption following capsid disassembly', *J Virol*, 79: 1992-2000.
Wold, W. S., and K. Toth. 2013. 'Adenovirus vectors for gene therapy, vaccination and cancer gene therapy', *Curr Gene Ther*, 13: 421-33.
Wright, J. F. 2009. 'Transient transfection methods for clinical adeno-associated viral vector production', *Hum Gene Ther*, 20: 698-706.
Wu, G. Q., Y. J. Liao, Z. Q. Qin, L. R. He, Y. C. Chen, Y. X. Zeng, H. F. Kung, and D. Xie. 2010. 'PYRIN domain of NALP2 inhibits cell proliferation and tumor growth of human glioblastoma', *Plasmid*, 64: 41-50.
Wu, K., D. Orozco, and P. Hearing. 2012. 'The adenovirus L4-22K protein is multifunctional and is an integral component of crucial aspects of infection', *J Virol*, 86: 10474-83.
Wu, Z., A. Asokan, and R. J. Samulski. 2006. 'Adeno-associated virus serotypes: vector toolkit for human gene therapy', *Mol Ther*, 14: 316-27.
Wu, Z., E. Miller, M. Agbandje-McKenna, and R. J. Samulski. 2006. 'Alpha2,3 and alpha2,6 N-linked sialic acids facilitate efficient binding and transduction by adeno-associated virus types 1 and 6', *J Virol*, 80: 9093-103.
Wustner, J. T., S. Arnold, M. Lock, J. C. Richardson, V. B. Himes, G. Kurtzman, and R. W. Peluso. 2002. 'Production of recombinant adeno-associated type 5 (rAAV5) vectors using recombinant herpes simplex viruses containing rep and cap', *Mol Ther*, 6: 510-8.

Xi, Q., R. Cuesta, and R. J. Schneider. 2005. 'Regulation of translation by ribosome shunting through phosphotyrosine-dependent coupling of adenovirus protein 100k to viral mRNAs', *J Virol*, 79: 5676-83.
Xiao, P. J., C. Li, A. Neumann, and R. J. Samulski. 2012. 'Quantitative 3D tracing of gene-delivery viral vectors in human cells and animal tissues', *Mol Ther*, 20: 317-28.
Xiao, X., J. Li, and R. J. Samulski. 1996. 'Efficient long-term gene transfer into muscle tissue of immunocompetent mice by adeno-associated virus vector', *J Virol*, 70: 8098-108.
———. 1998. 'Production of high-titer recombinant adeno-associated virus vectors in the absence of helper adenovirus', *J Virol*, 72: 2224-32.
Xiao, X., W. Xiao, J. Li, and R. J. Samulski. 1997. 'A novel 165-base-pair terminal repeat sequence is the sole cis requirement for the adeno-associated virus life cycle', *J Virol*, 71: 941-8.
Xie, Q., W. Bu, S. Bhatia, J. Hare, T. Somasundaram, A. Azzi, and M. S. Chapman. 2002. 'The atomic structure of adeno-associated virus (AAV-2), a vector for human gene therapy', *Proc Natl Acad Sci U S A*, 99: 10405-10.
Yan, S., P. J. Myler, and K. Stuart. 2001. 'Tetracycline regulated gene expression in Leishmania donovani', *Mol Biochem Parasitol*, 112: 61-9.
Yan, Y., B. Zhang, W. Hou, H. Lin, J. Rebetz, S. S. Hong, Y. Wang, L. Ran, and X. Fan. 2017. 'Active and separate secretion of fiber and penton base during the early phase of Ad2 or Ad5 infection', *Virology*, 505: 172-80.
Yang, Q., F. Chen, and J. P. Trempe. 1994. 'Characterization of cell lines that inducibly express the adeno-associated virus Rep proteins', *J Virol*, 68: 4847-56.
Yao, F., T. Svensjo, T. Winkler, M. Lu, C. Eriksson, and E. Eriksson. 1998. 'Tetracycline repressor, tetR, rather than the tetR-mammalian cell transcription factor fusion derivatives, regulates inducible gene expression in mammalian cells', *Hum Gene Ther*, 9: 1939-50.
Yi, Y., M. J. Noh, and K. H. Lee. 2011. 'Current advances in retroviral gene therapy', *Curr Gene Ther*, 11: 218-28.
Yin, H., R. L. Kanasty, A. A. Eltoukhy, A. J. Vegas, J. R. Dorkin, and D. G. Anderson. 2014. 'Non-viral vectors for gene-based therapy', *Nat Rev Genet*, 15: 541-55.
Young, C. S. 2003. 'The structure and function of the adenovirus major late promoter', *Curr Top Microbiol Immunol*, 272: 213-49.
Yuan, Z., C. Qiao, P. Hu, J. Li, and X. Xiao. 2011. 'A versatile adeno-associated virus vector producer cell line method for scalable vector production of different serotypes', *Hum Gene Ther*, 22: 613-24.
Zeltner, N., E. Kohlbrenner, N. Clement, T. Weber, and R. M. Linden. 2010. 'Near-perfect infectivity of wild-type AAV as benchmark for infectivity of recombinant AAV vectors', *Gene Ther*, 17: 872-9.
Zen, Z., Y. Espinoza, T. Bleu, J. M. Sommer, and J. F. Wright. 2004. 'Infectious titer assay for adeno-associated virus vectors with sensitivity sufficient to detect single infectious events', *Hum Gene Ther*, 15: 709-15.
Zhang, H. G., Y. M. Wang, J. F. Xie, X. Liang, H. C. Hsu, X. Zhang, J. Douglas, D. T. Curiel, and J. D. Mountz. 2001. 'Recombinant adenovirus expressing adeno-associated virus cap and rep proteins supports production of high-titer recombinant adeno-associated virus', *Gene Ther*, 8: 704-12.
Zhang, H., J. Xie, Q. Xie, J. M. Wilson, and G. Gao. 2009. 'Adenovirus-adeno-associated virus hybrid for large-scale recombinant adeno-associated virus production', *Hum Gene Ther*, 20: 922-9.
Zhang, W. W., L. Li, D. Li, J. Liu, X. Li, W. Li, X. Xu, M. J. Zhang, L. A. Chandler, H. Lin, A. Hu, W. Xu, and D. M. Lam. 2018. 'The First Approved Gene Therapy Product for Cancer Ad-p53 (Gendicine): 12 Years in the Clinic', *Hum Gene Ther*, 29: 160-79.
Zhang, X., and C. Y. Li. 2001. 'Generation of recombinant adeno-associated virus vectors by a complete adenovirus-mediated approach', *Mol Ther*, 3: 787-92.
Zhang, Y., and J. M. Bergelson. 2005. 'Adenovirus receptors', *J Virol*, 79: 12125-31.

Zhou, X., M. Vink, B. Klaver, B. Berkhout, and A. T. Das. 2006. 'Optimization of the Tet-On system for regulated gene expression through viral evolution', *Gene Ther*, 13: 1382-90.
Zincarelli, C., S. Soltys, G. Rengo, and J. E. Rabinowitz. 2008. 'Analysis of AAV serotypes 1-9 mediated gene expression and tropism in mice after systemic injection', *Mol Ther*, 16: 1073-80.

Appendix

1.1 DNA gBlock qPCR sequence standard:

Use with qPCR primers and probe: hFIX, Ad5 Fibre, EGFP, UTR, CMV, Ad5 Hexon, AAV2 ITR, TetR, AAV2 Rep, AAV2 Cap, AAV5 Cap, AAV9 Cap, AAV6 Cap, Ad5 packaging signal, AmpR, and KanR

GAGGCTGTGTTCCCTGATGTGGACTATGTGAACAGCACTGAGGCTGAAACCATCCTGGACAACATCACCC
AGAGCACCCAGAGCTTCAATGACTTCACCAGGGTGGTGGGTTTTGTTTTGGCTGTTAAAGGCAGTTTGGC
TCCAATATCTGGAACAGTTCAAAGTGCTCATCTTATTATAAGATTTGACGAAAATGGAGTGCTACTATTTT
GGTGAACCGCATCGAGCTGAAGGGCATCGACTTCAAGGAGGACGGCAACATCCTGGGGCACAAGCTGG
AGTACAACTACAACAGCCACAACGTCTATATCATGGCCGACAAGCAGATTTTCTTTGTCGATCCTACCATC
CACTCGACACACCCGCCAGCGGCCGCTGCCAAGCTTCCGAGCTCTCGAATTCTTTTCCCATATATGGAGTT
CCGCGTTACATAACTTACGGTAAATGGCCCGCCTGGCTGACCGCCCAACGACCCCCGCCCATTGACGTCA
ATAATGACGTATGTTCCCATAGTAACGCCAATAGGGTTTTGACACTCATATTTCTTACATGCCCACTATTA
AGGAAGGTAACTCACGAGAACTAATGGGCCAACAATCTATGCCCAACAGGCCTAATTTTGAATGAGGTG
GGAATTGAAGGACTCACTACTCGCAAGCTGGCACAGAAGCTGGGCGTCGAGCAGCCAACGCTGTACTG
GCATGTGAAGAATAAACGGGCGCTCCTAGACGCGCTTGCCATCGAAATGCTGGACTTTTCTAGGAACCCC
TAGTGATGGAGTTGGCCACTCCCTCTCTGCGCGCTCGCTCGCTCACTGAGGCCGGGCTTTTCCAGGCCTC
ATACATCTCCTTCAATGCGGCCTCCAACTCGCGGTCCCAAATCAAGGCTGCCTTGGACAATGCGGGAAAG
ATTATGAGCCTGACTAATCTAGAGATTCCGACCCAAGAGACTCAACTTCAAGCTCTTTAACATTCAAGTCA
AAGAGGTCACGCAGAATGACGGTACGACGACGATTGCCAATAACCTTACCAGCACGGTTCAGGTTTTTA
CCGCTTCGTGAGCACAAATAACACTGGCGGAGTCCAGTTCAACAAGAACCTGGCCGGGAGATACGCCAA
CACCTACAAAAACTTTTCTTGATGAATCCTGGACCTGCTATGGCCAGCCACAAAGAAGGAGAGGACCGTT
TCTTTCCTTTGTCTGGATCTTTAATTTTTGGCAAACAAGGAACTGGAAGAGACAACGTGTTACACATGTAA
GCGACGGATGTGGCAAAAGTGACGTTTTTGGTGTGCGCCGGTGTACACAGGAAGTGACAATTTTCGCGC
GGTTTTAGGCGGATGTTGTAGTAAATTTGGGCGTAACCGAGTAAGATTTCGACCGGAGATGTGCATGTT
ATGGGAGCCTTACCTGGAATGGTGTGGCAAGACAGAGACGTATACCTGCAGGGTCCTATTTGGGCCAAA
ATTCCTCACACGGATGGACATTTGAGCTGAATGAAGCCATACCAAACGACGAGCGTGACACCACGATGC
CTGTAGCAATGGCAACAACCTTGCGTAAACTATTAACTGGCGAACTACTTACTCTAGCTTCTTTCATCATG
GCTGATGCAATGCGGCGGCTGCATACGCTTGATCCGGCTACCTGCCCATTCGACCACCAAGCGAAACATC
GC

2.1 PCR Primers

Forward primer 5'-CACTGACTGACTGATACAATCGATGAAGAAAACGGTTTCCG-3' and reverse 5'-CTGCGGATCCAG AAATCGATATCGATGCCGAAGGGGGCGTGGTC-3'

2.2 PCR Primers

Forward primer 5'-GCGCAGTACTGGCAGCGGTGCACGGGCTGTACATCCTGCACGAG-3' and reverse 5'-CGCTGTATCTCAGTCAGTCAAGCTAGCGCAGCAGCCGCCGCGCC-3'

2.3 PCR Primers

Forward primer 5'-CTTAAAATCAGTTAGCAAATTTATGCATGCAGGAGGAGGTACCCACCATGTCGCGCCTGGACAAAAG-3' and reverse 5'-GAATAAGATCGCGACCTAGGATAGCCGTCGACCTTTAAAAAACCTCCCACAC-3'

2.4 PCR Primers

Forward primer 5'-GACGGCGATCGCTGGGGCGGCCGCCATCGATGGGTTAATTAATGTAGTGTATTTATACCCGG'-3 and reverse primer 5'-GACCCCCACCTTATATATTCTTTCCCACCCTTAATTAAGCCACGCCCACACATTTCAG TACCTC-3'

3.0 Alignment of the wt AAV genome sequence (AF043303.1) to pRepCap2 (Q1311) sequence map

